

**GEOTECHNICAL INFRASTRUCTURE ASSET
MANAGEMENT FOCUSING ON
PERFORMANCE DETERIORATION PROCESS
OF GROUND ANCHORS**

TAWEEPHONG SUKSAWAT

2014

**GEOTECHNICAL INFRASTRUCTURE ASSET MANAGEMENT FOCUSING ON
PERFORMANCE DETERIORATION PROCESS OF GROUND ANCHORS**

by

Taweephong Suksawat

A thesis submitted in partial fulfillment of the requirements for the
degree of Doctor of Engineering

Nationality: Thai

Previous Degree: Master of Engineering in Geotechnical Engineering
Asian Institute of Technology
Bangkok, Thailand

Scholarship Donor: Monbukagakusho Scholarship

Department of Urban Management,
Graduate School of Engineering,
Kyoto University
Japan

ACKNOWLEDGEMENT

The author wishes to express his deep gratitude to his supervisor Prof. Hiroyasu Ohtsu for his invaluable guidance, suggestions, encouragement, continuous supervision and help throughout the period of this thesis study especially allow and financial support the author to comeback home country for more than ten times during studied here.

Great appreciation is extended to Prof. Hirotaka Kawano and Prof. Junji Kiyono for their valuable suggestions and encouragement as well as for kindly serving as members of his examination committee.

I also would like to thank their support, great relation by doing research associated with Asian Institute of Technology, Dr. Noppadol Phien-wej and Dr. Pham Huy Giao as well as Kasetsart University, Dr. Suttisak Sornlalump for giving me opportunities to have great experiences in study during internship in Thailand.

In addition, I sincerely thank to Dr. Tomoki Shiotani, Dr. Shinya Inazumi, Dr. Tafumi Kitaoka, Noriko Oyagi-san and Hiromi Ito-san for their helping my study before coming to Japan and during in Japan especially for official documents.

Sincerest thanks to Dr. Nipawan Chaleiwchalad for her advice, teach, helpful, suggestions and guidance to the author's life during stay in Japan. The author would like to thank Miss. Supamas Rojjanapitakphan for her kind for preparing permission documents during working in Thailand. In addition, the author would like to sincerest thanks to Archan Raywatt Naimee, Mr. Sontisak Nakmanee, Mr. Nitinana Inanan, Mr. Sarawut Tessiri, Mr. Arsti Iyarak, Mr. Jo, Dr. Suthasinee Artidteang, and Miss. Salisa Chaiyaput for his/her kind for great dinners and parties during stay in Thailand.

I would like to give special thanks to Dr. Kenji Takahashi, Mr. Mitsuru Yabe and Mr. Yasunori Sakai for kind of them about operation of field monitoring and spending life some time in Phuket and Nakhon Nayok, Thailand.

My deep thank is to Kyoto University Global COE Program and Japanese Government who gave me the great opportunity with a scholarship to study in the program of PhD.

Degree here. I also sincerely express to Dr. Nagahisa Hirayama, Dr. Mamoru Yoshida, for their useful advices during my course works including of the internship program.

Many thanks to all members, Construction Engineering Systems Laboratory Agro Wunna Htun, Mr. Ryoji Kawai, Mr. Motoyoshi Goto, Mr. Junnosuke Okawa, Mr. Hirohisa Koga, Mr. Kunya Iwamoto, Mr. Sho Kimoto, Mr. Yasutaka Ota, Mr. Takayuki Isoda, Mr. Hiroshi Masuda, Mr. Naoya Matsuzuka, Mr. Naoki Okuno, Mr. Yuta Takada, Mr. Kodai Yamamoto, Mr. Junya Ikenaka, Mr. Satoshi Osawa, Miss. Sayaka Kumamoto (Sayapi), Miss. Hakamada Kaoru, Mr. Kanji Okuoka, Mr. Taku Kobayashi, Mr. Tomoya Shirai, Mr. Yuuki Takaoka, Mr. Toshihiro Nakai, Mr. and for giving encouragement each other and sharing students' life in our laboratory.

Especially, special thanks are contributed to Mr. Hirohisa Koga, Mr. Sho Kimoto, Mr. Hiroshi Masuda, Mr. Naoya Matsuzuka, Mr. Satoshi Osawa, Mr. Junya Ikenaka, Sayapi and Kaoruchan for their help during oversea working, translating language from Japanese to English, accommodation, credit card, driving and so on as well as Agro Wumma Htun for always making me not so lonely during lunch as well as Nomikai.

Thank you for my friends living in both Japan and Thailand who spend their life and time, and help solving the problem during in Japan.

Finally, my success in this studied and everything in my life devoted to my spouse and family for their encouragement and assistance throughout all periods of life. This work is lovingly dedicated to them.

ABSTRACT

Infrastructure systems are the basic physical and organizational structures needed for the services and facilities necessary for an economy to function. It provided a framework supporting an entire structure of a country's development. Generally, it refers to the technical structures that support a society, for instance, highway, bridge, dam, tunnel, water supply, etc. Moreover, it can be defined as the importance components of consistent systems supporting commodities and services indispensable to enable, sustain, or enhance societal living conditions.

The infrastructure systems were numerous developed in Japan for the last half century for the facility to societies. Highways were one of the infrastructure systems supplied as the connection linkage between cities from urban to sub-urban areas. They were dramatically expanded and enlarged until a present caused automobile gained popularity. Therefore, numerous highways were constructed at the foot of the hill which extensively man-made hazard. As a result, many countermeasures against to the slope collapse were acted.

Several ground improvement techniques, for instance, reinforcement retaining wall, shotcrete, soil nail, cement column and ground anchors were proposed to protect landslide as well as embankment failure along the highway recently. Particularly, ground anchors were used as the countermeasure for stabilizing both natural and man-cut slopes. Forty years since the first ground anchor was introduced to relief instable slope problems in Japan. Ground anchors have been installed more than 120,000 set in at least 30,000 projects. Since some of them have been constructed in early times, therefore, they were in heavily deteriorated condition. Consequently, their performances were severe condition such as lost in pre-stresses force, resulting in slope deformation and exposure of broken anchor heads.

In order to verify the present stability of those slopes, the Visual inspection test, the Lift off test and the Ultrasonic test were experimented on those slopes. They were employed to determine the capacity, potency and the remaining force of individual anchor. The Visual inspection test results were utilized as a preliminary evaluating the workability of the slopes since it is not complicated as well as the fastest method comparing with the others. The Lift off test was proposed to verify the actual remaining force in ground anchors at

present situation; however, this method is quite expensive and difficult to test on all the ground anchors. Therefore, it can be adopted only five to ten percent of the whole sample. The last method, namely the Ultrasonic test was introduced to approve and confirm the existing force in the ground anchors by mean of ultrasonic wave such as the amplitude voltage; however, due to the limitation of the data allowable, it was engaged to be the supplement method for the Lift off test.

The Visual inspection test results are provided by one of the Japanese expressway companies (hereafter called “the road administrator”) and the condition stages of ground anchor are categorized into six ratings, which are Excellent, Very good, Good, Fair, Marginal and Poor conditions corresponding to rank IV to rank I, respectively. Each rank of performance is determined by the visual inspection from the surface of the ground anchor head and hammering test from the anchor head by the expert engineer from the road administrator. However, it is quite low reliable because this method based only on the experience of the expert engineers.

The Lift off test was adopted as the direct method to determine the existing force; however, the cost of experiment is quite high compared with the other methods. Therefore, they were conducted on the selected slope with the limited number of testing. The kriging method was proposed to interpolate the unknown force of ground anchors adjacent to the testing results. In addition, Ultrasonic test results can also be calculated similarly with the Lift off test results; however, differences only to suggest the additional Lift off test by means of the indicator kriging. This method is one technique to indicate the weaker zone for the specify priority location for maintenance strategies.

In order to analyze the deterioration rate of the slope improved by ground anchors, the Weibull hazard model was employed as the represent statistical approach caused it quite more appropriate than the other models. It can simulate the deterioration process by means of failure probability and survival probability. Rod type and stand type as well as the different geological conditions were separately considering. Furthermore, the probability of failure as well as the three dimensional slope stability analysis was conducted on those risk slopes.

Due to allowance budget was limited to reinstalling on all ground anchors frequently, the economic performance of a risk slope over its entire life technique called the Life cycle

cost, *LCC* was considered. It was adopted as the indicators to evaluate the suitable scenario plan for repair/renew the risk slopes. Finally, the lowest expended on the maintenance strategy was selected as the appropriate scenario to prolong the life span of slope improved by ground anchors.

TABLE OF CONTENTS

Chapter	Title	Page
	Title Page	i
	Acknowledgement	iii
	Abstract	v
	Table of Contents	ix
	List of Figures	xiii
	List of Tables	xxi
1	INTRODUCTION	1
	1.1 General	1
	1.2 Research Objectives	7
	1.3 Scope of the Research Study	8
2	LITERATURE REVIEW	11
	2.1 Introduction	11
	2.2 Statistical Approach	12
	2.2.1 Normal distribution function	12
	2.2.2 Log-normal distribution function	14
	2.2.3 Markov chain model	15
	2.2.4 Weibull hazard model	21
	2.2.5 Poisson process model	24
	2.2.6 Exponential distribution function	26
	2.3 Deterioration Process of Cohesion	28
	2.4 Slope Stability Analysis	31
	2.5 Probability of Failure	37
	2.6 Monte Carlo Simulation	39
	2.7 Kriging Method	40
	2.8 Life Cycle Cost	44

TABLE OF CONTENTS

Chapter	Title	Page
	2.9 Case Study of Ground Anchor in Kinki District	45
3	METHODOLOGY	47
	3.1 Introduction	47
	3.2 Acquisition of Inspection Results and Identify of Current Conditoin	49
	3.2.1 Methodology of Visual Inspection Test Results	49
	3.2.2 Methodology of Lift off Test Results	52
	3.2.3 Methodology of Ultrasonic Test Results	58
	3.2.4 Comparison Scenario of Different Geological Conditions and Anchors types	59
	3.3 Modeling of Deterioration Process and Prediction of Future Condition	59
	3.3.1 Comparison Scenario of Different Markov chain model	59
	3.3.2 Comparison Scenario of Different Survival Probability Models	61
	3.4 Investigation on Stability and Failure Proability	63
	3.5 Estimate of Life Cycle Cost and Decision Making on Maintenance	64
4	THE ACQUISITION OF TESTING RESULTS AND IDENTIFICATION OF CURRENT CONDITION	65
	4.1 Introduction	65
	4.2 The Visual Inspection Data	67
	4.3 The Lift off Test Data	76
	4.3.1 The Kriging Results	78

TABLE OF CONTENTS

Chapter	Title	Page
	4.3.2 Comparison of the Survival Probability of the Lift off test and kriging results	83
4.4	The Ultrasonic test result	85
	4.4.1 Statistic Approach	89
	4.4.2 Comparison between Lift off test and Ultrasonic Results	93
5	MODELING OF THE DETERIORATION PROCESS AND PREDICTION OF FAILURE CONDITION	97
5.1	Introduction	97
5.2	The Visual Inspection Test Results	97
	5.2.1 Comparison of Three Markov Models Results	97
	5.2.2 Comparison of Several Statistical Models Results	98
5.2.3	Comparison of Survival Probability between Ground Anchors Types and Geological Conditions	102
5.3	The Lift off Test Results	106
	5.3.1 Comparison of Survival Probability between Ground Anchors Types and Geological Conditions	106
5.4	Comparison between the Lift off Test and Visual Inspection Test Results	111
6	INVESTIGATION ON STABILITY OF RISK SLOPES AND PROBABILITY OF FAILURE	115
6.1	Introduction	115
6.2	The Safety Factor Analysis	115
6.3	Annual Probability of Failure of the Risk Slopes	124

TABLE OF CONTENTS

Chapter	Title	Page
7	ESTIMATE OF THE LIFE CYCLE COST AND DECISION- MAKING ON MAINTENANCE	131
7.1	Introduction	131
7.2	The Concept of Life Cycle Cost, <i>LCC</i>	132
7.3	<i>LCC</i> Considering the Macroscopic Viewpoint	134
7.3.1	<i>LCC</i> of the Visual inspection test	134
7.3.2	<i>LCC</i> of the Lift off test	138
7.3.3	Comparison of <i>LCC</i> Results between the Visual Inspection and Lift off tests	139
7.4	<i>LCC</i> Considering the Microscopic Viewpoint	141
8	CONCLUDING REMARKS AND FURTHER RECOMMENDATIONS	147
8.1	Concluding Remarks	147
8.2	Further Recommendations	150
	REFERENCE	153
	APPENDIX A	A-1

LIST OF FIGURES

Figure	Title	Page
1.1	Total number of ground anchor used in Japan since 1970 (Miyatake et al, 2007)	2
1.2	Example of deterioration of ground anchors	3
1.3	Type of ground anchor	4
1.4	Type of ground anchor	5
1.5	Scopes and frame work of the study	9
2.1	Probability and cumulative density function of Normal distribution function (Casella et al, 2001).	13
2.2	Probability and cumulative density function of Log-normal distribution function (Casella et al, 2001).	14
2.3	Six-state Markov chain model	16
2.4	Transition matrixes for Markov original method	18
2.5	Transition matrixes for Markov simplify method	18
2.6	Markov hazard transition matrix calculated by MS excel	20
2.7	The effect of m on failure rate of Weibull hazard model	22
2.8	The regression curve for calculation parameters of the Weibull Hazard model	23
2.9	Probability and cumulative density function of Poisson process model	25
2.10	Probability and cumulative density function of Exponential distribution function	27
2.11	Relationship between K_c and C_r after Otani et al (2004)	29
2.12	Deterioration curve of cohesion after Otani et al (2004)	29
2.13	Random path of decrease of cohesion after Otani et al (2004)	30
2.14	Random path of decrease of cohesion after Ohtsu et al (2004)	30
2.15	Slices and forces in a sliding mass (Krahn, 2002)	32
2.16	Example of slope stability analysis by SV slope software for circular failure pattern	34

LIST OF FIGURES

Figure	Title	Page
2.17	Example of slope stability analysis by SV slope software for plan failure pattern (a) Two dimensions and (b) Three dimensions	35
2.18	The slope configuration for analysis in previous studied (Kimoto et al, 2011)	36
2.19	Relationship between performance function and failure probability	39
2.20	Example of results of factor safety analysis employed Monte Carlo technique	40
2.21	Semi- variogram (Bohling, 2005)	41
2.22	Component of Semi-Variogram (Bohling, 2005)	41
2.23	Example of indicator kriging	43
2.24	Schematic diagram of the performance strategies of various scenarios based on Weibull model	44
2.25	Prioritization of the road slope to be repaired (Ohtsu, 2011)	46
3.1	Flowchart of this study	48
3.2	Example results of the Visual inspection test	50
3.3	Example results of the Visual inspection results of Ibaraki No.12	50
3.4	Flow chart of visual inspection test data	51
3.5	The Lift off test performance and results	53
3.6	Flow chart describes the criteria of each rank	55
3.7	Flow chart of Lift off test results	57
3.8	Flow chart of the Ultrasonic test results.	58
3.9	Comparison scenario of this study	59
3.10	Survival Probability models	62
4.1	Routes and number of testing slopes obtained from the Visual inspection test	67
4.2	Compareson number of samples among of different geological conditions different geological conditions	71
4.3	The installation year as well as the cumulative number of ground anchors in Kansai district	72

LIST OF FIGURES

Figure	Title	Page
4.4	Percent sharing on each rank at 8, 16 and 28 years since installation	73
4.5	The percentage of failure and survive ground anchors of the Scenario I	74
4.6	The percentage of failure and survive ground anchors of the Scenario II	75
4.7	Routes and data of the Lift off test obtained from field test	76
4.8	Comparison between rod type and strand type of the Lift off test	78
4.9	Example results of semi-variogram	79
4.1	Kriging results of Fukushi No.15	80
4.11	Kriging results of Ibaraki No.2	80
4.12	Histogram comparison among of four models and the Lift off test	81
4.13	Total anchors force of each models based on kriging results	82
4.14	Comparison between survival probabilities of kriging and lift off test results	84
4.15	The percentages of failures and survives ground anchors of the rod and strand types	84
4.16	The percentages of failures and survives ground anchors of the sedimentary and igneous rock	85
4.17	The basic concept of the Ultrasonic test	86
4.18	The Ultrasonic test results fluctuated varying from each testing	86
4.19	The example of the Ultrasonic test on ground anchors	87
4.20	The reflection characteristics of Ultrasonic wave	88
4.21	Location of the Lift off test on Fukushi No.20	89
4.22	Results of the Lift off test	91
4.23	Relationship between amplitude from Ultrasonic test versus existing force from Lift off test	91
4.24	Confidence interval	92

LIST OF FIGURES

Figure	Title	Page
4.25	Calibration on the Lift off test results with the Ultrasonic test results on 90%, 95% and 99% confidence interval	94
4.26	Comparison among of the Lift off test result and the Ultrasonic test with 90%, 95% and 99% confidence intervals	96
5.1	Comparison of results among of Markov models with observation data at (a) 8 years (b) 26 years (c) 18 years and (d) 22 years	98
5.2	Comparison of survival probability based on three Markov models	99
5.3	Comparison of survival probability among of several models.	101
5.4	Comparison of survival probability among Weibull, Normal and Log-Normal models together with histogram and PDF of scenario I and II	102
5.5	Comparison of survival probability among of new type, old type and all data	103
5.6	Comparison results between rod and strand types	104
5.7	Comparison of survival probability between different geological conditions.	105
5.8	Comparison of survival probability between different geological conditions as well as	106
5.9	Comparison of survival probabilities between rod and strand types.	107
5.10	Comparison of survival probabilities between different geological conditions.	108
5.11	Comparison of survival probabilities between different geological conditions as well as strand and rod types	109
5.12	The name of risk slopes that shall be a priority investigate the F.S. of the sedimentary rock	110
5.13	Comparison of simulation results between the Visual inspection and Lift off test	111
5.14	Comparison of survival probabilities between the Visual inspection and Lift off test	112

LIST OF FIGURES

Figure	Title	Page
6.1	The example of three dimensional slope stability analysis for this study	116
6.2	Example slope configuration (Fukushi No.9)	117
6.3	The example FS results of Fukushi No.9	118
6.4	The example to simulate force with time	120
6.5	The example of deteriorated on anchor force on a slope	121
6.6	FS with time of sedimentary (a) rod type and (b) strand type	121
6.7	Relationship between percentages of reduction in performance function versus survival probability	123
6.8	The reduction of the existing force with time	123
6.9	Existing forces of ground anchor versus performance function	124
6.10	Performance function and Existing force versus elapsed time	125
6.11	Conditional probabilities of failure of risk slopes	126
6.12	Annual probabilities of failure of risk slopes	127
6.13	Cumulative Annual Probabilities of Failure of risk slopes	128
6.14	The relationship between F.S. and cumulative probability of failure	129
7.1	Performance of ground anchors with maintenance strategies	132
7.2	Comparison of LCC results of the Rod type (MC-I)	135
7.3	Comparison of LCC results of the Rod type (MC-II)	135
7.4	Comparison of LCC results of the Rod type (WB-I)	135
7.5	Comparison of LCC results of the Rod type (WB-II)	136
7.6	Comparison of LCC results of the Strand type (MC-I)	136
7.7	Comparison of LCC results of the Strand type (MC-II)	136
7.8	Comparison of LCC results of the Strand type (WB-I)	137
7.9	Comparison of LCC results of the Strand type (WB-II)	137
7.10	Comparison of LCC results of the Rod type	138
7.11	Comparison of LCC results of the Strand type	138

LIST OF FIGURES

Figure	Title	Page
7.12	Comparison of LCC results between ground anchors type of the Visual inspection test	139
7.13	Comparison of LCC results between statistical models of the Visual inspection test	140
7.14	Comparison of LCC results between the Visual Inspection test and the Lift off test results	140
7.15	Comparison of LCC with difference repair scenarios of Ibaraki No.4	142
7.16	Comparison of LCC with difference repair scenarios of Ibaraki No.2	142
7.17	Comparison of LCC with difference repair scenarios of Wagayama No.8	143
7.18	Comparison of LCC with difference repair scenarios of Kobe No.2	143
7.19	Comparison of LCC with difference repair scenarios of Kyotan No.4	143
7.20	Comparison of LCC with difference repair scenarios of Fukushi No.8	144
7.21	Comparison of LCC with difference repair scenarios of Ibaraki No.12	144
7.22	LCC versus volume of failure of risk slopes	145
7.23	Optimum LCC versus number of anchors installed	146
7.24	Number of ground anchor versus optimum inspection interval	146

LIST OF TABLE

Table	Title	Page
1.1	Evaluation criterion of condition rating	4
1.2	Comparison among pros and cons of three experiments	6
2.1	Statics satisfied and interslice forces in various methods (Krahn, 2002)	33
3.1	Criteria for calculation the failure and survival probability	51
3.2	Criteria of each ranking based on Lift off test results	54
4.1	Evaluation criterion of condition rating by Visual inspection test	65
4.2	Summary of the Visual inspection data, Old type ground anchor	68
4.3	Summary of the Visual inspection data, New type ground anchor	69
4.4	Summary of the Lift off test data	77
4.5	Summary of the Lift off test data and survival probability	83
4.6	Summary of Lift off test results of Fukushi No.20	90
4.7	Summary results of indicator kriging	95
6.1	Summary of Safety Factor analysis results	119
7.1	Summary of the LCC results of the Visual inspection test	137
7.2	Summary of the LCC results of the Lift off test	139
7.3	Summary of input parameters for analysis the LCC	141
7.4	Summary of Life Cycle Cost analysis results	144

CHAPTER 1

INTRODUCTION

1.1 General

Infrastructure systems are basic physical and organizational structures needed for the services essential to the operation of a society or enterprise. It refers collectively to the roads, highways, bridges, tunnels and similar public works that are required for an economic growth. Moreover, it can be defined as the important components of consistent systems supporting commodities and services indispensable to enable, sustain, or enhance societal living conditions.

Several infrastructure systems have been developed in Japan since last half century. It is the integrated, multidisciplinary set of strategies in sustaining public infrastructure assets. Therefore, the concept of infrastructure asset management has proposed to strategically operate, construction, maintenance and renewal of infrastructures. The infrastructure asset management is a systematic process of maintaining, upgrading, and operating physical assets provide at the lowest life-cycle cost. The lowest life-cycle cost refers to the best appropriate cost for rehabilitating, repairing or replacing an asset.

The reduction rate of performance of the infrastructure is the predominate factor to investigate life-cycle cost. Generally, the service level is continuously decreased after construction or maintenance depending on the frequency of the usage or the types of infrastructures. For instance, the amount of the traffic for the highway pavement and the damage level of the pavement is increasing proportionally to the frequency of the usage. On the other hand, it is quite different from the viewpoint of the geotechnical infrastructure, such as slopes, tunnels and dams. Its damage level increases caused the deterioration process as well as the service level is independent of the amount of traffic or the number of usages. Therefore, the safety factor, $F.S.$ is more appropriate to describe the service level in the viewpoint of geotechnical engineering. Moreover, the $F.S.$ reflects the risk and probability of failure of those infrastructures, which regarding to the concern of road user. Highways play an important component supplied the connection linkage between cities and

sub-urban areas. They were dramatically expanded and enlarged until the present caused automobile gained popularity. As a result, several highways were constructed in mountainous areas, which extensively expand man-made hazard. Therefore, many countermeasures against to the slope collapse were acted. Several ground improvement techniques, for instance, reinforcement retaining wall, shotcrete, soil nail, cement column and ground anchors were proposed to protect landslide and embankment failure along the highway slope recently. Particularly, ground anchors, they were used as the countermeasure in order to stabilize both natural and man-cut slopes for road and dam construction, improve structural stability, control floating of structures caused by underground water, etc.

Forty years since the first ground anchor was installed in western Japan; ground anchors have been employed for various purposes, more than 120,000 ground anchors in at least 30,000 projects (see Fig 1.1) Some of them constructed in earlier times have aged and deteriorated their performance, such as lost in pre-stresses force, resulting in slope deformation and exposure of broken anchor heads (Miyatake et al, 2007). The deterioration of ground anchors indicated the reduction on quality or strength with time as a result of fatigue and collusion, multiple aggressive environment factor, poor workmanship, inadequate design and lack of maintenance (Ohtsu, 2011). Therefore, it is necessary to predict the deterioration rate of ground anchor quantitatively, and to do the strategic maintenance from the viewpoint of the asset management (Kimoto et al, 2011).

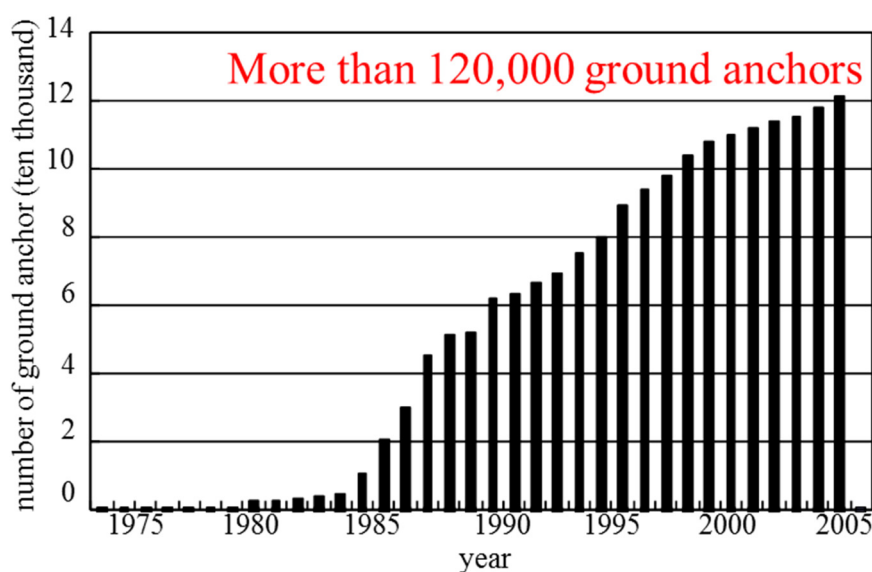


Figure 1.1 Total number of ground anchor used in Japan since 1970 (Miyatake et al, 2007)

Figure 1.2 illustrate the example of ground anchors deterioration in several modes. Some of them showed concrete head broken, which increasing rusting on the tendon bar or wire as demonstrated in Fig 1.2 (a). Generally, after time gone by, rust might occur on the tendon bar or wire, it directly affected to force in the ground anchors since load depending on the cross-section area of the tendon bar (see Fig 1.2 (b)). Moreover, no remaining force on several ground anchors because a tendon bar might be broken due to over-stresses or heavily corroded on the tendon bar as illustrated in Fig 1.2 (c). Finally, concrete cover on slope might crack due to over-deformation (see Figure 1.2 (d)), then slopes danger to collapse in the near future.

Ground anchors can be divided into two categories, which are rod type and strand type as shown in Fig 1.3 (a) rod type and (b) strand type, respectively. The rod type is the single rod, the size of this type is called as the dimension of a tendon whereas the strand type is the multiple cables that are separated or braided together. The rod types are commonly available in 26 mm, 32 mm, 36 mm, 45 mm, and 64 mm in diameters while the strand types call as the number of 15 mm diameter strands.



(a) Ground anchor head broke



(b) Rust on the ground anchor (rod type)

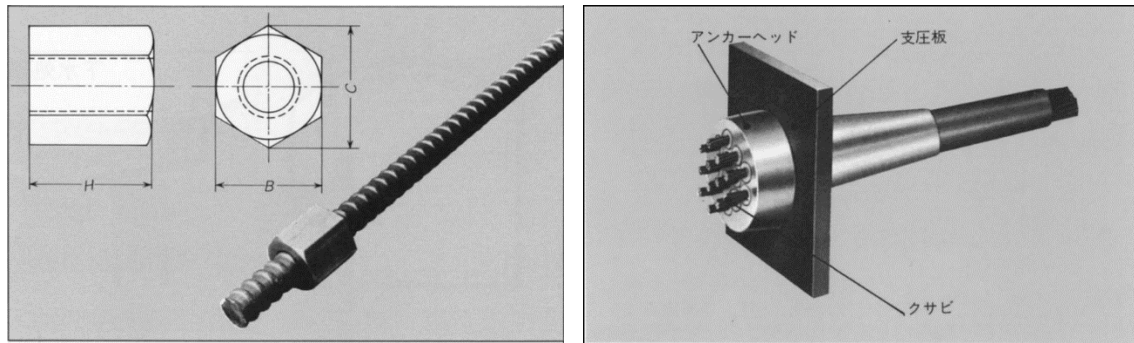


(c) No existing force in anchor



(d) Crack on the concrete

Figure 1.2 Example of deterioration of ground anchors



(a) Rod type anchor

(b) Strand type anchor

Figure 1.3 Type of ground anchor

In order to analyze the life span of ground anchors, it can be divided into three types of experiment consisting of Visual Inspection test, Lift-off test and Ultrasonic test. Three types of testing quite different results that Visual Inspection test results showed as the raking rate, the Lift-off test results provided direct force as well as a force-deformation curve and the Ultrasonic test results showed amplitude and voltage.

The Visual inspection test results are provided by one of the Japanese expressway companies (hereafter called “the road administrator”), and the condition states of ground anchor are categorized into six ratings as tabulated in Table 1.1. The degrees of deterioration conditions were classified as Excellent, Very good, Good, Fair, Marginal and Poor conditions corresponding to rank IV to rank I, respectively. Each rank of performance deterioration level of ground anchors is determined by the visual inspection from a surface of the ground anchor head and hammering test from the anchor head by the expert engineer from the road administrator (Kimoto et al, 2010).

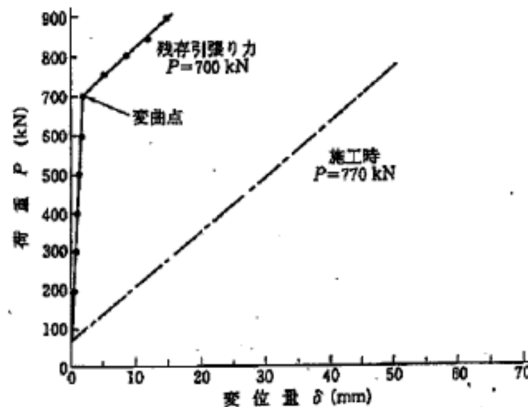
Table 1.1 Evaluation criterion of condition rating

Condition Rating	Physical Meaning
I	Poor condition: replacement required
II	Marginal condition: possible replacement required
III	Fair condition: repair required
IV	Good condition: possible minor maintenance/repair
V	Very good condition: no maintenance/repair needs
VI	Excellent condition: ground anchor is as new

The Lift-off test provided the existing force to verify the capability of ground anchors. It was adopted as the direct method to measure residual force as well as the abnormality of bonding and tendon portions. However, the cost of the lift-off testing is more expensive than the visual inspection test; moreover, the lift-off test is also difficult to test, because it takes longer time for setting up equipment and platform while the visual inspection test is an only observation on the head of ground anchor with a lightweight equipment. In contrast, life-off test will give more accuracy.



(a) Schematic of the Lift-off test



(b) Result of the Lift-off test

Figure 1.4 Type of ground anchor

Figure 1.4 (a) and (b) provided the schematic and the ideal result of the Lift-off test, respectively. According to the figure, the Lift-off test is very difficult to conduct because it takes time to set up the platform as well as testing by heavy equipment. The testing result

was plotted as the pull-out force, P as well as deformation, δ as illustrated in Fig 1.4 (b). The turning point is the remaining force of the anchor while the stiffness of the tendon and bonding portions can be described by mean of slope incline before and after yielding point, respectively.

The last method, Ultrasonic test was conducted on each ground anchor by means of wave to measure indirect force. The basic concept of this method is that the amplitude is a proportion increase with the remaining force of the tendon. The pros of this method such as detected flaws which undetected by the naked eye, quick and inexpensive. This method quite easier than the Lift-off test, however, the results still complicate to verify the exact force on ground anchor; the validation is required. Finally, it can be used to suggest the additional spot for Lift-off test, if the Ultrasonic results showed failure zone by considering indicator kriging results.

Table 1.2 Comparisons among pros and cons of three experiments

Type of Test	Visual Inspection test	Lift Off test	Ultrasonic test
Pros	<ul style="list-style-type: none"> • Easiest • Fastest • Cheapest • Preliminary reconnaissance • All anchor inspected • Quick results • Non hazardous waste 	<ul style="list-style-type: none"> • High accuracy • Measure T directly • Detect abnormality of Bonding portion/tendon • Stress-strain curve allow. • Non-destructive test 	<ul style="list-style-type: none"> • Easy • Quick • Inexpensive • Preliminary reconnaissance • Detect flaws which undetected by naked eye • All anchor inspected
Cons	<ul style="list-style-type: none"> • Based on expert inspector only, human error • Low accuracy • Cannot measure T • Cannot Detect abnormality of Bonding portion/tendon 	<ul style="list-style-type: none"> • Expensive • Time consumed • Difficult • Limited testing spot • Interpreted time req. • Hazardous waste (oil) • Heavy equipment req. 	<ul style="list-style-type: none"> • Unrecognized condition of bonding • Human error • irregular shape/ inhomogeneous are difficult to inspect • Cannot measure T directly

Three methods have different advantages and disadvantages, for instance; the Visual Inspection test is quite cheap, fast and easy to test. However, it is a very subjective result caused based only on the experience of the expert engineer without any calculation. On the

other hand, the Lift-off test might be better since it measured the remaining force directly, but it is too expensive and impossible to test on every anchor. In addition, the Ultrasonic test seems to be more appropriate, because it can obtain the existing force on every sample with inexpensive expense and can detect the flaws which undetected by the naked eye; however, it is a still indirect method hence validation is needed to verify. Both pros and cons of those experiments were tabulated in Table 1.2.

The methodology to analyze the deterioration process of slope improved by ground anchor can be evaluated by mean of survival probability considering with several statistic models, for example, Weibull hazard model, Markov chain model, Poisson process model, Normal and Log-normal distribution model, etc. Then, slope stability analysis was conducted as the index to classify the situation of individual slope. The conditional probability of failure was also employed to evaluate the risk of slope failure at the curtain time. Finally, this studied established maintenance strategies focussing on life cycle cost to evaluate the geotechnical infrastructure asset management on slope improved by ground anchors.

1.2 Research Objectives

The main objective of this study was to evaluate the present condition and maintenance decision on the risky slope which improved the stability by ground anchors. The specific purposes include:

- ◆ To acquire and identify the current situation of the slopes improved by ground anchors based on three testing methods, including the Visual inspection test, the Lift off test and the Ultrasonic test.
- ◆ To determine and compare on the failure probability results as well as the future prediction of the deterioration process by means of statistic approach, for example Weibull hazard model, Markov chain model, Poisson process model, Normal and Log-normal distribution, etc.
- ◆ To evaluate the stability and performance function of risk slopes at the present situation and future prediction, including the annual failure probability on each risky slope.
- ◆ To analyze the maintenance strategies associated with the Life Cycle Cost, *LCC* in

order to decision-making to maintenance on both the inspection interval and the experimental method.

1.3 Scope of the Research Study

The overall framework and scope of research study based on the risk evaluation of slope improved by ground anchor in Kansai district, Japan, which is caused by the deterioration process as presented in Fig 1.5. The dissertation consists of eight chapters, and comprehensive contents are introduced as follows:

- Chapter 1: general introduction of this research, the objectives and scope of the study
- Chapter 2: Reviewed the literatures related to this research study, including statistical approach such as Weibull model, Markov model and Weibull hazard model, three dimensions safety factor analysis, failure probability and life cycle cost.
- Chapter 3: Presented the methodology of this study, including the flow charts of calculation on three testing results, the procedure of stability analysis and the process of the evaluation on the life cycle cost.
- Chapter 4: The acquisition of the inspection results as well as the identify of current condition. In this chapter, three inspection results were illustrated in the current situation of the ground anchor.
- Chapter 5: Modeling of deterioration process and prediction of future condition. The statistic approach for determining the survival probabilities were calculated and compared to determine the appropriate model.
- Chapter 6: Investigation on stability and failure probability. This section demonstrated the results of stability analysis and performance function based on the Lift-off test. Note that, the Visual inspection result was abandoned because it cannot evaluate the existing force by this result.
- Chapter 7: Estimate of life cycle cost and decision making on maintenance. This chapter evaluated the maintenance strategies based on life cycle cost technique to establish the maintenance plan to repair/replace.
- Chapter 8: Conclusions of this research study and recommendations for future work.

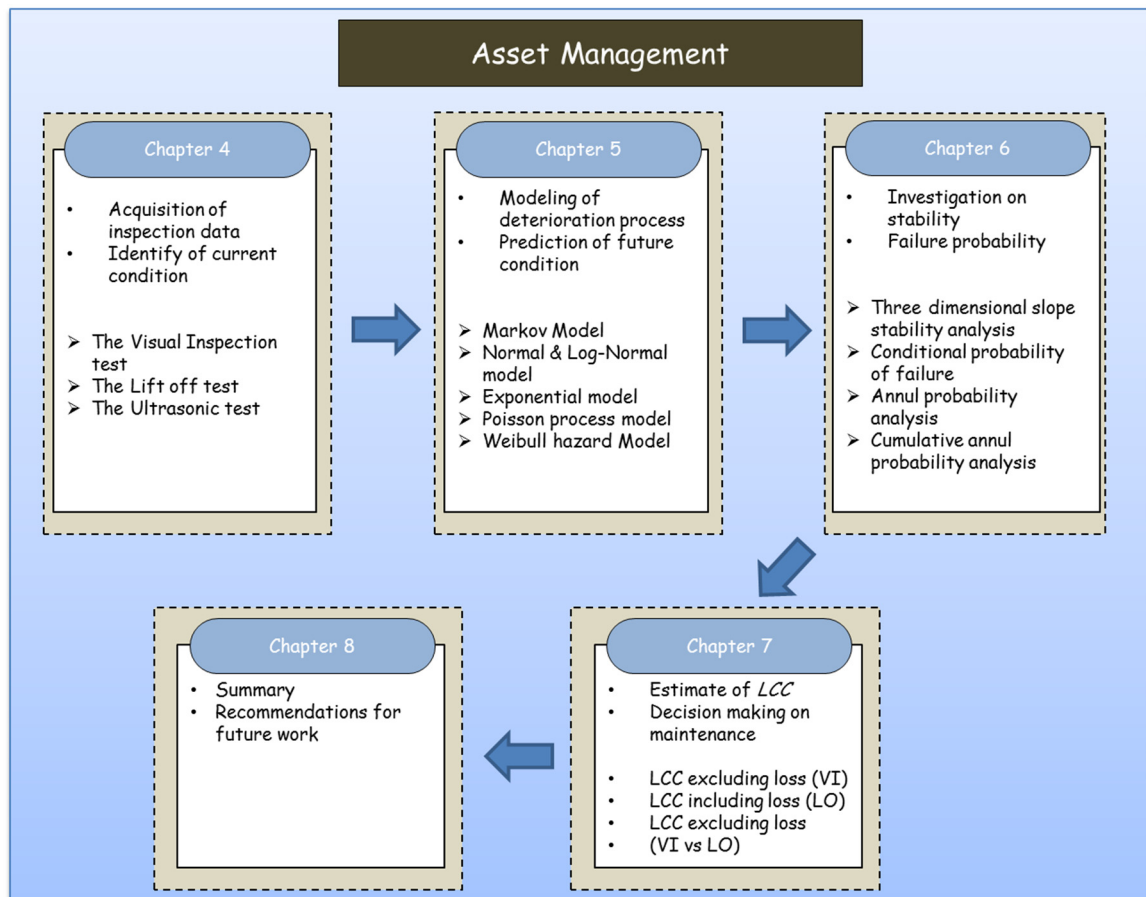


Figure 1.5 Scopes and framework of the study

CHAPTER 2

LITERATURE REVIEW

2.1 Introduction

Several studies were proposed focusing on prevention of embankment slope failure or slope stabilization along the highway slope recently. Numerous geotechnical engineering techniques, for example, reinforcement retaining wall, shotcrete, soil nail, cement column and ground anchors were adopted as the countermeasure on this matter. Particularly, ground anchors were served in order to stabilize both natural and man-cut slopes for road and dam construction, improve structural stability, control floating of structures caused by underground water, etc.

Fifty years since the first ground anchors were installed in Japan; the anchors have been employed for various purposes in at least 120,000 ground anchors of 30,000 projects. Some of them were constructed in early time, which have aged and deteriorated their performance, such as lost in pre-stresses load as well as some of them were overstress caused by deformation of slope, resulting in slope deformation and exposure of broken anchor heads (Miyatake et al, 2007).

Statically approaches such as Normal and Log-normal distribution functions, Markov model and Weibull distribution function were studied in order to predict life time of ground anchors by consider regarding the geological condition of road slopes where the ground anchor is installed. However, stability of slope not depending on only the deterioration of ground anchor, but also depending on weathering process of soil. Which means that strength parameters like cohesion, c and internal friction angle, ϕ of soil were also taken into an account.

In case of stability analysis, both statistical (performance function, Q) and mechanical (factor of safety, $F.S.$) methods were used as the index to estimate the stability of these slopes at the certain time. Both two and three dimensions were employed as well as both plan and circular failure pattern were also considered.

In terms of maintenance strategy, the life cycle cost, *LCC* was adopted as another index to evaluate the scenario plan for repair/renew the ground anchors as well as the life span of ground anchors.

2.2 Statistical Approach

Statistical approach is a method of analyzing or representing statistical data can be called that body of analytical and computational methods by which characteristics of a population are inferred through observations made in a representative sample from that population. This study considers five famous statistical methods which are Normal models, Log-Normal distribution function, Markov models, Poisson process model and Weibull distribution function to predict the lifespan of ground anchors by meaning of survival probability and failure probability with time. The briefs of each method are described below;

2.2.1 Normal distribution function

The normal distribution function is a continuous probability distribution that is the most widely known for the statistical methodology to approximate many natural phenomena. The normal distribution function is often used in the natural, social, sciences and engineering. This distribution function is the real-valued random variables. Moreover, it has severally developed into a standard of reference for many probability problems. The normal distribution is considered the most possible probability distribution in statistics.

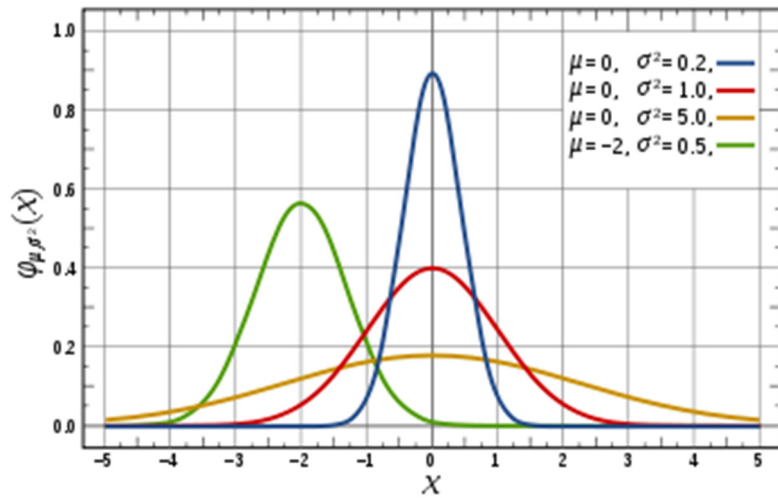
In probability theory, the normal (or Gaussian) distribution has a bell-shaped probability density function, known as the Gaussian function or informally the bell curve (Casella et al, 2001). The probability density function of the normal distribution is given as follow;

$$f(x) = \frac{1}{\sqrt{2\pi\sigma^2}} e^{-\frac{(x-\mu)^2}{2\sigma^2}} \quad (2.1)$$

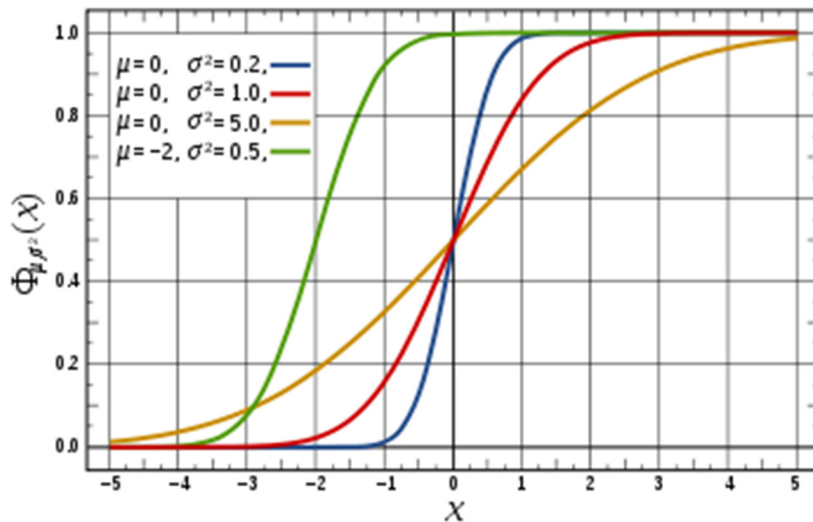
The cumulative distribution function of normal distribution is given as follow;

$$f(x) = \int_{-\infty}^{\infty} \frac{1}{\sqrt{2\pi\sigma^2}} e^{-\frac{(x-\mu)^2}{2\sigma^2}} \quad (2.2)$$

where parameter μ is the mean or expectation (location of the peak), σ^2 is the variance and σ is the standard deviation of the data.



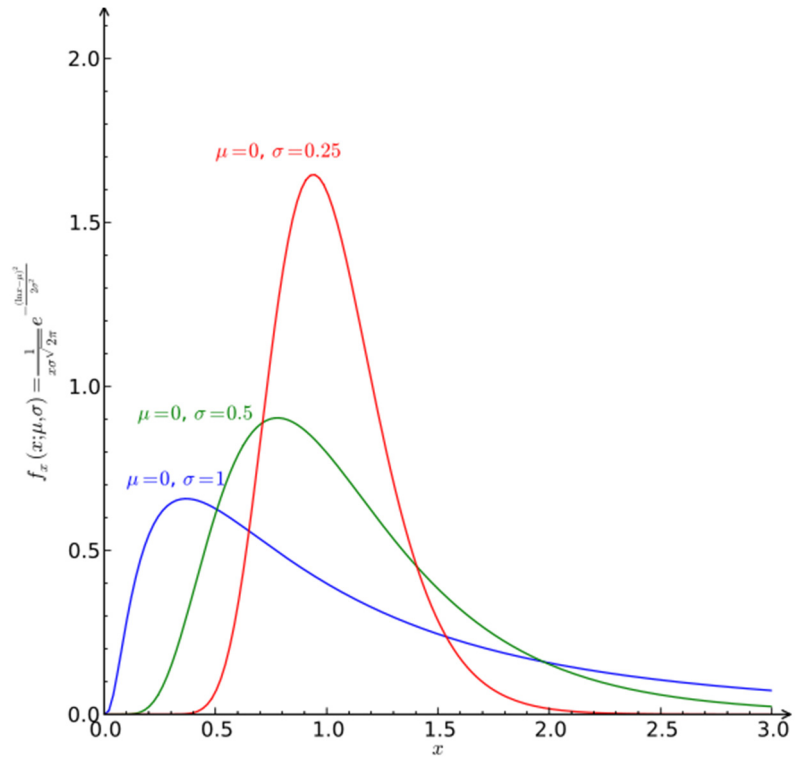
(a) Probability density function



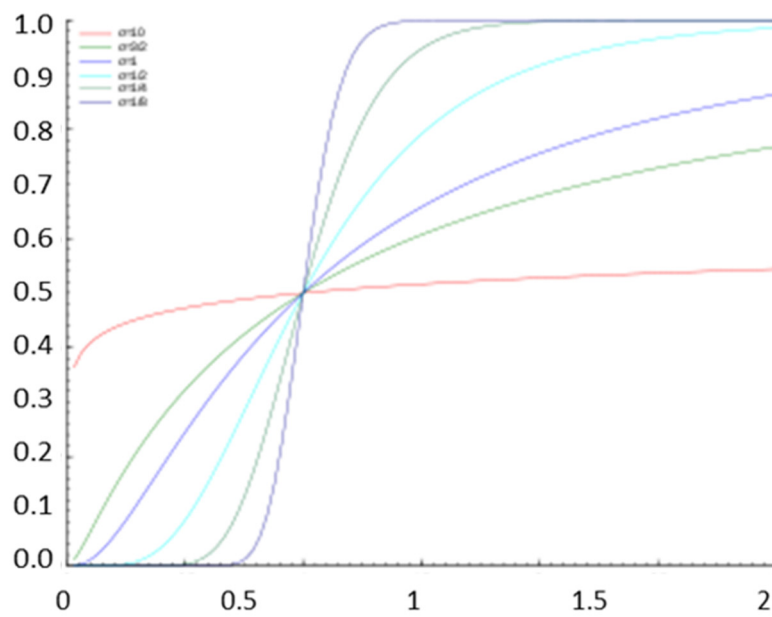
(b) Cumulative distribution function

Figure 2.1 Probability density function and cumulative distribution function of Normal distribution function (Casella et al, 2001).

Normal distribution function and Cumulative distribution function are illustrated in Fig. 2.1. It is symmetric around the mean value μ , which same as the mode, the median and the mean of the distribution, whereas σ illustrated how much variation exists from the average or expected value. A low σ shows that the data tend to be very close to the average, while high σ indicates that the data are spread out over a large range of average values.



(a) Probability density function



(b) Cumulative distribution function

Figure 2.2 Probability density function and cumulative distribution function of Log-normal distribution function (Casella et al, 2001).

2.2.2 Log-normal distribution function

The log-normal distribution function is a continuous probability distribution function of a random variable which is similar to the normal distribution functions; however the log-normal distribution function does not contain the non-negative value. The log-normal distribution is occasionally referred to as the Galton's distribution.

The probability density function of a log-normal distribution is;

$$f(x) = \frac{1}{x\sigma\sqrt{2\pi}} e^{-\frac{(\ln x - \mu)^2}{2\sigma^2}}, x > 0 \quad (2.3)$$

The cumulative distribution function is;

$$f(x) = \frac{1}{2} \operatorname{erfc} \left[-\frac{\ln x - \mu}{\sigma\sqrt{2}} \right] = \Phi \left[-\frac{\ln x - \mu}{\sigma} \right] \quad (2.4)$$

Where erfc is the complementary error function, and Φ is the cumulative distribution function of the standard normal distribution. The probability and cumulative distribution function are illustrated in Fig. 2.2

2.2.3 Markov chain model

The Markov chain is a stochastic process with the Markov property. The Markov process was characterized as memory-less or discrete (discrete-time) random process. The next condition depends only upon the current condition and not on the sequence of events that preceded it. The Markov chain model is a sequence of random variables x_1, x_2, x_3, \dots with the Markov property given the present condition; the future and past conditions are independent.

In general formula, the Markov chain model can be expressed as follows;

$$P(X_{t+1} = i_{t+1} | X_0 = i_0, X_1 = i_1, \dots, X_t = i_t) = P(X_{t+1} = i_{t+1} | X_t = i_t) \quad (2.5)$$

Where i is the conditional state at time t , P is the conditional probability of any future condition given present and past conditions (Kimoto, 2011). The general formulation to calculate the Markov process as follows;

$$S(\tau) = S(0) \cdot T^\tau \quad (2.6)$$

In which

$$T = \begin{bmatrix} T_{nn} & T_{nn-1} & \cdots & T_{n1} \\ T_{n-1n} & T_{n-1n-1} & \cdots & T_{n-11} \\ \vdots & \vdots & \ddots & \vdots \\ T_{1n} & T_{1n-1} & \cdots & T_{11} \end{bmatrix} \quad (2.7)$$

Where $S(\tau)$ is the condition of the system at time τ and $S(0)$ is the initial stage of the system

In this study, the Markov model is used to calculate the deterioration process of ground anchor's performance by defining discrete condition states and accumulating the probability of transition from one condition to another over multiple discrete time intervals. Based on the assumption of the Markov chain, the transition probability matrix can be depicted in Fig.2.3. The higher state allows to change state to lower rank while impossible to transit to upper state.

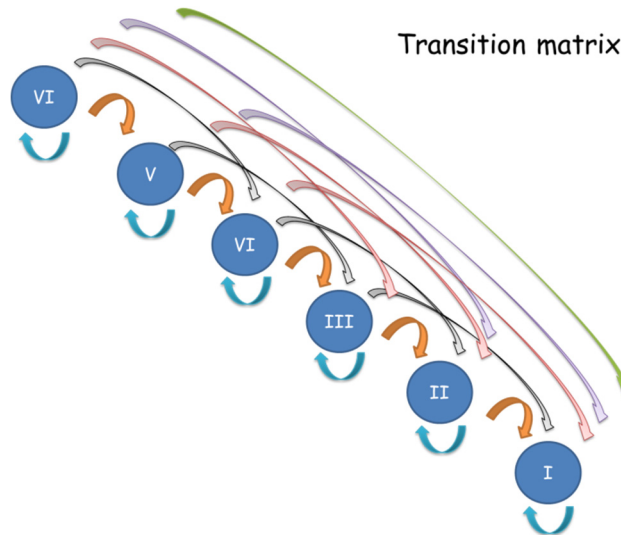


Figure 2.3 Six-state Markov chain model

The assumption of determination of the deterioration process by the Markov chain should be, firstly, clarified by neglecting some conflicts, which are (Kimoto et al, 2011 and Ohtsu, 2011);

- All ground anchors are assumed to have same deteriorating nature.
- The transition matrix of each ground anchor is set up for one year incensement in interval time.
- The Markovian deterioration of ground anchor is assumed to be homogeneous discrete Markov process through its life time.

Based on the assumptions described above, considering the condition ratings, the state of the system at time t is presented by a number of observed ground anchors corresponding to each condition rating as shown below;

$$S(t) = [S_{VI} \quad S_V \quad S_{IV} \quad S_{III} \quad S_{II} \quad S_I] \quad (2.8)$$

In this study, the transition probability matrix can be divided into three methods. However, the basic concept for calculation the Markov process is same. The difference of these three methods is that only in the transition probability matrix which are;

1. The original method: the basic assumption that ground anchor can transform the state forward (i to $i+1, i+2, \dots, J$) as well as still in a current state (still in i state). This method allows the ground anchors can be transferred from the excellent condition (rank VI) to the poor condition (rank I) within one time step (in this study is one year) or another word, this method implied that deterioration might be skipped to another condition more than one state forward. Figure 2.4 illustrates the meaning for the transition matrix for original method, which is the upper triangular matrix type (only all entries below the main diagonal are zero. The transition matrix of the original method shown in Eq. below;

$$T = \begin{bmatrix} T_{VI,VI} & T_{VI,V} & T_{VI,IV} & T_{VI,III} & T_{VI,II} & T_{VI,I} \\ 0 & T_{V,V} & T_{V,IV} & T_{V,III} & T_{V,II} & T_{V,I} \\ 0 & 0 & T_{IV,IV} & T_{IV,III} & T_{IV,II} & T_{IV,I} \\ 0 & 0 & 0 & T_{III,III} & T_{III,II} & T_{III,I} \\ 0 & 0 & 0 & 0 & T_{II,II} & T_{II,I} \\ 0 & 0 & 0 & 0 & 0 & T_{I,I} \end{bmatrix} \quad (2.9)$$

2. The simplify method: the basic assumption is quite similar to the original method; however, it can only transform one state forward (i to $i+1$) and without transformation, still in a current state (still in i state) as illustrated in Eq. (2.10). Figure 2.5 shows the meanings

of transition matrix for simplify method that is the square matrix which is close to diagonal matrix type.

$$T = \begin{bmatrix} T_{VI,VI} & T_{VI,V} & 0 & 0 & 0 & 0 \\ 0 & T_{V,V} & T_{V,IV} & 0 & 0 & 0 \\ 0 & 0 & T_{IV,IV} & T_{IV,III} & 0 & 0 \\ 0 & 0 & 0 & T_{III,III} & T_{III,II} & 0 \\ 0 & 0 & 0 & 0 & T_{II,II} & T_{II,I} \\ 0 & 0 & 0 & 0 & 0 & T_{I,I} \end{bmatrix} \quad (2.10)$$

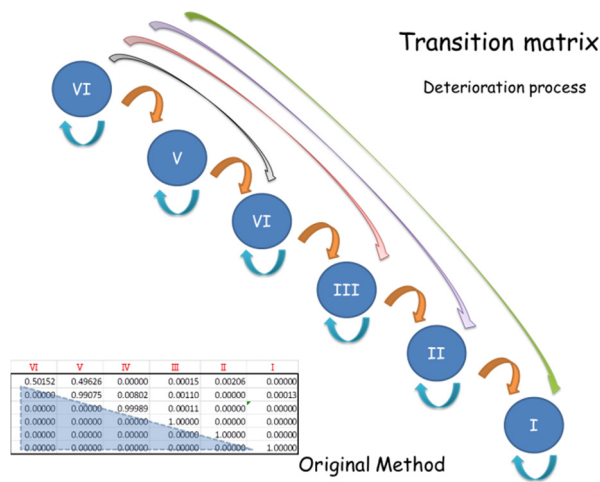


Figure 2.4 Transition matrixes for Markov original method

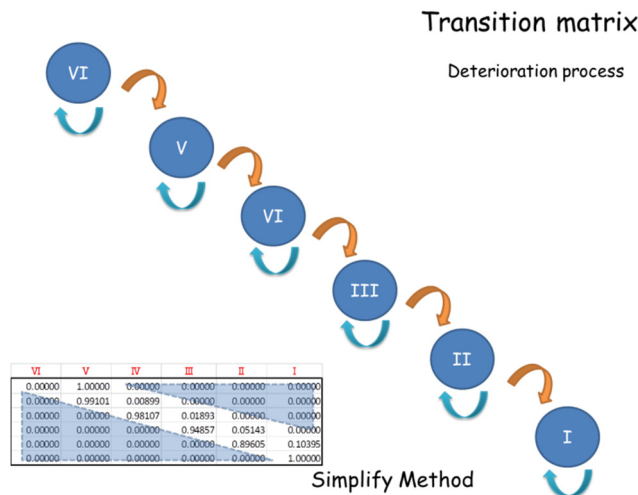


Figure 2.5 Transition matrixes for Markov simplify method

3. The Markov hazard model: this model was proposed by Tsuda et al (2006) has a wide range of application in various infrastructure systems. This model is also one branch of the

Markov model that based on the assumption of the exponential distribution. Process for calculation of this model for transition matrix quite different from the both methods mentioned above; however, after that is the same calculation process. The general expressions of the Markov hazard mode are;

$$P[h(y_B) = i | h(y_A) = i] = \exp(-\theta_i Z) \quad (2.11)$$

Where Z expresses the interval between two inspection times, θ is the hazard rate of the i state. Kaito (2009) and Thanh (2009) proposed the hazard rates depended on traffic volume as well as slab area; however, in this study; the hazard rates were assumed to be the unknown parameters, β , as describe in in Eq. (2.12),

$$\theta_i = \beta_i \quad (2.12)$$

The transition matrix of the Markov hazard model can be described as follows;

$$\pi_{ij} = P[h(y_B) = i | h(y_A) = j] \quad (2.13)$$

$$\pi_{ij} = \sum_{k=i}^j \prod_{m=i}^{k-1} \frac{\theta_m}{\theta_m - \theta_k} \prod_{m=i}^{k-1} \frac{\theta_m}{\theta_{m+1} - \theta_k} \exp(-\theta_i Z) \quad (2.14)$$

$$T = \begin{bmatrix} \pi_{VI,VI} & \pi_{VI,V} & \pi_{VI,IV} & \pi_{VI,III} & \pi_{VI,II} & \pi_{VI,I} \\ 0 & \pi_{V,V} & \pi_{V,IV} & \pi_{V,III} & \pi_{V,II} & \pi_{V,I} \\ 0 & 0 & \pi_{IV,IV} & \pi_{IV,III} & \pi_{IV,II} & \pi_{IV,I} \\ 0 & 0 & 0 & \pi_{III,III} & \pi_{III,II} & \pi_{III,I} \\ 0 & 0 & 0 & 0 & \pi_{II,II} & \pi_{II,I} \\ 0 & 0 & 0 & 0 & 0 & \pi_{I,I} \end{bmatrix} \quad (2.15)$$

For convenient to calculate, the general forms of Markov transition probabilities are given in the following simplify equations which are;

$$\pi_{ii} = \exp(-\theta_i Z) \quad (2.16)$$

$$\pi_{ii+1} = \frac{\theta_i}{\theta_i - \theta_{i+1}} \{ \exp(-\theta_i Z) + \exp(-\theta_{i+1} Z) \} \quad (2.17)$$

$$\pi_{ij} = \sum_{k=i}^j \prod_{m=i}^{k-1} \frac{\theta_m}{\theta_m - \theta_k} \prod_{m=i}^{k-1} \frac{\theta_m}{\theta_{m+1} - \theta_k} \exp(-\theta_i Z) \quad (2.18)$$

$$\pi_{iJ} = 1 - \sum_{j=i}^{J-1} \pi_{ij} \quad (2.19)$$

where

$$i = 1, \dots, J-1$$

$$j = i, \dots, J$$

In addition, the well know commercial software, namely *MS excel* was used to calculate the Markov hazard transition matrix as shown in Fig 2.6 following Eq (2.16) to (19), respectively.

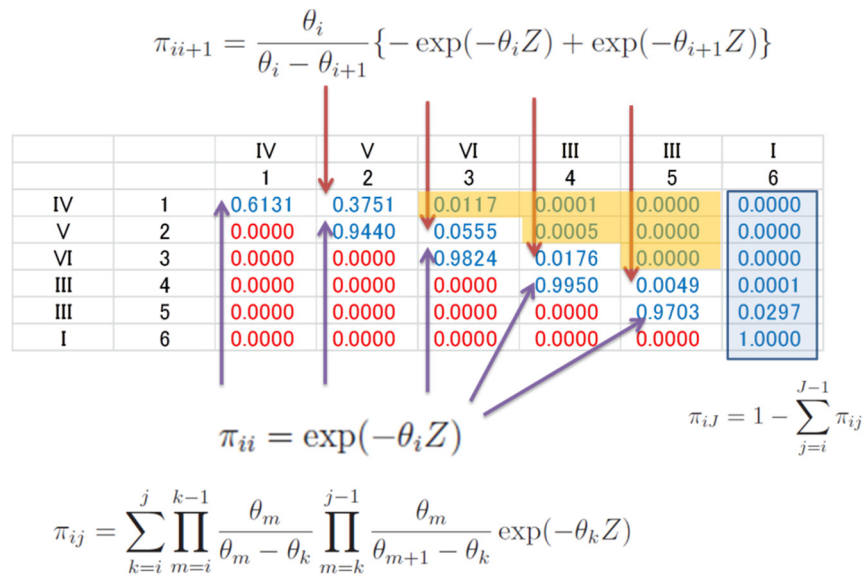


Figure 2.6 Markov hazard transition matrix calculated by MS excel

Finally, the transition probability matrix of three methods can be calculated by a trial and error method in order to obtain the appropriate matrix by using *Solver* in *MS excel* worksheet. The *Solver* is part of a suite of commands sometimes called what-if analysis, a process of changing the values in cells to see how those changes affect the outcome of formulas on the worksheet. The difference between observation and simulation value were compared by minimizing those values.

2.2.4 Weibull hazard model

The Weibull hazard model is a method for modeling data sets containing values greater than zero, for example, failure data of produce in the factories. The Weibull analysis can make predictions about a product's life, compare the reliability of competing product designs, statistically establish warranty policies or proactively manage spare parts. In General form, survival probability, $\tilde{F}_i(t)$ can express as follows;

$$\tilde{F}_i(t) = 1 - F_i(t) \quad (2.20)$$

Where $F_i(t)$ represents the cumulative probability of transition in the condition state

The conditional probability that the condition state of a component at time t advances from t to $t+1$ during time interval $[t, t + \Delta t]$ is defined as;

$$\lambda_i(t)\Delta t = \frac{f_i(t)\Delta t}{\tilde{F}_i(t)} \quad (2.21)$$

Where the probability density $\lambda_i(t)$ is referred as the hazard function, therefore;

$$\frac{d\tilde{F}_i(t)}{dt} = -f_i(t) \quad (2.22)$$

Eq. (2.21) then became.

$$\begin{aligned} \lambda_i(t) &= \frac{f_i(t)}{\tilde{F}_i(t)} = -\frac{\frac{d\tilde{F}_i(t)}{dt}}{\tilde{F}_i(t)} \\ &= \frac{d}{dt} \left(-\log \tilde{F}_i(t) \right) \end{aligned} \quad (2.23)$$

Considering that $\tilde{F}_i(0) = 1 - F_i(0) = 1$, and by integrating Eq. (2.20), we obtained;

$$\tilde{F}_i(t) = \exp \left[- \int_0^t \lambda_i(u) du \right] \quad (2.24)$$

The Weibull hazard function, $\lambda_i(t)$ can be obtained by the following equation..

$$\lambda_i(t) = \theta_i m t^{m-1} \quad (2.25)$$

Where θ_i and m are hazard rate and the Weibull shape parameter, respectively.

Probability density function, $f_i(t)$ and Survival probability, $\tilde{F}_i(t)$ can be expressed:

$$f_i(t) = \theta_i m t^{m-1} \exp(-\theta_i t^m) \quad (2.26)$$

$$\tilde{F}_i(t) = \exp(-\theta_i t^m) \quad (2.27)$$

where

$m < 1$ indicated a failure rate that decreases with time, “early-life failures”

m close to 1 indicated a fairly constant failure rate, “useful life or random failures”

$m > 1$ indicated a failure rate that increases with time, also known as wear-out failures

Figure 2.7 demonstrates the effect of m value on the failure rate of the Weibull hazard model. The high failure rate was found in the early stage sometime call infant failure, then the failure rate decreases continuously to the useful life that mostly seem to be constant. Finally, the failure rate increased drastically in the last, which call wear-out failure.

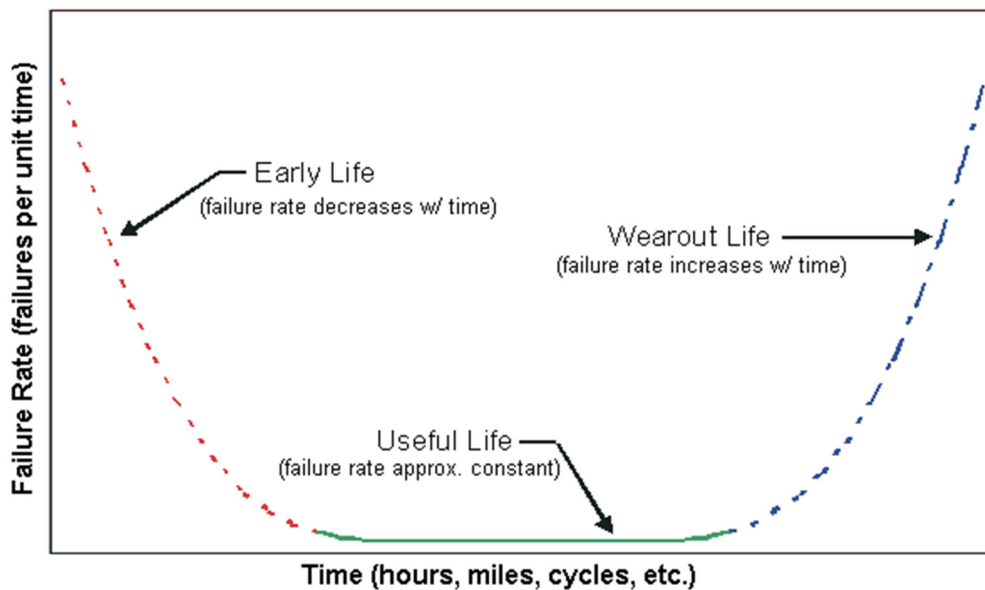


Figure 2.7 The effect of m on failure rate of Weibull hazard model

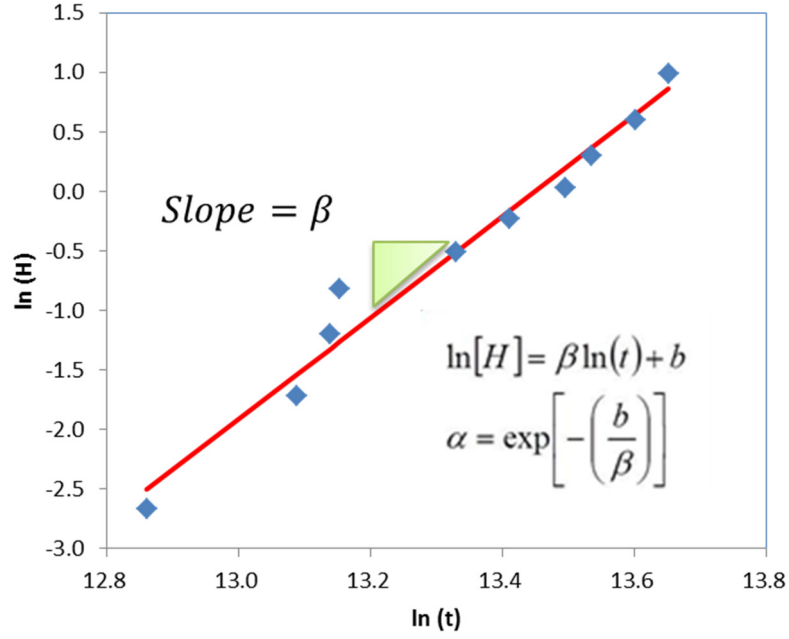


Figure 2.8 The regression curve for calculation parameters of the Weibull Hazard model

For convenient, the Weibull parameters are simply given in the following equation;

$$m = \beta \quad (2.28)$$

$$\theta = \frac{1}{\alpha^\beta} \quad (2.29)$$

In this case, H which is the cumulative hazard rate is expressed as follows;

$$H = \int_0^t \lambda_i(u) du = \theta_i t^m = \left(\frac{t}{\alpha}\right)^\beta \quad (2.30)$$

Take the natural logarithm of both sides, the Equation can be described as follows;

$$\begin{aligned} \ln[H] &= \beta \ln\left(\frac{t}{\alpha}\right) \\ &= \beta \ln t - \beta \ln \alpha \end{aligned} \quad (2.31)$$

Finally, it can be expressed in terms of linear equation as illustrated in Fig. 2.8, the slope of the line became β parameter and α can be calculated by using as following;

$$\alpha = \exp\left[-\frac{b}{\beta}\right] \quad (2.32)$$

To analyze failure probability and survival probability based on the Weibull hazard function, they can be calculated as follows:

$$f(t, \alpha, \beta) = \frac{\beta}{\alpha^\beta} t^{\beta-1} e^{-\left(\frac{t}{\alpha}\right)^\beta} \quad (2.33)$$

$$\tilde{F}(t, \alpha, \beta) = e^{-\left(\frac{t}{\alpha}\right)^\beta} \quad (2.34)$$

2.2.5 Poisson process model

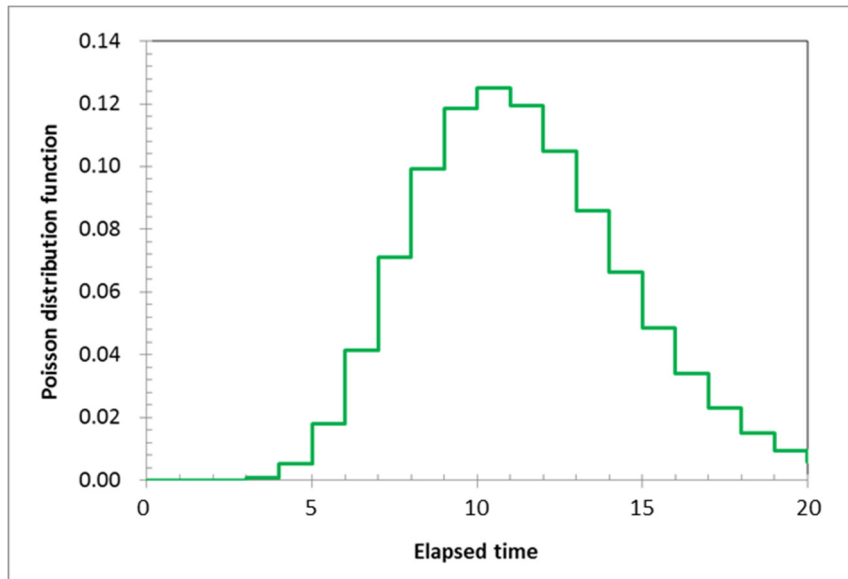
The Poisson process is a stochastic process which counts the number of events, and the time that these events occur in a given time interval. The time between each pair of consecutive events has an exponential distribution with a failure rate, λ and each of these inter-arrival times are assumed to be independent of other inter-arrival times. The Poisson process is a continuous-time process; the sum of a Bernoulli process can be thought of as its discrete-time counterpart. A Poisson process is a pure-birth process, the simplest example of a birth-death process. It is also a point process on the really half-line (Wikipedia, 2013).

The basic form of the Poisson process is a continuous-time counting process $\{N(t), t \geq 0\}$ that possesses the following properties;

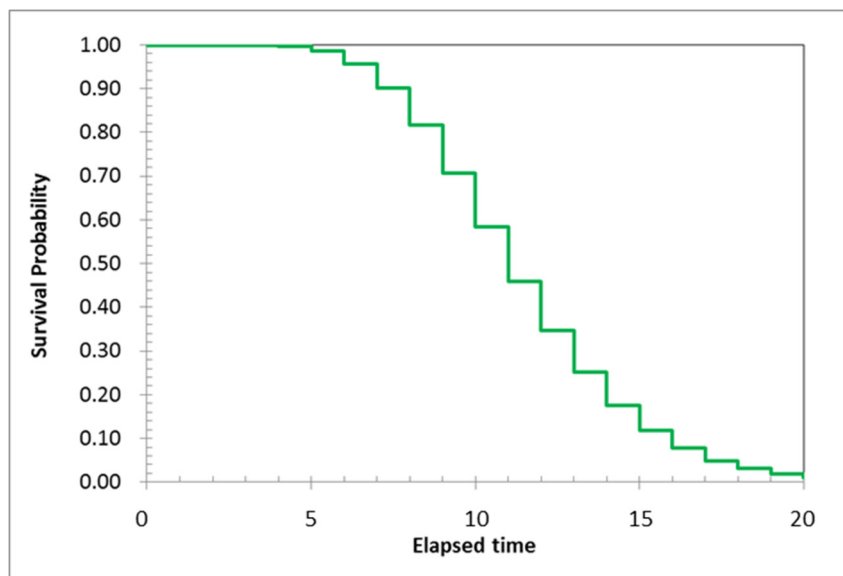
- $N(0) = 0$
- Independent increments (the numbers of occurrences counted in disjoint intervals are independent of each other)
- Stationary increments (the probability distribution of the number of occurrences counted in any time interval only depends on the length of the interval)
- The probability distribution of $N(t)$ is a Poisson distribution
- No counted occurrences are simultaneous.

Consequences of this definition include;

- The probability distribution of the waiting time until the next occurrence is an exponential distribution.
- The occurrences are distributed uniformly on any interval of time. (Note that $N(t)$, the total number of occurrences, has a Poisson distribution over $(0, t)$, whereas the location of an individual occurrence on $t \in (a, b)$ is uniform.)



(a) Probability density function



(b) Cumulative distribution function

Figure 2.9 Probability density function and cumulative distribution function of Poisson process model

This process is characterized by a failure rate, λ also known as intensity, such that the number of events in the time interval $(t, t + \tau]$ follows a Poisson distribution function with an associated failure rate parameter, λt as illustrated in Fig 2.9 (a). This relation is given as;

$$P[(N(t + \tau) - N(t)) = k] = \frac{e^{-\lambda t} (\lambda t)^k}{k!} \quad k = 0, 1, \dots, \quad (2.35)$$

This cumulative distribution function of the Poisson process was shown in Fig 2.9 (b) can be expressed as follows;

$$\sum_{i=0}^k P[(N(t + \tau) - N(t)) = i] = \sum_{i=0}^k \frac{e^{-\lambda t} (\lambda t)^i}{i!} \quad k = 0, 1, \dots, \quad (2.36)$$

2.2.6 Exponential distribution function

The exponential distribution is the continuous probability distribution described the time between events in a Poisson process as mentioned in section 2.2.5. In addition, to be used for the analysis of Poisson processes, it is found in various other contexts.

The probability density function of an exponential distribution is;

$$f(x, \lambda) = \begin{cases} \lambda e^{-\lambda x} & x \geq 0 \\ 0 & x < 0 \end{cases} \quad (2.37)$$

The cumulative distribution function is given by;

$$F(x, \lambda) = \begin{cases} 1 - e^{-\lambda x} & x \geq 0 \\ 0 & x < 0 \end{cases} \quad (2.38)$$

Where

λ is the failure rate that can be expressed as;

$$\text{Failure Rate, } \lambda = \frac{r}{\sum t + (n - r)T} \quad (2.39)$$

$$\text{Mean Time to Failure, } \theta = \frac{1}{\lambda} \quad (2.40)$$

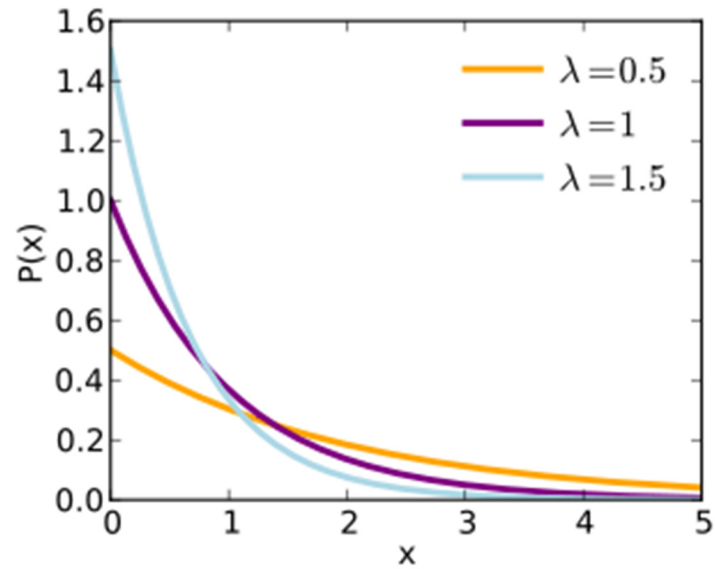
Where

r = No. of failure data

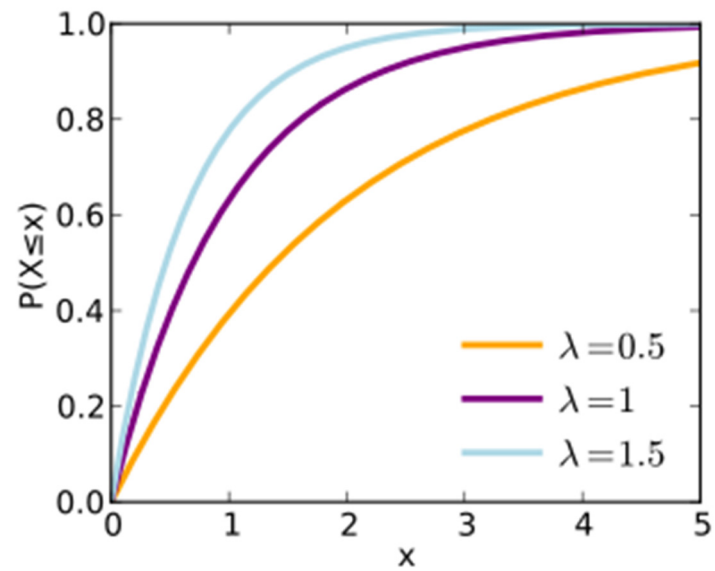
t = time at failure of each failure data

n = No. of total data

T = total time to test



(a) Probability density function



(b) Cumulative distribution function

Figure 2.10 Probability density function and cumulative distribution function of Exponential distribution function

The exponential distribution model is also famous for calculating the reliability curve to predict the deterioration rate of the system. In this study, this model is the one of the several models which used to compare the appropriate with another model. The probability density and cumulative density functions demonstrated in Fig 2.10 (a) and (b), respectively.

2.3 Deterioration Process of Cohesion

Otani et al (2004) studied on the deterioration rate of cohesion in improved slopes by a shortcrete in rock slopes based on observed data of several projects in by the Japan Highway administration. These slopes have more than thirty years in service, in addition; some of them illustrated some creaking and bulging obviously. In these projects, durability of shortcrete slopes is evaluated and established the standard for maintenance. The deterioration of cohesion as well as depth of weathering was calculated by considering the elastic wave velocity obtained by field survey for several years.

The recession coefficient of cohesion K_c was calculated following Fig2.11. For the initial cohesion, C_0 is measured by unconfined compressive strength test in laboratory test. The cohesion at time t was calculated by following Eq.;

$$C_r = 1 - \left(\frac{Vp}{Vp_0} \right)^2 \quad (2.41)$$

$$C = K_c \cdot C_0 \quad (2.42)$$

Where

C_r is fissure coefficient

Vp is elastic wave velocity of ground (m/s)

Vp_0 is velocity of ultrasonic pulse (m/s)

K_c is recession coefficient of cohesion,

C_0 is initial cohesion

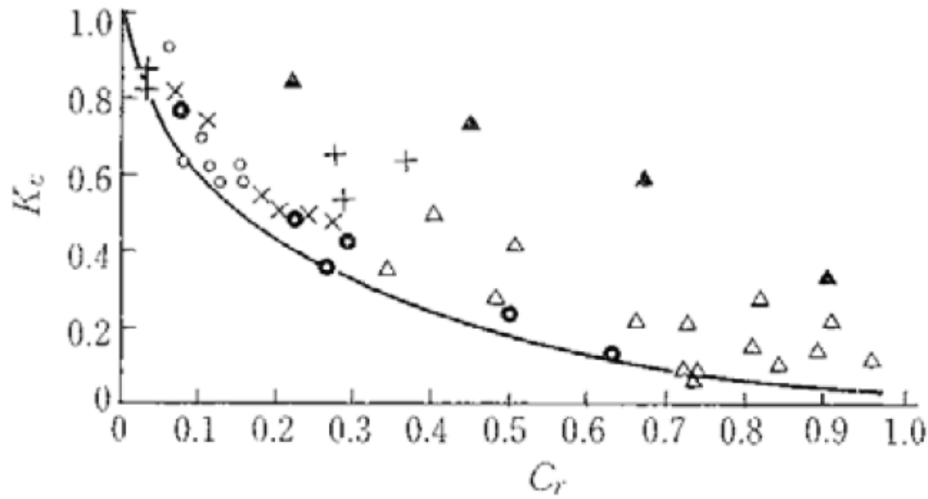


Figure 2.11 Relationship between K_c and C_r after Otani et al (2004)

Finally, calculate the trend line of cohesion deterioration rate by dealing with regression of the exponential model as demonstrated in one case study in the Fig 2.12. Figure 2.13 illustrates random path of the decrease of cohesion. It can be divided into three categories that random path whose initial value is the mean (black line), the random path whose initial is from 95% upper confidence interval (gray line) and the random path whose initial is from 95% lower confidence interval (dotted line). Generally, the drift rate of deterioration change after time gone by. Note that, the deterioration rate of internal friction angle, ϕ was neglected in this study because its quite an insignificant reduction comparing with cohesion or other word the internal friction angle, ϕ was assumed to be constant.

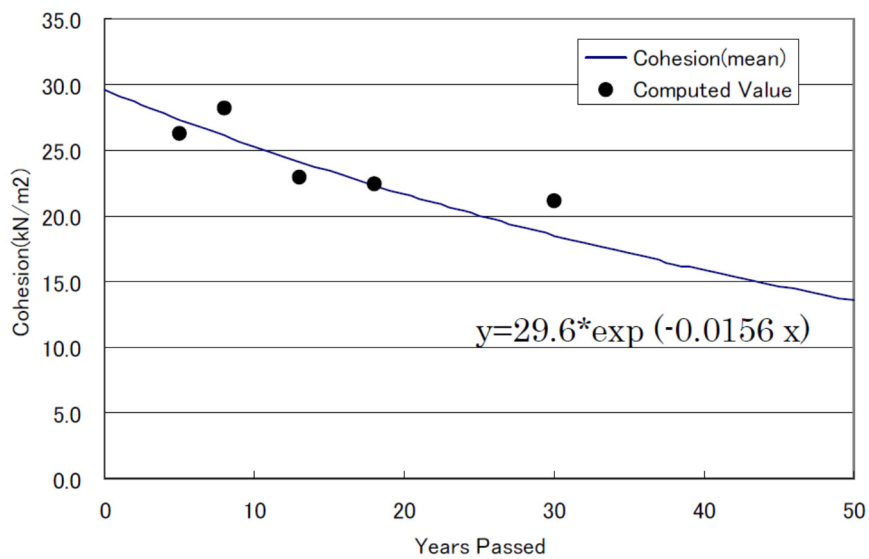


Figure 2.12 Deterioration curve of cohesion after Otani et al (2004)

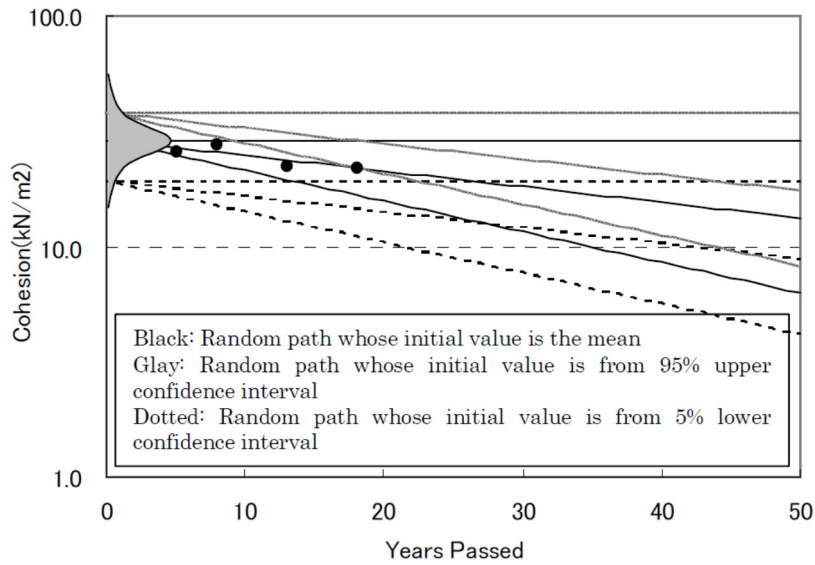


Figure 2.13 Random path of decrease of cohesion after Otani et al (2004)

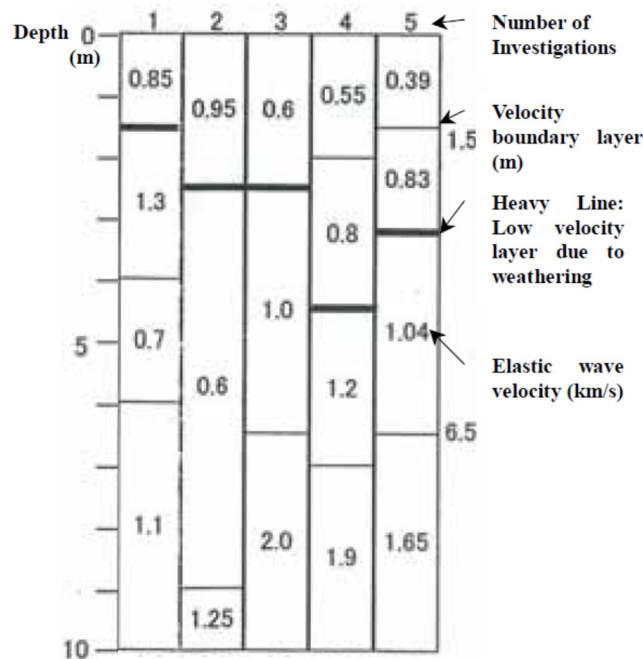


Figure 2.14 Random path of decrease of cohesion after Ohtsu et al (2004)

In case of depth of weathering layer also studied by Otani et al (2004). However, the depth of weathering is varying from 1.5m to 4.5m depending on the slopes. The methodology to evaluate the weathering depths is assumed by considering the boundary of low velocity layers obtained by an elastic wave from seismic prospecting. Figure 2.14 shows an

example result of the low velocity layers range, which indicated the chronological weathering zone as shown in the heavy line. Moreover, it is also indicated that the weathering layer thickness trend to increases with the number of inspections as illustrated in the horizontal axis. It seems to be apparently seen that inadequate number of borehole, the results weathering depth is inappropriate as well as low accuracy comparing with a high number of investigations.

2.4 Slope Stability Analysis

Slope stability analysis is performed to assess the safe design of a human-made or natural slope and the equilibrium conditions, for example, slope along the highway, borrow pit and deep excavation. Generally, slope stability is often used in geotechnical engineering field for describing slope condition, whether stable or not by mean of the factor of safety.

Factor of safety is a term describing the structural capacity of a system beyond the expected loads or actual loads. It can express as the proportional of resisting force/moment over the acting force/moment. The resisting force/moment represents strength or capacity of its material, whereas the acting force/moment is the design load and/or self-weight of material that attempt to act the structure to collapse.

In geotechnical engineering, factor of safety indicated the stability of slopes that can be divided into two major categories of calculation methods, which are limit equilibrium and numerical simulation method. The idea of the limit equilibrium method is to discretion a potential sliding mass into small vertical slices, then determine the proportion of moment or force equilibrium of each slice. Finally, cumulate the moment or force equilibrium proportion of all slices to be the safety factor. However, it does not consider strain and displacement compatibility.

The factor of safety evaluated by the limit equilibrium method can be expressed in the simplified equation form as follows;

$$FS = \frac{\text{Resisting force} + \text{Anchor (force/moment)}}{\text{Driving (force/moment)}} \quad (2.43)$$

For the numerical simulation method both total shear resistance and the total mobilized

shear stress on a slip surface can be computed and used to determine the factor of safety. The factor of safety based on the numerical simulation method can express in the simplified form as follows;

$$FS = \frac{\text{Initial strength of soil}}{\text{Strength at Failure}} \quad (2.44)$$

However, this method quite complicated because it needed more geotechnical parameters than limit equilibrium method such as elasticity, Poisson ratio and so on which difficult to determine. Therefore, the limit equilibrium was only employed to study.

The Limit equilibrium method was introduced early in the 20th century. In 1916, Petterson (1955) presented the methodology for evaluates the factor of safety by dividing the sliding mass into several slices for slope in Stigberg Quay in Gothenberg, Sweden. The next couple of decades, Fellenius (1936) introduced the Ordinary or Swedish method of slices (Krahn, 2002). Several advance methods for limit equilibrium were developed; for instant, Janbu (1954), Bishop (1955), Morgenstern and Price (1965) and Spencer (1967) that most of them look similar, however, different in the detail of the calculation. Figure 2.15 illustrates schematic diagrams of slice and force in sliding masses (Krahn, 2002) and Table 2.1 lists the statics satisfied and inter-slice forces in various methods.

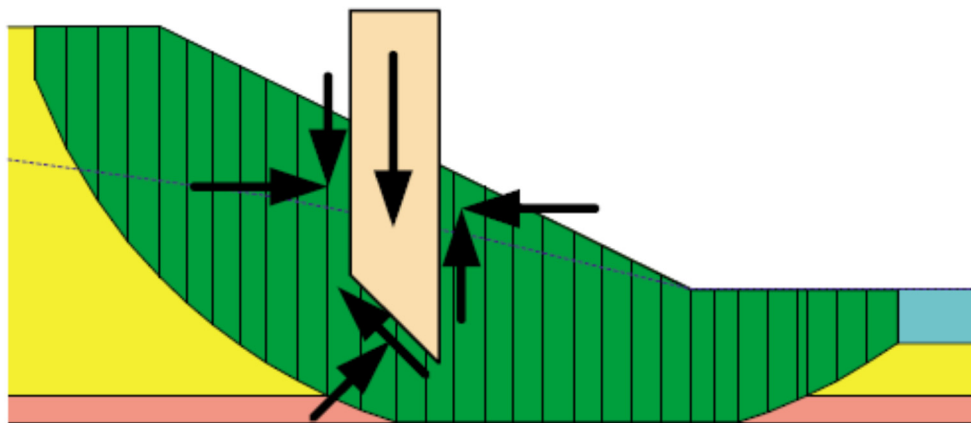


Figure 2.15 Slices and forces in a sliding mass (Krahn, 2002)

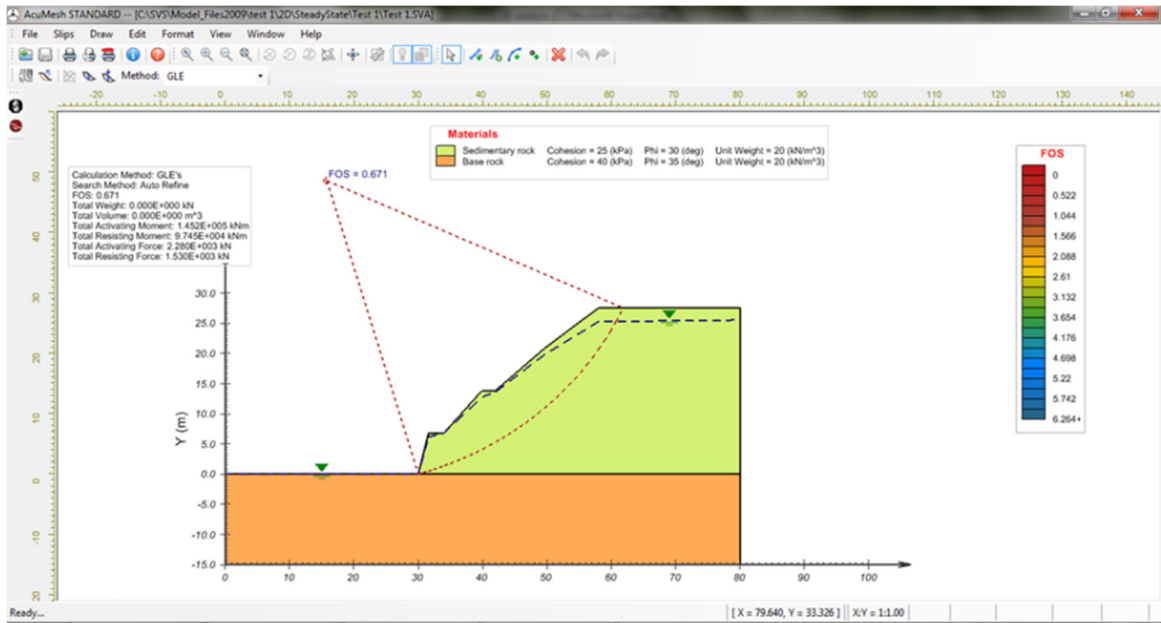
Table 2.1. Statics satisfied and interslice forces in various methods (Krahn, 2002)

Method	Moment equilibrium	Horizontal force equilibrium	Interslice normal (E)	Interslice shear (X)
Ordinary or Fellenius	Yes	No	No	No
Bishop's simplified	Yes	No	Yes	No
Janbu's simplified	No	Yes	Yes	No
Spencer	Yes	Yes	Yes	Yes
Morgenstern-Price	Yes	Yes	Yes	Yes
Corps of Engineers – 1	No	Yes	Yes	Yes
Corps of Engineers – 2	No	Yes	Yes	Yes
Lowe-Karafiath	No	Yes	Yes	Yes

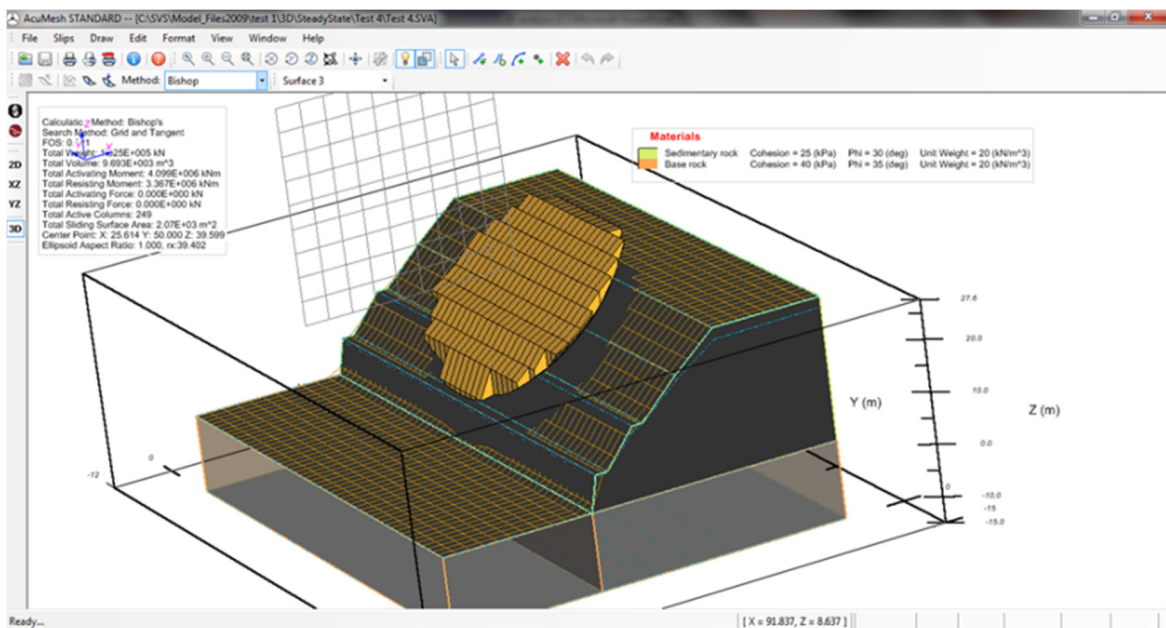
In this paper, the ordinary or Fellenius's method was used to evaluate three dimensional safety factor due to simplicity, which neglects the horizontal force in between slices. However, the results of F.S. are not obvious difference comparing with the others. The ordinary or Fellenius's method can be described as follows;

$$F.S. = \frac{\sum cb_i + (w_i \cos \theta_i - u_i b_i) \tan \phi + \sum T_j \cos \theta_j \tan \phi + \sum T_j \sin \theta_j}{\sum w_i \sin \theta_i} \quad (2.45)$$

The commercial software, namely *SV slope* which developed by *Soil Vision Systems Ltd.* was introduced to evaluate the safety factor. Note that, the three-dimensional model was conducted in this study. The reason is it seems to be more suitable than two dimensions model because slope does not the plane strain problem. Moreover, ground anchor can be simulated as spots which more compatible with three dimension model. The mode of failure can be divided into two patterns, which are circular and plan failures as shows in Fig 2.16 and 2.17, respectively. Figure 2.16 (a) and (b) indicate the plane failure pattern which always occurs in case of high cohesion material like clay and sill slopes, whereas the plane failure pattern (see Fig 2.17 (a) and (b)) always appear on the cohesion-less slope like sand and rock. Usually, the plane failures were regularly simulated in case of rock slopes caused the orientation of rock mass controlled the location of the failure occurrence. Therefore, the plane failure pattern which more suitable for weathering rock slopes was assumed to analysis.

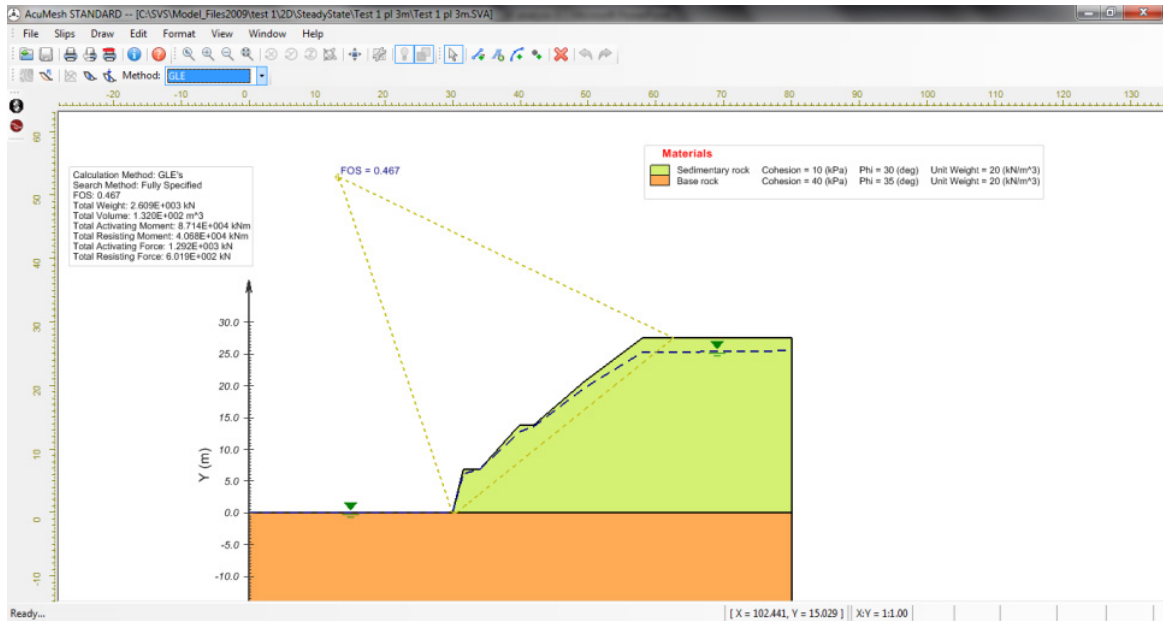


(a) Two dimensions

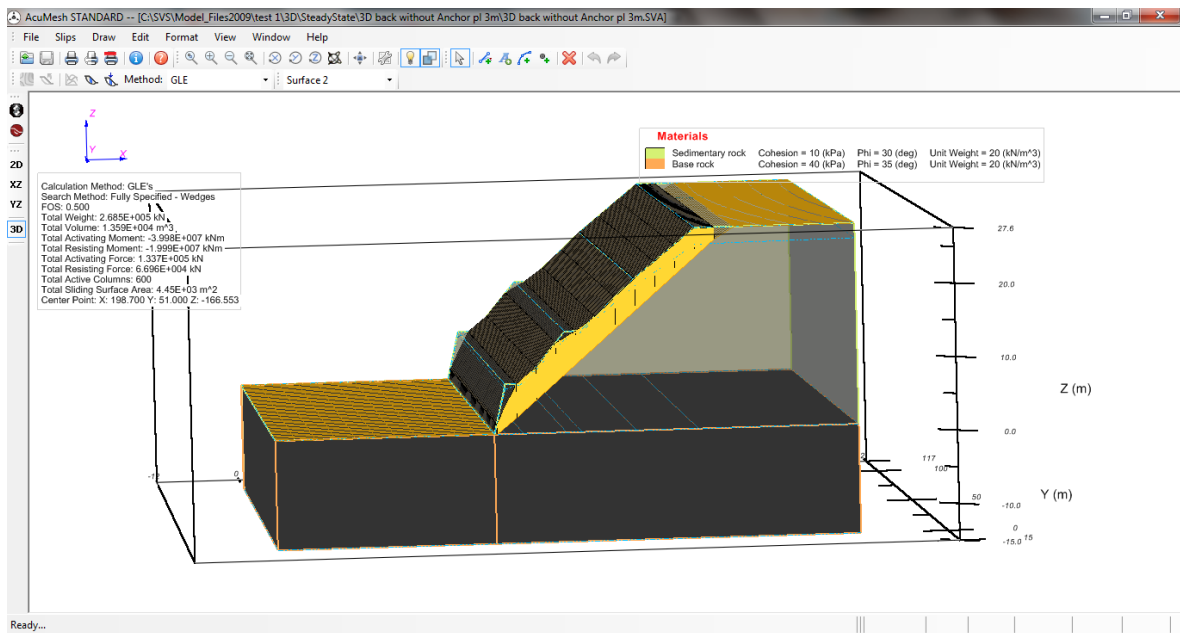


(b) Three dimensions

Figure 2.16 Example of slope stability analysis by *SV slope* software for circular failure pattern (a) Two dimensions and (b) Three dimensions



(a) Two dimension



(b) Three dimension

Figure 2.17 Example of slope stability analysis by SV slope software for plan failure pattern (a) Two dimensions and (b) Three dimensions

Figure 2.18 demonstrates a slope configuration for analysis in a previous study by Kimoto et al, 2011. The height of slope is 27m consisting of 2 berms and width of slopes is 26m. Some part of this slope presented the gradient greater than 1:1 in horizontal to vertical which quite dangerous and potential to collapse anytime during monsoon season. Ten ground anchors were installed to increase the stability of slopes; the inclination of each ground anchor is 20°. In addition, ground water level was fixed in the worst case which means that groundwater is reach to near the ground surface.

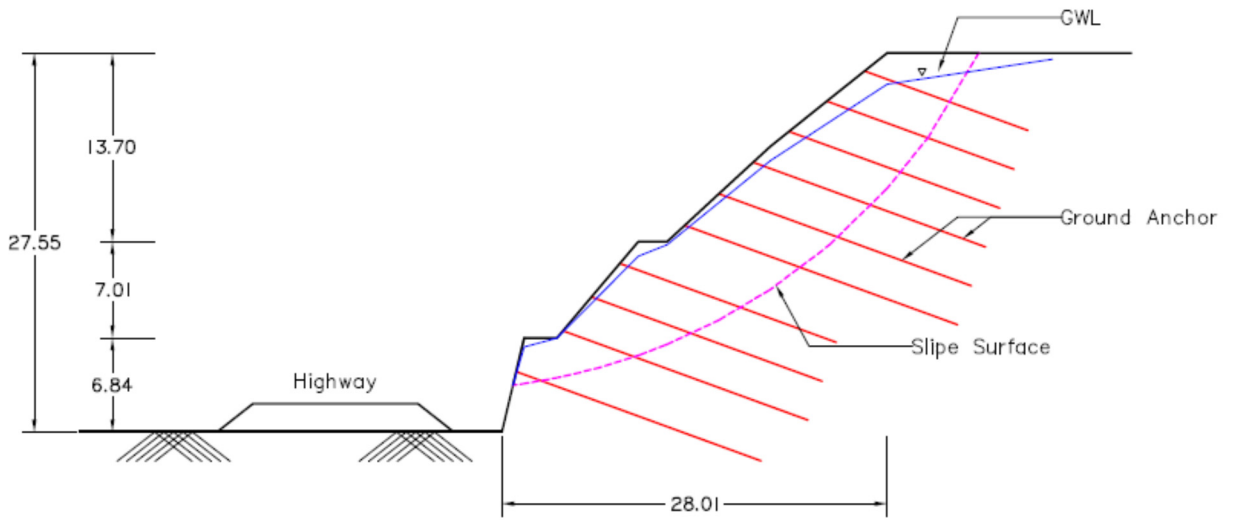


Figure 2.18 The slope configuration for analysis in previous studied (Kimoto et al, 2011)

The formulation to calculate given as follow;

$$Q = a_0 + a_1 C + a_2 \tan \phi + \sum_{j=1}^l (a_{j+2,1} + T_j) + \sum_{j=1}^l (a_{j+2,2} + T_j) \tan \phi \quad (2.46)$$

Where

$$a_0 = -1$$

$$a_1 = \frac{\sum_{i=1}^n b_i \sec \theta_i}{\sum_{i=1}^n w_i \sin \theta_i}$$

$$a_2 = \frac{\sum_{i=1}^n (w_i \cos \theta_i - u_i b_i \sec \theta_i)}{\sum_{i=1}^n w_i \sin \theta_i}$$

$$a_{j+2,1} = \frac{\sin\theta_i}{\sum_{i=1}^n w_i \sin\theta_i}$$

$$a_{j+2,2} = \frac{\cos\theta_i}{\sum_{i=1}^n w_i \sin\theta_i}$$

in which, where C and ϕ are cohesion and internal friction of soil, w_i and b_i are weight and wide of slide i , respectively. θ_i is the inclination of slice base referred to horizontal line. u_i is pore water pressure in i slice. T_j means pre-stresses induce to ground anchor and angle between anchor direction and normal line to the critical surface. Finally, n and m represented the number of slices and anchors, respectively (Ohtsu, 2011).

It is clearly stated that the physical meaning of performance function, Q is summarized as follows;

- $Q < 0$; Instable Condition
- $Q = 0$; Critical Condition
- $Q > 0$; Stable Condition

In order to clarify the relationship between factor of safety and performance function, it can be simplifies the relationship as follow;

$$F.S. = Q + 1 \tag{2.47}$$

However, the safety factor is varying depending on the slope configuration, including the number of ground anchors, size of slopes, gradient of slope face, the depth of weathering zone, strength parameters, etc. Therefore, it shall evaluate the safety factor individually based upon the actual slope scheme.

2.5 Probability of Failure

The conditional probability of failure described the tentative of slope failure at time t . Considering the mean, $\mu_{Q(t)}$ and standard deviation, $\sigma_{Q(t)}$ at time (t) of Q ; therefore, the equation of probability density function of a performance function $f_{Q(t)(x)}$ is expressed as follows;

$$f_{Q(t_i)}(x) = \frac{1}{\sigma_{Q(t_i)}\sqrt{2\pi}} \exp\left[-\frac{1}{2}\left(\frac{x - \mu_{Q(t_i)}}{\sigma_{Q(t_i)}}\right)^2\right] \quad (2.48)$$

Therefore, $P(0)$ is the probability that reflect Q less than zero can be calculated by the following equation;

$$P(0) = \int_{-\infty}^0 \frac{1}{\sigma_{Q(t_i)}\sqrt{2\pi}} \exp\left[-\frac{1}{2}\left(\frac{x - \mu_{Q(t_i)}}{\sigma_{Q(t_i)}}\right)^2\right] dx \quad (2.49)$$

Where

$$s = \frac{x - \mu_{Q(t_i)}}{\sigma_{Q(t_i)}} \quad (2.50)$$

Then, by substitution a variable conversion showed in Eq.(2.50), $P(0)$ is converted to Eq.(2.51)

$$\begin{aligned} P(0) &= \int_{-\infty}^{\left(\frac{\mu_{Q(t_i)}}{\sigma_{Q(t_i)}}\right)} \frac{1}{\sqrt{2\pi}} \exp\left[-\frac{1}{2}s^2\right] ds = \Phi\left(-\frac{\mu_{Q(t_i)}}{\sigma_{Q(t_i)}}\right) \\ &= \Phi(-\beta) \quad \left(\beta = \frac{\mu_{Q(t_i)}}{\sigma_{Q(t_i)}}\right) \end{aligned} \quad (2.51)$$

In which, $\Phi(x)$ is the operator for calculating a reliability index that represents the cumulative probability function of the random variable x , and β is the reliability index as expressed in Eq.(2.52);

$$\Phi(-\beta) = 1 - \Phi(\beta) \quad (2.52)$$

To clarify the physical meaning of equations mentioned above, the shading areas in Fig 2.19 (a) represent the conditional probability of failure, $p_f(t_i)$ at time (t_i) calculated by the Eq. (2.48) to Eq.(2.52). The probability of failure per year as illustrated in Fig 2.19 (b) can be calculated by the following equation;

$$p_f(t_i) = \prod_{j=1}^{i-1} (1 - \Delta p_f(t_j)) \Delta p_f(t_i) \quad (2.53)$$

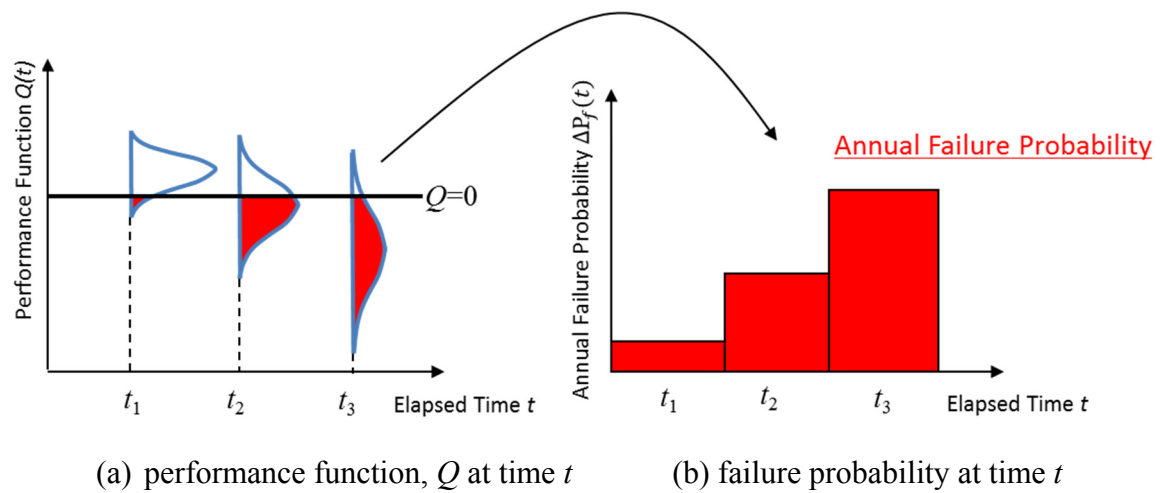


Figure 2.19 Relationship between performance function and failure probability

2.6 Monte Carlo Simulation

Monte Carlo methods (or Monte Carlo experiments) are the computational algorithms that multiple trials the expected value of the random variable by repeated random sampling to compute their results. They are frequently used in mathematical problems in several fields of study such as engineering and science. Moreover, there are most appropriate to be applied when it is impossible to obtain a closed-form expression or infeasible to apply a deterministic algorithm.

Monte Carlo methods are mostly employed in three similar problems, which consisting of optimization, numerical integration and generation of samples from a probability distribution. Generally, the Monte Carlo methods are especially useful for simulating systems with many coupled degrees of freedoms. They are used to model phenomena with significant uncertainty in inputs, such as the calculation of risk and sensitivity analysis in business and engineering field.

The Monte Carlo simulation arises from the interactive, co-linear and non-linear behavior of typical process simulations. For example, in geo-statistics, Monte Carlo methods were often employed to designing, analyzing and contributing to quantitative risk analysis. Another example is to evaluate the factor of safety for slope stability analysis under uncertainty several strength parameters.

Figure 2.20 demonstrated the example of results of factor safety analysis employed Monte Carlo technique with different location of slopes at k.p. of 6.30, 10.80, 49.80 and 49.60, correspondingly where the safety factor and probability density function was shown in horizontal and vertical axis, respectively.

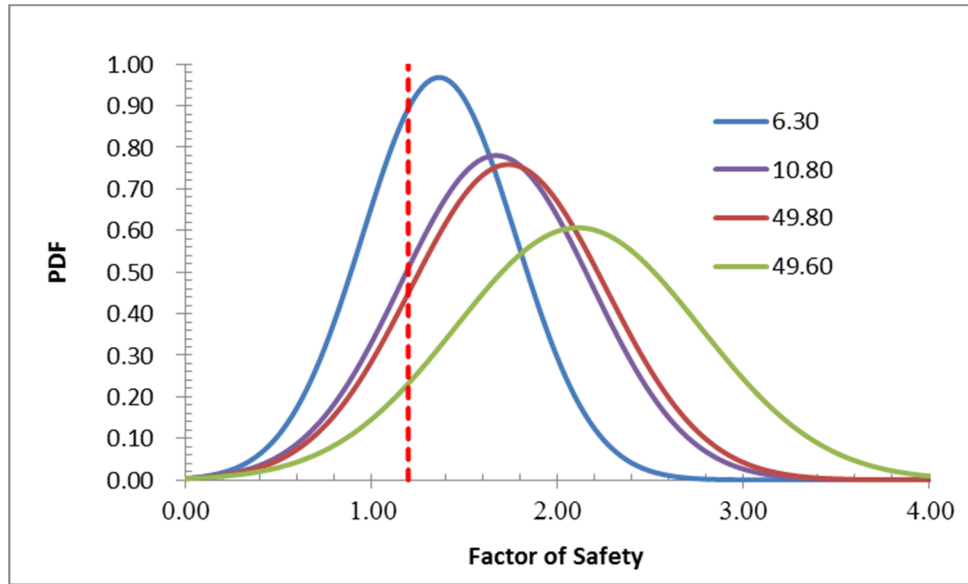


Figure 2.20 Example of results of factor safety analysis employed Monte Carlo technique

2.7 Kriging Method

Kriging is an advanced geo-statistical procedure that generates an estimated the unknown values from a scattered set. Kriging is based on the regionalized variable theory assumed that the spatial variation in the phenomenon represented by the z -values is statistically homogeneous throughout the surface.

The spatial variation is quantified by the semi-variogram in which computed from the average squared difference in z -value between pairs of input sample points. The sample semi-variogram is calculated from the sample data with the equation shown below;

$$\gamma(h) = \frac{1}{2n} \sum_{i=1}^k \{z(x_i) - z(x_i + h)\}^2 \quad (2.54)$$

Where

$\gamma(h)$ is experiment semi-variogram

$z(x_i)$ is the determine position of the random variable

$z(x_i + h)$ is the determine next position of the random variable

n and k are number of the pair samples and total number of pair samples, respectively

Figure 2.21 shows the comparison among of several semi-variogram model results, however, most of them illustrated almost same results. Figure 2.22 demonstrated the component of the semi-variogram which composed of sill, range, and nugget.

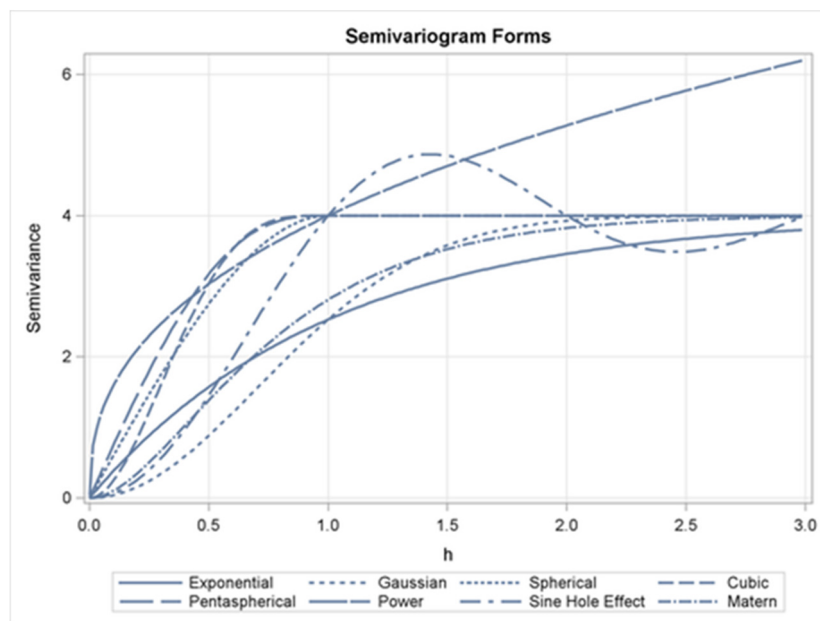


Figure 2.21 Semi- variogram (Bohling, 2005)

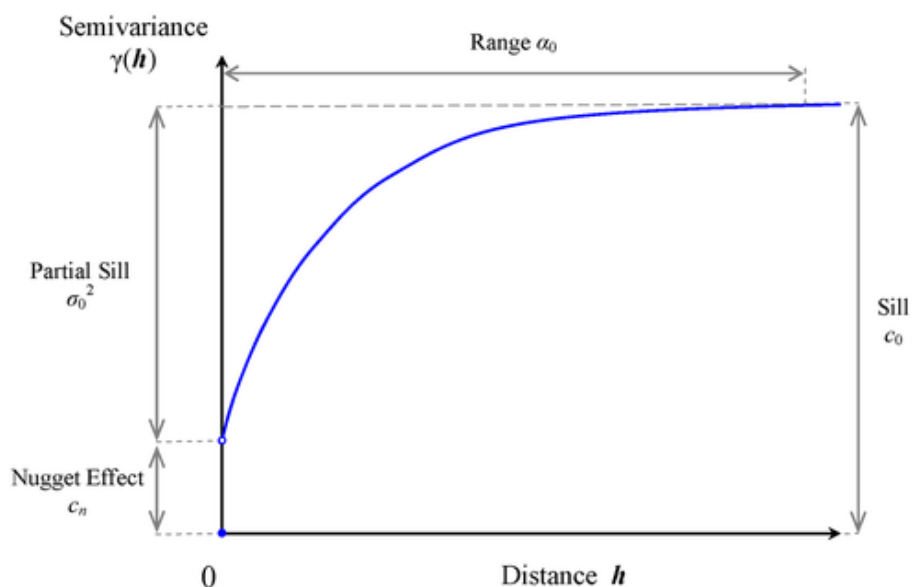


Figure 2.22 Component of Semi-Variogram (Bohling, 2005)

The characteristics of each component of semi-variogram are composed as follows;

1. Sill: this is the amplitude which the semi-variogram value at the levels off.
2. Range: the lag distance at which the semi-variogram reach to sill value.
3. Nugget: the value of semi- variogram at original point. In theory the semi-variogram value should be zero.

In this study, four empirical famous models were employed to simulate the semi-variogram, can be expressed as follows;

$$\text{Spherical: } g(h) = \begin{cases} c \cdot \left(1.5 \left(\frac{h}{a} \right) - 0.5 \left(\frac{h}{a} \right)^3 \right) & \text{if } h \leq a \\ c & \text{otherwise} \end{cases} \quad (2.55)$$

$$\text{Exponential: } g(h) = c \cdot \left(1 - \exp \left(\frac{-3h}{a} \right) \right) \quad (2.56)$$

$$\text{Gaussian: } g(h) = c \cdot \left(1 - \exp \left(\frac{-3h^2}{a^2} \right) \right) \quad (2.57)$$

$$\text{Power: } g(h) = c \cdot h^\omega \quad \text{with } 0 < \omega < 2 \quad (2.58)$$

Where

h represent lag distance,

a represent (practical) range,

c represent sill,

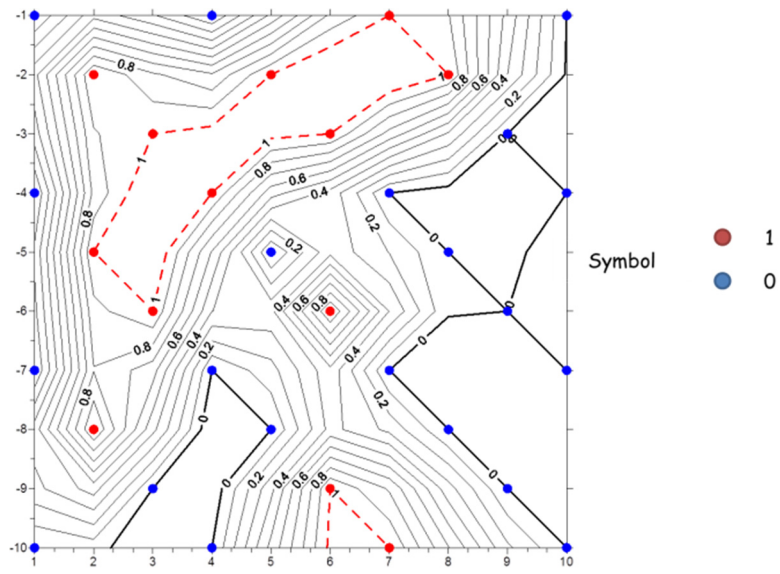
Furthermore, the indicator kriging was also utilized to indicate the weak zone for giving priority sequent to maintenance. Both Lift-off test and Ultrasonic test results were considered and compared in this study. The indicator kriging is an estimation technique with the same basis of kriging, which considering value exceeding than the indicator value. The indicator kriging was set up as shown in Eq.2.59 belows;

$$I(x; z_k) = \begin{cases} 1 & \text{if } z(x) \leq z_k \\ 0 & \text{if } z(x) > z_k \end{cases} \quad (2.59)$$

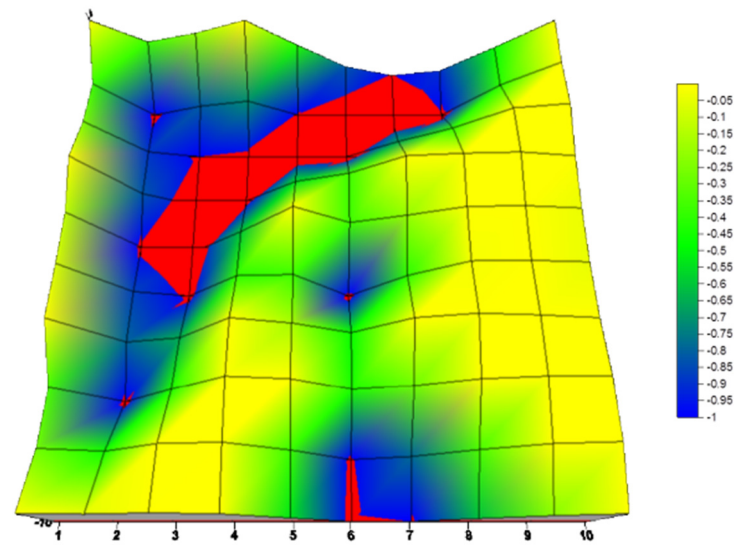
Where

z_k represent the indicator value

$z(x)$ represent the determine value at the position x



(a) Contour map



(b) Surface map

Figure 2.23 Example of indicator kriging

Figure 2.23 (a) to (b) illustrate the example of indicator kriging results demonstrated as the contour map as well as the surface map. Both types distinctly showed the risk zone by the red dotted line for the contour map (see Fig 2.23 (a)) and color filled in the surface map (see Fig 2.23 (b)), respectively. The risk zone of a surface map might be clearly to understand from the color filled than the contour map, but it is fairly complicated to count the areas of failure. On the other hand, contour map is moderately easy to appraise the areas on both risk zones ($z < z_k$) and survive zone ($z > z_k$).

2.8 Life Cycle Cost

In terms of maintenance strategy, the life cycle cost, LCC was adopted as the indicators to evaluate the suitable scenario plan for repair/renew as well as its life span. Figure 2.24 showed the performance profile of a slope improved by ground anchor considering probability of survival decrease after time gone by. The maintenance conducted at a certain time, for example, substituting ground anchor, the probability of survival increased as a new again and dropped since the deterioration process another time as presented in a dashed line. In case of non-maintenance, the probability of survival continuously decreased until reach to the failure condition as shown in red continuous line. In this paper, the Weibull hazard model is served to describe a deterioration rate of ground anchor.

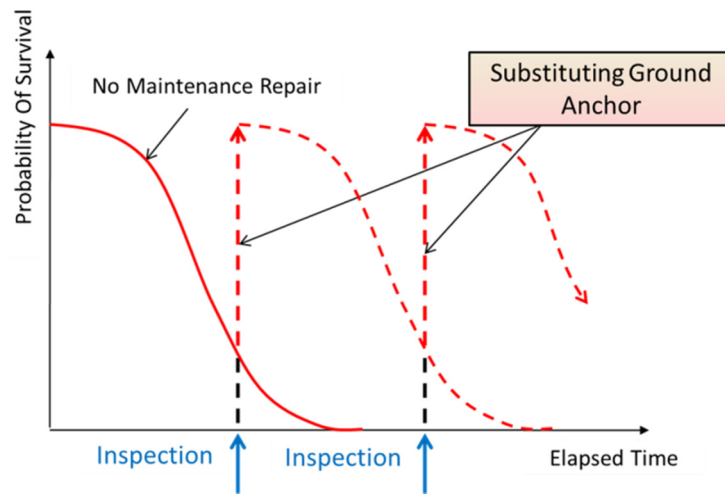


Figure 2.24 Schematic diagram of the performance strategies of various scenarios based on Weibull model

The LCC composed of three terms, which are inspection cost, repair/replace cost and recovery cost due to slope failure as denote as C_{ins} , C_{rep} and C_h , respectively. In addition, ρ is the social discount rate that assumes to be 4%, j represented time after maintenance, i is time after slope failure occurrence, t_m is maintenance time and k is the inspection interval. The inspection intervals were considered at 2, 5, 10, 15, 17 and 20years. The cost of recovery was calculated following equation proposed by Ohtsu, 2011.

$$C_h = (C_{v0}V + C_{A0}A)x(1 + a) + C_{M0}n \quad (2.60)$$

The *LCC* can be expressed with the equation as follows;

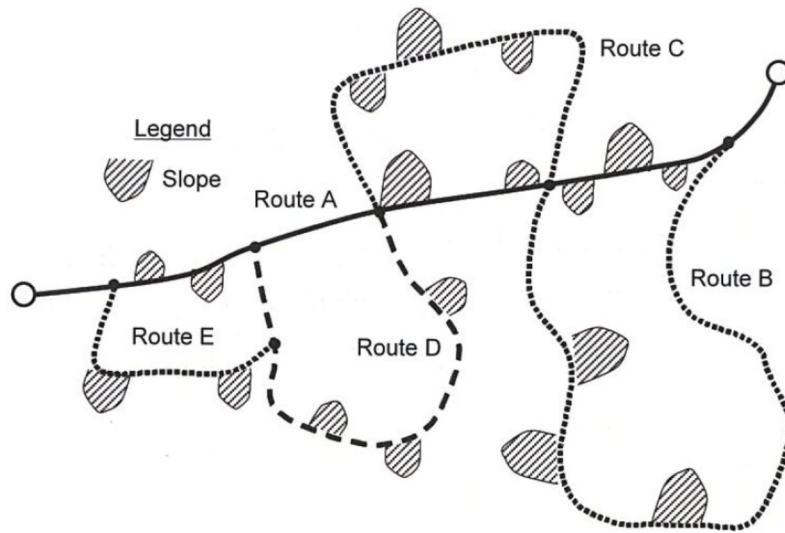
$$\begin{aligned}
 LCC = & \sum_{k=1}^x \sum_{j=1}^{k-t_m} IC_{ins} \left(\frac{1}{1+\rho} \right)^{k-t_m} \\
 & + \sum_{k=1}^x \sum_{j=1}^{k-t_m} \left[\prod_{j=1}^{i-1} (1-\Delta p_f(t_j)) \Delta p_f(t_i) \right] C_{rep} \left(\frac{1}{1+\rho} \right)^{k-t_m} \\
 & + \sum_{i=1}^t \left[\prod_{j=1}^{i-1} (1-\Delta p_f(t_j)) \Delta p_f(t_i) \right] C_h \left(\frac{1}{1+\rho} \right)^i
 \end{aligned} \tag{2.61}$$

2.9 Case Study of Ground Anchor in Kinki District

Ohtsu (2011) suggested that the viewpoint of infrastructure asset management, slope maintenance/reinforcement strategy required two types of investigation, which are the macroscopic view point that considering on the routes and the microscopic viewpoint focusing on an individual slope as illustrated in Fig 2.25 (a) and (b).

The experiment to verify the ability of ground anchors on risk slope were started by dealing with the Visual Inspection test in 2000 and were reported by Ohtsu, 2009 and Ohtsu et al, 2010. Moreover, the Lift-off test was introduced adopted as the direct method to determinate remaining force. Suksawat, et al, 2013 proposed the advance geo-statistical approach, namely kriging and indicator kriging to evaluate the unknown force caused insufficient data allowable. Finally, the Ultrasonic test was proposed starting in 2013 in order to measure the existing force indirectly, for saving on both cost and time.

The statistical approach for modeling to maintenance strategies on ground anchors were proposed by the server statistical models, for example, Markov chain model (Ohtsu et al, 2009 and Ohtsu, 2011), Markov hazard model (Kimoto et al, 2011 and Kimoto, 2013), Weibull Hazard model (Thanh, 2009 and Suksawat et al, 2012), etc. However, those methods involved only on the statistical methods which seem to be inadequate to evaluate the stability of those risk slopes; therefore, two and dimensional stability analysis was introduced by Kimoto, 2013 and Suksawat et al, 2013. In order to give priority to maintenance on risk slopes, *LCC* was applied as the countermeasure by Ohtsu et al, 2006.



(a) Macroscopic view point



(b) Microscopic view point

Figure 2.25 Prioritization of the road slope to be repaired (Ohtsu, 2011)

CHAPTER 3

METHODOLOGY

3.1 Introduction

The methodology to evaluate the deterioration process of slopes reinforced by ground anchors can be divided into four phases, which are the acquisition of inspection results & identify of current condition, modeling of deterioration process & prediction of future condition, investigation on stability & failure probability, estimate of life cycle cost & decision making on maintenance. The acquisition of inspection data & identify of current condition deals with the obtained data, including the Visual inspection test, Lift off test and Ultrasonic test. The Visual inspection test results were utilized to preliminary survey to evaluate the workability of the slopes caused it is not complicated as well as fastest method comparing with the other; however, it is a low reliable because this method based only on the simple experience of the expert engineers. Consequently, the Lift off test was used instead to verify the actual force remaining in ground anchors at present situation, but this method quite expensive and difficult to test all the ground anchors. Therefore, it can be adopted only five to ten percent of whole anchors. The last method, namely, Ultrasonic test was introduced to approve as the additional method to confirm the existing force indirectly on ground anchors by mean of ultrasonic wave such as the amplitude wave. This method was proposed as the supplement to the Lift off test results because it was conducted only on a slope.

The flowchart of this study was shown in Fig 3.1. It can divided into 8 chapters, including the introduction (chapter 1), literature review (chapter 2), methodology (chapter 3), acquisition of inspection results & identify of current condition (chapter 4), modeling of deterioration process & prediction of future condition (chapter 5), investigation on stability & failure probability (chapter 6), estimation on life cycle cost, *LCC* & decision-making on maintenance (chapter 7) and summary (chapter 8). The acquisition of the inspection results and identify of current condition can be categorized into three types of results, which are the Visual inspection test, Lift off test as well as Ultrasonic test.

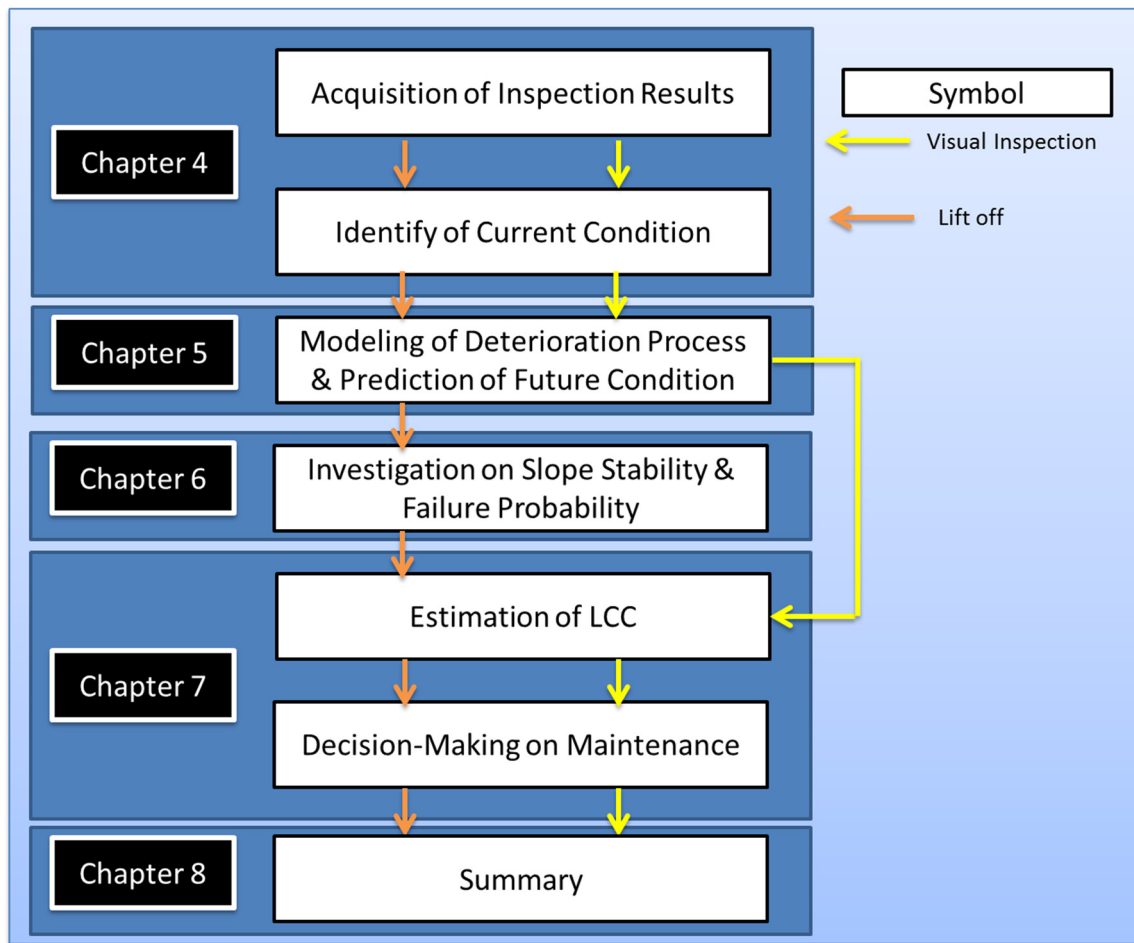


Figure 3.1 Flowchart of this study

The Visual inspection test can calculate the deterioration process by means of statistic approach, for example, the probability of failure and the survival probability. Several probabilistic models were compared the results to evaluate the appropriate model for representing the deterioration rate by deals with this testing results because the data allowable are adequate to calculate.

The Lift of test results were analyzed by considering the kriging interpolation, post-yielding ($Tan\theta$) analysis, statistic approach, stability/performance function and probability of failure, respectively. Both of two results were compared relationship and considered the maintenance strategies following the Life cycle cost analysis.

The last testing method, the Ultrasonic test was served as an alternative way to calculate remaining force, indicator kriging interpolation was used to indicate the risky zone of the failure. Both indicator kriging results from the Lift off test and the Ultrasonic test were

compared and calibrated the suitable technique for approximating the existing force indirectly. Finally, all of result was summarized as a concluding remark as well as future recommendation.

3.2 Acquisition of Inspection Results and Identify of Current Conditoin

In this chapter, three testing results were described the acquisition of inspection results as well as to identify of current condition. The detail of each testing result was summarized as follows;

3.2.1 Methodology of Visual Inspection Test Results

The Visual inspection test results are provided by one of the Japanese expressway companies. The condition states of ground anchors are categorized into six ratings as mentioned in the previous section. The degree of deterioration of ground anchor was classified as Excellent, Very good, Good, Fair, Marginal and Poor conditions corresponding to rank IV to rank I, respectively. Each rank of performance deterioration level of ground anchor is determined by the visual test from the surface of ground anchor's head such as hammering by an expert engineer from the road administrator (Kimoto et al, 2011).

Figure 3.2 presents the example results of the Visual inspection test, for example, head plate whether loose or tight and then remove the cover head to check the rusting on the tendon. The example results showed in Fig 3.2 demonstrates the SHS S5-4, strand type anchors, classified the ranking rate as the rank I caused the head plate does not tight, heavy rusting on the tendon and hydraulic oil leakage surrounds the rubber seal.

Furthermore, each Visual inspection test result was summarized by considering on individual slope as presented, for example, of Ibaraki No.12 showing in Fig 3.3. For more information, the results of Visual inspection test on all slopes was individually presented in Appendix A. Next, all the results were cumulated by classified on each inspection year of testing for convenient to analysis of the next phase.

The criterion to classify the failure ranking plays an important role for computing statistical approach and classifying the survival and failure probabilities. Therefore, they were established divided into two scenarios which are rank I and II corresponding to fail, is denoted as the scenario I and the rank I, II and III corresponding to fail as the scenario II, respectively, (see Table 3.1). On the other hand, the criteria for survival rank are rank III to VI and rank IV to VI corresponding to survive anchors for scenario I and II, respectively. In addition, the scenario I can be called as the optimistic scenario while the scenario II might be called as the pessimistic scenario.

Table 3.1 Criteria for calculation the failure and survival probability

Scenario	Criteria for Failure	Criteria for Survival
I	Rank I+II	Rank III to VI
II	Rank I+II+III	Rank IV to VI

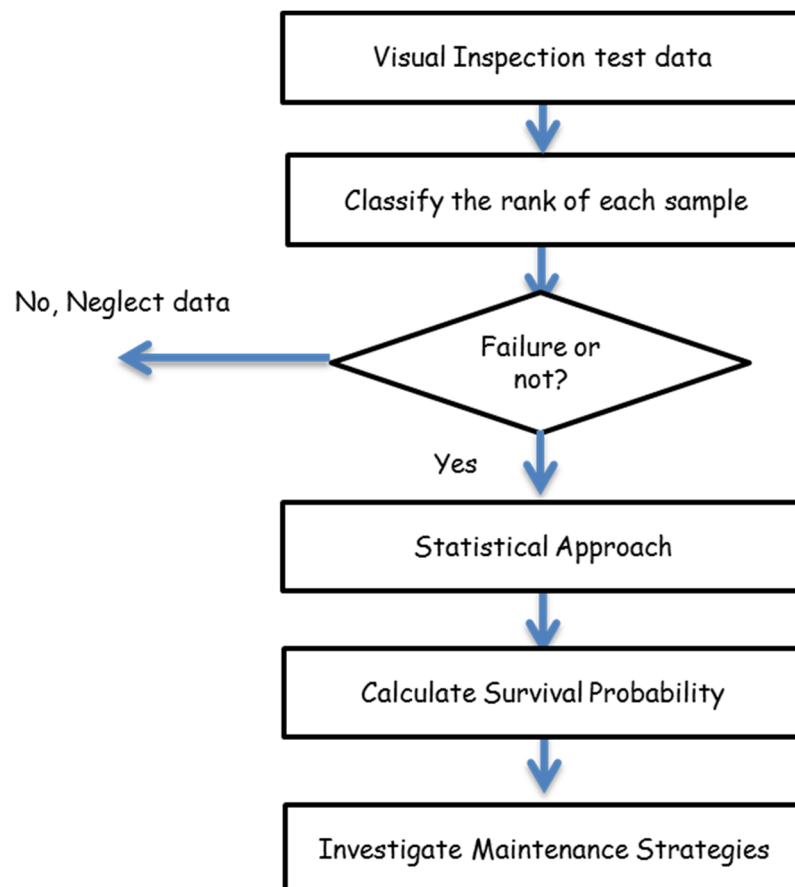


Figure 3.4 Flow chart of visual inspection test data

Figure 3.4 presented a flow chart to determine the deterioration process based on the Visual inspection data. These data were classified to be either failure or survive by considering two criteria as mention in Table 3.1. The failure data were summarized on each elapsed year, then calculated the probability of failure associated with several statistical approaches, including Weibull hazard model, Markov chain model, Poisson process model, Normal and Log-normal distribution function, etc. Those results were compared with the obtained data by means of survival probability to search the best-fitting model. The appropriate model was extremely important applying as the representative statistical model to predict the further state, life span, deterioration rate, and so on of risk slope reinforced by ground anchors. Finally, the simulation result of the deterioration process of the Visual inspection test was investigated the maintenance strategies.

3.2.2 Methodology of Lift off Test Results

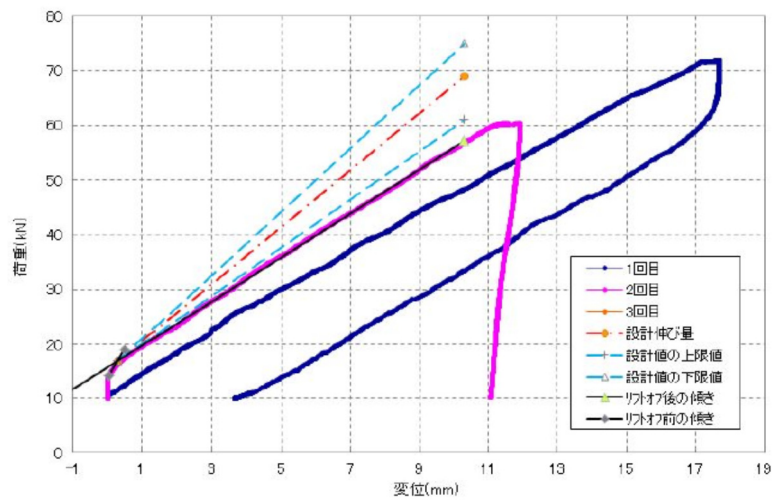
The Lift off test was adopted as the direct method to measure the existing pre-stress or residual force which remaining in ground anchors. The important advantages of this testing method are non-destructive test, actual force directly obtained, post-yielding behavior acquired and abnormality on both tendon and bonding zone detected but the higher expense than the Visual inspection test. Moreover, the Lift off test is too difficult to conduct because it takes longer time for setting up the equipment and platform while the Visual inspection test is only observed on the head of ground anchor with lightweight equipment. However, the Lift off test results gave more reasonable comparison with the Visual inspection results because it offered to measure pre-existing force directly as well as it can measure the behavior of ground anchors after yielding.

Figure 3.5 demonstrates the example of the Lift off test which conducted by pull-out on the ground anchor head employing loading jack as shown in Figure 3.5 (a) to measure the magnitude of the load in the anchor tendon and displacement. The resultant of load-displacement curves are presented in Fig 3.5 (b), where executed at least twice cyclic tests. The dashed lines are the gradients which represented the tendon stiffness that depending on the definition of measurement such as initial elasticity, tangent elasticity and elasticity at 50% of the yield point. These results can be used to investigate the abnormalities on the tendon or the bonding portion of the anchor. Moreover, it can be used to judge the need for

investigating the back of anchor heads, conducting maintenance tests and re-stressing or prolonging the life span (Miyatake et al, 2007).



(a) The Lift off test performed by the hydraulic jack



(b) Results of the Lift off test

Figure 3.5 The Lift off test performance and results

The results of the Lift off test can be divided as the ranking as listed in Table 3.2. The ranking consisting of five ranks which are I, II, III, IV and OK arranged from worst

condition to good condition, respectively. To give the ranking relates, it was considered on both observed anchor forces as well as elastic zone/bonding portion together.

Table 3.2 Criteria of each ranking based on Lift off test results

Rank (New)	Description		
	Observed Anchor Force	Elastic zone/ Bonding portion	$\tan \theta$
I	a) No Yielding point b) $T_L > 1.2 T_d$ c) $1.0 T_d < T_L < 1.2 T_d$ d) $T_L < 1.0 T_d$	a) – b) – c) No elastic zone d) No elastic zone	
II	a) $1.0 T_d < T_L < 1.2 T_d$ & $T_y < 1.1 T_L$ b) $T_L < 0.2 T_d$ & $T_y < 1.1 T_L$ c) $0.2 T_d < T_L < 1.0 T_d$ & $T_y < 1.1 T_L$	a) Elastic zone is observed & Bonding portion NG b) Elastic zone is observed & Bonding portion NG c) Elastic zone is observed & Bonding portion NG	
III	a) $T_L < 0.2 T_d$ & $T_y > 1.1 T_L$ b) $0.2 T_d < T_L < 1.0 T_d$ & $T_y > 1.1 T_L$	a) Elastic zone is observed & Bonding portion NG b) Elastic zone is observed & Bonding portion NG	
IV	$0.2 T_d < T_L < 1.0 T_d$	Elastic zone is observed/ Bonding portion OK	NG
OK	$0.2 T_d < T_L < 1.0 T_d$	Elastic zone is observed/ Bonding portion OK	OK

For the rank I, that was stipulated to be the failure rank which considered the observed anchor force as (a) no yield point, (b) $T_L > 1.2 T_d$, (c) $1.0 T_d < T_L < 1.2 T_d$ and (d) $T_L < 1.0 T_d$ together with the elastic zone was not observed. The rank II considered the range of the observed anchor force in these criteria; (a) $1.0 T_d < T_L < 1.2 T_d$ & $T_y < 1.1 T_L$, (b) $T_L < 0.2 T_d$ & $T_y < 1.1 T_L$ and (c) $0.2 T_d < T_L < 1.0 T_d$ & $T_y < 1.1 T_L$ whereas elastic zone/bonding portion are observed and stable, respectively. Rank III considered a measured force as follow; (a) $T_L < 0.2 T_d$ & $T_y > 1.1 T_L$ and (b) $0.2 T_d < T_L < 1.0 T_d$ & $T_y > 1.1 T_L$ while the elastic zone/bonding portion are observed and stable, respectively. In case of the Rank IV measured the observed anchor force as $0.2 T_d < T_L < 1.0 T_d$ and the elastic zone/bonding

portion are observed and stable, respectively. Finally, the rank OK was considered similar to the rank IV but new criterion namely $\tan \theta$ was added that the results should be reasonable. For the rank II to rank OK are corresponding to survival rank that will not use to analyze the failure probabilities.

Where

T_L represented the tensile strength obtained by the Lift off test

T_d represented the design ground anchor force

T_y represented the yield force of ground anchor

T_a represented the allowable force of ground anchor

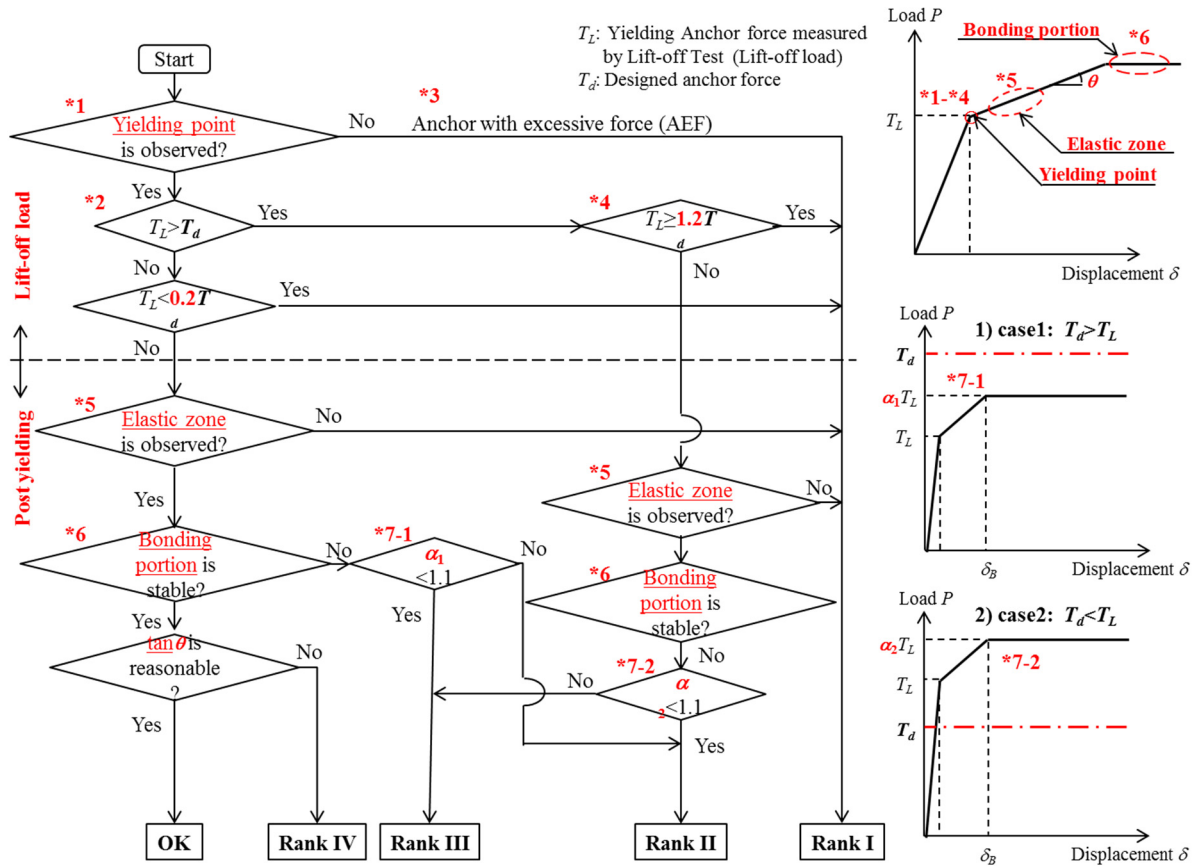


Figure 3.6 Flow chart describes the criteria of each rank

The criteria of each rank were shown as a flow chart in Fig 3.6. The procedure to classify considered the yield point (*1) that was observed or not, if not the results was classified as the rank I which is failure rank in this study. The physical meaning of this behavior is the

ground anchor with excessive force (AEF, *3). On the other hand, if it was observed, the magnitude of tensile strength was considered for the next step that if $T_L > 1.2 T_d$ (*2 to *4) & $T_L < 0.2 T_d$ corresponding to rank I as well. In contrast, if $1.2 T_d > T_L > 0.2 T_d$, the post yielding portion was additionally considered. Moreover, if the $T_L > 1.2 T_d$ (*4) the elastic zone was considered whether observed or not. If it was observed and the bonding portion was stable, the ultimate force, a_1 and a_2 obtained from the Lift off test were calculated. In case of $a_2 < 1.1$, it can be categorized as rank II, otherwise rank III.

The post yielding part consisting of three important parameters which are elastic zone (*5), bonding portion (*6) and $Tan\theta$ as shown on the upper right of Fig 3.6. The elastic zone was diagnosed (*5) that if it does not observe, it becomes rank I. Conversely, if the elastic is observed, but the bonding portion is instable, it shall be considered the existing force with the design forces of anchors. This procedure can be divided into two categories that $T_d > T_L$ and $T_d < T_L$ corresponding to a_1 and a_2 as illustrated on the middle right (case 1, *7-1) and lower right (case 2, *7-2) of Fig 3.6, respectively. The bonding portion was checked that if not stable as well as $a_2 < 1.1$, this results corresponding to rank II. In addition, if $a_1 < 1.1$ & $a_2 > 1.1$ as well as the post yielding zone similar properties with rank II, it can be classified as rank III.

Rank IV and OK were almost the same properties that differentiate only on the $Tan\theta$ parameter. For the rank OK, the $Tan\theta$ results shall be reasonable while rank IV, the $Tan\theta$ results was abandoned. For the other parameters of post-yielding part, which are elastic zone as well as a bonding portion shall be observed and stable, respectively; otherwise, this result shall be rank I to rank III, respectively.

Figure 3.7 demonstrates the flow chart to analyze the present condition of the Lift off test results. The first phase is to interpolate the unknown ground anchor force nearby the testing spots employed the advance geo-statistic technique call kriging method. The semi-variogram was calculated to investigate the appropriate model to simulate the kriging, for example, Spherical, Exponential and Power models. Then evaluate the unknown force and classify all results, whether failure or not associated with the flow chart mentioned above.

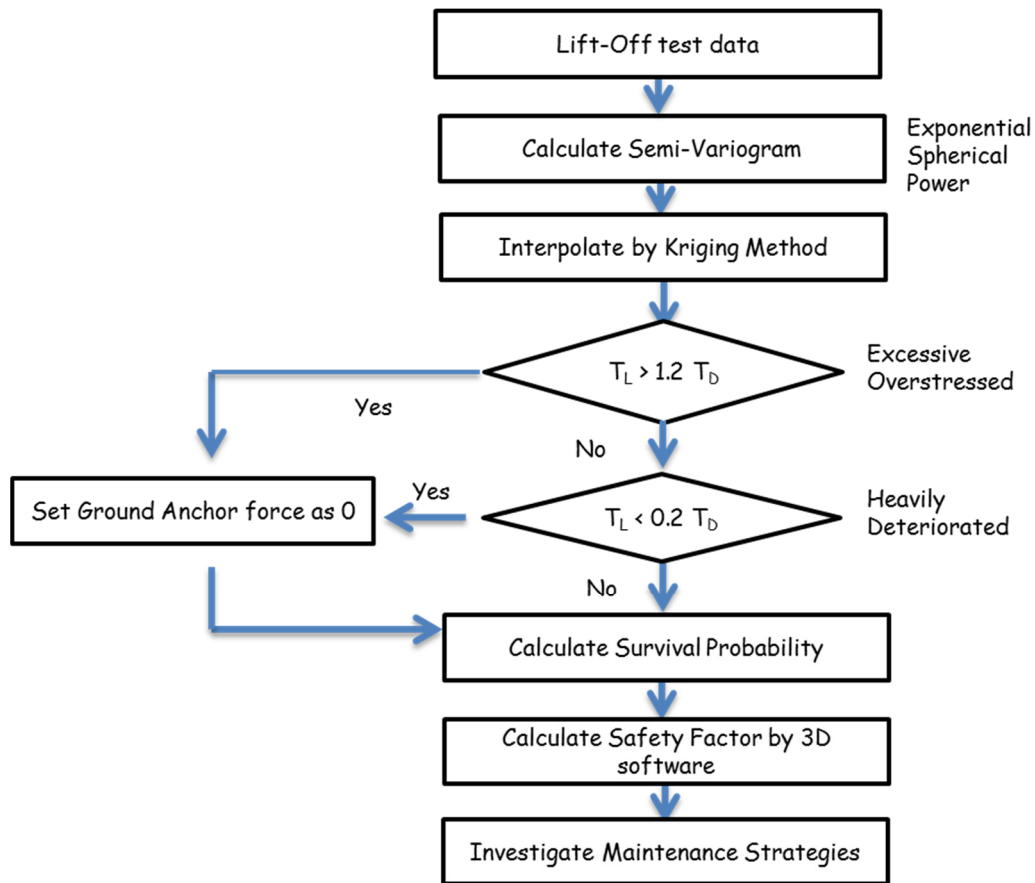


Figure 3.7 Flow chart of Lift off test results

The failure's criteria can be divided into two groups, which are the anchors force excess of a hundred twenty percent and less than twenty percent compared with the design force corresponding to fail (excessive overstressed and heavily deteriorated, respectively). In case of failure ground anchors, the force was assumed to be zero; otherwise, the force of each ground anchor was set based on kriging results.

The deterioration process was evaluated by dealt with the survival probability that evaluated from the failure ground anchors; however, the number of testing was limited; therefore, the appropriate model obtained from the Visual inspection test was adapted. The stability analysis was the analysis in the next phase by employing a commercial software namely *SV slope*. The Limit equilibrium method, *LEM* was used to evaluate the safety factor of each risk slope. Finally, the maintenance strategies associated with life cycle cost, *LCC* was established for determining the appropriate inspection interval and to making-decision for maintenance.

3.2.3 Methodology of Ultrasonic Test Results

The methodology to analyze associated with the Ultrasonic test results can also be calculated similarly with the Lift off test results; however, differences only abandoned the safety factor and predict the future state. The indicator kriging is one technique to indicate the weaker zone for the specify priority location for maintenance work. In fact, the indicator kriging is an estimation technique with the same basic of kriging, which is considering value exceed or beneath the indicator value, z_k as presented in the flow chart in the Fig 3.8.

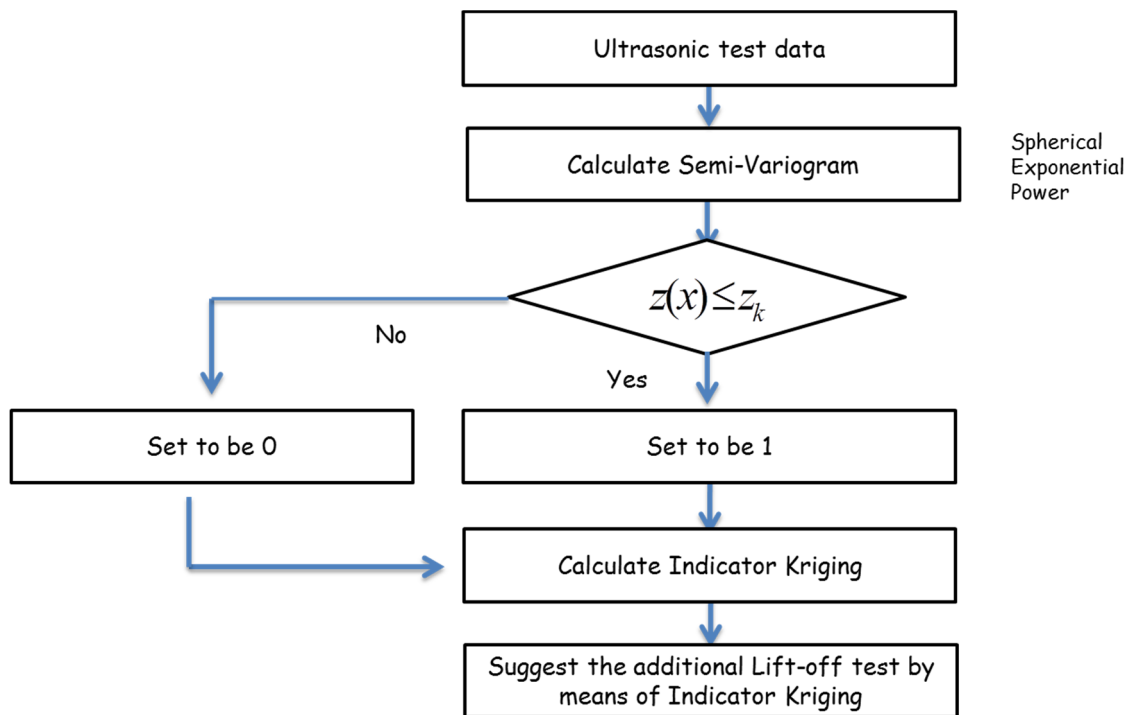


Figure 3.8 Flow chart of the Ultrasonic test results.

The first phase is to calculate semi-variogram to determine the proper model. Generally, the suitable semi-variogram can be employed same as the kriging calculation from the Lift off test results. Next, calculate the indicator kriging by considered the amplitude of the Ultrasonic results, whether rather or less than the value, z_k . Finally, these results were applied to be the guidance for suggesting spots for Lift off test in order to verify the remaining force additionally.

3.2.4 Comparison Scenario of Different Geological Conditions and Anchors types

All results of this study can be demonstrated into several comparison scenarios, for example, geological condition (sedimentary rock versus igneous rock) and type of ground anchors (strand type versus rod type) as depicted in Fig.3.9. Moreover, they also can be compared between same type of geological conditions with distinctive types of ground anchor as well as alike type of ground anchors types with different geological conditions. Moreover, it is also can be separated between the new and old types.

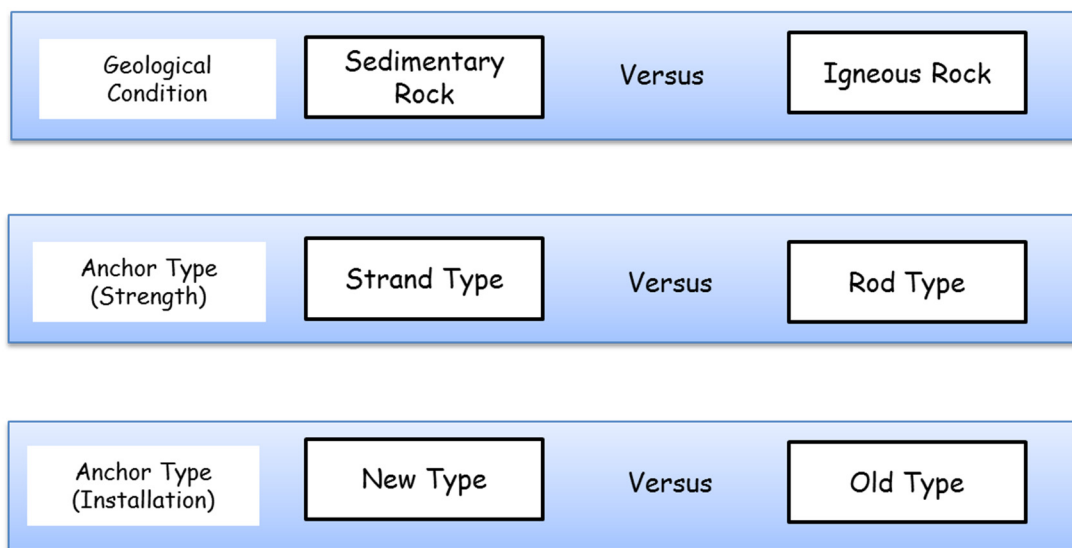


Figure 3.9 Comparison scenario of this study

3.3 Modeling of Deterioration Process and Prediction of Future Condition

3.3.1 Comparison Scenario of Different Markov chain model

Because the Markov chain models can be calculated divided into three models which are Original method, Simplify method and Markov hazard model, in order to select the suitable model for represent the Markov model, it have to compare the results to verify the appropriate model; however, the basic concept of calculating is same but different only the transition probability matrixs which are;

1. Original method: the basic assumption that ground anchor can transform the state forward (i to $i+1, i+2, \dots, J$) as well as still in current state (still in i state) as shown in Eq. (3.1).

$$T = \begin{bmatrix} T_{VI,YI} & T_{VI,Y} & T_{VI,IV} & T_{VI,III} & T_{VI,II} & T_{VI,I} \\ 0 & T_{V,Y} & T_{V,IV} & T_{V,III} & T_{V,II} & T_{V,I} \\ 0 & 0 & T_{IV,IV} & T_{IV,III} & T_{IV,II} & T_{IV,I} \\ 0 & 0 & 0 & T_{III,III} & T_{III,II} & T_{III,I} \\ 0 & 0 & 0 & 0 & T_{II,II} & T_{II,I} \\ 0 & 0 & 0 & 0 & 0 & T_{I,I} \end{bmatrix} \quad (3.1)$$

2. Simplify method: the basic assumption is quite similar to the original method, however, it can transform only one state forward (i to $i+I$) and without transformation, still in current state (still in i state) as illustrated in Eq. (3.2).

$$T = \begin{bmatrix} T_{VI,YI} & T_{VI,Y} & 0 & 0 & 0 & 0 \\ 0 & T_{V,Y} & T_{V,IV} & 0 & 0 & 0 \\ 0 & 0 & T_{IV,IV} & T_{IV,III} & 0 & 0 \\ 0 & 0 & 0 & T_{III,III} & T_{III,II} & 0 \\ 0 & 0 & 0 & 0 & T_{II,II} & T_{II,I} \\ 0 & 0 & 0 & 0 & 0 & T_{I,I} \end{bmatrix} \quad (3.2)$$

3. Markov hazard model: this model was proposed by Tsuda et al (2006) has a wide range of applications in various infrastructure systems. This model is also one branch of Markov model that base on the assumption of the exponential distribution.

$$P[h(y_B) = i | h(y_A) = i] = \exp(-\theta_i Z) \quad (3.3)$$

Where Z expresses the interval between two inspection times, θ is the hazard rate of the i state. Kaito (2009) and Thanh (2009) proposed the hazard rates depended on traffic volume as well as slab area, however in this study; the hazard rates were assumed to be the unknown parameters, β , as describe in in Eq. (3.4),

$$\theta_i = \beta_i \quad (3.4)$$

The transition matrix of the Markov hazard model can be described as follows;

$$\pi_{ij} = P[h(y_B) = i | h(y_A) = i] \quad (3.5)$$

$$\pi_{ij} = \sum_{k=i}^j \prod_{m=i}^{k-1} \frac{\theta_m}{\theta_m - \theta_k} \prod_{m=i}^{k-1} \frac{\theta_m}{\theta_{m+1} - \theta_k} \exp(-\theta_i Z) \quad (3.6)$$

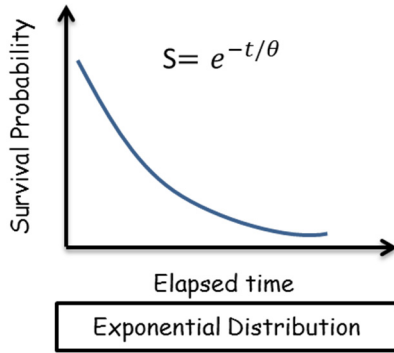
$$T = \begin{bmatrix} \pi_{VI,VI} & \pi_{VI,V} & \pi_{VI,IV} & \pi_{VI,III} & \pi_{VI,II} & \pi_{VI,I} \\ 0 & \pi_{V,V} & \pi_{V,IV} & \pi_{V,III} & \pi_{V,II} & \pi_{V,I} \\ 0 & 0 & \pi_{IV,IV} & \pi_{IV,III} & \pi_{IV,II} & \pi_{IV,I} \\ 0 & 0 & 0 & \pi_{III,III} & \pi_{III,II} & \pi_{III,I} \\ 0 & 0 & 0 & 0 & \pi_{II,II} & \pi_{II,I} \\ 0 & 0 & 0 & 0 & 0 & \pi_{I,I} \end{bmatrix} \quad (3.7)$$

Finally, the transition probability matrix of three methods can be calculated by trial and error technique to obtain the appropriate value by using *Solver* in *MS Excel* worksheet. *Solver* is part of a suite of commands sometimes called what-if analysis, a process of changing the values in cells to see how those changes affect the outcome of formulas on the worksheet. The difference between the observed and simulated value were compared by minimizing those values. Then, until different value showed lowest distinct values, the transition probability matrix will be used to analyze the deterioration rate of ground anchor in the next phase.

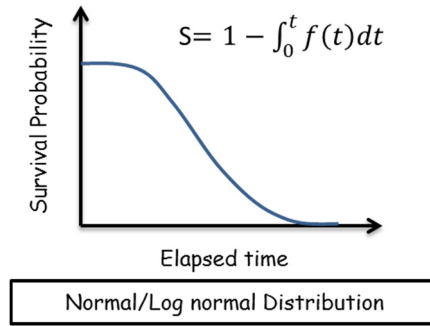
3.3.2 Comparison Scenario of Different Survival Probability Models

As mentioned previously, several models were proposed to evaluate the deterioration rate of ground anchors. In this study, the Exponential model, Normal/Log-normal distribution model, Weibull model and Poisson process model were utilized and compare results. The first group consisting of four models called the continuous probability distribution, whereas the second group composed of two models, which are the Poisson process model as well as the Markov model was the discrete probability distribution.

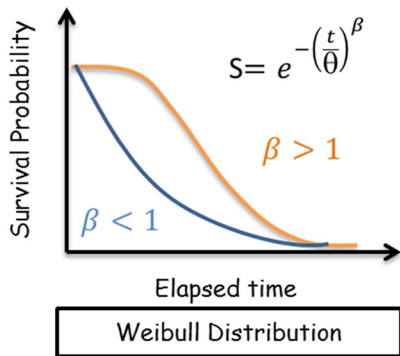
Survival probability curves of each model were illustrated in Fig 3.10 (a) to (e) corresponding to Exponential model, Normal/Log-normal distribution model, Weibull model, Poisson process model and Markov model, respectively. The Markov model was illustrated as the shading color corresponding to percent sharing of each rank, whereas the other models presented as the continuous line represented the deteriorated rate. The deteriorated curve of the Weibull hazard model is quite similar to Normal and Log-normal distribution model if the shape parameter rather than one; in contrast, it is quite the same shape of the exponential distribution model if the shape parameter lower than one. The Poisson process model showed the different deteriorated path that decreases as a step down.



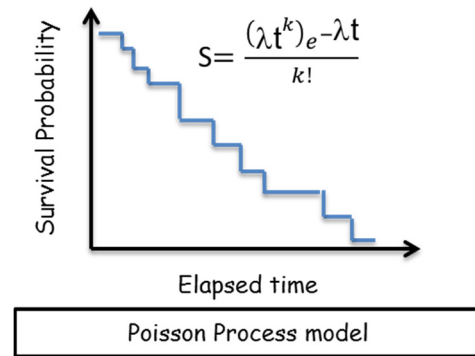
(a) Exponential model



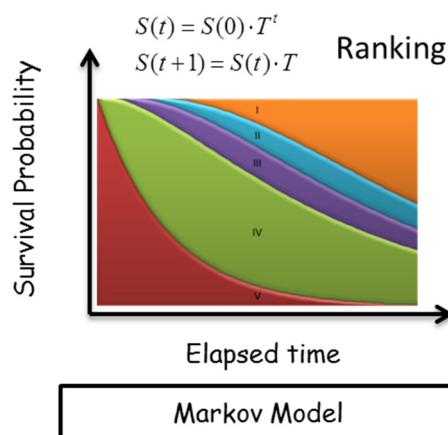
(b) Normal/Log-normal distribution model



(c) Weibull model



(d) Poisson Process model



(e) Poisson Process model

Figure 3.10 Survival Probability models

Where

$$\text{Failure Rat, } \lambda = \frac{r}{\sum t + (n-r)T}$$

$$\text{Mean Time to Failure, } \theta = \frac{1}{\lambda}$$

r = No. of failure data

t = time at failure of each failure data

n = No. of total data

T = total time to test

k = No. of failure data (Poisson process model)

In order to determinate the appropriate model to represent the deterioration rate; it was conducted on all data on the Visual inspection test results because the number of samples is quite adequate to analyze.

(7) Investigation on Stability and Failure Proability

In this section, three dimensional stability analysis and the failure probability were proposed to conduct on the risk slopes in order to predict the future condition of those slopes. The ordinary or Fellenius's method was engaged because this method is quite simple which is the most simplify technique; anyway, the results of *F.S.* are not obvious the difference from the other method.

The appropriate strength parameters like cohesion, c and internal friction angle, ϕ of each slope were calculated by deal with the back calculated technique on the without improvement state. Next, apply the anchors force following the design force to consider the initial state and adopted the force from the kriging results for analyzing stability on the present condition.

The failure probability of the risk slope was calculated considering the reduced rates of anchors force caused deterioration processes by assuming the decayed rate following Weibull hazard model. The conditional probabilities of failure, annual probability of failure and cumulative annual probability of failure were calculated to verify the risk of failure on individual slope. Finally, they were compared and discussed to establish the sequent for the maintenance strategies.

(1) Estimate of Life Cycle Cost and Decision Making on Maintenance

The last section of this study is to estimate of life cycle cost, *LCC* and decision-making on maintenance of the slope improved by ground anchors. The *LCC* calculation can be divided into two ways which are;

1. *LCC* of the Visual inspection test results: considering the failure probability based on the Weibull hazard model and the Markov model with neglect the loss due slope failure caused the Visual inspection test cannot calculate slope stability. It can be considered as the macroscopic viewpoint.
2. *LCC* of both Visual inspection test and Lift off test results: considering the failure probability based on the Weibull hazard model, excluding the losses because of slope failure. This result was considered in decision-making on the testing method for establishing the maintenance strategies.
3. *LCC* of the Lift off test results: considering the failure probability based on the Weibull hazard model, including the losses due to slope failure. It can be considered as the microscopic viewpoint.

CHAPTER 4

THE ACQUISITION OF TESTING RESULTS AND IDENTIFICATION OF CURRENT CONDITION

4.1 Introduction

Nowadays, several risk slopes improved by ground anchors were detected that they might tentatively collapse caused continuously decreasing on its performance due to deterioration process. In order to identify the present stability of those slopes, the Visual inspection test, the Lift off test and the Ultrasonic test were proposed to conduct. The Visual inspection test as well as the ultrasonic test can be experimented on every ground anchors while the Lift off test cannot because of too expensive and difficult to be performed.

The Visual inspection results of the ground anchors are provided by one of the Japanese expressway companies, and the condition states of ground anchors are categorized into six ratings as tabulated in Table 4.1. The degree of deterioration of ground anchor conditions was classified as Excellent, Very good, Good, Fair, Marginal and Poor conditions corresponding to rank IV to rank I, respectively. The Visual inspection tests were easier to perform comparison with the Lift off test since it used only light weight equipment for roughly evaluating to judge the rating of the sample. Moreover, this method is the fastest and cheapest method comparing with the Lift off test and Ultrasonic test.

Table 4.1 Evaluation criterion of condition rating by Visual inspection test

Condition Rating	Physical Meaning
I	Poor condition: replacement required
II	Marginal condition: possible replacement required
III	Fair condition: repair required
IV	Good condition: possible minor maintenance/repair
V	Very good condition: no maintenance/repair needs
VI	Excellent condition: ground anchor is as new

On the other hand, the Lift off test directly provided the actual remaining force. Although, strength parameters like cohesion and internal friction angle of the rock are the predominating factor which controlled the stability of slopes, the existing force is additionally reinforced to enhance resisting capacity of slopes as well. In addition, the Lift off test results not only demonstrated existing ground anchor force, but also can express behavior on both pre and post yielding portions, as described in terms of force versus displacement. However, the cost of experiment is quite high compared with the other methods.

The Lift off test was conducted on selected slopes with the limited number of testing caused its cost and the difficulty of experiments. The kriging method was adopted to interpolate force of ground anchors adjacent to the testing spots. However, the kriging method can be calculated by numerous models, i.e. Spherical, Exponential, Gaussian and Power models. Therefore, it has to verify with semi-variogram in order to investigate an appropriate model to be the representative for interpolating the force.

The post yielding portion was considered in this chapter by means of $Tan\theta$. This parameter can be used to indicate the abnormality on the post-yield portion. It provided the knowledge to classify the failure patterns, whether occurring on either bonding or tendon portion. The results on $Tan\theta$ can be categorized into three types, including abnormal anchors on the tendon portion, abnormal anchors on the bonding portion and normal anchors types. The abnormal on the tendon bar means the size of tendon too small while abnormal on bonding portion means bonding length is too short; otherwise, it becomes the normal anchor type.

The Ultrasonic test is a non-destructive method using very short ultrasonic pulse-waves penetrated into the sample in order to observe internal flaws or to characterize materials by means of signal amplitude. Common examples of Ultrasonic tests are included monitoring pipework corrosion, detection/evaluation, dimensional measurements, material characterization, and more. It is composed of several functional units, such as the pulser/receiver, transducer, and display devices. However, this method was categorized as the supplementary data to the Lift off test because it was conducted on a slope.

4.2 The Visual Inspection Data

This study was conducted on slope reinforced by ground anchors along the expressways in the Kinki district, including Kyoto, Osaka, Kobe and Himeji prefectures. The Visual inspection test results obtained from those areas consisting of eight routes, 83 slopes, comprised of 17 slopes in Fukuchiyama, 10 slopes in Himeji, 13 slopes in Kobe, 1 slope in Fukusaki, 6 slopes in Kyotan, 16 slopes in Ibaraki, 11 slopes in Minami and 9 slopes in Wakayama. The total number of testing is 22,976 data set as presented in Fig 4.1.

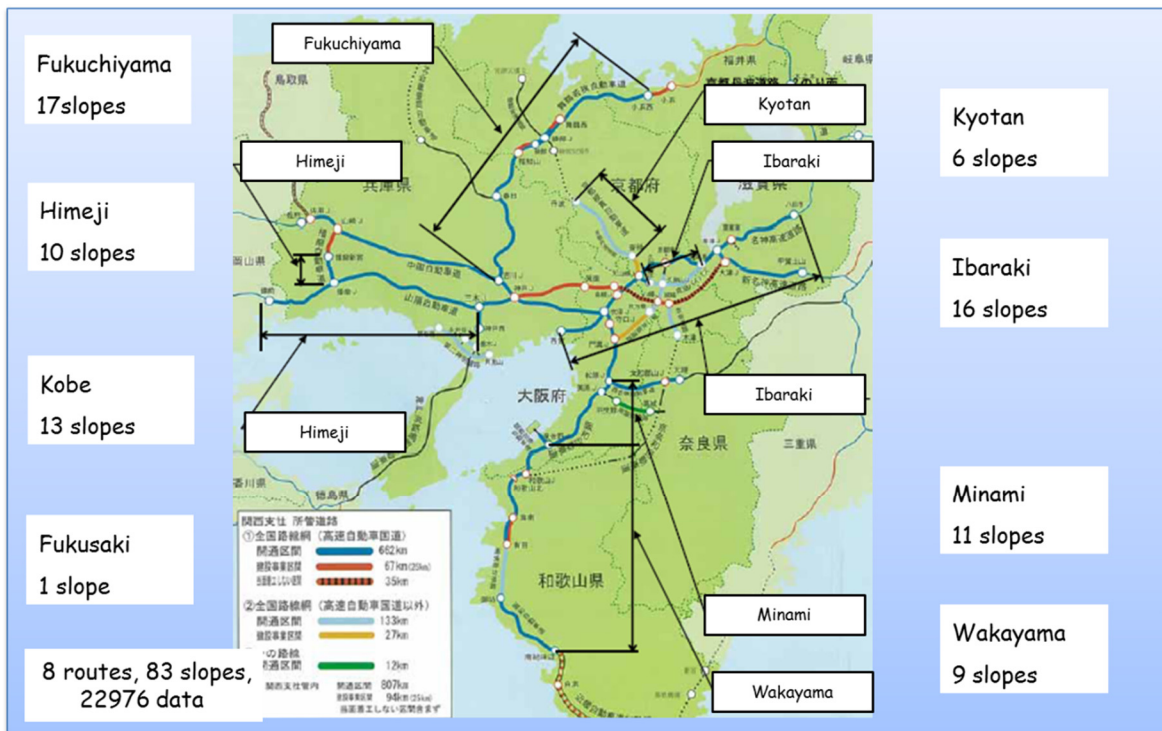


Figure 4.1 Routes and number of testing slopes obtained from the Visual inspection test

The Visual inspection results obtained from field test were summarized as tabulated for old type and new type in Table 4.2 and 4.3, correspondingly. First column demonstrated the ground anchors types, the strand type denoted as *S* whereas the rod type symbolized as *R*. Moreover, these tables illustrated the number of ground anchors failure that can be divided into two scenarios which are rank I & II and rank I, II & III corresponding to failure for scenario I and II, respectively (denoted as the S-I and S-II in these tables).

Table 4.2 Summary of the Visual inspection data, Old type ground anchor

Type	Site	Visula Inspection							Geological Condition	Inspection Year	Install	Elasped time	No of Failure		Survival Prob	
		I	II	III	IV	V	VI	Sum					s - I	s - II	s - I	s - II
R	Fukuchiyama-3		2					34	Sedimentary Rock	2000	1986	14.0	2	2	0.94	0.94
R	Fukuchiyama-3		2	1	7	24		34	Sedimentary Rock	2009	1986	23.0	2	3	0.94	0.91
R	Fukuchiyama-4					61		61	Sedimentary Rock	2000	1986	14.0	0	0	1.00	1.00
R	Fukuchiyama-4		1	4	6	50		61	Sedimentary Rock	2009	1986	23.0	1	5	0.98	0.92
S	Fukuchiyama-5		1	31	19	278		329	Sedimentary Rock	2000	1985	15.0	1	32	1.00	0.90
S	Fukuchiyama-5	3	44	122	74	86		329	Sedimentary Rock	2009	1985	24.0	47	169	0.86	0.49
R	Fukuchiyama-6					54		54	Sedimentary Rock	2000	1985	15.0	0	0	1.00	1.00
R	Fukuchiyama-6		1	2	6	45		54	Sedimentary Rock	2009	1985	24.0	1	3	0.98	0.94
R	Fukuchiyama-7	4				80		84	Sedimentary Rock	2000	1985	15.0	4	4	0.95	0.95
R	Fukuchiyama-7	15	9	8	11	41		84	Sedimentary Rock	2009	1985	24.0	24	32	0.71	0.62
S	Fukuchiyama-8					116		116	Sedimentary Rock	2000	1986	14.0	0	0	1.00	1.00
S	Fukuchiyama-8		6	2	3	116		127	Sedimentary Rock	2009	1986	23.0	6	8	0.95	0.94
R	Fukuchiyama-9					48		48	Sedimentary Rock	2000	1985	15.0	0	0	1.00	1.00
R	Fukuchiyama-9	5	1	1	1	40		48	Sedimentary Rock	2009	1985	24.0	6	7	0.88	0.85
R	Fukuchiyama-10		2			69		71	Sedimentary Rock	2000	1985	15.0	2	2	0.97	0.97
R	Fukuchiyama-10		4	3		64		71	Sedimentary Rock	2009	1985	24.0	4	7	0.94	0.90
R	Fukuchiyama-11	1	2	0	0	62		65	Sedimentary Rock	2000	1985	15.0	3	3	0.95	0.95
R	Fukuchiyama-11	4	7	1	1	49		62	Sedimentary Rock	2009	1985	24.0	11	12	0.82	0.81
R	Fukuchiyama-12					53		53	Sedimentary Rock	2000	1985	15.0	0	0	1.00	1.00
R	Fukuchiyama-12		1			52		53	Sedimentary Rock	2009	1985	24.0	1	1	0.98	0.98
R	Fukuchiyama-13					248		248	Sedimentary Rock	2000	1985	15.0	0	0	1.00	1.00
R	Fukuchiyama-13			5		243		248	Sedimentary Rock	2009	1985	24.0	0	5	1.00	0.98
S	Fukuchiyama-14					143		143	Sedimentary Rock	2000	1988	12.0	0	0	1.00	1.00
S	Fukuchiyama-14	1	2	3	13	124		143	Sedimentary Rock	2009	1988	21.0	3	6	0.98	0.96
R	Fukuchiyama-15					45		45	Gabbro	2000	1988	12.0	0	0	1.00	1.00
R	Fukuchiyama-15		6	1	3	35		45	Gabbro	2009	1988	21.0	6	7	0.87	0.84
R	Fukuchiyama-16					102		102	Gabbro	2000	1988	12.0	0	0	1.00	1.00
R	Fukuchiyama-16			1		101		102	Gabbro	2009	1988	21.0	0	1	1.00	0.99
S	Fukuchiyama-17					26		26	Sedimentary Rock	2000	1988	12.0	0	0	1.00	1.00
S	Fukuchiyama-17				2	24		26	Sedimentary Rock	2009	1988	21.0	0	0	1.00	1.00
S	Fukuchiyama-18					78		78	Sedimentary Rock	2000	1988	12.0	0	0	1.00	1.00
S	Fukuchiyama-18					78		78	Sedimentary Rock	2009	1988	21.0	0	0	1.00	1.00
S	Himeji-1		1	4	36	11		52	Rhyolite	2000	1988	12.0	1	5	0.98	0.90
S	Himeji-1		1	13	33	15		62	Rhyolite	2009	1988	21.0	1	14	0.98	0.77
S	Himeji-2					223		299	Rhyolite	2000	1981	19.0	0	76	1.00	0.75
S	Himeji-2	1			77	221		299	Rhyolite	2009	1981	28.0	1	78	1.00	0.74
S	Himeji-3					92		92	Rhyolite	2000	1981	19.0	0	0	1.00	1.00
S	Himeji-3					92		92	Rhyolite	2009	1981	28.0	0	0	1.00	1.00
R	Himeji-4		2			206		208	Rhyolite	2000	1981	19.0	2	2	0.99	0.99
R	Himeji-4	2	8	24	174			208	Rhyolite	2009	1981	28.0	10	34	0.95	0.84
S	Minami-1			3	76	1		80	Granite	2000	1988	12.0	0	3	1.00	0.96
S	Minami-1		5	2	73			80	Granite	2009	1988	21.0	5	7	0.94	0.91
S	Minami-2			10	47			57	Granite	2000	1988	12.0	0	10	1.00	0.82
S	Minami-2		3	10	44			57	Granite	2009	1988	21.0	3	13	0.95	0.77
S	Minami-3			5	127			132	Granite	2000	1988	12.0	0	5	1.00	0.96
S	Minami-3	1	4	27	100			132	Granite	2009	1988	21.0	5	32	0.96	0.76
S	Minami-4		4	1	55			60	Granite	2000	1988	12.0	4	5	0.93	0.92
S	Minami-4	3	28	1	28			60	Granite	2009	1988	21.0	31	32	0.48	0.47
S	Minami-5			9	45			54	Granite	2000	1988	12.0	0	9	1.00	0.83
S	Minami-5	1	3	6	44			54	Granite	2009	1988	21.0	4	10	0.93	0.81
S	Minami-6		2	11	178			191	Granite	2000	1988	12.0	2	13	0.99	0.93
S	Minami-6		3	44	49	95		191	Granite	2009	1988	21.0	3	47	0.98	0.75
S	Minami-7			4	106			110	Granite	2000	1988	12.0	0	4	1.00	0.96
S	Minami-7			25	86	1		112	Granite	2009	1988	21.0	0	25	1.00	0.78
S	Minami-8				44			44	Granite	2000	1988	12.0	0	0	1.00	1.00
S	Minami-8		7		37			44	Granite	2009	1988	21.0	7	7	0.84	0.84
R	Minami-9				22	17		39	Granite	2000	1988	12.0	0	0	1.00	1.00
R	Minami-9			1	32	6		39	Granite	2011	1988	23.0	0	1	1.00	0.97
R	Wakayama-1				2	695		697	Granite	2000	1988	12.0	0	0	1.00	1.00
R	Wakayama-1			202	120	375		697	Granite	2009	1988	21.0	0	202	1.00	0.71
R	Wakayama-2				216			216	Sedimentary Rock	2000	1988	12.0	0	0	1.00	1.00
R	Wakayama-2			2	214			216	Sedimentary Rock	2009	1988	21.0	0	2	1.00	0.99
R	wakayama-3				48	6		54	Sedimentary Rock	2000	1988	12.0	0	0	1.00	1.00
R	wakayama-3			54				54	Sedimentary Rock	2009	1988	21.0	0	54	1.00	0.00

Table 4.2 Summary of the Visual inspection data, Old type ground anchor (Continue)

Type	Site	Visula Inspection							Geological Condition	Inspection Year	Install	Elasped time	No of Failure		Survival Prob	
		I	II	III	IV	V	VI	Sum					I+II	I+II+III	I+II	I+II+III
R	wakayama-4				1	67		68	Sedimentary Rock	2000	1988	12.0	0	0	1.00	1.00
R	wakayama-4				1	67		68	Sedimentary Rock	2009	1988	21.0	0	0	1.00	1.00
R	Wakayama-5			2	34			36	Sedimentary Rock	2000	1987	13.0	0	2	1.00	0.94
R	Wakayama-5		7	29				36	Sedimentary Rock	2009	1987	22.0	7	36	0.81	0.00
S	Ibaragi-1				6	222		228	Sedimentary Rock	2000	1987	13.0	0	0	1.00	1.00
S	Ibaragi-1		7	6	116	99		228	Sedimentary Rock	2009	1987	22.0	7	13	0.97	0.94
R	Ibaragi-2		6	2	24			32	Sedimentary Rock	2000	1987	13.0	6	8	0.81	0.75
R	Ibaragi-2	10	17	31	189			247	Sedimentary Rock	2009	1987	22.0	27	58	0.89	0.77
R	Ibaragi-3				40			40	Sedimentary Rock	2000	1987	13.0	0	0	1.00	1.00
R	Ibaragi-3				40			40	Sedimentary Rock	2009	1987	22.0	0	0	1.00	1.00
R	Ibaragi-4	3	20	2	229	20		274	Sedimentary Rock	2000	1987	13.0	23	25	0.92	0.91
R	Ibaragi-4	16	61	27	172			276	Sedimentary Rock	2009	1987	22.0	77	104	0.72	0.62
S	Kyotan-1				8	85		93	Sedimentary Rock	2000	1988	12.0	0	0	1.00	1.00
S	Kyotan-1			5	9	79		93	Sedimentary Rock	2009	1988	21.0	0	5	1.00	0.95
R	Kyotan-2				40			40	Sedimentary Rock	2000	1988	12.0	0	0	1.00	1.00
R	Kyotan-2				40			40	Sedimentary Rock	2009	1988	21.0	0	0	1.00	1.00

Table 4.3 Summary of the Visual inspection data, New type ground anchor

Type	Site	Visula Inspection							Geological Condition	Inspection Year	Install	Elasped time	No of Failure		Survival Prob	
		I	II	III	IV	V	VI	Sum					I+II	I+II+III	I+II	I+II+III
S	Himeji-5				8			8	Rhyolite	2000	1989	11.0	0	0	1.00	1.00
S	Himeji-5				8			8	Rhyolite	2010	1989	21.0	0	0	1.00	1.00
S	Himeji-6		7	68	65			140	Rhyolite	2000	1994	6.0	7	75	0.95	0.46
S	Himeji-6		7	68	65			140	Rhyolite	2010	1994	16.0	7	75	0.95	0.46
S	Himeji-7		2	19	74	23		118	Rhyolite	2000	1990	10.0	2	21	0.98	0.82
S	Himeji-7		2	19	74	23		118	Rhyolite	2010	1990	20.0	2	21	0.98	0.82
S	Himeji-8				450			450	Rhyolite	2000	1990	10.0	0	0	1.00	1.00
S	Himeji-8				450			450	Rhyolite	2010	1990	20.0	0	0	1.00	1.00
S	Himeji-9				390			390	Rhyolite	2000	1990	10.0	0	0	1.00	1.00
S	Himeji-9				390			390	Rhyolite	2010	1990	20.0	0	0	1.00	1.00
S	Himeji-10				339			339	Rhyolite	2000	1990	10.0	0	0	1.00	1.00
S	Himeji-10				339			339	Rhyolite	2010	1990	20.0	0	0	1.00	1.00
S	Kobe-1				16			16	Sedimentary Rock	2000	1994	6.0	0	0	1.00	1.00
S	Kobe-1				16			16	Sedimentary Rock	2010	1994	16.0	0	0	1.00	1.00
S	Kobe-2				45	42		87	Sedimentary Rock	2000	1995	5.0	0	0	1.00	1.00
S	Kobe-2	1			45	41		87	Sedimentary Rock	2010	1995	15.0	1	1	0.99	0.99
S	Kobe-3				58			58	Sedimentary Rock	2000	1993	7.0	0	0	1.00	1.00
S	Kobe-3				58			58	Sedimentary Rock	2010	1993	17.0	0	0	1.00	1.00
S	Kobe-4				35			35	Sedimentary Rock	2000	1993	7.0	0	0	1.00	1.00
S	Kobe-4				35			35	Sedimentary Rock	2010	1993	17.0	0	0	1.00	1.00
S	Kobe-5				10	57		67	Sedimentary Rock	2000	1993	7.0	0	0	1.00	1.00
S	Kobe-5				10	57		67	Sedimentary Rock	2010	1993	17.0	0	0	1.00	1.00
S	Kobe-6				321			321	Sedimentary Rock	2000	1995	5.0	0	0	1.00	1.00
S	Kobe-6				321	295		616	Sedimentary Rock	2010	1995	15.0	0	0	1.00	1.00
S	Kobe-7				9			9	Sedimentary Rock	2000	1995	5.0	0	0	1.00	1.00
S	Kobe-8				5	101		106	Sedimentary Rock	2000	1995	5.0	0	0	1.00	1.00
S	Kobe-8				6	100		106	Sedimentary Rock	2010	1995	15.0	0	0	1.00	1.00
S	Kobe-9				27			27	Sedimentary Rock	2000	1994	6.0	0	0	1.00	1.00
S	Kobe-9				27			27	Sedimentary Rock	2010	1994	16.0	0	0	1.00	1.00
S	Kobe-10				48			48	Sedimentary Rock	2000	1994	6.0	0	0	1.00	1.00
S	Kobe-10				48			48	Sedimentary Rock	2010	1994	16.0	0	0	1.00	1.00
S	Kobe-11				372			372	Sedimentary Rock	2000	1994	6.0	0	0	1.00	1.00
S	Kobe-11				372			372	Sedimentary Rock	2010	1994	16.0	0	0	1.00	1.00
S	Kobe-12				31	80		111	Sedimentary Rock	2000	1994	6.0	0	0	1.00	1.00
S	Kobe-12				31	80		111	Sedimentary Rock	2010	1994	16.0	0	0	1.00	1.00
R	Kobe-13				43	122		165	Sedimentary Rock	2000	1996	4.0	0	0	1.00	1.00
R	Kyotan-3					12		12	Sedimentary Rock	2000	1994	6.0	0	0	1.00	1.00
R	Kyotan-3					12		12	Sedimentary Rock	2011	1994	17.0	0	0	1.00	1.00
R	Kyotan-4				3	167		170	Sedimentary Rock	2000	1994	6.0	0	0	1.00	1.00
R	Kyotan-4		3	3	4	160		170	Sedimentary Rock	2011	1994	17.0	3	6	0.98	0.96

Table 4.3 Summary of the Visual inspection data, New type ground anchor (Continue)

Type	Site	Visula Inspection							Geological Condition	Inspection Year	Install	Elasped time	No of Failure		Survival Prob	
		I	II	III	IV	V	VI	Sum					I+II	I+II+III	I+II	I+II+III
S	Kyotan-5				124	390		514	Sedimentary Rock	2000	1994	6.0	0	0	1.00	1.00
S	Kyotan-5	1		5	425	83		514	Sedimentary Rock	2011	1994	17.0	1	6	1.00	0.99
R	Kyotan-6				123			123	Sedimentary Rock	2000	1994	6.0	0	0	1.00	1.00
R	Kyotan-6		1	1	111			113	Sedimentary Rock	2011	1994	17.0	1	2	0.99	0.98
R	Ibaraki-5			1	40	308		349	Sedimentary Rock	2000	1994	6.0	0	1	1.00	1.00
R	Ibaraki-5			1	89	256		346	Sedimentary Rock	2012	1994	18.0	0	1	1.00	1.00
S	Ibaraki-6			1	87			88	Sedimentary Rock	2000	1996	4.0	0	1	1.00	0.99
S	Ibaraki-6			1	87			88	Sedimentary Rock	2012	1996	16.0	0	1	1.00	0.99
R	Ibaraki-7					305		305	Sedimentary Rock	2000	1994	6.0	0	0	1.00	1.00
R	Ibaraki-7				55	250		305	Sedimentary Rock	2012	1994	18.0	0	0	1.00	1.00
R	Ibaraki-8					365		365	Sedimentary Rock	2000	1996	4.0	0	0	1.00	1.00
R	Ibaraki-8				94	271		365	Sedimentary Rock	2012	1996	16.0	0	0	1.00	1.00
R	Ibaraki-9			3	2	69		74	Sedimentary Rock	2000	1996	4.0	0	3	1.00	0.96
R	Ibaraki-9			3	38	33		74	Sedimentary Rock	2012	1996	16.0	0	3	1.00	0.96
R	Ibaraki-10			1	220	117		338	Sedimentary Rock	2000	1996	4.0	0	1	1.00	1.00
R	Ibaraki-10		2	17	262	58		339	Sedimentary Rock	2012	1996	16.0	2	19	0.99	0.94
R	Ibaraki-11			1		15		16	Sedimentary Rock	2000	1996	4.0	0	1	1.00	0.94
R	Ibaraki-11			3	4	9		16	Sedimentary Rock	2012	1996	16.0	0	3	1.00	0.81
S	Ibaraki-12				282			282	Sedimentary Rock	2000	1996	4.0	0	0	1.00	1.00
S	Ibaraki-12		10	16	257			283	Sedimentary Rock	2012	1996	16.0	10	26	0.96	0.91
R	Ibaraki-13				18			18	Sedimentary Rock	2000	1996	4.0	0	0	1.00	1.00
R	Ibaraki-13				18			18	Sedimentary Rock	2012	1996	16.0	0	0	1.00	1.00
R	Ibaraki-14				30	70		100	Sedimentary Rock	2000	1996	4.0	0	0	1.00	1.00
R	Ibaraki-14			1	76	22		99	Sedimentary Rock	2012	1996	16.0	0	1	1.00	0.99
R	Ibaraki-15				30			30	Sedimentary Rock	2000	1996	4.0	0	0	1.00	1.00
R	Ibaraki-15		2	1	27			30	Sedimentary Rock	2012	1996	16.0	2	3	0.93	0.90
R	Ibaraki-16					78		78	Sedimentary Rock	2000	1999	1.0	0	0	1.00	1.00
R	Ibaraki-16					78		78	Sedimentary Rock	2012	1999	13.0	0	0	1.00	1.00
S	Fukusaki-1				24	105		129	Sedimentary Rock	2000	1995	5.0	0	0	1.00	1.00
S	Fukusaki-1				24	105		129	Sedimentary Rock	2012	1995	17.0	0	0	1.00	1.00
S	Minami-10				1	51		52	Granite	2000	1994	6.0	0	0	1.00	1.00
S	Minami-10				2	50		52	Granite	2011	1994	17.0	0	0	1.00	1.00
S	Minami-11				19	42		61	Granite	2000	1992	8.0	0	0	1.00	1.00
S	Minami-11	3	0	8	17	33		61	Granite	2011	1992	19.0	3	11	0.95	0.82
S	wakayama-6				5	11		16	Sedimentary Rock	2000	1992	8.0	0	0	1.00	1.00
S	wakayama-6			2	9	5		16	Sedimentary Rock	2011	1992	19.0	0	2	1.00	0.88
S	wakayama-7				10	24		34	Sedimentary Rock	2000	1992	8.0	0	0	1.00	1.00
S	wakayama-7			2	13	19		34	Sedimentary Rock	2011	1992	19.0	0	2	1.00	0.94
R	wakayama-8		6			389		395	Sedimentary Rock	2000	1994	6.0	6	6	0.98	0.98
R	wakayama-8	8	12	16	16	343		395	Sedimentary Rock	2011	1994	17.0	20	36	0.95	0.91
S	wakayama-9			1	10	135		146	Sedimentary Rock	2000	1994	6.0	0	1	1.00	0.99
S	wakayama-9		1	1	20	124		146	Sedimentary Rock	2011	1994	17.0	1	2	0.99	0.99

Four geological conditions were sedimentary, gabbro, rhyolite and granite rock type as tabulated on the 4th column. The last two columns showed the calculated of survival probability based on the scenario I and II, respectively. Note that, some slopes provided two or three data set caused the Visual inspection test were experimented two periods in 2000 and inspected again during 2009 to 2012.

The first anchor set was installed in Himeji No.2, No.3 and No.4 (Rhyolite rock) during 1981, the strand type was employed, whereas the last group was installed in Ibaraki No.16 (sedimentary rock) engaged rod type. Before 1988, the ground anchors called the old types,

after that they were improved by coated with additional chemicals to enhance rust resistance on the tendon bar, call as a new type. Therefore, the new type shall be longer life span caused its resisting for decaying; however, both types are still divided into rod and strand types.

The number of samples was compared among of different geological condition, including sedimentary, gabbro, rhyolite and granite rock as presented in Fig 4.2. They were installed in sedimentary rock about two third of whole data set, which is the largest group, on the other hand, they were installed in gabbro rock just one percent. Moreover, rhyolite and granite shared only 18% and 14%, respectively. It might be an inadequate sample to analysis the deterioration process if considers individually, therefore, gabbro, rhyolite and granite were regrouped as the igneous rock. Finally, the ground anchors installed in the igneous rock was found 33% that about one-third of total inspected data.

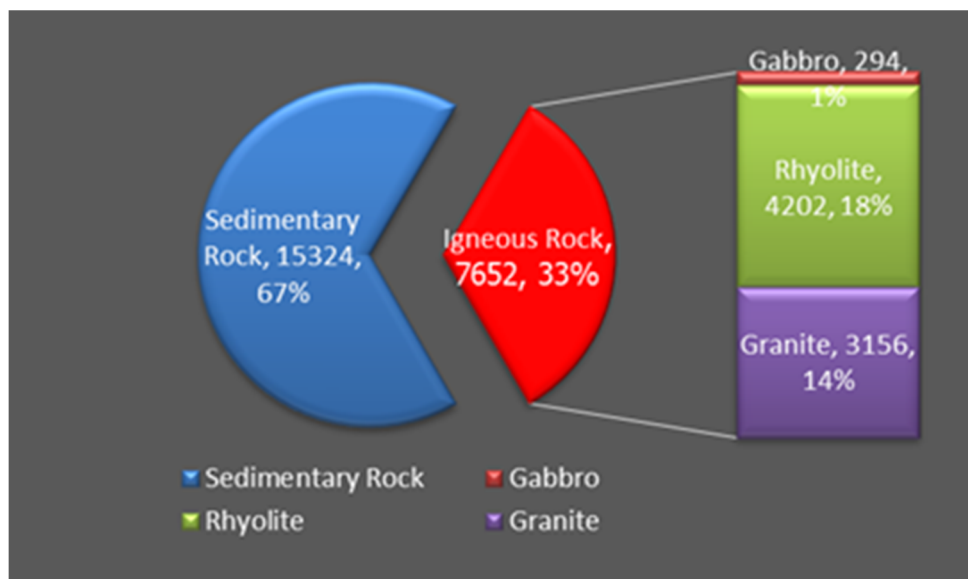
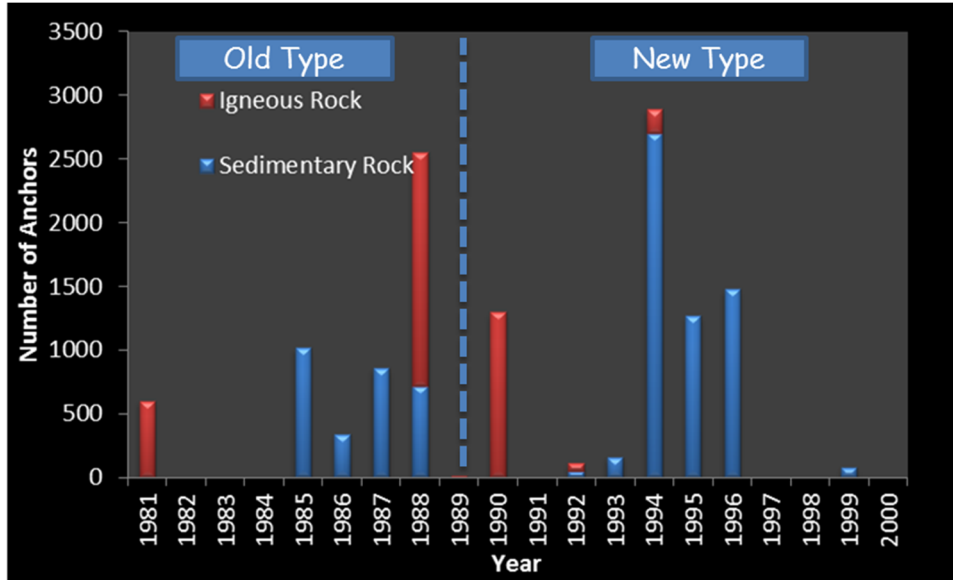


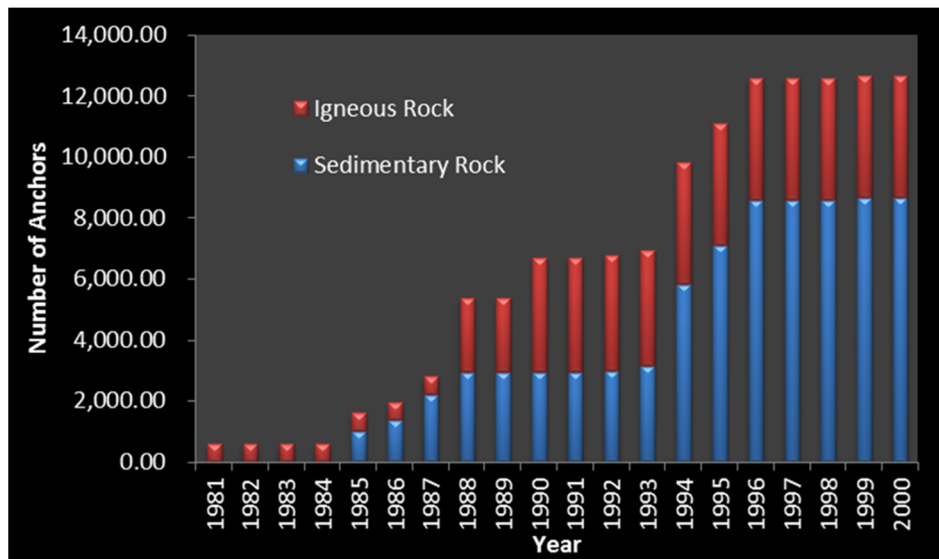
Figure 4.2 Comparison number of samples among of different geological conditions

Figure 4.3 (a) showed that the ground anchors were installed starting from 1981 until 1999. The cumulative of ground anchor installation in Kinki district were about 12,000 anchors (see Fig 4.3(b)). The first group about five hundred anchors were installed in igneous rock during 1981, and then installed on other slopes during 1985 to 1988. All the anchors installed in this period are the old type. After 1989, the new type anchors were adopted

started from 1990 in igneous rock. From 1992 to 1996, numerous anchors were installed particularly in 1994, however, mostly in sedimentary rock. The last group, only 78 ground anchors, was installed in 1999 in sedimentary rock.

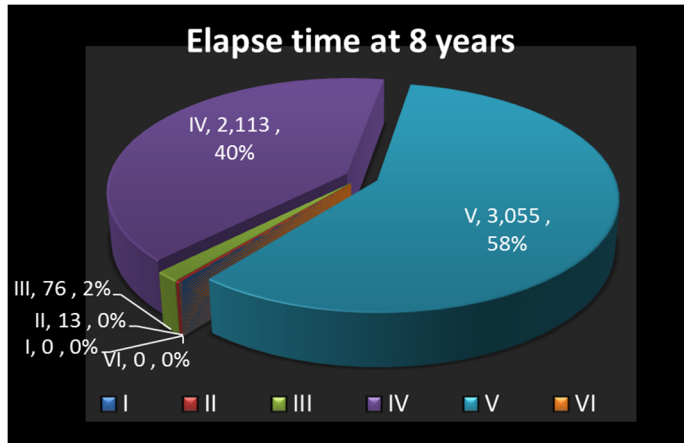


(a) Summary of ground anchor installation year

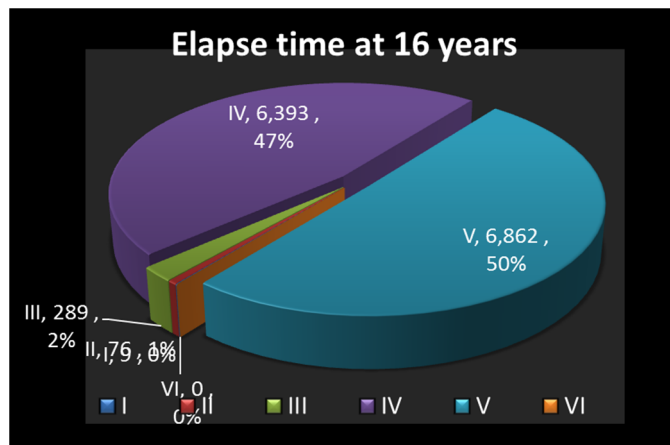


(b) Cumulative ground anchor installation

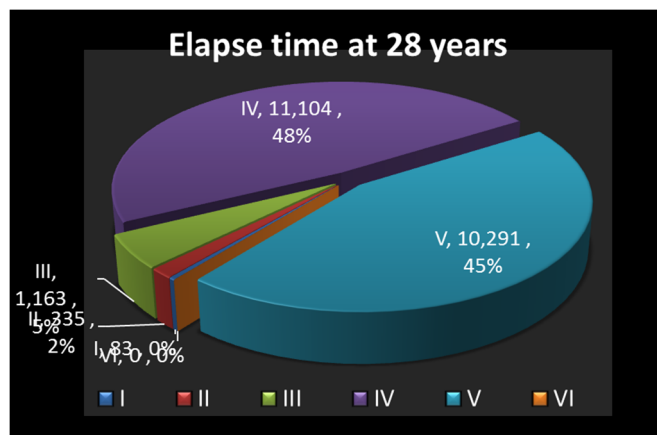
Figure 4.3 The installation year as well as the cumulative number of ground anchors in Kansai district



(a) Elapse time at 8 years



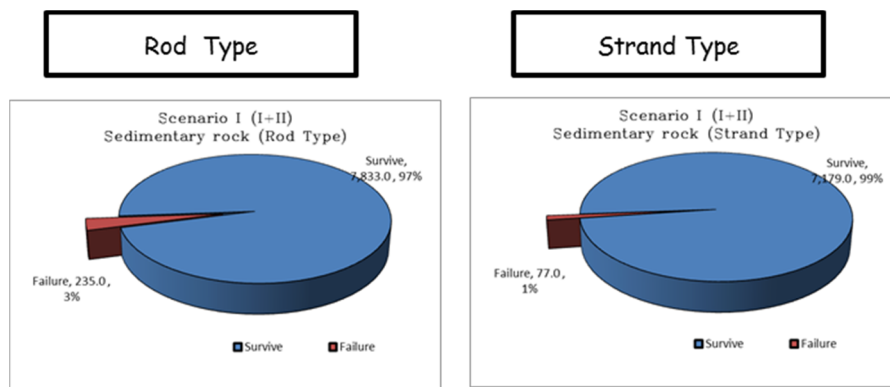
(b) Elapse time at 16 years



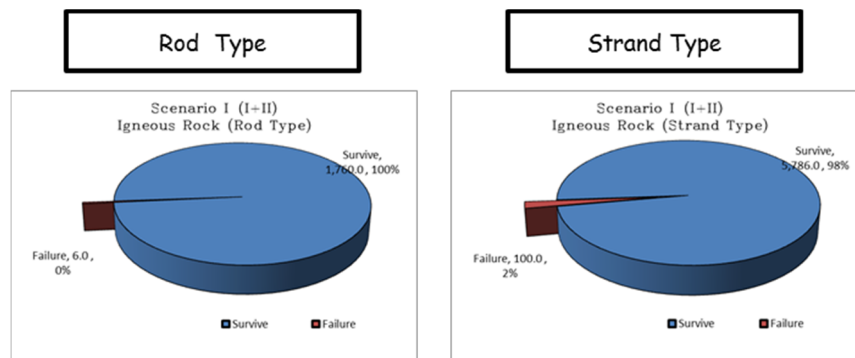
(c) Elapse time at 28 years

Figure 4.4 Percent sharing on each rank at 8, 16 and 28 years since installation

Figure 4.4 (a) to (c) illustrated the percent sharing on each rank at 8, 16 and 28 years since installation, respectively. These results indicated that the rank I, II, III and IV are increasing with time while rank V decrease because deterioration phenomenal of the ground anchors that transformed from the excellent condition to poor condition. In fact, percentage of the poor, marginal and fair conditions (rank I, II and III) which corresponding to failure ranks were slightly increased with time; however, they slightly rise compared with survival rank. Perhaps, because the conservatively judged by the expert engineer, the rank I seem to be quite rare to be found.



(a) Sedimentary Rock



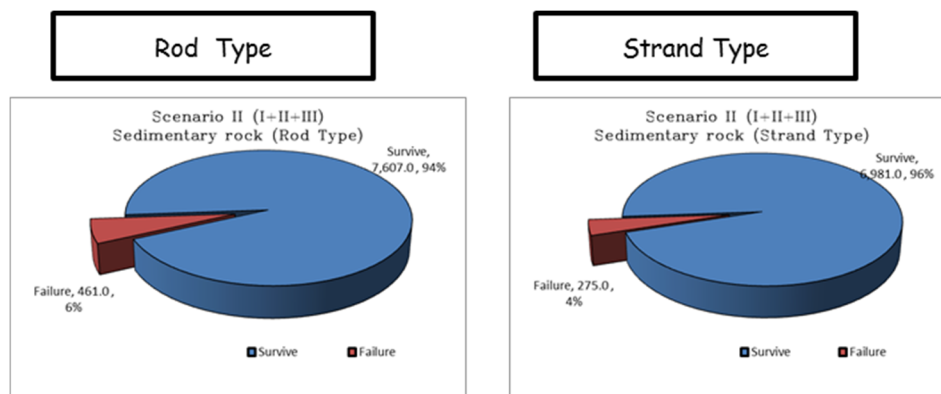
(b) Igneous Rock

Figure 4.5 The percentage of failure and survive ground anchors of the Scenario I

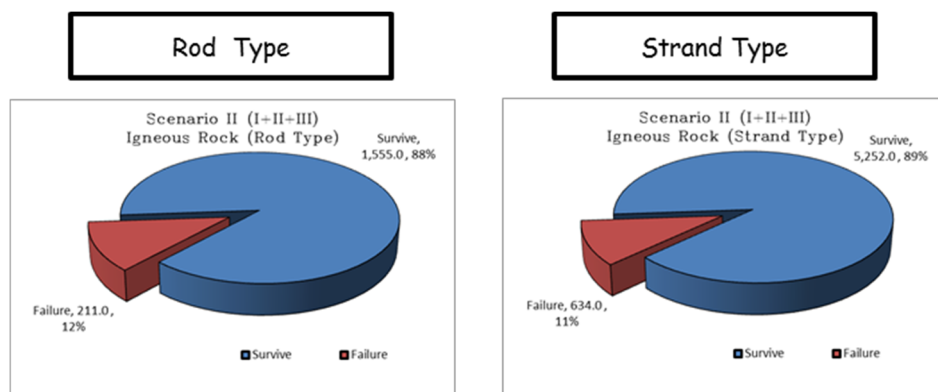
Figure 4.5 (a) and (b) illustrated the comparison on percentage of failure between rod and stand types of scenario I for sedimentary rock and igneous rock, respectively. The results revealed that just a few percentages of failure were found, especially in rod type of igneous rock demonstrated the non-failure data. On the same matter, the comparison of percentage

of failure between rod and strand types of scenario II of sedimentary rock and igneous rock were summarized as present in Fig 4.6 (a) and (b) respectively.

By comparing all data set, the scenario I showed lower percentages of failure, comparing with scenario II as expected since scenario I considered only rank I and II corresponding to failure while scenario II including rank III. By comparing the percentage of failure, rod type seems to be greater than the strand type except igneous rock of scenario I. Furthermore, sedimentary rock demonstrated lower percentage of failure, compared with the igneous rock on the same type of anchor; however just rod type of scenario I showed opposite results. The reason is that the amount of data allowance is limited, only 1,760 samples, while the other contained data more than 5,000 samples.



(a) Sedimentary Rock



(b) Igneous Rock

Figure 4.6 The percentage of failure and survive ground anchors of the Scenario II

4.3 The Lift off Test Data

This study, the Lift off tests were experimented during 2000 and 2009 to 2012 on the slopes along the highways same location with the Visual inspection test. However, the budget allocated was limited to conduct all anchors, the selected spots, including seven routes, 38 slopes, which comprise of Fukuchiyama 9 slopes, Himeji 5 slopes, Kobe 3 slopes, Kyotan 3 slopes, Ibaraki, 4 slopes, Minami 9 slopes and Wakayama 5 slopes, which are total 240 samples as presented in Fig 4.7.

Four geological conditions were grouped, which are sedimentary, gabbro, rhyolite and granite rock types which are same with the Visual inspection test. Therefore, for convenient to analysis, there were re-categorized to be two rock groups, which are sedimentary and igneous rocks. Moreover, the ground anchors were compared by divided into two types, which are rod and strand types because it cannot separately analyze between new and old type of ground anchors due to inadequate data.

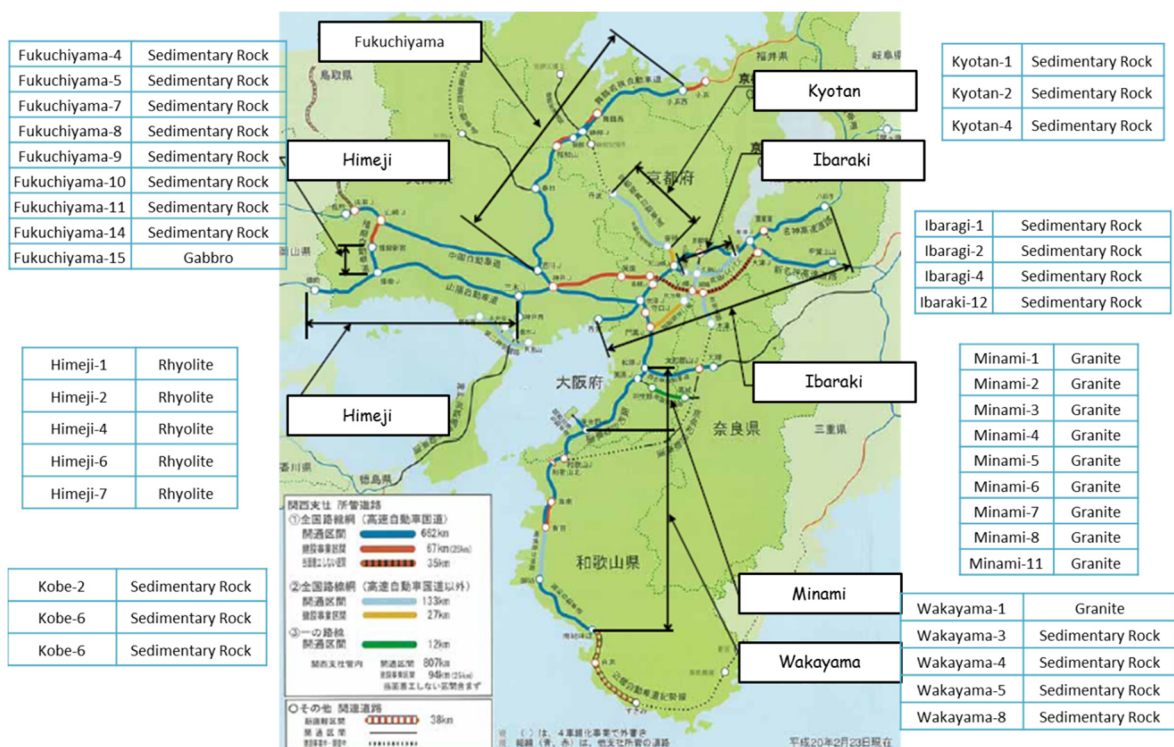


Figure 4.7 Routes and data of the Lift off test obtained from field test

The Lift off test was experimented on each slope about five to ten anchors scattering on whole improved areas. The testing spots were decided by expert engineers considered from the Visual inspection results to verify the anchors force. The *R* and *S* in the first column of Table 4.4 denotes the rod and strand types, respectively. The failure criteria were divided into two categories with are the present anchors force excess of 120% and less than twenty percent compared with the design force corresponding to fail (excessive overstressed and heavily deteriorated, respectively).

Table 4.4 Summary of the Lift off test data

Type	Site	Rock Type	Inspection Year	Install	Elapsed time	Lift-off test		
						No of Anchor	No of Failure	Survival Prob
R	Fukuchiyama-4	Sedimentary Rock	2009	1986	23	5	1	0.80
S	Fukuchiyama-5	Sedimentary Rock	2009	1985	24	5	0	1.00
R	Fukuchiyama-7	Sedimentary Rock	2009	1985	24	5	1	0.80
S	Fukuchiyama-8	Sedimentary Rock	2009	1986	23	5	3	0.40
R	Fukuchiyama-9	Sedimentary Rock	2010	1985	25	10	2	0.80
R	Fukuchiyama-10	Sedimentary Rock	2009	1985	24	5	0	1.00
R	Fukuchiyama-11	Sedimentary Rock	2009	1985	24	5	2	0.60
S	Fukuchiyama-14	Sedimentary Rock	2010	1988	22	5	0	1.00
R	Fukuchiyama-15	Gabbro	2010	1988	22	8	7	0.13
S	Himeji-1	Rhyolite	2009	1988	21	5	0	1.00
S	Himeji-2	Rhyolite	2009	1981	28	6	0	1.00
S	Himeji-4	Rhyolite	2010	1984	26	10	0	1.00
S	Himeji-6	Rhyolite	2010	1994	16	5	0	1.00
S	Himeji-7	Rhyolite	2010	1990	20	5	0	1.00
S	Minami-1	Granite	2009	1988	21	5	0	1.00
S	Minami-2	Granite	2009	1988	21	5	0	1.00
S	Minami-3	Granite	2010	1988	22	5	0	1.00
S	Minami-4	Granite	2009	1988	21	6	2	0.67
S	Minami-5	Granite	2009	1988	21	7	1	0.86
S	Minami-6	Granite	2009	1988	21	5	1	0.80
S	Minami-7	Granite	2009	1988	21	13	5	0.62
S	Minami-8	Granite	2009	1988	21	5	2	0.60
S	Minami-11	Granite	2011	1992	19	5	0	1.00
R	Wakayama-1	Granite	2009	1988	21	5	1	0.80
R	wakayama-3	Sedimentary Rock	2009	1988	21	5	0	1.00
R	wakayama-4	Sedimentary Rock	2009	1988	21	5	2	0.60
R	Wakayama-5	Sedimentary Rock	2010	1987	23	5	0	1.00
R	Wakayama-8	Sedimentary Rock	2011	1994	17	12	5	0.58
S	Ibaragi-1	Sedimentary Rock	2010	1987	23	5	0	1.00
R	Ibaragi-2	Sedimentary Rock	2010	1987	23	10	9	0.10
R	Ibaragi-4	Sedimentary Rock	2010	1987	23	14	6	0.57
S	Ibaraki-12	Sedimentary Rock	2012	1995	17	12	3	0.75
S	Kyotan-1	Sedimentary Rock	2010	1988	22	5	0	1.00
R	Kyotan-2	Sedimentary Rock	2009	1988	21	5	0	1.00
S	Kyotan-4	Sedimentary Rock	2011	1994	17	10	9	0.10
S	Kobe-2	Sedimentary Rock	2010	1995	15	6	4	0.33
S	Kobe-6	Sedimentary Rock	2010	1995	15	5	0	1.00
S	Kobe-6	Sedimentary Rock	2000	1995	5	13	0	1.00

The comparisons of the obtained results between two types of geological conditions were presented in Fig 4.8. The ground anchors installed in sedimentary and igneous rock were 3,431 and 2,082 anchors, corresponding to 62% and 38% percent, respectively. It implied that the mainly results obtained from the ground anchors installed in sedimentary rock while only one-third were obtained from the igneous rock.

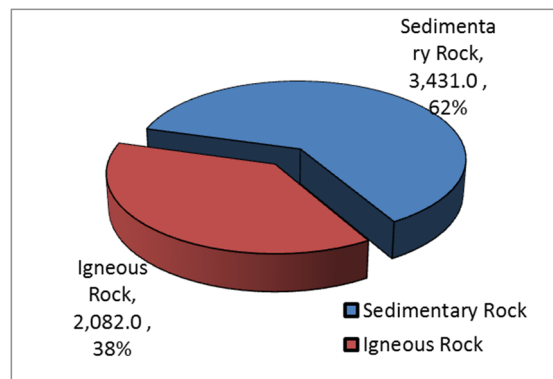


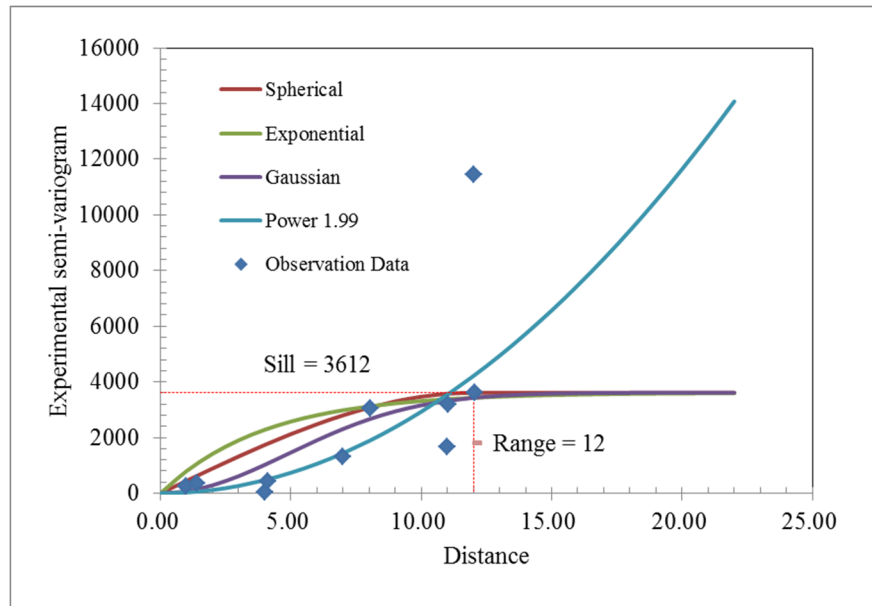
Figure 4.8 Comparison between rod type and strand type of the Lift off test

4.3.1 The Kriging Results

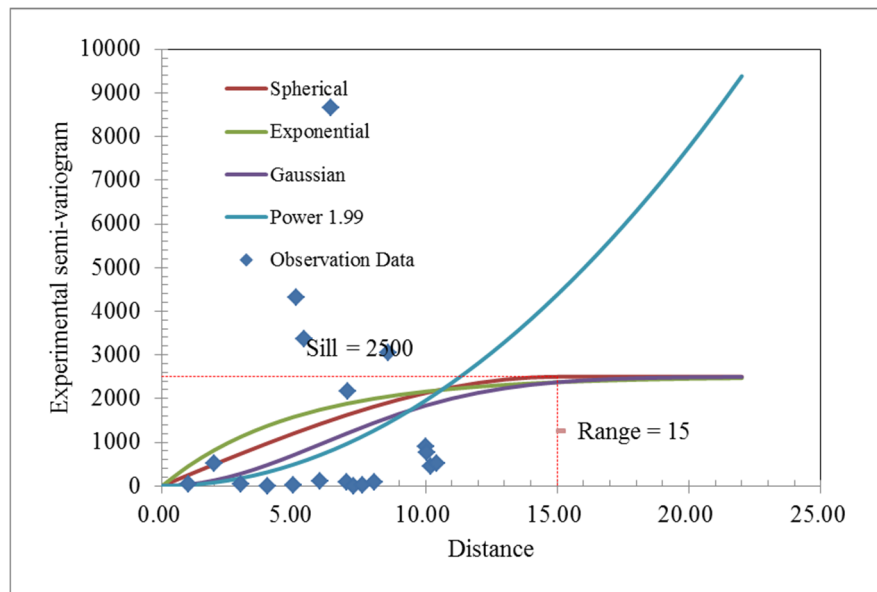
The semi-variogram was calculated and compared to judge the suitable model for calculating kriging. Figure 4.9 (a) to (b) illustrate the example of the comparison results of four empirical semi-variogram models consisting of Spherical, Exponential, Gaussian and Power models of Wakayama No.5 and Ibaraki No.2, respectively. By comparing, the results of three semi-variogram models, which are Spherical, Exponential and Gaussian models show similar trends. At the early stage of experimental semi-variogram, the Exponential, Spherical and Gaussian models showed its value from high to low, respectively. In case of Power model, the values of the semi-variogram shows drastically increase with distance from the original point.

In addition, kriging results can be presented as the contour line together with filled color as illustrated in Fig 4.10 for Fukuchiyama No.15 and Fig 4.11 for Ibaraki No.2, respectively. The shading color indicated the contour line of remaining anchor force. The red color means high deteriorated zones whereas green is lower deteriorated portions. The black dashed line specified the failure zone corresponding to the existing force lower than twenty

percent of the initial installed force. The results among of four models showed similar outcomes than low deteriorated on the lower left portion in Fukuchiyama No.15 corresponding to one-fourth of whole anchors are still survive approximately. Ibaraki No.2 illustrated lower left zone is high remaining force which about ten percent still survived. However, the Gaussian model results of Ibaraki No.2 showed the strange shape comparing with the others because it is depending on the semi-variogram.



(a) Wakayama No.5



(b) Ibaraki No.2

Figure 4.9 Example results of semi-variogram

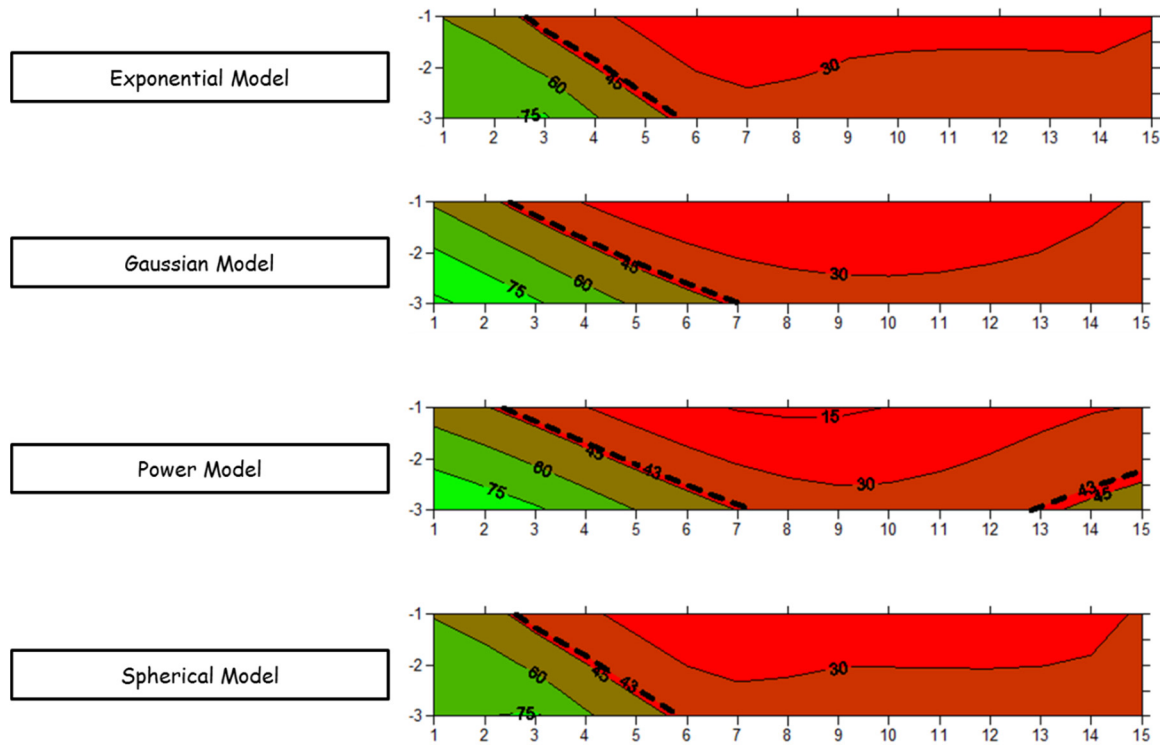


Figure 4.10 Kriging results of Fukuchiyama No.15

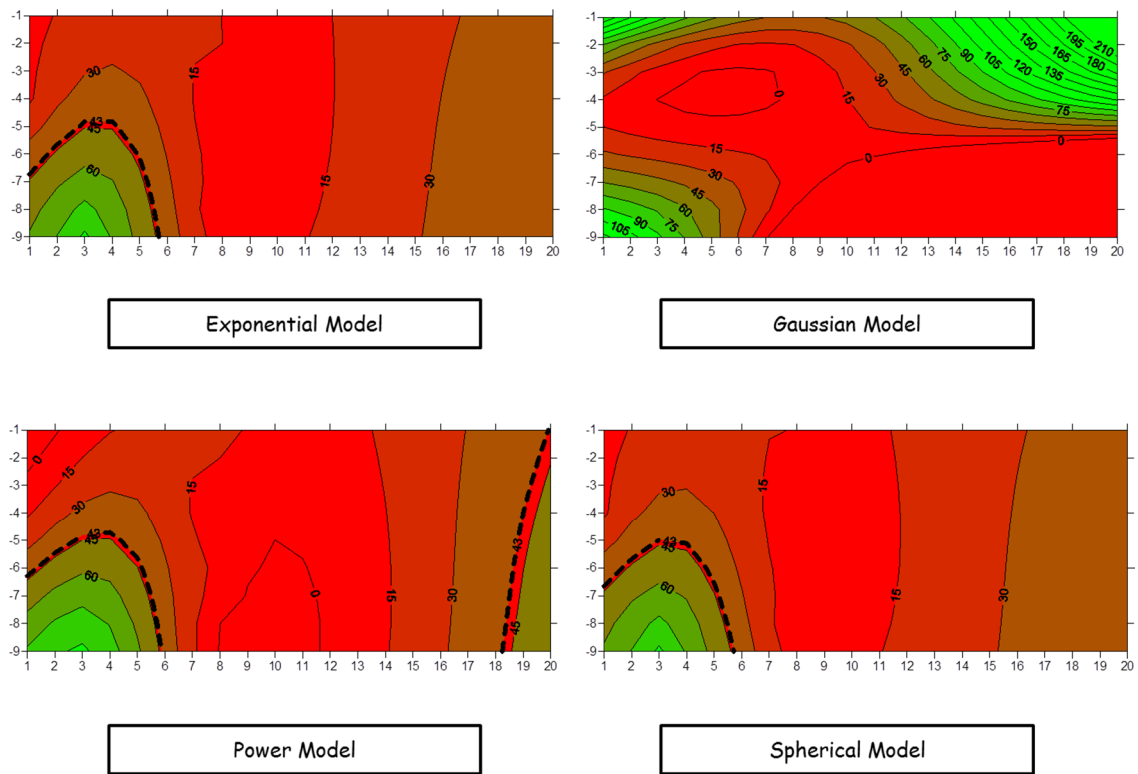
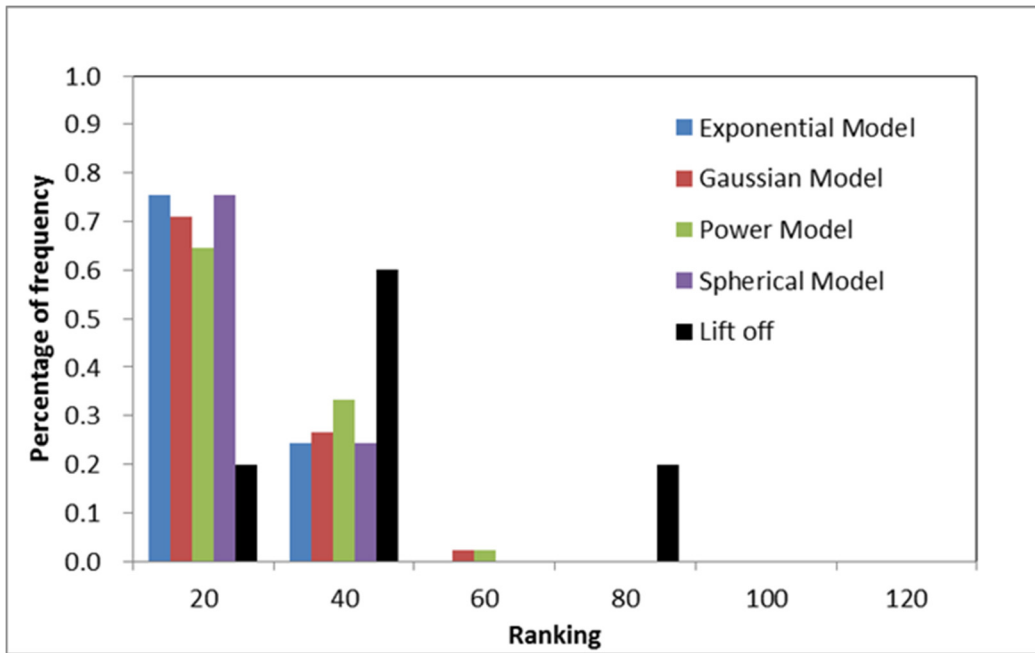
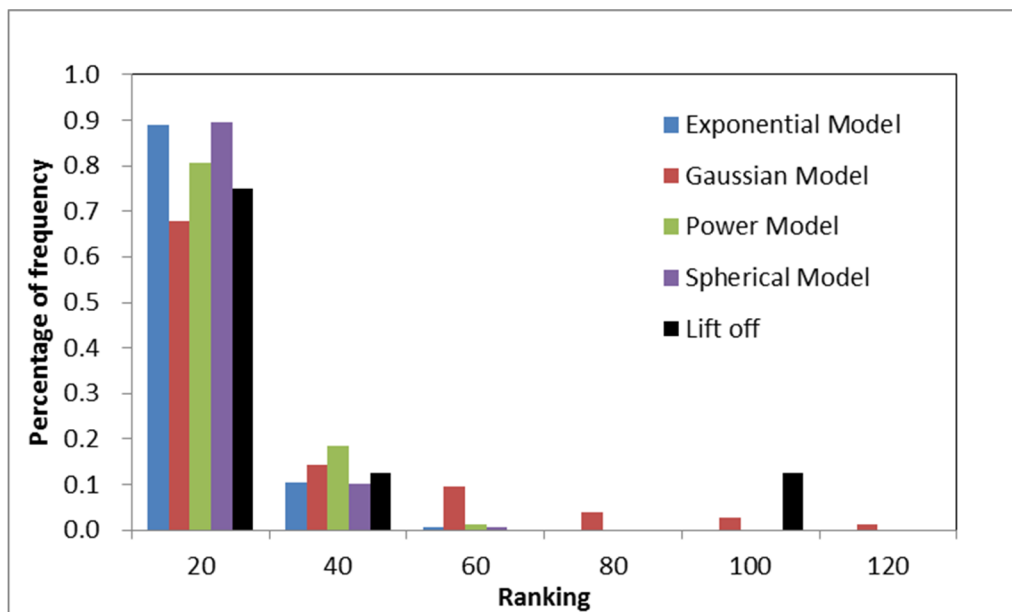


Figure 4.11 Kriging results of Ibaraki No.2



(a) Fukuchiyama No.15



(b) Ibaraki No.2

Figure 4.12 Histogram comparison among of four models and the Lift off test

Figure 4.12 (a) and (b) present the results of histogram compared between simulated by four semi-variogram models and the field data obtained by Lift off tests, the horizontal axis showed the ranking considered the twenty percent interval of the remaining force while the vertical axis presented percentage of frequency. Four simulated models revealed almost

same results and close to the Lift off test; particularly, on the Ibaraki No.2. In fact, the number of Lift off test was conducted only five and ten samples on Fukuchiyama No.15 and Ibaraki No.2, respectively; therefore, the comparison results of Ibaraki No.2 seem to be closer than Fukuchiyama No.15. The magnitude of the anchor's force directly affected to the stability of slopes; therefore, the interpolate results by kriging technique plays an important role in the safety of factor. The summaries of anchor's forces on each model were presented in Fig 4.13 (a) and (b) for Fukuchiyama No.15 and Ibaraki No.12, respectively. By comparing, all of kiging results revealed almost same total anchors forces except the Gaussian models of Ibaraki No.2. Therefore, every model might be able to interpolate kriging.

However, consider the tendency of data associated with semi-variogram as demonstrated in Fig 4.9, the Power model with ω of 1.99 might be more suitable because the calculated semi-variogram of obtained data increasing with distance as well as sill does not clearly appear. Therefore, the kriging interpolate based on the Power model with ω of 1.99 was employed as the representative model in this study.

	Exponential Model	Gaussian Model	Power Model	Spherical Model
Σ_{force}	1,724.27	1,753.07	1,787.94	1,720.53

(a) Fukuchiyama No.15

	Exponential Model	Gaussian Model	Power Model	Spherical Model
Σ_{force}	4,940.17	7,440.54	4,570.27	4,937.19

(b) Ibaraki No.2

Figure 4.13 Total anchors force of each models based on kriging results

4.3.2 Comparison of the Survival Probability of the Lift off test and kriging results

The results of kriging on individual slopes were summarized as listed in Table 4.5. By comparing, the survival probability from both kriging and the Lift off test results revealed similar outcomes.

Table 4.5 Summary of the Lift off test data and survival probability

Type	Site	Rock Type	Inspection Year	Install	Elapsed time	Lift-off test			Kriging		
						No of Anchor	No of Failure	Survival Prob	No of Anchor	No of Failure	Survival Prob
R	Fukuchiyama-4	Sedimentary Rock	2009	1986	23	5	1	0.80	61	8	0.87
S	Fukuchiyama-5	Sedimentary Rock	2009	1985	24	5	0	1.00	180	17	0.91
R	Fukuchiyama-7	Sedimentary Rock	2009	1985	24	5	1	0.80	84	22	0.74
S	Fukuchiyama-8	Sedimentary Rock	2009	1986	23	5	3	0.40	116	82	0.29
R	Fukuchiyama-9	Sedimentary Rock	2010	1985	25	10	2	0.80	48	6	0.88
R	Fukuchiyama-10	Sedimentary Rock	2009	1985	24	5	0	1.00	71	0	1.00
R	Fukuchiyama-11	Sedimentary Rock	2009	1985	24	5	2	0.60	81	35	0.57
S	Fukuchiyama-14	Sedimentary Rock	2010	1988	22	5	0	1.00	133	0	1.00
R	Fukuchiyama-15	Gabbro	2010	1988	22	8	7	0.13	45	32	0.29
S	Himeji-1	Rhyolite	2009	1988	21	5	0	1.00	52.0	11	0.79
S	Himeji-2	Rhyolite	2009	1981	28	6	0	1.00	299.0	0	1.00
S	Himeji-4	Rhyolite	2010	1984	26	10	0	1.00	112.0	6	0.95
S	Himeji-6	Rhyolite	2010	1994	16	5	0	1.00	138.0	0	1.00
S	Himeji-7	Rhyolite	2010	1990	20	5	0	1.00	74.0	0	1.00
S	Minami-1	Granite	2009	1988	21	5	0	1.00	80.0	0	1.00
S	Minami-2	Granite	2009	1988	21	5	0	1.00	57.0	0	1.00
S	Minami-3	Granite	2010	1988	22	5	0	1.00	132.0	0	1.00
S	Minami-4	Granite	2009	1988	21	6	2	0.67	60.0	7	0.88
S	Minami-5	Granite	2009	1988	21	7	1	0.86	54.0	21	0.61
S	Minami-6	Granite	2009	1988	21	5	1	0.80	115.0	11	0.90
S	Minami-7	Granite	2009	1988	21	13	5	0.62	110.0	49	0.55
S	Minami-8	Granite	2009	1988	21	5	2	0.60	44.0	18	0.59
S	Minami-11	Granite	2011	1992	19	5	0	1.00	61.0	5	0.92
R	Wakayama-1	Granite	2009	1988	21	5	1	0.80	649.0	260	0.60
R	wakayama-3	Sedimentary Rock	2009	1988	21	5	0	1.00	54	0	1.00
R	wakayama-4	Sedimentary Rock	2009	1988	21	5	2	0.60	63	11	0.83
R	Wakayama-5	Sedimentary Rock	2010	1987	23	5	0	1.00	36	0	1.00
R	Wakayama-8	Sedimentary Rock	2011	1994	17	12	5	0.58	395	213	0.46
S	Ibaragi-1	Sedimentary Rock	2010	1987	23	5	0	1.00	228.0	0	1.00
R	Ibaragi-2	Sedimentary Rock	2010	1987	23	10	9	0.10	180	161	0.11
R	Ibaragi-4	Sedimentary Rock	2010	1987	23	14	6	0.57	234	114	0.51
S	Ibaraki-12	Sedimentary Rock	2012	1995	17	12	3	0.75	209.0	64	0.69
S	Kyotan-1	Sedimentary Rock	2010	1988	22	5	0	1.00	93	3	0.97
R	Kyotan-2	Sedimentary Rock	2009	1988	21	5	0	1.00	40	0	1.00
S	Kyotan-4	Sedimentary Rock	2011	1994	17	10	9	0.10	172.0	124	0.28
S	Kobe-2	Sedimentary Rock	2010	1995	15	6	4	0.33	85.0	24	0.72
S	Kobe-6	Sedimentary Rock	2010	1995	15	5	0	1.00	629.0	0	1.00
S	Kobe-6	Sedimentary Rock	2000	1995	5	13	0	1.00	239.0	0	1.00

Alternatively, they also can be compared as presented in Fig 4.14 for convenience to be comprehended. The horizontal axis is the survival probability calculated by kriging while the vertical axis is directly calculated by the Lift off test. In addition, the dashed red line is the reference line that indicated the ideal relationship. Survival probability results of each slope were plotted, and whole data seem to lay nearby the reference line. Additionally, the trend line was plotted to validate the relationship of both methods; they showed an acceptable correlation. Therefore, kriging technique appeared the applicable method to

estimate the force nearby testing results; moreover, if more obtained data allowable, the kriging results might be more pleasurable.

The comparison results between of the survive (blue) and the failure (red) anchors of different anchors types were presented in Fig 4.15. The results illustrated the failure anchor about 30% and 11%, approximately corresponding to rod type and strand type, respectively. This percentage of sharing results implied that the life span of the rod type shall be shorter than the strand types; therefore, the rod type should be closely inspected the tension force efficiency.

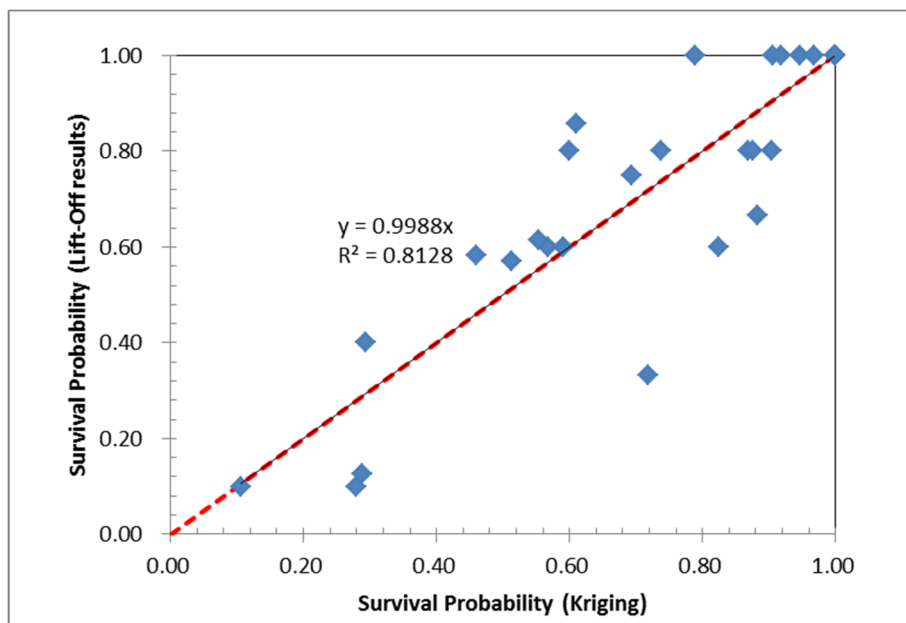


Figure 4.14 Comparison between survival probabilities of kriging and lift off test results

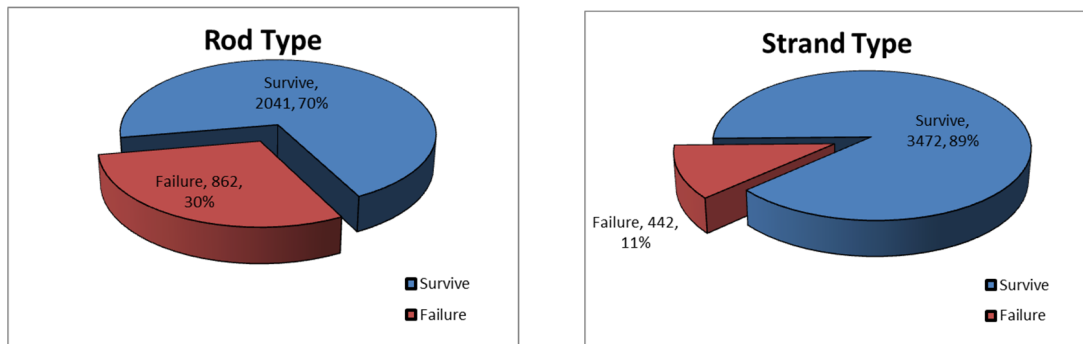


Figure 4.15 The percentages of failures and survives ground anchors of the rod and strand types

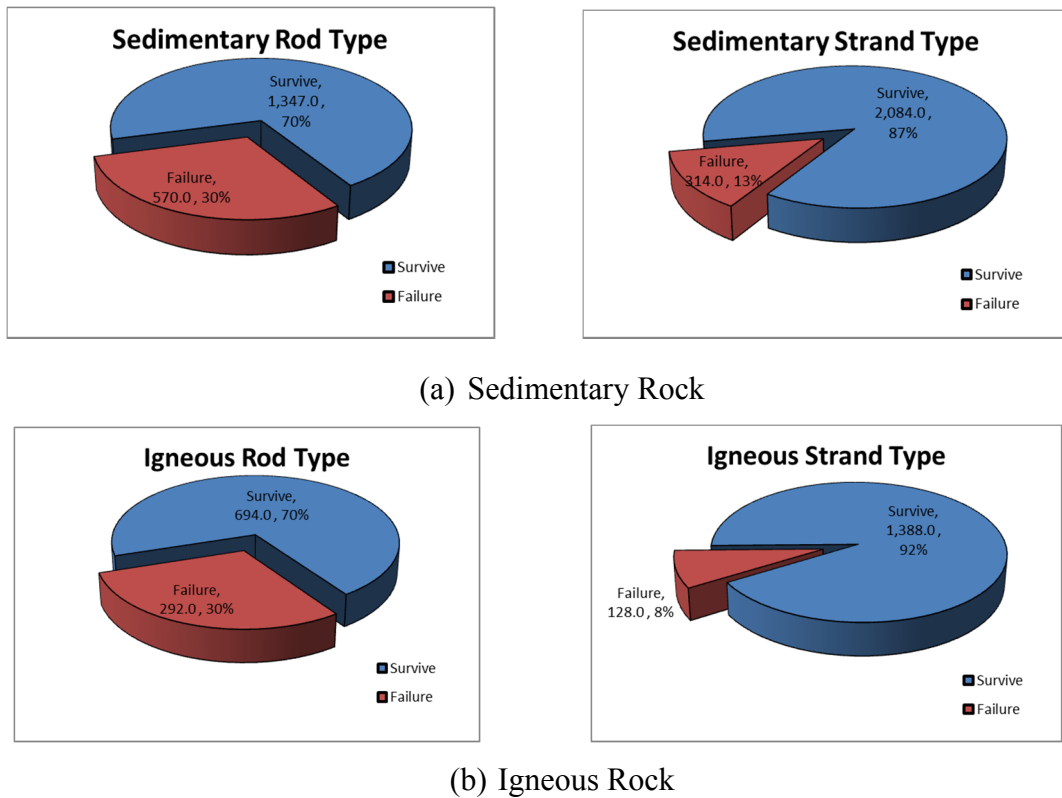


Figure 4.16 The percentages of failures and survives ground anchors of the sedimentary and igneous rock

4.4 The Ultrasonic test result

The results of Ultrasonic test were presented as an amplitude wave, a measurement of the size of a wave. In ultrasonic testing, changes in signal amplitude may indicate defects in a material as illustrated in Fig 4.17. The sound energy is to propagate in the wave form of the samples. The Ultrasonic wave signal is transformed into an electrical signal by the transducer and back to the receiver by displayed on a screen. This wave is presented versus the time for signal generation. When there is a flaw (such as a crack or discontinuity) detected, a part of the wave will be reflected back from the defect surface. It also related to the distance that the signal traveled through the samples.

Some of the pros of Ultrasonic inspection that are often cited included non-destructive tests, does not require access to both sides of the sample, easily deployed, inexpensive test, etc. In contrast, there are still some disadvantages such as calibration requires for each

material, good contact with the material is necessary, cannot take a measurement over rust and interpretation needs experience.

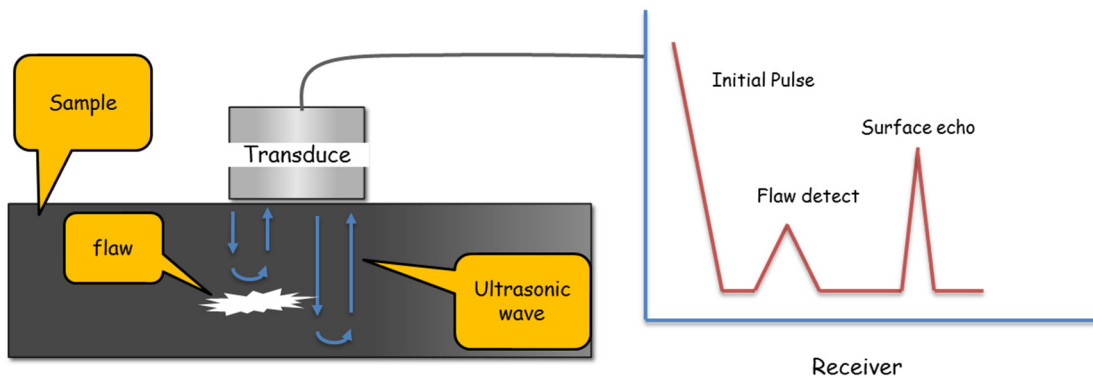


Figure 4.17 The basic concept of the Ultrasonic test

In this studied, the Ultrasonic tests were proposed to evaluate the existing force of ground anchors as an indirect method because they are faster comparing with the Lift off tests. The assumption of this studied was an amplitude of the Ultrasonic test proportionally increased with the remaining force obtained from Lift off tests. However, the results of Ultrasonic tests fluctuated varying from each testing (see Fig 4.18). Therefore, it is necessary to calibrate associate with statistical approaches.

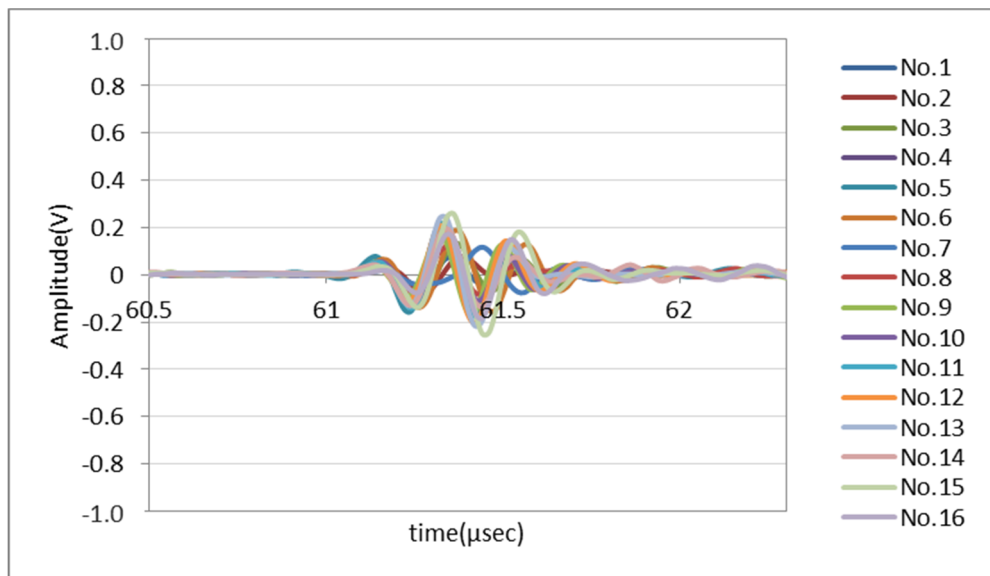
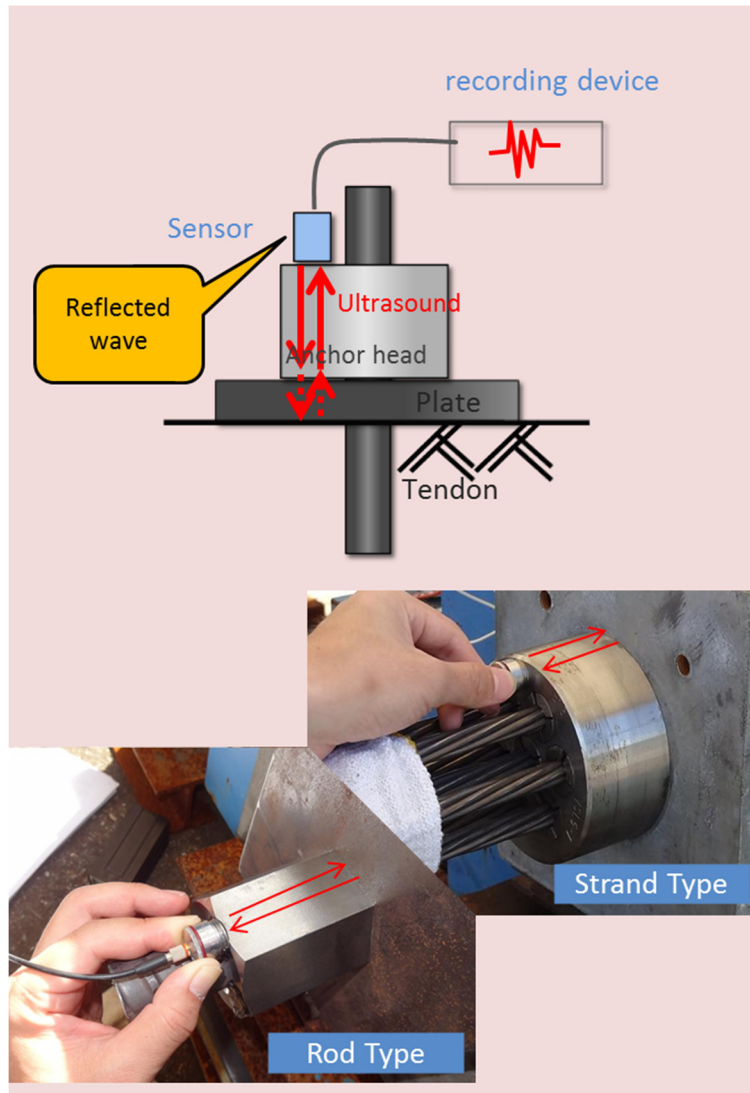
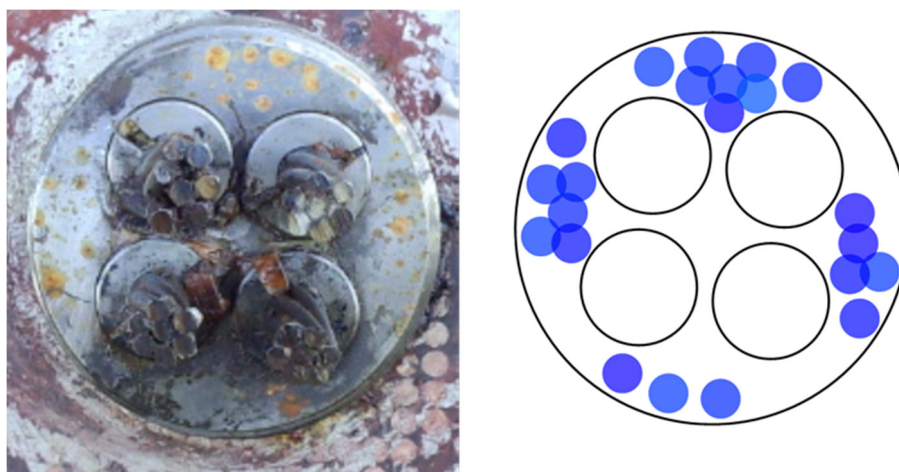


Figure 4.18 The Ultrasonic test results fluctuated varying from each testing



(a) Ultrasonic test on the anchor's head



(b) Testing spots on anchors head

Figure 4.19 The example of the Ultrasonic test on ground anchors

The Ultrasonic tests were experimented with a transformed ultrasonic wave via ground anchors head as illustrated in Fig 4.19 (a). Before testing, ground anchors shall be clean and dry conditions because its results are quite sensitive to the contact between transducers and sample's surface. This method can be adopted on both rod and strand types. Usually, Ultrasonic tests were conducted spreading on whole anchor's head (see Fig 4.19 (b)) to eliminate errors due to equipment as well as human. The average values of each anchor were calibrated with actual existing forces to be obtained the regression curve.

Ultrasonic testing is generally referred as an acoustic wave propagated into material from the transducer and reflected back to the receivers to be detected the discontinuities, composition of layers, defect in a material, thickness and so on. Its results can be demonstrated by acoustic reflection versus time-varying. Many different patterns of vibrational motion are shown in Fig 4.20; depending on changing of their materials or layers.

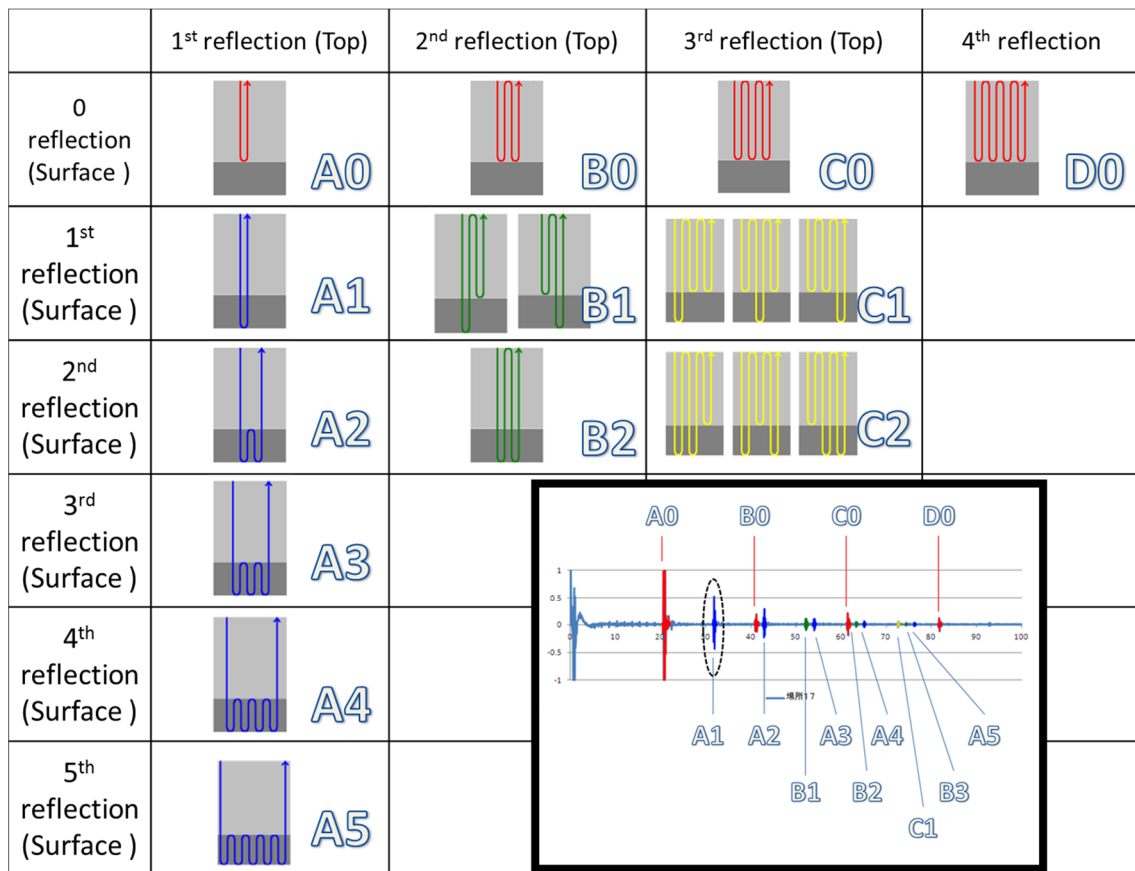


Figure 4.20 The reflection characteristics of Ultrasonic wave

The results of reflections on an acoustic wave can be divided into several patterns, for example, the first, second, third and fourth reflections are corresponding to single, double, triple and quadruple reflected from the second layer (*A0*, *B0*, *C0* and *D0*, respectively) while *A1* is an echo of the top of third layers. However, it is too difficult to explain the behaviors after second reflecting on top of third layers because it cannot identify whether an echo from which layers; therefore, it was abandoned. Moreover, its magnitude is so small and combining with other resonances. Therefore, the *A1* was determined the results of Ultrasonic test to be calibrated with actual existing force obtained by Lift off test results.

4.4.1 Statistic Approach

Fifteen ground anchors were experimented spreading on a slope, namely Fukuchiyama No.20, by both Lift off tests and the Ultrasonic tests as illustrated Fig 4.21. The locations of testing were marked as the red circles. This slope consists of a hundred ground anchors, five raw and twenty column, a SHS S5-4 type (strand type, allowable force of 440 kN). Therefore, the failure criteria of ground anchors were 70kN for heavily deteriorated condition and 442 kN for excessive overstressed condition, corresponding to 20% and 120% of the design force, respectively. In addition, the Lift off test results were summarized as tabulated in Table 4.6. In brief, only two anchors were in heavily deteriorated condition on the fifth row No.3 and 15 whereas excessive overstressed condition was not found.

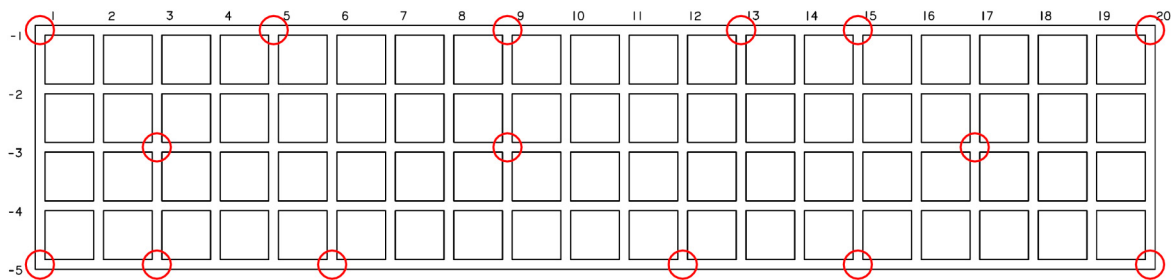


Figure 4.21 Location of the Lift off test on Fukuchiyama No.20

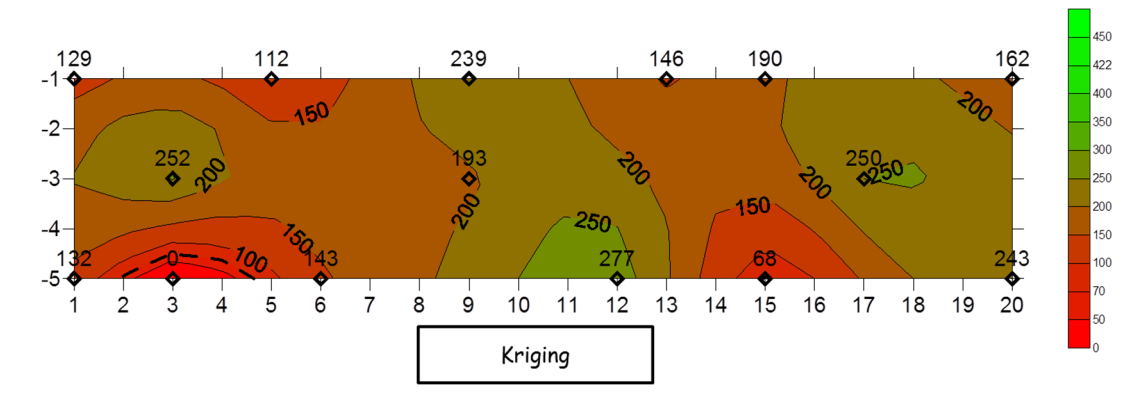
Table 4.6 Summary of Lift off test results of Fukuchiyama No.20

Coordinate		Lift off results (kN)
X	Y	
3	-5	0
15	-5	68
5	-1	112
1	-5	132
6	-5	143
13	-1	146
9	-3	193
9	-1	239
20	-5	243
3	-3	252
12	-5	277
20	-1	162
17	-3	250
15	-1	190
1	-1	129

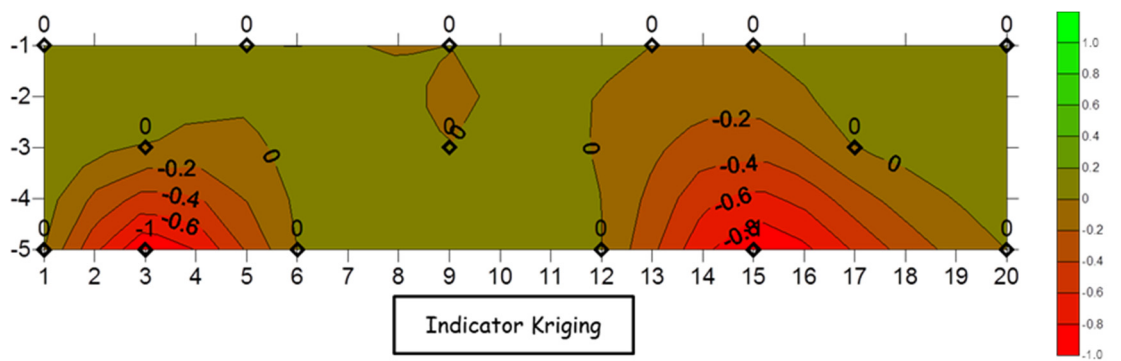
The Lift off test results was analyzed associated with the both kriging and indicator kriging in order to specify the failure zone of the anchors. The power model was applied to be a representative model since it is the most appropriate comparing with others as mentioned on early chapter. In addition, the criteria of indicator kriging can set up and expressed as follows;

$$IK(T_D, T_L) = \left\{ \begin{array}{ll} -1 & \text{if } T_L < 0.20T_D \\ 0 & \text{if } 0.20T_L \leq T_L \leq 1.20T_D \\ +1 & \text{if } T_L > 1.20T_D \end{array} \right\} \quad (4.1)$$

The danger zones were indicated as the dashed black line for kriging results, whereas the red color shading with the number defined of -1 for the indicator kriging result as presented in Fig 4.22 (a) and (b), respectively. Their results revealed that only two areas were in heavily deteriorated condition, which located on the 5th row; however, without the overstress condition on this slope. Moreover, some zone showed risky condition such as on the top left of kriging results. In contrast, critical zone does not find on the indicator kriging result.



(a) Kriging result



(b) Indicator kriging

Figure 4.22 Results of the Lift off test

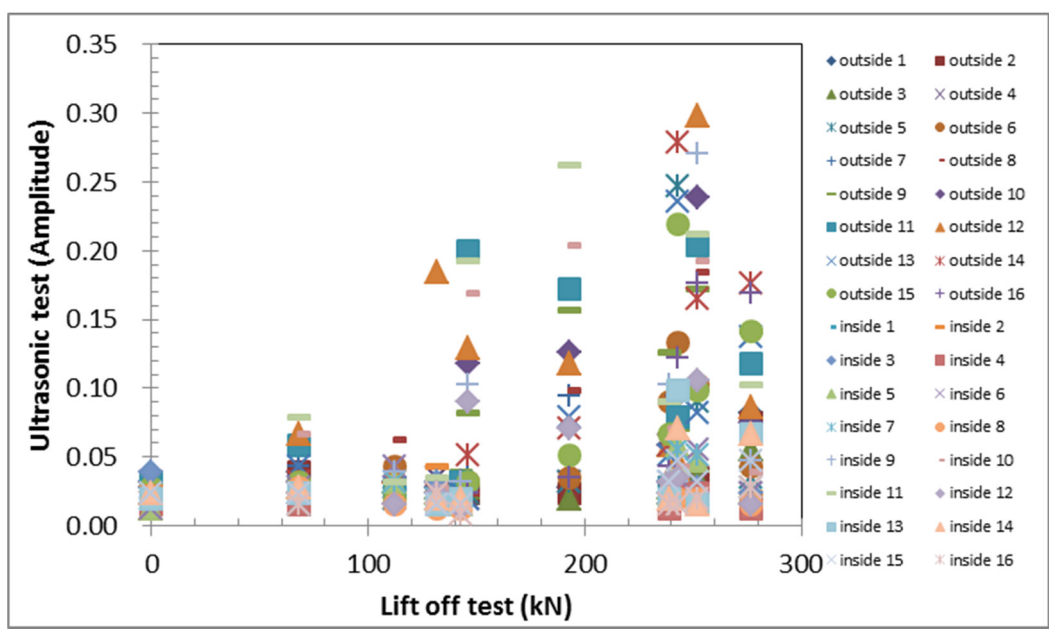


Figure 4.23 Relationship between amplitude from Ultrasonic test versus existing force from Lift off test

The relationship between the Ultrasonic test results versus the Lift off test results was displayed in Fig 4.23 that the existing forces obtained from the Lift off test were in horizontal axis while the results of the Ultrasonic test were plotted in terms of amplitude on the vertical axis. The results revealed that the amplitude proportionally increased with remaining force; however, they were quite low accuracy since obtained data were numerous scattered, particularly higher existing force. Therefore, the average value of ultrasonic test might not be appropriate for calibrating the correlations.

In order to release this problem, the confidence interval was adapted to eliminate bias on the Ultrasonic test results that might be occurred from human and/or equipment error. This technique is used to indicate the reliability of an estimate with varying on the level of confidence. The confidence interval can be simply expressed as a range of good estimates on the unknown population parameters. Figure 4.24 presents the upper and lower boundaries of the sample. In this study, they were considered at 99%, 95% and 90%, respectively, and can be calculated by following equation:

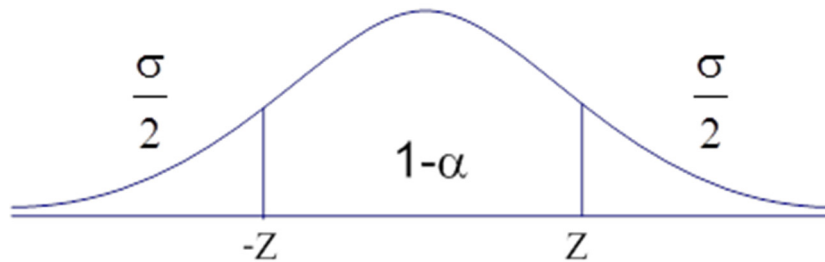


Figure 4.24 Confidence interval

$$\text{Confidence interval} = \mu \pm z \left(\frac{\sigma}{\sqrt{n}} \right) \quad (4.2)$$

Where

μ is the expected value

σ is the standard deviation

n is the number of sample

99%; $z = \pm 2.580$

95%; $z = \pm 1.960$

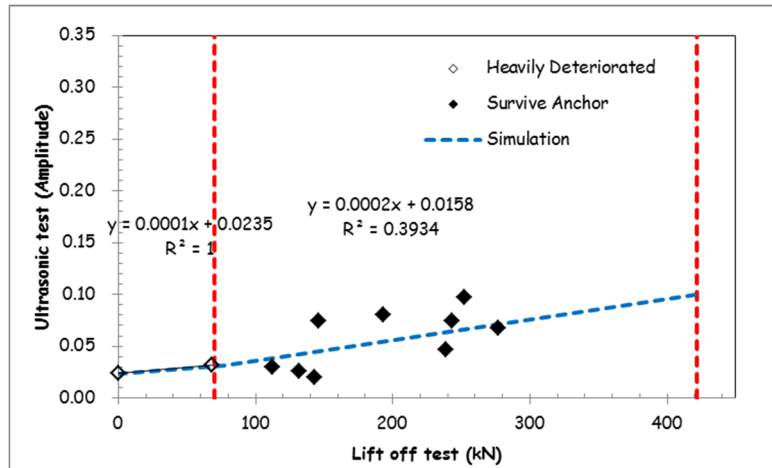
90%; $z = \pm 1.645$

The remaining data which excluded bias were used to re-calculate the expected value of the amplitude of the Ultrasonic test, neither less than the lower boundary nor more than the upper boundary. The averages of amplitude versus the Lift off test results were plotted and drawn the regression curve to obtain the correlation of both results. The linear prediction function was applied to estimate the existing force by giving the amplitude value of the Ultrasonic test.

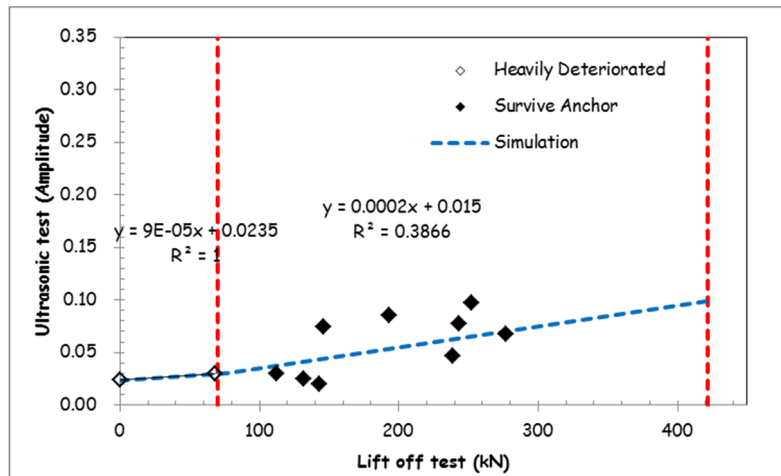
Figure 4.25 (a) to (c) present the calibration curve between the Lift off test results and the Ultrasonic test results of 90%, 95% and 99% confidence intervals, respectively. The obtained data significantly increased with the existing force grew up. Both red dashed lines were drawn as the boundaries of the both failure zones. The first boundary was twenty percent of the design force, whereas the second line was 120% of design force corresponding to heavily deteriorate and excessive overstress conditions, respectively. The regression curves were divided into two parts separated at 77kN following tentative of the average data. The gradient of a prediction line is quite mild on the first part with high accuracy indeed while the second part is steeper. However, the *R-square* values do not high on the second part due to too scatter data. Finally, the threshold was set up for analyzing the indicator kriging.

4.4.2 Comparison between Lift off test and Ultrasonic Results

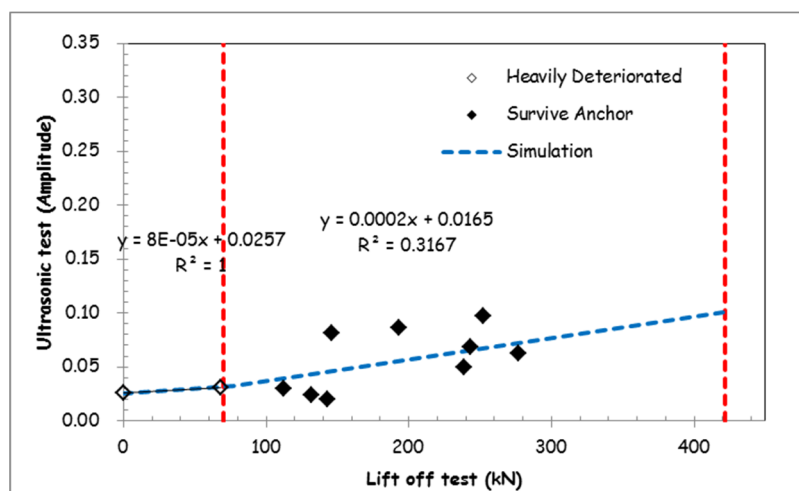
The threshold of Ultrasonic test was separately stipulated into three sets at 0.0312, 0.0304 and 0.0319 following 90%, 95% and 99% confidence intervals, respectively. Note that, these values are focusing only under the lower boundary while the data above the upper boundary was neglected since the excessive overstresses condition does not find. The methodology for calculating is following Eq.4.5. The results of the indicator kriging were summarized as tabulated in Table 4.7. Most of the results demonstrated almost same with each other except for 90% confidence interval that only ground anchor at point X = 15, Y = -5.



(a) 90% confidence interval



(b) 95% confidence interval



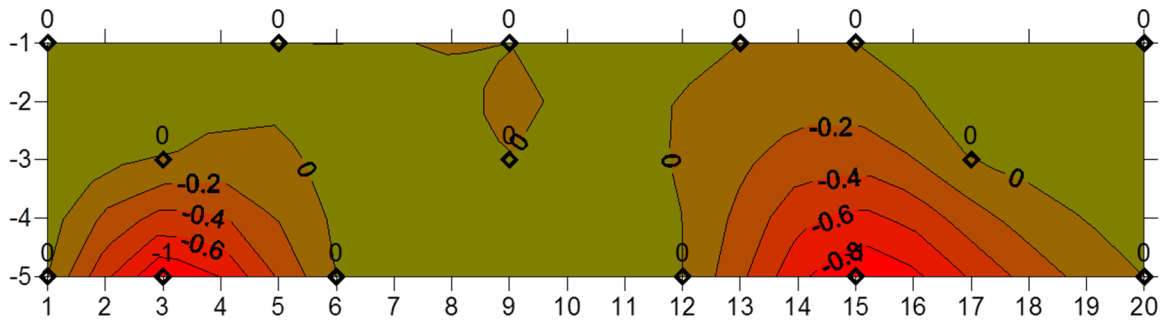
(c) 99% confidence interval

Figure 4.25 Calibration on the Lift off test results with the Ultrasonic test results on 90%, 95% and 99% confidence interval

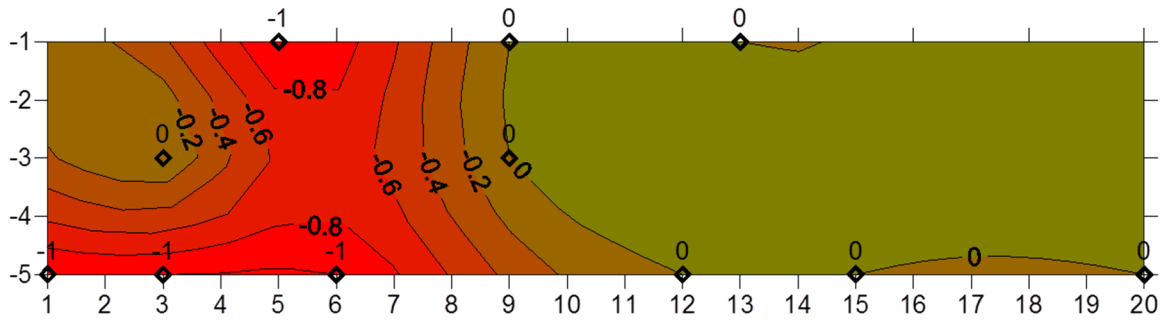
Table 4.7 Summary results of indicator kriging

Coordinate		90% confidence interval	95% confidence interval	99% confidence interval	Indicator kriging		
X	Y				90% confidence interval	95% confidence interval	99% confidence interval
3	-5	0.0235	0.0235	0.0257	-1	-1	-1
15	-5	0.0314	0.0294	0.0308	0	-1	-1
5	-1	0.0302	0.0302	0.0302	-1	-1	-1
1	-5	0.0260	0.0247	0.0234	-1	-1	-1
6	-5	0.0196	0.0196	0.0203	-1	-1	-1
13	-1	0.0745	0.0745	0.0814	0	0	0
9	-3	0.0804	0.0857	0.0863	0	0	0
9	-1	0.0471	0.0471	0.0497	0	0	0
20	-5	0.0739	0.0770	0.0684	0	0	0
3	-3	0.0974	0.0974	0.0974	0	0	0
12	-5	0.0672	0.0672	0.0627	0	0	0

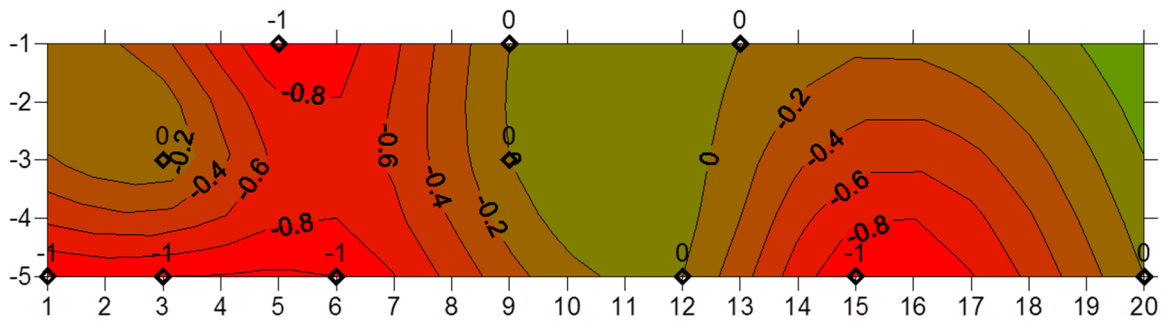
The results of indicator kriging were shown as the contour line filled with color to convenient to understand. The red shading color represented an unsafe zone while the green shading means the safe zone. In addition, the changing from red to green is corresponding to the reduction of risky degree proportional, the interval value is 0.2. Figure 4.26 (a) to (c) were the results of Lift off test, Ultrasonic test of 90% and 95% confidence intervals, respectively. Note that, the kriging results of an Ultrasonic test of 95% and 99% confidence intervals are same; therefore, only 95% confidence interval was displayed. The indicator kriging were adopted for interpreting results of an Ultrasonic test in order to suggest the additional location for the Lift off test. The 90% and 95% confidence intervals demonstrated almost same results on the left part, but totally the difference to the right of the improved zone. The 95% confidence interval result seems to be the more appropriate cause it is well-matched with the actual result obtained from Lift off test, particularly on the right zone. Even though, the left zones of both results are obviously different, the Ultrasonic test results are quite compatible with the kriging results of the Lift off test (see Fig 4.29 (a)).



(a) The Lift off test result



(b) The Ultrasonic test result with 90% confidence interval



(c) The Ultrasonic test result with 95% and 99% confidence intervals

Figure 4.26 Comparison among of the Lift off test result and the Ultrasonic test with 90%, 95% and 99% confidence intervals

In brief, the degree of the confidence interval plays an important role in the indicator kriging results. Generally, the confidence interval at least of 95% was adequate to analyze because too low confidence interval is an inappropriate results, while too high value is dispensable due to the same result. Finally, the results of the Ultrasonic test can be used as the indirect method to evaluate the failure location of each slope for giving an additional spot to conduct the Lift off test to confirm the remaining forces in ground anchor.

CHAPTER 5

MODELING OF THE DETERIORATION PROCESS AND PREDICTION OF FAILURE CONDITION

5.1 Introduction

This chapter, the modeling of the deterioration process and prediction of failure condition were presented. In order to predict the deterioration process of the ground anchors, several statistic models were adopted, including the Weibull hazard model, Markov chain model, Exponential model, Normal distribution model, Log-normal distribution model and Poisson process model. The ground anchors can be categorized into two types, which are strand type and rod types. In addition, they can also be divided into the new type and old type that different on a rusting protection coat which directly affected on its life span. Finally, all of statistical approach results were compared and discussed in order to verify the best-fitting model for representing model to analysis on the next step.

5.2 The Visual Inspection Test Results

5.2.1 Comparison of Three Markov Models Results

Firstly, the Markov models were proposed to calculate the life span of slope improved by ground anchor. Figure 5.1(a) to (d) illustrate the comparison of all data set among of simulated results by three models, showed as the line while the observed data demonstrated as the column bar, in 8, 16, 18 and 22 years, respectively. These simulated results show similar trends, especially Simplify model and Markov hazard model show almost same results while the original method demonstrated some different results, however, no obvious divergence.

Figure 5.2 (a) and (b) show the comparison among three Markov models by considering the survival probability for scenario I and II, respectively. The scattering dot represented the Visual inspection test results, whereas the simulation results are shown as color lines. The results indicated that the Markov original model showed higher survival probability comparing with the other models. The Markov simplify model presented closer to the field

monitoring meaning that this model is appropriate for predicting the deterioration path. Furthermore, this model showed a more pessimistic scenario than others in the long term. Therefore, we decided to apply the Markov simplify method as the representative of Markov models in this paper.

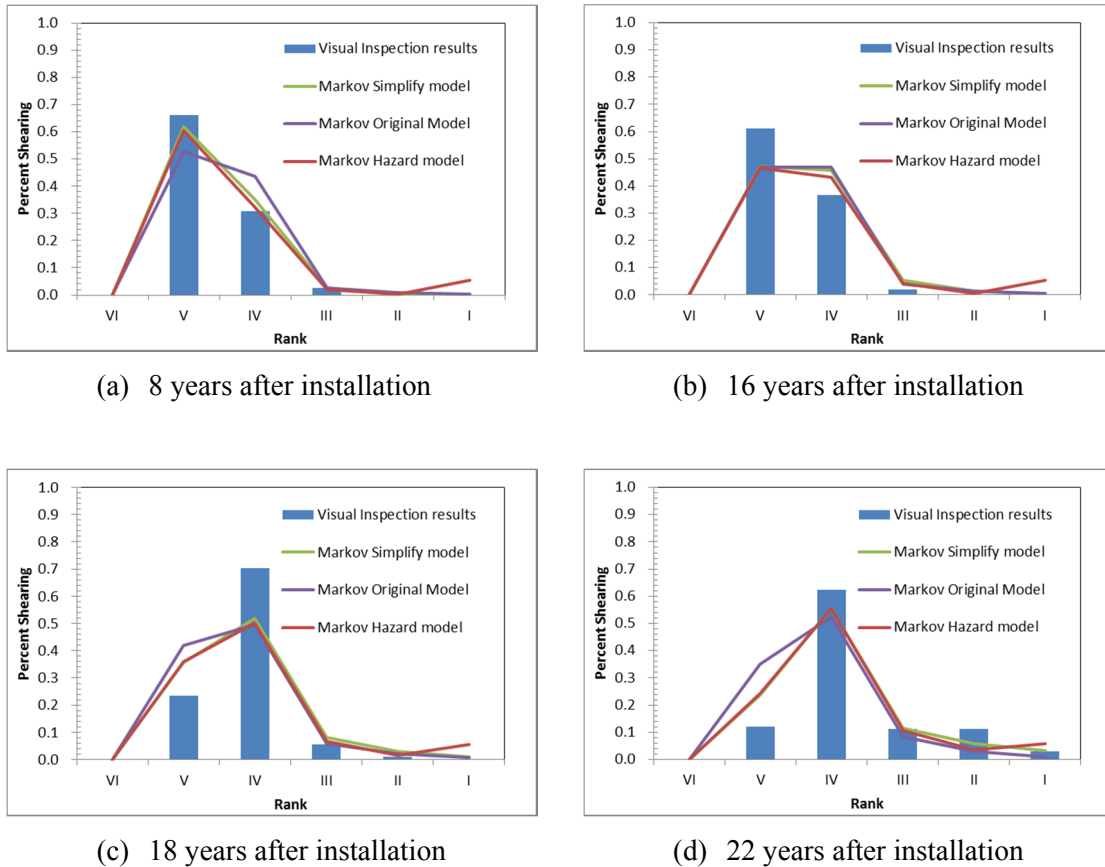
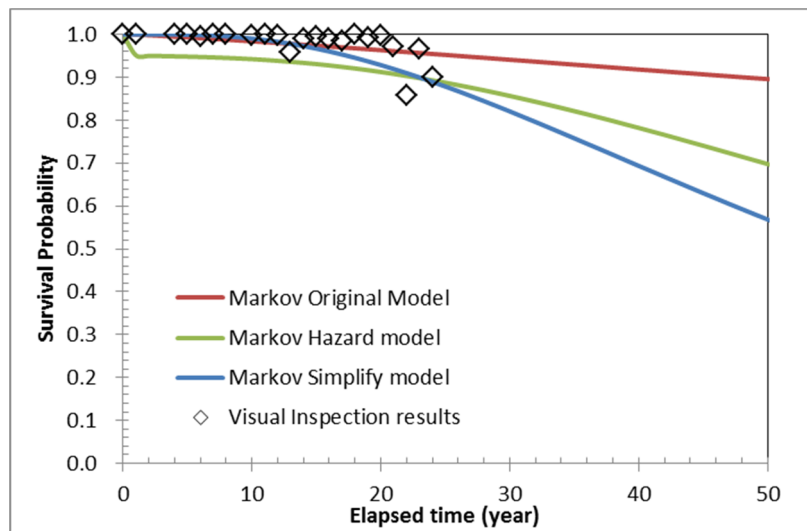


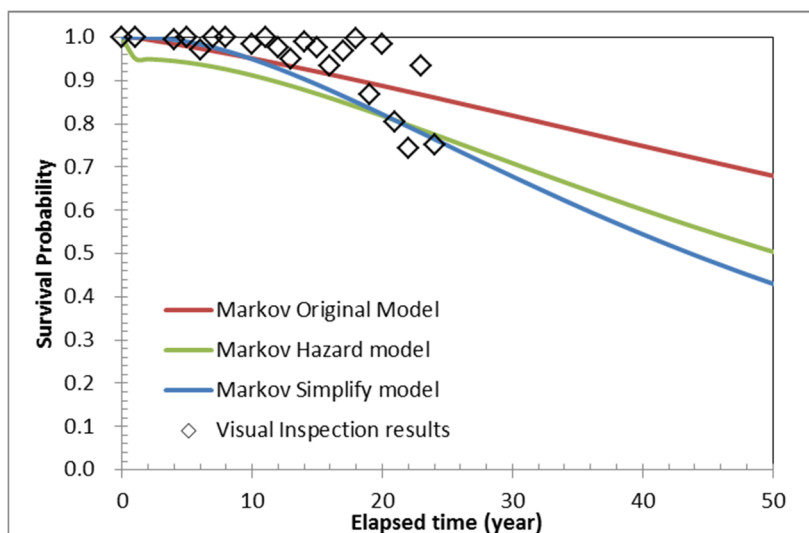
Figure 5.1 Comparison of results among of Markov models with observation data at (a) 8 years (b) 26 years (c) 18 years and (d) 22 years

5.2.2 Comparison of Several Statistical Models Results

The results of survival probability, for example, Weibull hazard model, Markov model, Exponential model, Normal distribution model, Log-normal distribution model and Poisson process model were compared together in this section in order to find the appropriate model for analyzing the deterioration process as illustrated in Fig 5.3 (a) and (b) for scenario I and II, respectively. All of the data set was engaged as the observed data since unsuitable to break into different geological conditions or type of ground anchors caused limitation of data allowance.



(a) Scenario I



(b) Scenario II

Figure 5.2 Comparison of survival probability based on three Markov models

The results of Markov models presented as the shading color represented each ranking while the other models demonstrated as the continuous line. Survival probability based on the Markov model can be expressed as the boundary line above shading areas of rank II, which corresponding to survive for scenario I (Figure 5.3 (a)), whereas scenario II starting from the lower boundary line of rank III (Figure 5.3 (b)). The results revealed that the Markov model and the Exponential model seemed to be overestimated predict the deterioration path on both scenarios I and II since too high survival probability at present

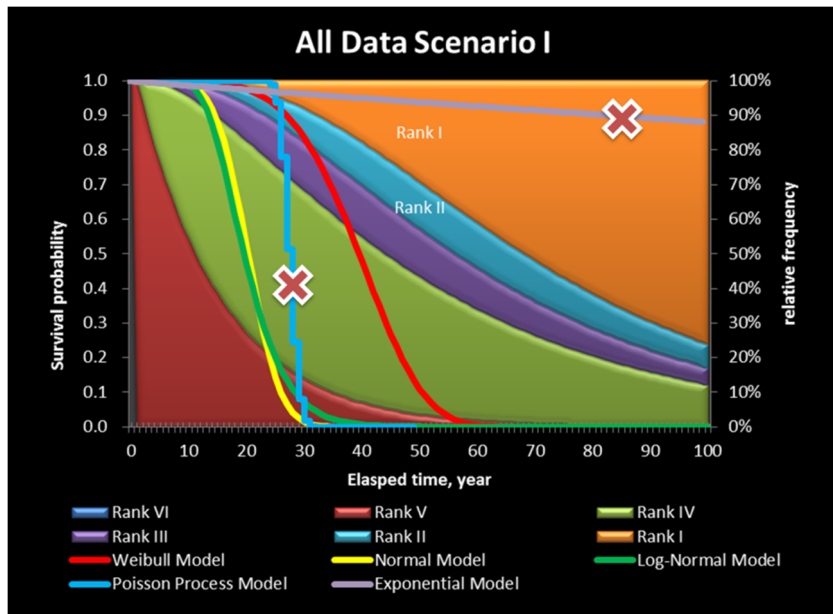
(around 30 years) as well as the failure does appear even if a hundred year passed. In addition, the Poisson process models presented survival probability suddenly decreased after twenty five years passed. Their results demonstrated the enormous drop down started from 100% to failure within five years which impossible to occur. It is also might not be appropriate to be employed for expecting the deterioration curve.

Therefore, three remaining models which are the Weibull hazard, Normal and Log-normal distribution models might be able to be a representative model for predicting the deterioration rate. The Normal and Log-normal distribution models illustrated the almost alike results with a shorter life span than the Weibull hazard model. In addition, the Weibull hazard model obviously presented different results of the life span between scenario I and II, which are 50 and 55 years, respectively, on the other hand, both Normal and Log-normal distribution model demonstrated same life span of 30 years approximately. However, these two figures do not appropriate to evaluate the suitable model.

The alternative way to compare these results is to plot with the observation data by considering survival probability and histogram. The left figure in Fig 5.4 indicates the survival probability with no distinctly different between the Normal and Log-normal distribution models; however, their results quite unlike, while compared with the Weibull hazard model as mentioned previously. The Weibull hazard model indicated the life span longer than 50 years while the Normal distribution and Log-normal distribution models showed approximately 30 years.

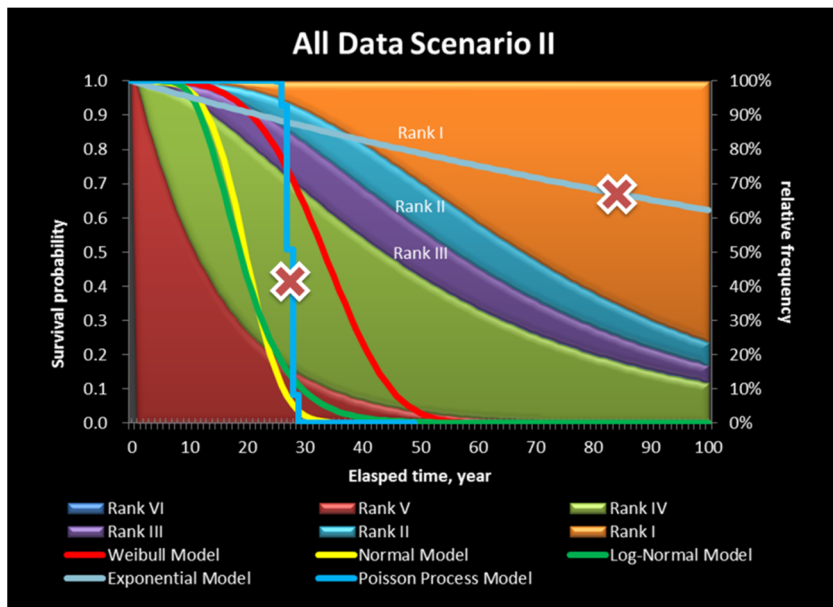
Considering on the right of Fig 5.4, it presented as the histogram of failure data and probability density function of three models. Normal and the Log-normal distribution model illustrated quite same shape of probability density function, although the number of failure data increased from the scenario I to the scenario II whereas the Weibull hazard model illustrated opposite results. It is implied that the density of the failure data predominated to the shape of probability density function than the number of failure data in case of the Normal and Log-Normal distribution model; however the results of the Weibull hazard model depended on both survive as well as failure data. Therefore, the Weibull hazard model is more appropriate to be the representative model. Furthermore, the

numbers of failure data in the scenario I seem to be inadequate for analysis, accordingly, scenario II were applied to be the best scenario in this study.



Scenario	Criteria for Failure	Criteria for Survival
I	Rank I+II	Rank III~VI

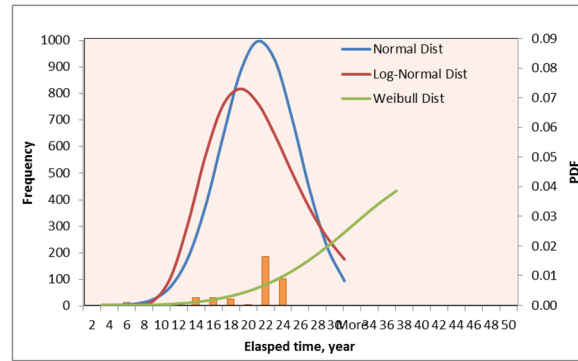
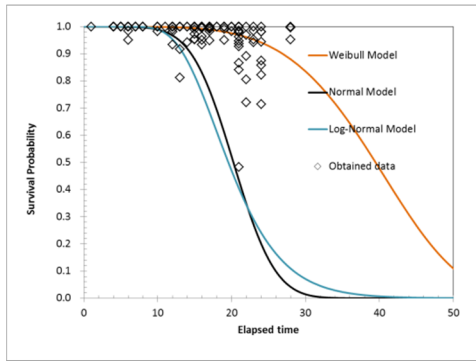
(a) Scenario II



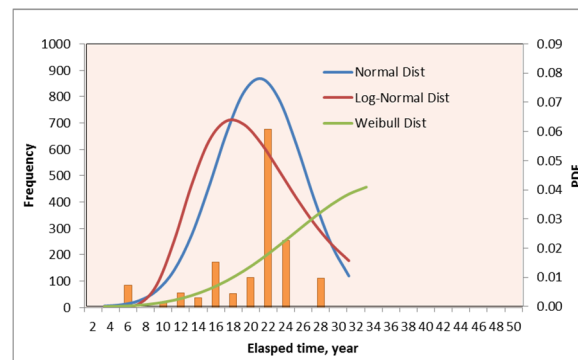
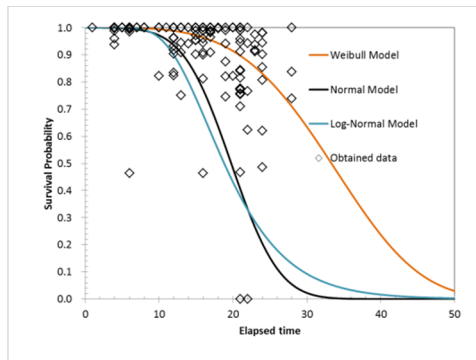
Scenario	Criteria for Failure	Criteria for Survival
II	Rank I+II+III	Rank IV~VI

(b) Scenario II

Figure 5.3 Comparison of survival probability among of several models.



(a) Scenario I



(b) Scenario II

Figure 5.4 Comparison of survival probability among Weibull, Normal and Log-Normal models together with histogram and PDF of scenario I and II

5.2.3 Comparison of Survival Probability between Ground Anchors Types and Geological Conditions

The simulated results based on the Weibull hazard model were plotted to compare the life span of ground anchor based on the different rusting protections which are new type and old type as presented in Fig 5.5. The new type ground anchors were installed 60%, approximately while the old types were about 40%. The inspection data showed that the new type anchors were tested since the first year after installing whereas the rod type anchors were inspected after twelve years passed.

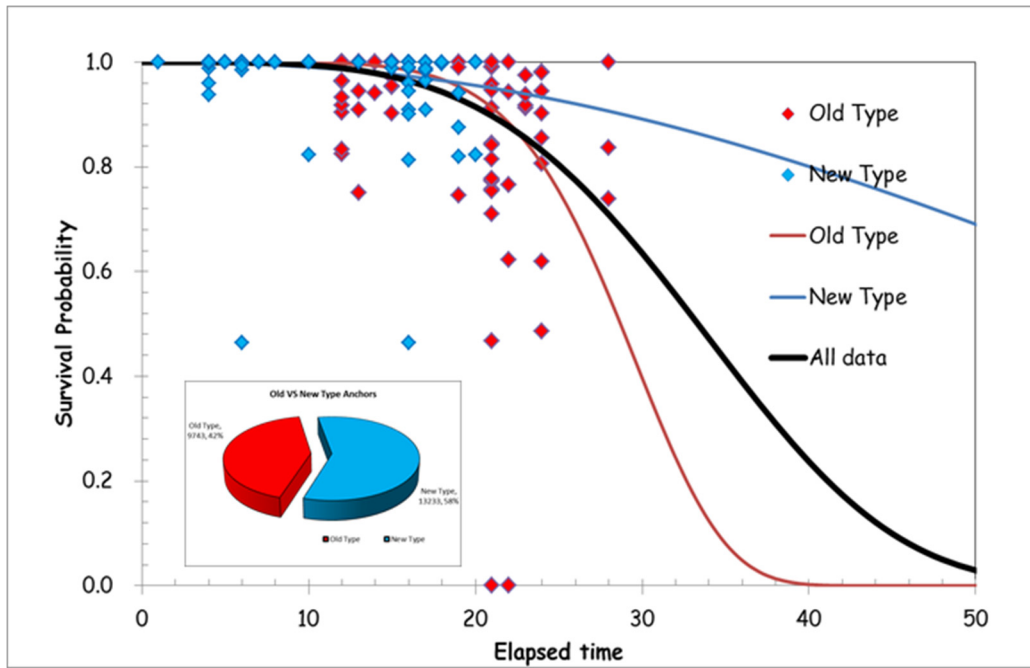


Figure 5.5 Comparison of survival probability among of new type, old type and all data

The blue, black and red lines corresponding to the results of the deterioration rate of new type, all data and old type ground anchors while the blue and red dot are the survival probability calculated from the Visual inspection test results. The new type ground anchors presented longer life span than the old type ground anchors; the new type showed life span longer than 50 years while the old types reached to the failure condition within 40 years after installation. The reason is that the new type anchors were coated with additional chemical admixture in order to reduce the decay rate by the rust while non-coated on the old type anchors.

Figure 5.6 shows comparison results between different physical properties of ground anchors, strand type and rod type. These comparison results do not separate the type of geological condition. The rod type was used 40%, approximately while the strand type was adopted around 60%. The red line indicated the simulation of strand type's failure rate, whereas the blue line is the rod type. The Visual inspection data were plotted as the red and blue dot corresponding to strand type and rod type, respectively. The inspection tests were experimented starting from one to twenty-eight year since installation. Mostly, inspection data is still high survival probability even though twenty-eight years passed, particularly

strand type. In addition, some slopes of rod type showed completely failure after 21 and 22 years; nevertheless, the minimum failure probabilities of strand type were only about 50%.

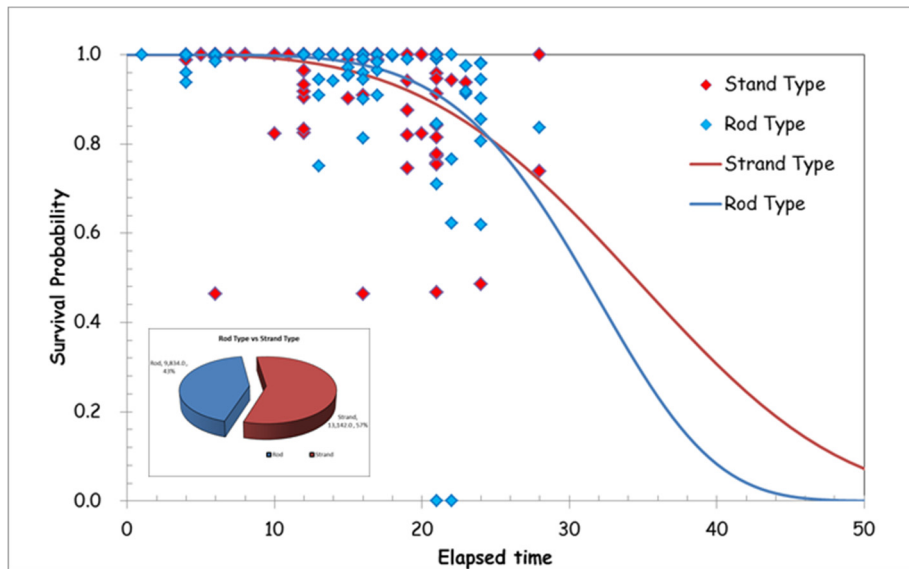
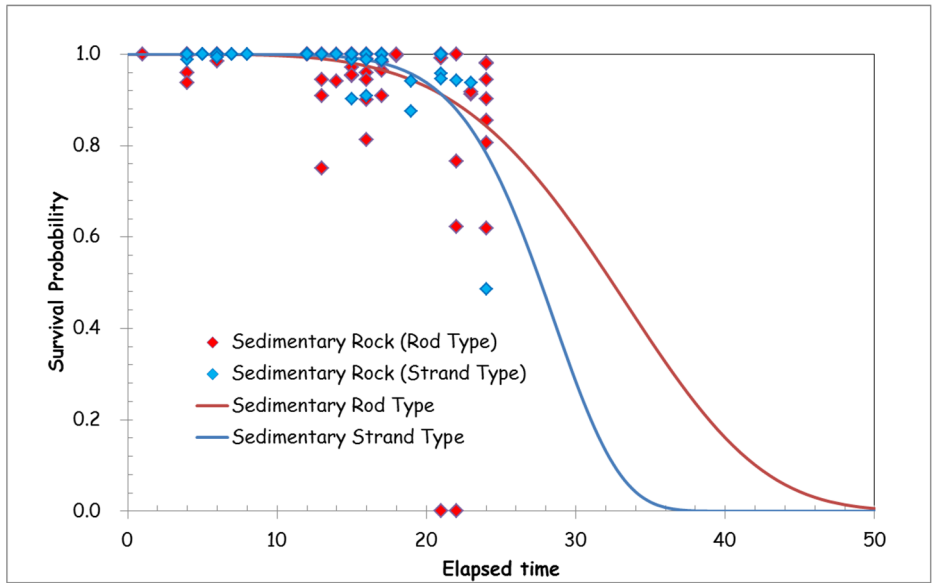


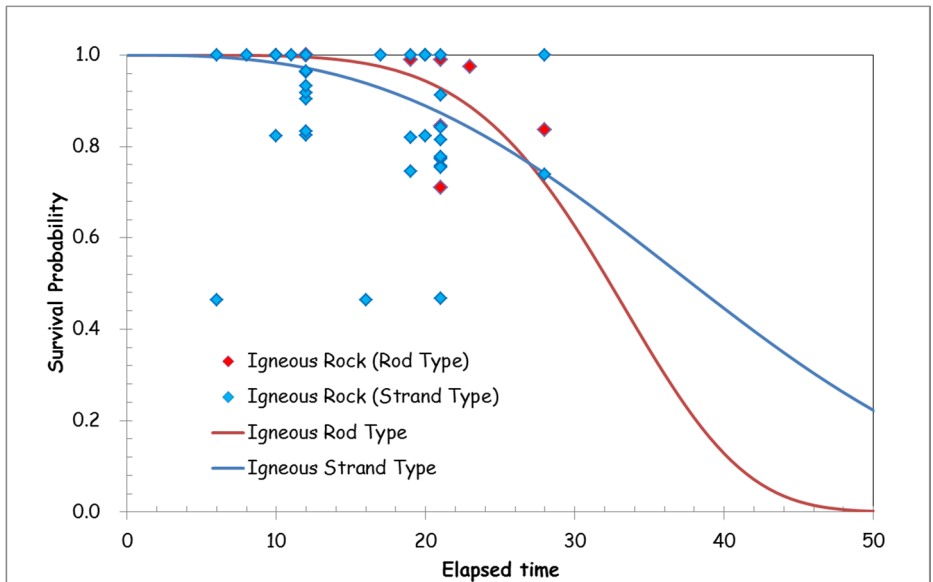
Figure 5.6 Comparison results between rod and strand types

The simulated results indicated that the strand type showed longer life span than the rod type as expected because the more installed force in strand type; therefore the deteriorated process should be taken longer time. In addition, numerous slopes of rod type survival probability lesser than strand type slope on average.

Figure 5.7 shows the comparison results between rod and strand types considering the different geological conditions which are sedimentary rock (see Fig 5.7 (a)) and igneous rock (see Fig 5.7 (b)), respectively. The scatter points represented survival probability calculated from each slope obtained from the Visual inspection test while the continuous line is the simulated results based on the Weibull hazard model. However, both results showed diverged trends that life span of rod type was shorter than the strand type in the case of the igneous rock while the results of the sedimentary rock indicated opposite outcome. These consequences showed completely the conflict with the previous results that strand type should be longer life span than rod type.



(a) Sedimentary rock



(b) Igneous rock

Figure 5.7 Comparison of survival probability between different geological conditions.

Furthermore, the simulation results of both sedimentary and igneous rocks with different ground anchors types were plotted together as illustrated in Fig 5.8. The dashed lines indicated the rod type while the continuous lines were strand types. The red lines represented igneous rocks, whereas the blue lines denoted as the sedimentary rocks. The results cannot explain which types of ground anchor were longer life spans caused rod type presented similar results on both rock types while strand type explicitly difference.

Moreover, in case of the igneous rock, the rod type showed shorter life span than the strand type, quite similar to previous results as shown in Fig 5.6, whereas the sedimentary rock showed distinct. However, a number of failure data of the igneous rock - rod types were small points that are only four slopes as well as allowable short inspection time during 18 to 28 years only.

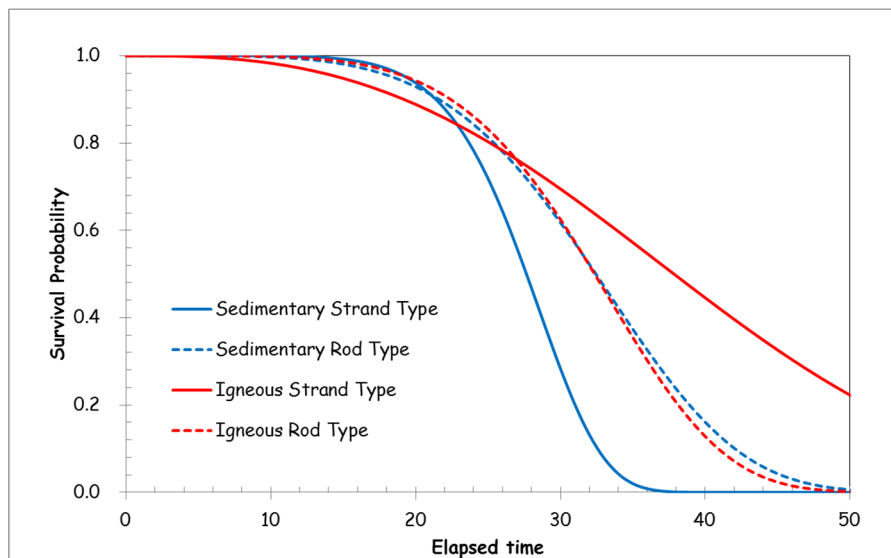


Figure 5.8 Comparison of survival probability between different geological conditions as well as strand and rod types

Finally, these outcomes might be indicated that the Visual inspection test would be the preliminary reconnaissance to roughly classify condition state of the ground anchors and for quick maintenance on a spot; however, it might not be appropriate to stipulate as a primary method for analysis an anchor's life span since it judged by the human eye without validation by heavy equipment.

5.3 The Lift off Test Results

5.3.1 Comparison of Survival Probability between Ground Anchors Types and Geological Conditions

The Weibull hazard model was adopted to evaluate the deterioration process of the risk slopes improved by ground anchors of the Lift off test results caused its predicted curve is more fitted with the obtained data comparing with the others as mentioned in the previous

section. The dwindling rate of the rod and strand types were plotted as illustrated in Fig 5.9. The obtained data were plotted as scattered dot while the simulated results were presented by continuous lines, blue and red color corresponding to rod type and strand type, respectively. Survival probabilities displayed slowly decayed rated on the early stages; afterward drastically reduced after fifteen years. These results revealed the strand type longer life span that the rod type which consistent with the percentage of failure anchors as mentioned earlier. Both results demonstrated that these slopes might reach to a critical point after thirty to thirty-five years after installation for rod and strand types, respectively. In brief, they will reach to failure points within forty years since reinforced.

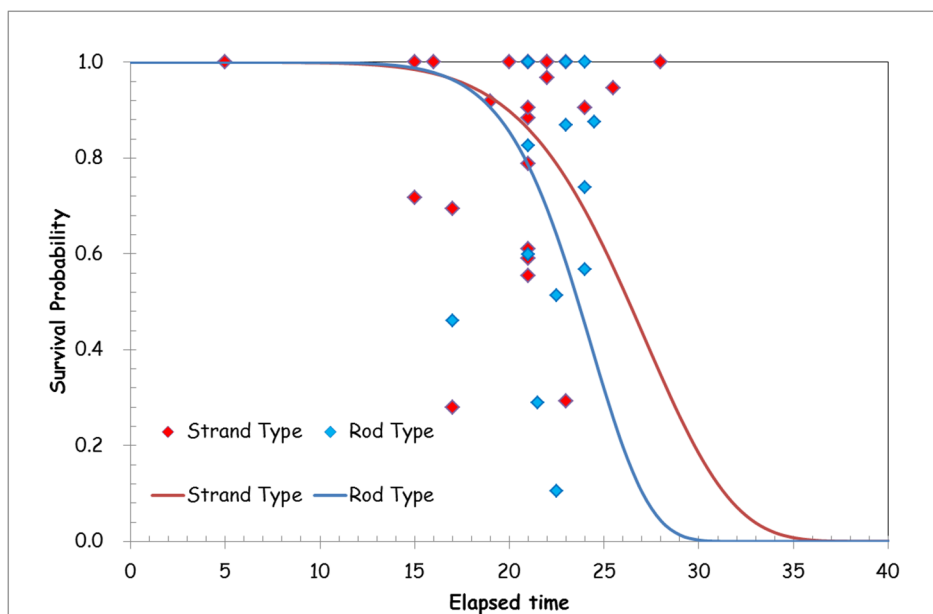
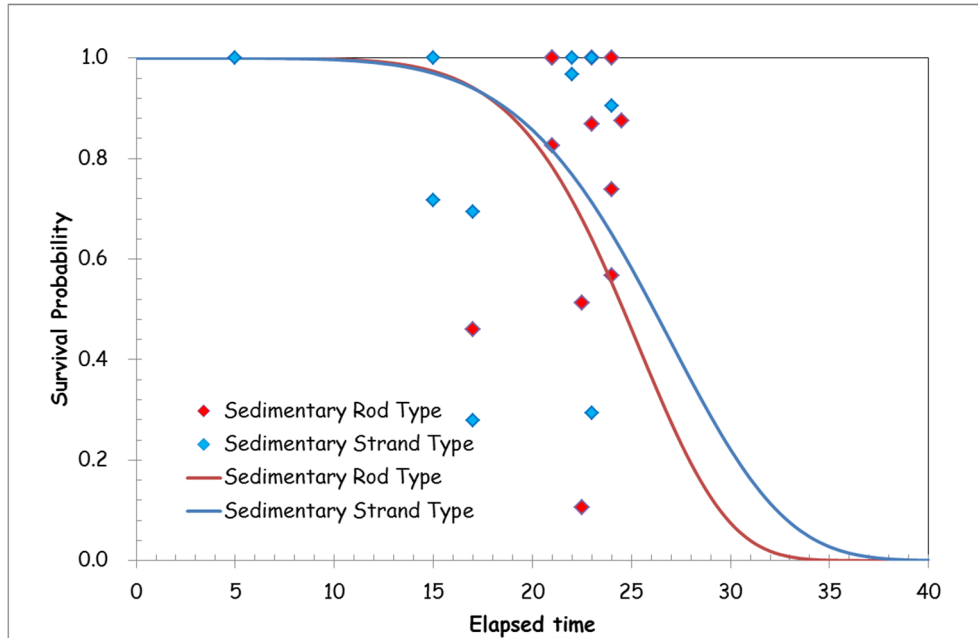


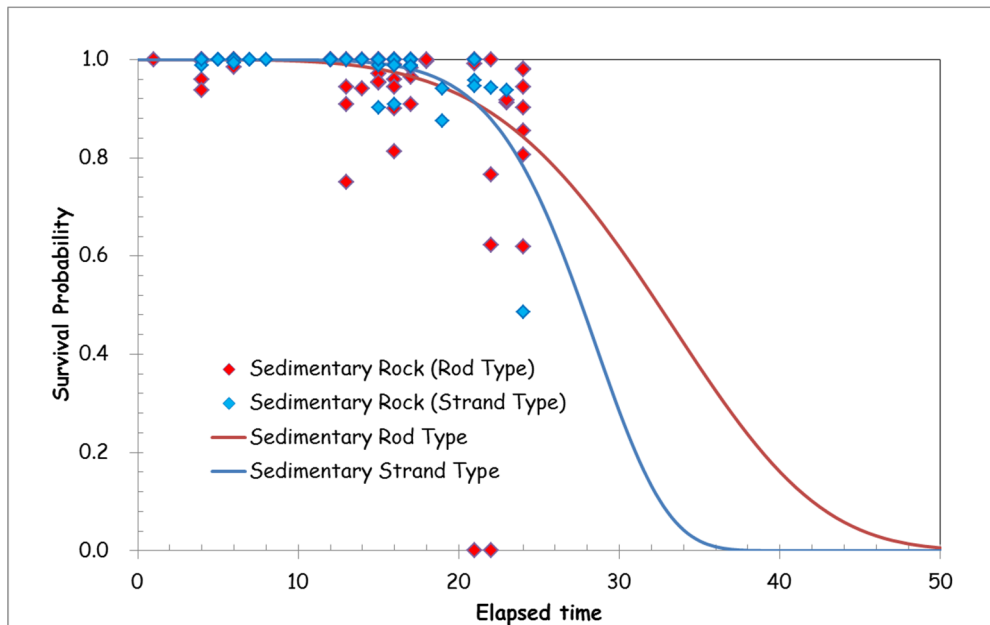
Figure 5.9 Comparison of survival probabilities between rod and strand types.

The deterioration processes were considered separating into sedimentary and igneous rocks as displayed in Fig 5.10 (a) and (b), respectively. Furthermore, these results were also plotted separately between rod and strand types for convenience to understand. As expected, strand type illustrated longer life span than the rod type on either sedimentary or igneous rocks. However, the obtained Lift off test data seemed to be inadequate to analyze, for example, igneous rod type, deterioration curve displayed to suddenly drop after twenty-years as presented in Fig 5.10 (b). Moreover, the obtained data of the igneous rock showed limited testing time started from fifteen to twenty-three years, thereby, its curve trend to be rapidly deteriorating after the first result was taken unlike the sedimentary rock.

Consequently, this study was considering only the sedimentary rock for determining the life span, stability of slopes as well as the probability of failure while the igneous was considered only for reference as the other geological condition.



(a) sedimentary rock



(b) igneous rock

Figure 5.10 Comparison of survival probabilities between different geological conditions.

Figure 5.11 illustrates comparison results between different geological condition as well as types of ground anchors from simulation results. Strand types were presented as blue lines, whereas the red lines represented the rod types. In addition, the dashed and continuous lines were igneous and sedimentary rocks, respectively. Strand types displayed the longer life span on either sedimentary rock or igneous rock. Furthermore, ground anchors installed in sedimentary rocks illustrated longer life span than the igneous rocks. As mentioned in the previous section, however, sedimentary rock seems to be the smoother curve than the igneous caused the allowable data more adequate to analyze.

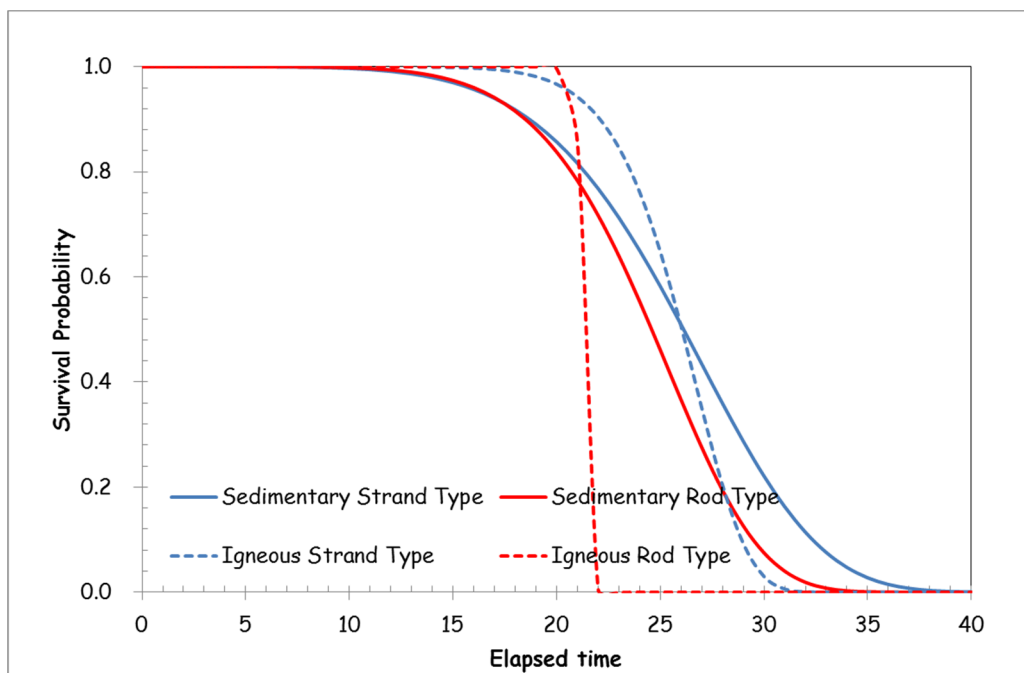
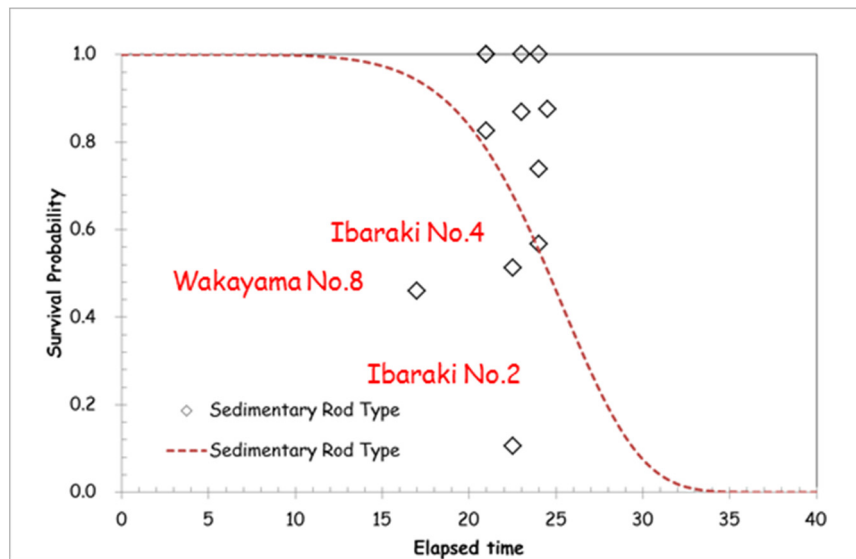


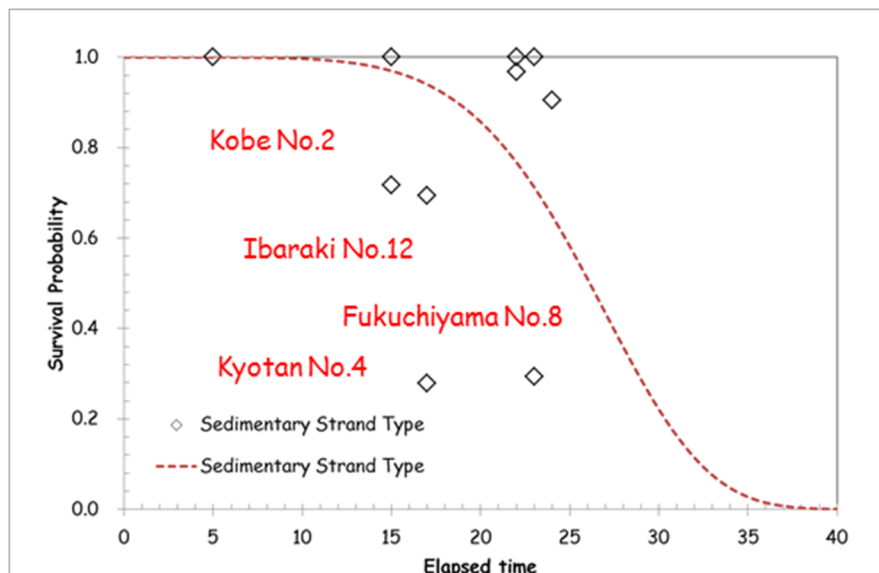
Figure 5.11 Comparison of survival probabilities between different geological conditions as well as strand and rod types

In order to evaluate the risk of slopes failure, the stability analysis employed three-dimensional safety factor analysis was conducted by dealing with limit equilibrium method. In this part, only sedimentary rock slopes were investigated because the data allowable adequate to analyze. The red dashed line represents the threshold calculated from the Weibull hazard model. The slopes showed survival probabilities under the threshold line mean heavily deterioration, which shall be priority considered the safety factor, including Ibaraki No.4, Wagayama No.8 and Ibaraki No.2 for rod type whereas Kobe No.2, Ibaraki No.12, Kyotan No.4 and Fukushi No.8 for strand types as presented in Fig 5.12 (a) to (b),

respectively. Because a safety factor of each slope involved several factors, individual slope was analyzed separately based on its configurations depending on a number of ground anchors, slope shape, inclination of slope, strength parameters such as cohesion, friction angle, etc. On the other hand, those slopes which illustrated higher survival probabilities than the threshold lines were inessential to conduct stability analysis caused their performances are still high capacities to act against acting force.



(a) Sedimentary rod type



(b) Sedimentary strand type

Figure 5.12 The name of risk slopes that shall be a priority to investigate the *F.S.* of the sedimentary rock

5.4 Comparison between the Lift off Test and Visual Inspection Test Results

In this section, the results of survival probabilities between the Lift off test and Visual inspection test based on the Weibull hazard model were compared and discussed. As mentioned in the previous chapter, the scenario II (rank I+II+III corresponding to fail) based on the Visual inspection test results was a suitable scenario to evaluate the deterioration process of slopes improved by ground anchors.

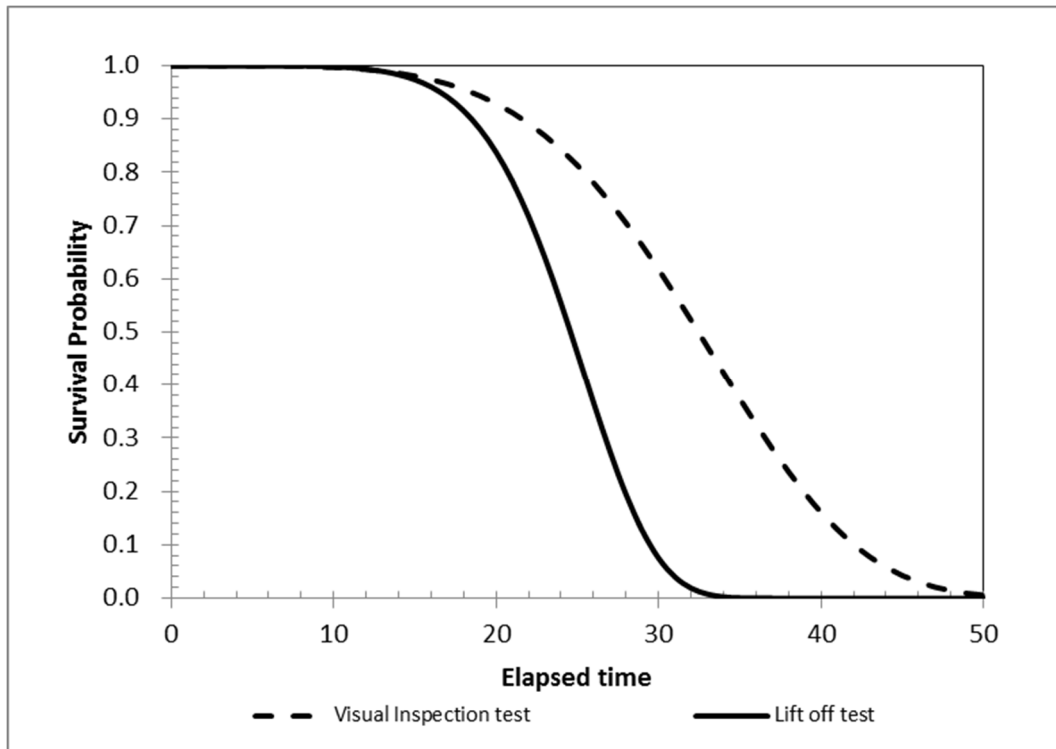


Figure 5.13 Comparison of simulation results between the Visual inspection and Lift off test

Figure 5.13 shows the comparison of survival probability results between the Lift off test (continuous line) and the Visual inspection test (dashed line) of sedimentary rock-rod type. The deteriorated rate based on Visual inspection showed the slower rate than the Lift off test; moreover, it seemed to be reaching to failure after fifty years past while the Lift off test indicated the life span was about 33 years, approximately. However, at an early stage before fifteen years since installed, both results demonstrated quite same survival probabilities, subsequently, both simulated results decreased with different rates. Considering at 28 years, (the 1st anchor was installed in 1981 and the 1st Lift off test was

conducted in 2009) survival probability based on Lift off test was 0.19 while Visual inspection result was very high about 0.70 that quite large different outcome. Therefore, this result revealed that the Visual inspection results significantly seen to be overestimated life span.

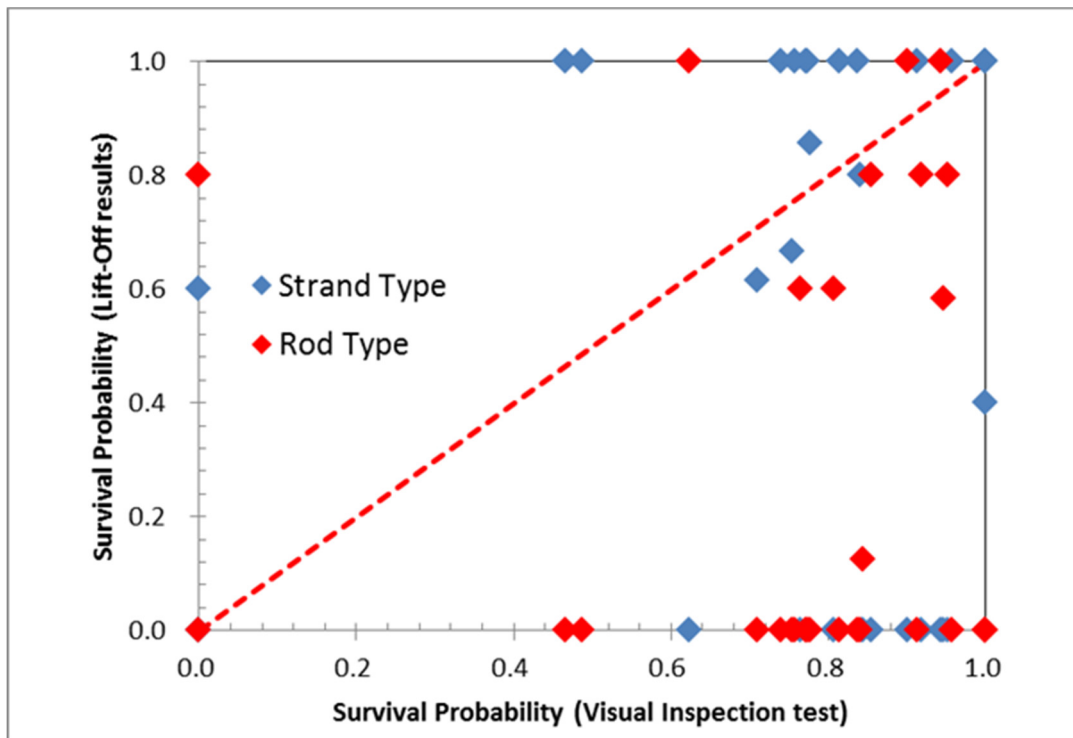


Figure 5.14 Comparison of survival probabilities between the Visual inspection and the Lift off test

By considering the microscopic viewpoint, the survival probabilities of both Visual inspection and Lift off test were compared as shown in Fig 5.14. The scatter red and blue points represented survival probabilities of each slope for rod type and strand type, respectively. The red dashed line is the ideal relationship or the reference line. These results point out that non-relationship on both methods that some slopes showed very high survival probabilities based on the Visual inspection test but some of them fails when considering Lift off test. In contrast, their demonstrated opposite results as well.

Therefore, the Visual inspection results might not be appropriate to simulate the deterioration rate; however, it can be used for preliminary test to judge whether ground

anchors failure or survives on each spot. Subsequently, individual ground anchor was decided to re-stressed or reinstall depending on the Lift off test results.

CHAPTER 6

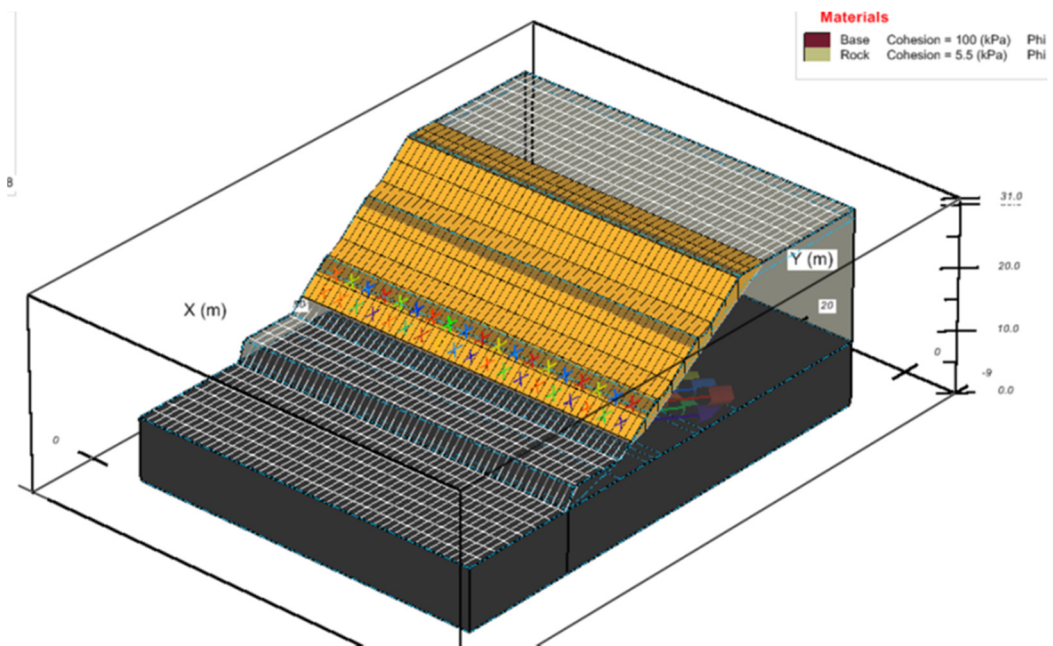
INVESTIGATION ON STABILITY OF RISK SLOPES AND PROBABILITY OF FAILURE

6.1 Introduction

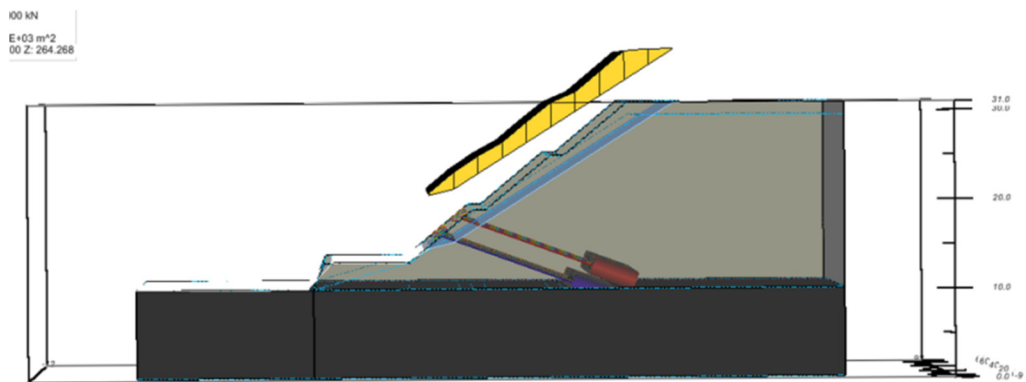
In this chapter, the ordinary or Fellenius's method was used to evaluate the three-dimensional safety factor because this method is quite simple that abandoned horizontal force in between the slices, anyway the results of *F.S.* do not obvious the difference from the others. The back analysis technique was proposed to investigate the appropriate strength parameters of the slope such as cohesion, c' , internal friction angle, ϕ' and the unit weight, γ . The commercial software, *SVslope* which developed by *Soil Vision Systems Ltd.* was introduced to analyze the stability of slopes in this study. This slope stability analysis was considering only plane failure patterns which more suitable for weathering rock slopes as demonstrated in Fig. 6.1. The pros of three dimensional safety factor analysis are to provide the actual shape of a slope that shall be better than the two dimensional analysis, especially slope reinforced by ground anchors because it can consider as the improved spots unlike the two dimensional analysis that transferred the ground anchor to be the plain-strain problem.

6.2 The Safety Factor Analysis

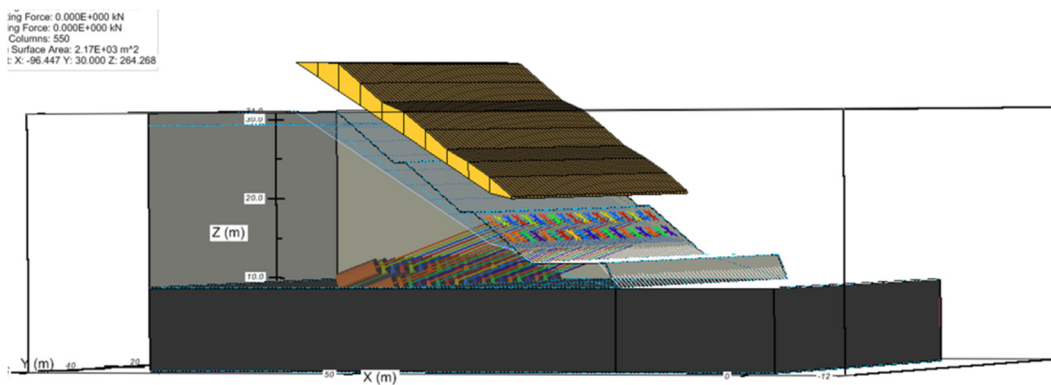
The number, location, length, size and force of ground anchors as well as shapes of each slope are simulated based on information provided by the road administrator. Therefore, each slope are considered individually caused depended on its configuration, for example, some slope is very steep and large while the others quite small and mild slope. For instance, Figure 6.2 shows slope attribute of Fukuchiyama No.9, which composed of two sets of ground anchors on the upper and lower part of the slope. Ground anchors of each part composing of two rows @ 3.00m spacing in both directions. Forty-eight ground anchors were installed with inclination angle of 20 degrees below the horizontal line.



(a) Perspective view

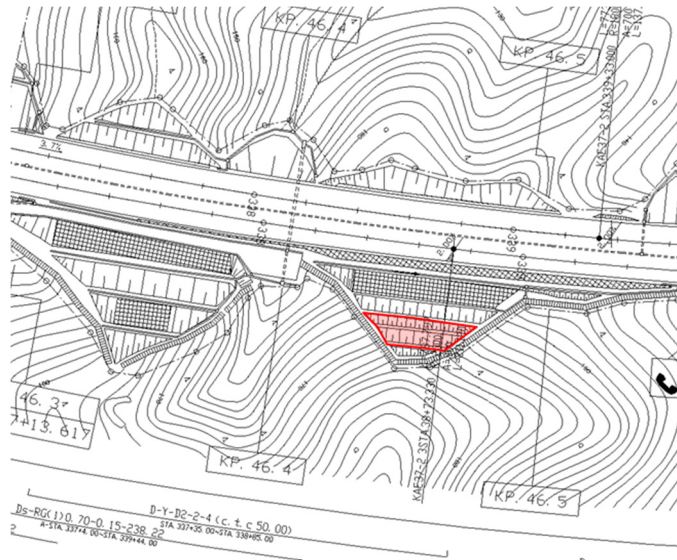


(b) Left view



(c) Right view

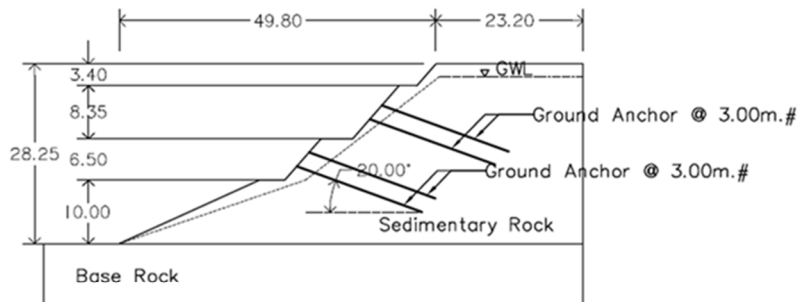
Figure 6.1 The example of three dimensional slope stability analyses for this study



(a) Plan



(b) Side view



Fukuchiyama - 9

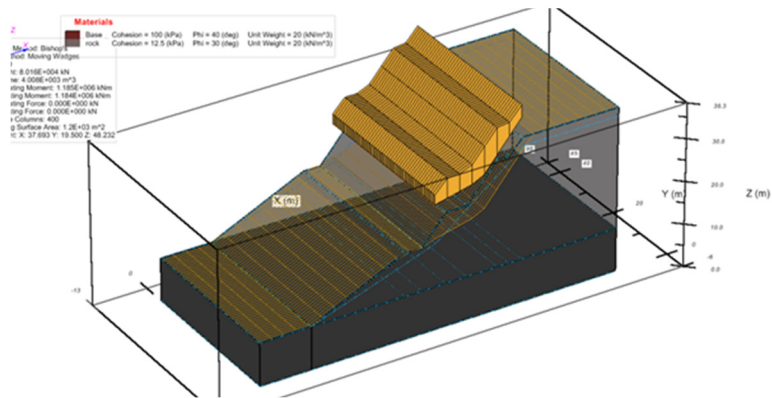
Section

Not to Scale

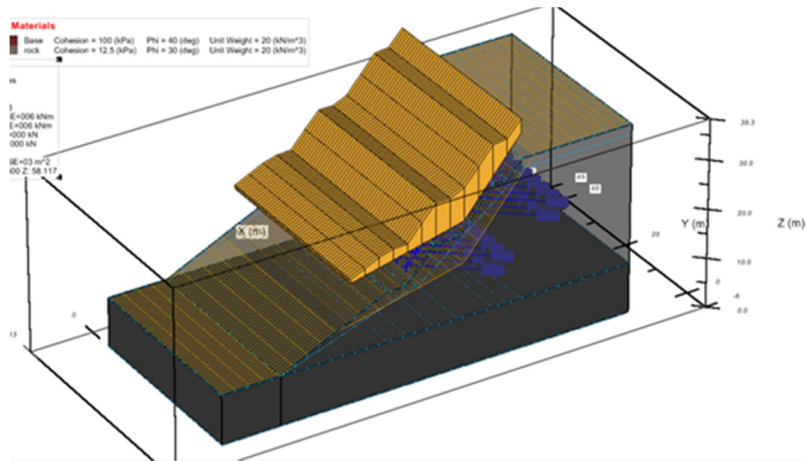


(c) Cross – section

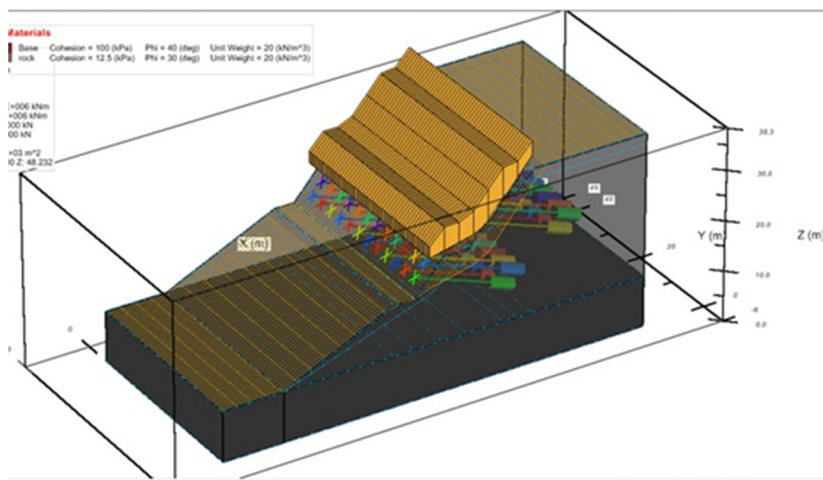
Figure 6.2 Example slope configuration (Fukuchiyama No.9)



(a) Without Ground Anchor



(b) Initial condition



(c) Present condition

Figure 6.3 The example *FS* results of Fukuchiyama No.9

In order to evaluate the strength parameters such as cohesion and internal friction angle of each slope, the back-analysis technique was adopted by trial and error on those parameters until the *F.S.* close to one at without ground anchors stage considering the pessimistic scenario that the GWT level close to the surface. Because slope shall be risk to collapse or instable before reinforced, otherwise it is meaningless to reinforcement. Next, apply the anchors force to calculate initial condition (after reinforcing) as well as present condition, respectively.

The example results of slope stability analysis, including, without ground anchor, initial conditions and present conditions are presented in Fig 6.3 (a) to (c), respectively for Fukuchiyama No.9. These results indicated the different location of the critical failure plane that without ground anchors case showed a critical plane on the top of the slope which almost the same place with a present condition case. However, the initial condition case demonstrated the failure mass larger than the others because the ground anchors installed with full design load can be against acting force more than other cases.

Table 6.1 Summary of Safety Factor analysis results

Slope name	<i>F.S.</i> (Without AC)		<i>F.S.</i> (Initial)		<i>F.S.</i> (Present)		<i>Survival Prob</i> (Present)
	Pessimistic scenario	Optimistic scenario	Pessimistic scenario	Optimistic scenario	Pessimistic scenario	Optimistic scenario	
GWT Condition							-
Wakayama No.8	1.00	1.28	1.10	1.38	1.00	1.29	0.46
Ibaraki No.4	1.00	1.22	1.60	1.68	1.18	1.36	0.51
Ibaraki No.2	1.00	1.22	1.46	1.69	1.04	1.27	0.11
Fukuchiyama No.8	1.00	1.37	1.17	1.54	1.06	1.45	0.29
Kyotan No.4	1.00	1.26	1.21	1.56	1.05	1.35	0.29
Kobe No.2	1.00	1.14	1.11	1.25	1.05	1.18	0.72
Ibaraki No.12	1.00	1.12	1.75	2.66	1.60	2.35	0.69

The results of *F.S.* were summarized, for instance, without ground anchor, initial condition and present condition cases of those risky slope as tabulated in Table 6.1. Moreover, they

can be divided the GWT level to be two scenarios which are the GWT level close to the surface of slope and lower than the failure plane, corresponding to the pessimistic and the optimistic scenarios, respectively. The $F.S.$ at an initial condition increase after ground anchors were installed; subsequently, decrease continuously depending on the number of ground anchors as well as slope shape. The GWT level plays an important factor to the of $F.S.$ of slope that the pessimistic scenarios always show lower than the optimistic scenarios. In addition, some of them seem to reach a critical condition at present considering pessimistic scenario, except Ibaraki No.4, and Ibaraki No.12 caused their survival probabilities is still high as well as high number of anchors installed, which are 234 and 209 anchors, respectively.

The reduced rates of anchors force caused deterioration processes were assumed following Weibull hazard model. In addition, its reduction rate shall be considered individually since the results of existing force at present obtained by Lift off test were differences depending on the performance of the anchor. The predictions of deteriorated forces were supposed to be same rate, but different elapse time. The assumption to forecast these forces are the percentage of the remaining force over the design force, $\frac{T_L}{T_d}$ equal to survival probability. Therefore, the average simulated deterioration rate, a continuous line (see Fig.6.4) shifted back to the equivalent survival probability of obtaining data demonstrated as the dashed line in Fig 6.4. Finally, all of anchors on a slope are simulated the deteriorated rate with same technique as illustrated in Fig 6.5, it can be seen that the results of the reduction rate on anchor's forces were parallel with the others. Furthermore, the $F.S.$, average force, μ , standard deviation, σ and covariant of variation, COV of on at time t can be obtained.

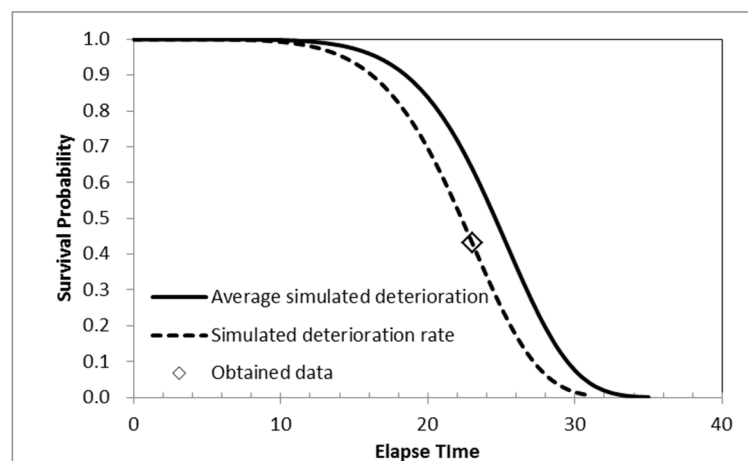


Figure 6.4 The example to simulate force with time

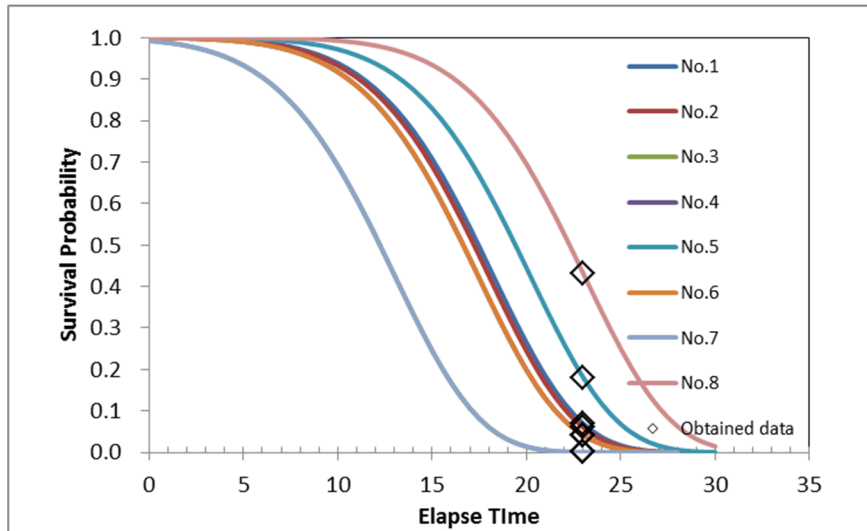
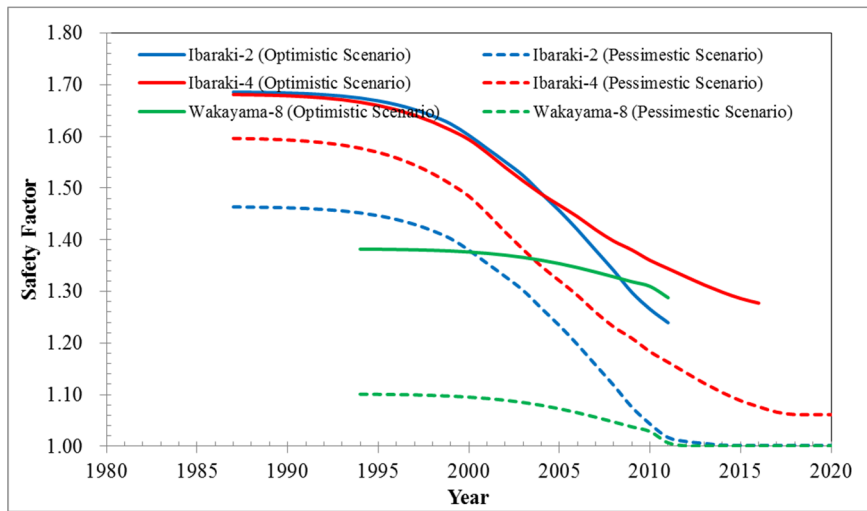
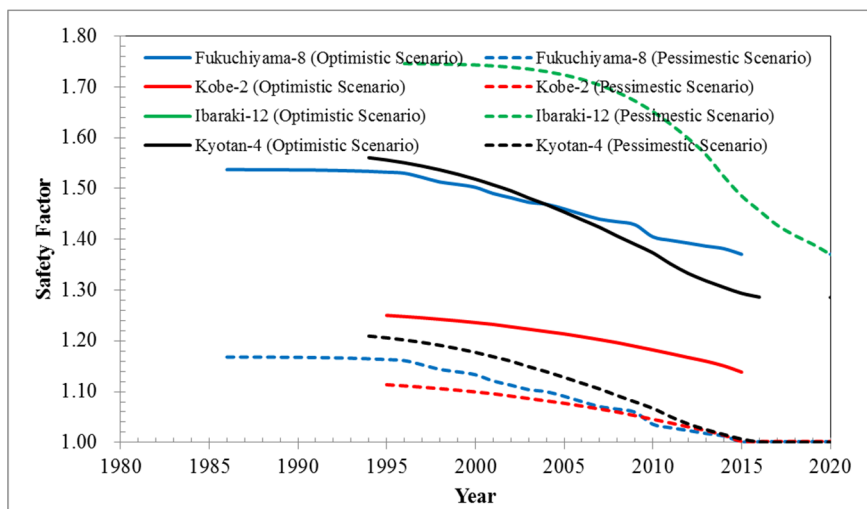


Figure 6.5 The example of deteriorated on anchor force on a slope



(a) Rod type



(b) Strand type

Figure 6.6 FS with time of sedimentary (a) rod type and (b) strand type

The results of *F.S.* versus time are plotted for rod and strand types of the sedimentary rock as illustrated in Fig 6.6 (a) and (b), respectively. The dashed lines represent the pessimistic scenarios, while the continuous lines are the optimistic scenarios. Considering the pessimistic scenario, Ibaraki No.2 and Wakayama No.8 seem to be severe deteriorated conditions while Ibaraki No.4 is still stable for the rod type as presented in Fig 6.6 (a). Ibaraki No.12 seems to be low risk to collapse, whereas Kyotan No.4, Kobe No.2 and Fukuchiyama No.8 may reach to critical stage after 2015 for strand type. These results confirmed that both Ibaraki No.4 and Ibaraki No.12 which still high survival probabilities does not reach to critical condition. On the other hand, the optimistic scenarios reveal higher *F.S.* and might not reach to a critical situation in near future. It implies that the pessimistic scenarios are more proper to investigate the failure probability.

By comparing, the relationships between *F.S.* and survival probabilities may not be appropriate to compare, for example, *F.S.* result of Wakayama No.8 was only 1.00, but the survival probability is high at 0.46; nevertheless, survival probability of Ibaraki No.2 is quite low (0.11) and *F.S.* is also low (1.04). Consequently; the percentage of reduction in performance function seems to be more appropriate for comparing together with the survival probability. The performance function was related to the *F.S.*, which can be calculated as follows;

$$Q = F.S. - 1 \quad (6.1)$$

Hence, the percentage of reduction in performance function can be express as follows;

$$\text{Percentage of Performance Function} = \frac{Q (\text{present})}{Q (\text{initial})} \quad (6.2)$$

Figure 6.7 shows the relationship between percentages of reduction on performance function versus survival probabilities of seven risk slopes. The hollow dot represented the calculated results of those risk slopes while the red dashed line was a one to one relationship corresponding to the ideal correlation line. Survival probabilities presented overestimated results compared with percentages of reduction in performance function.

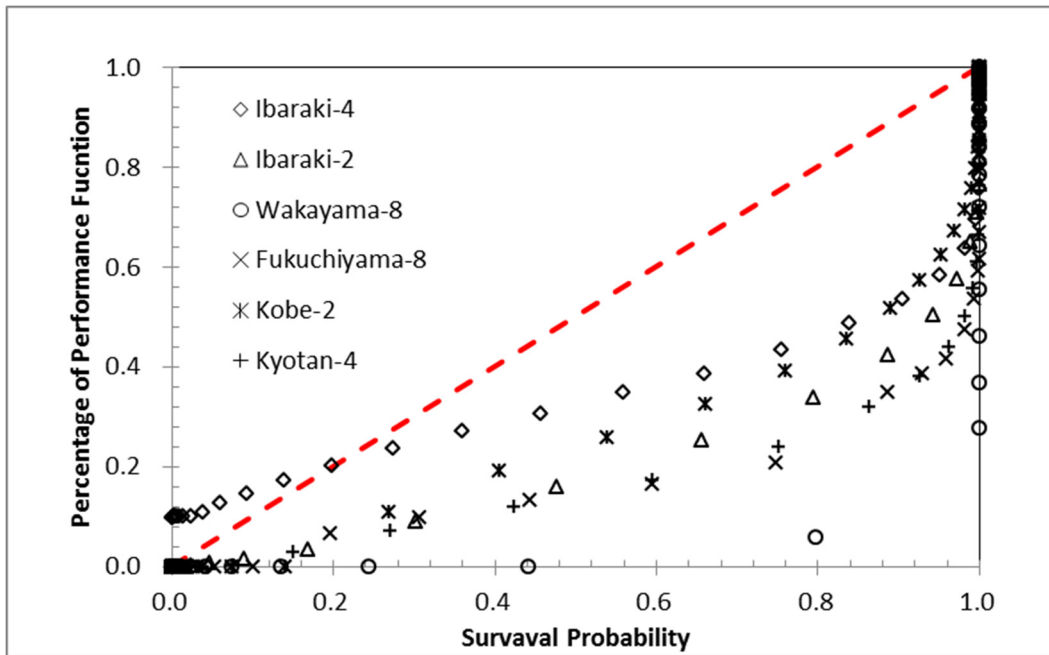


Figure 6.7 Relationship between percentages of reduction in performance function versus survival probability

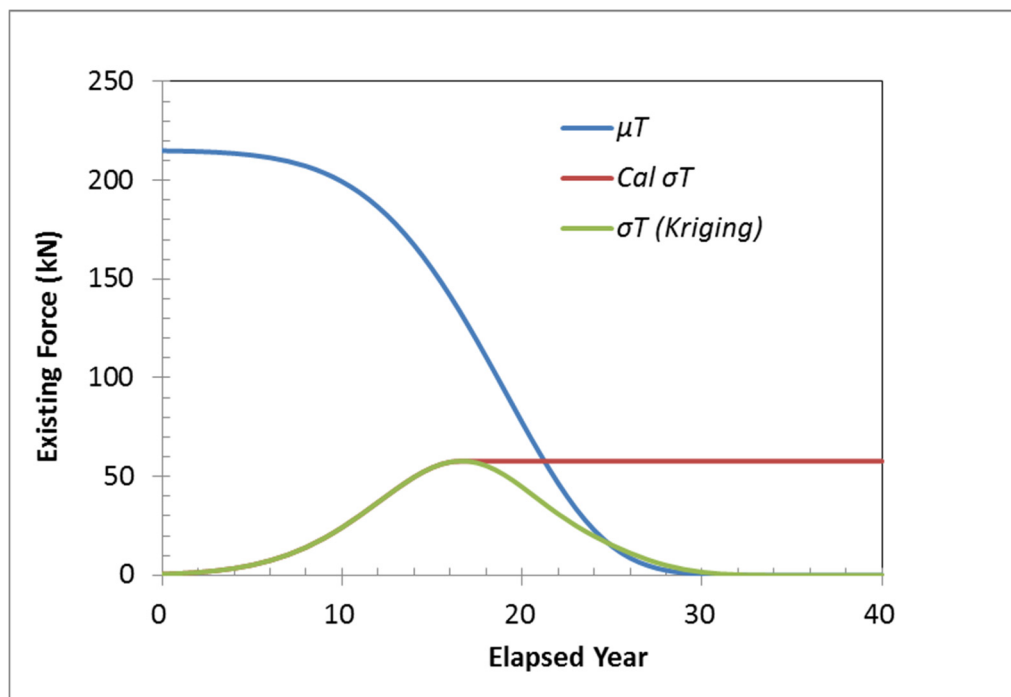


Figure 6.8 The reduction of the existing force with time

6.3 Annual Probability of Failure of the Risk Slopes

Even though, the Safety Factor, $F.S.$ can be used as an indicator for making decision and judge, whether those slopes stable or instable; however, it might not be an adequate cause

it does not deal with variation of the data. Therefore, the annual failure probability might be more appropriate to consider regarding this matter.

In this section, the annual failure probability of each risk slope was conducted and compared. The risk slopes were divided following anchor's type into two groups as rod and strand types. As mentioned in previous sanction, the performance function, Q can be calculated from the safety factor, $F.S.$ as illustrated in Eq. 6.1. The reduction of anchors forces versus time can be simulated by means of the Weibull hazard model as mentioned in section 6.2, hereafter average, μ and standard deviation, σ of the anchors force can be evaluated as presented in Fig 6.8. Average existing force, μ_T of each year continuously declined with time as presented by blue line; on the other hand, standard deviation, σ_T rose gradually with time as shown by the green line, however, it went down after reach to certain time. Therefore, the red line represented an adjusted standard deviation for calculation, $Cal\sigma_T$ which assumed constant σ_T after reaching to the zenith point because the μ_T is close to zero, the coefficient of variation will approach infinity and is therefore sensitive to small changes in the mean.

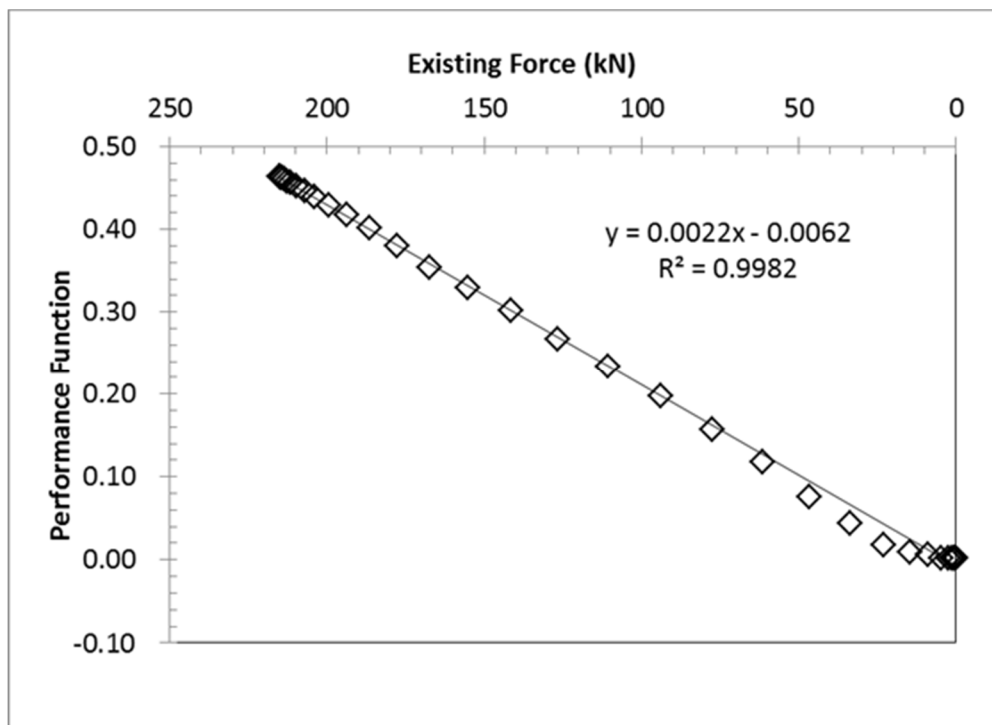
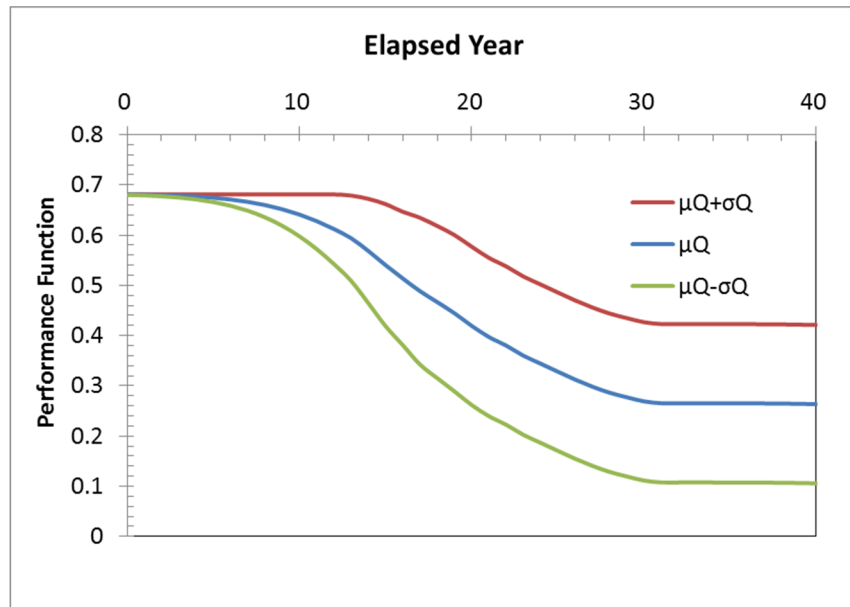
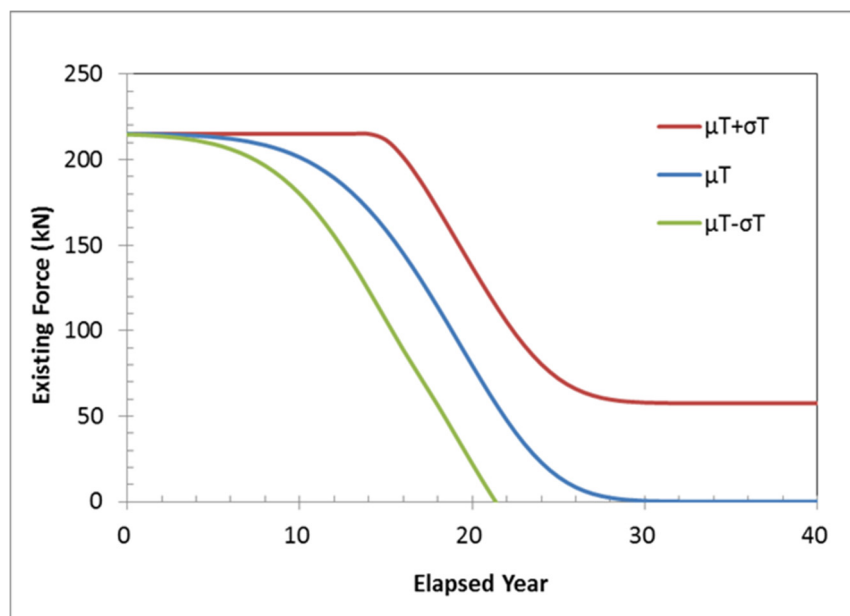


Figure 6.9 Existing forces of ground anchor versus performance function

Figure 6.9 presents the average existing force of ground anchor on the horizontal axis versus the performance function on the vertical axis. The regression curve between both parameters demonstrated as a linear relationship with high R -squared. Therefore, it can be expressed that the average existing force was a function of the performance function.



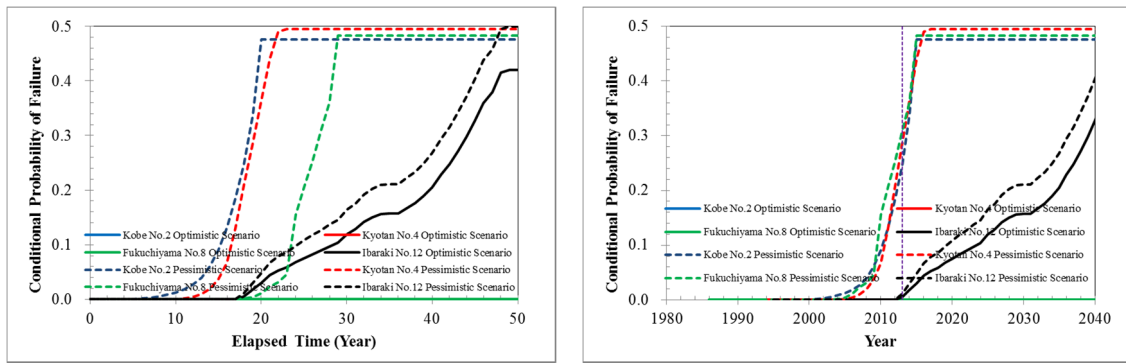
(a) Performance function with time



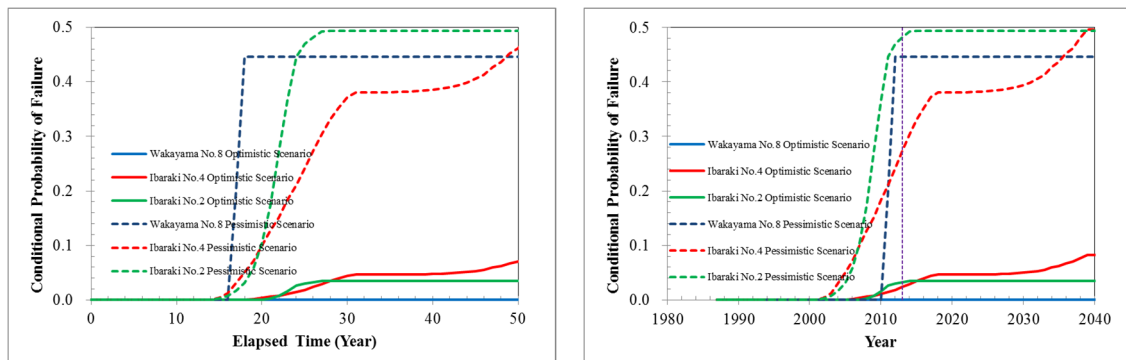
(b) Existing force with time

Figure 6.10 Performance function and Existing force versus elapsed time

Figure 6.10 (a) and (b) demonstrate the performance function as well as the existing force versus elapsed time, respectively. The expectation value was plotted as blue color while the red and green corresponding to average value plus and minus standard deviation, respectively.



(a) Strand type

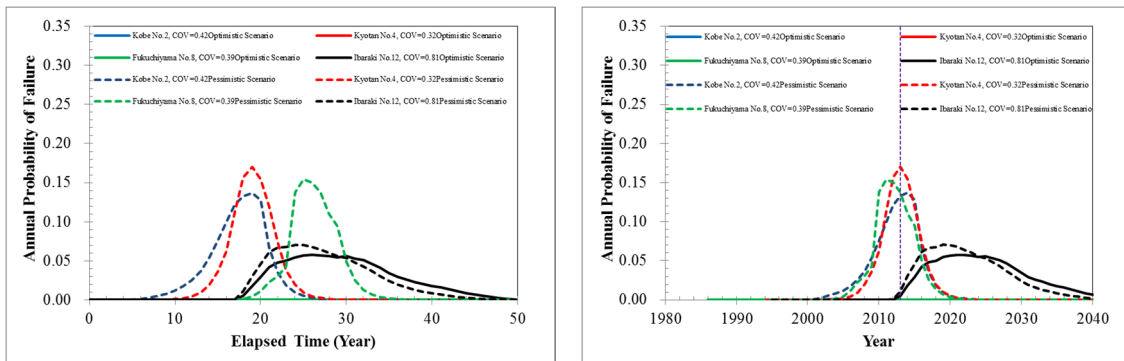


(b) Rod type

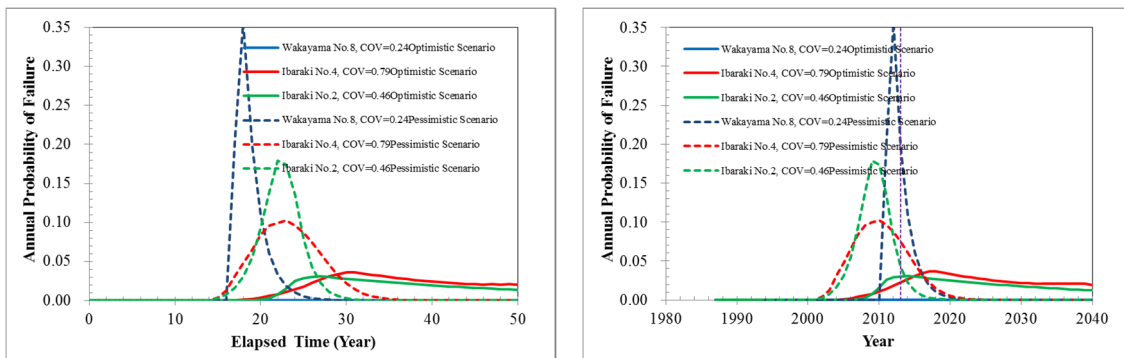
Figure 6.11 Conditional probabilities of failure of risk slopes

The conditional probabilities of failure are illustrated in Fig 6.11 for (a) strand type and (b) rod type, respectively. The left pictures represent conditional probabilities of failure versus elapsed time while the right demonstrate as the years. Considering the pessimistic scenario, Kobe No.2, Kyotan No.4 and Fukuchiyama No.8 reached to maximum value after 20, 23 and 30 years, respectively, whereas Ibaraki No.12 does not reach to maximum point even if 40 years has passed which corresponding to strand type. By considering as the year, most of them reach to the maximum conditional probability of failure at 2015 except Ibaraki No.12. In case of Rod type, Wakayama No.8, Ibaraki No.2 touched to zenith at 18 and 29 after installation; on the other hand, Ibaraki No.4 do not reach to maximum point even 40

passed. Wakayama No.8 reached to the maximum point before present while others touch the highest conditional probability of failure after 2015. The results quit same with strand types. It implied that only Wakayama No.8 might be dangerous at present while Ibaraki No.12 is still stable after 40 years have passed. Others might be a serious condition after 2015. However, the optimistic scenarios always show lower conditional probability of failure.



(a) Strand type

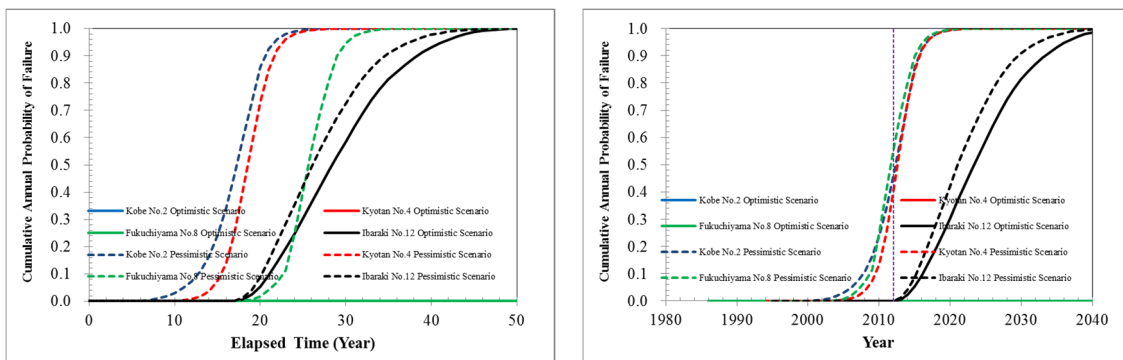


(b) Rod type

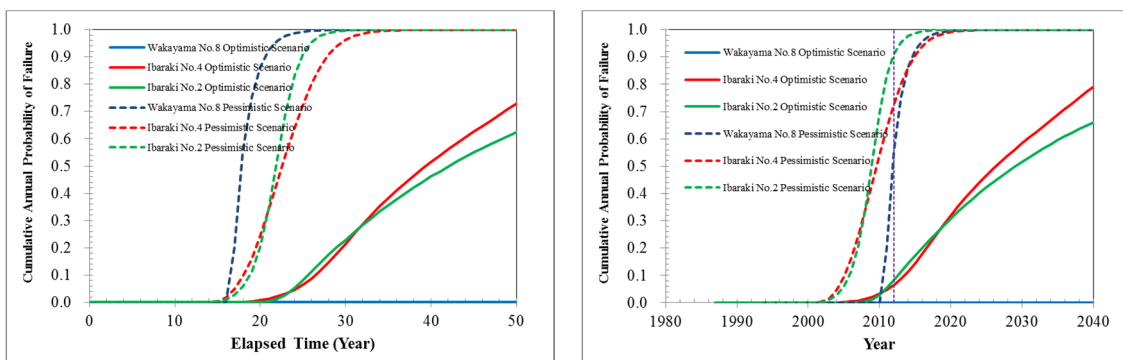
Figure 6.12 Annual probabilities of failure of risk slopes

Figure 6.12 (a) and (b) present the annual probabilities of failure, which calculated by formulae given in Chapter 2. It can be demonstrated into elapsed time as well as the years. The coefficient of variation, COV at present, which obtained from kriging results directly affected to the shape of probability density function, PDF that larger COV , the base of PDF expanded and crest point decreased, in contrast to the smaller COV ; the base decreased while peak increased. For instance, Wakayama No.8's COV , 0.24, narrow base with high peak point while Ibaraki No.12 was 0.79; the pedestal is the larger with lower zenith.

In case of strand type, considering the pessimistic scenario, the expectation of annual probabilities of failure closed to present year (2013) except Ibaraki No.12, on the other hand, the rod type illustrated the peak point at early present year. Its peak point revealed strand types seem to be more durable than rod type, which is quite the consistent reason with the results of the deteriorated rate from the Weibull hazard model. In addition, the probability density function based on the optimistic scenarios does not appear since several slopes are very low risk to collapse.



(a) Strand type

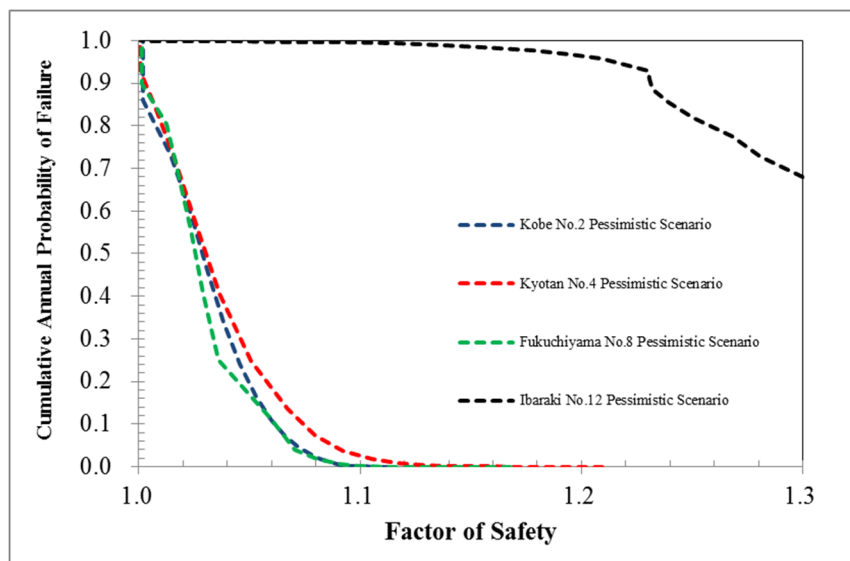


(b) Rod type

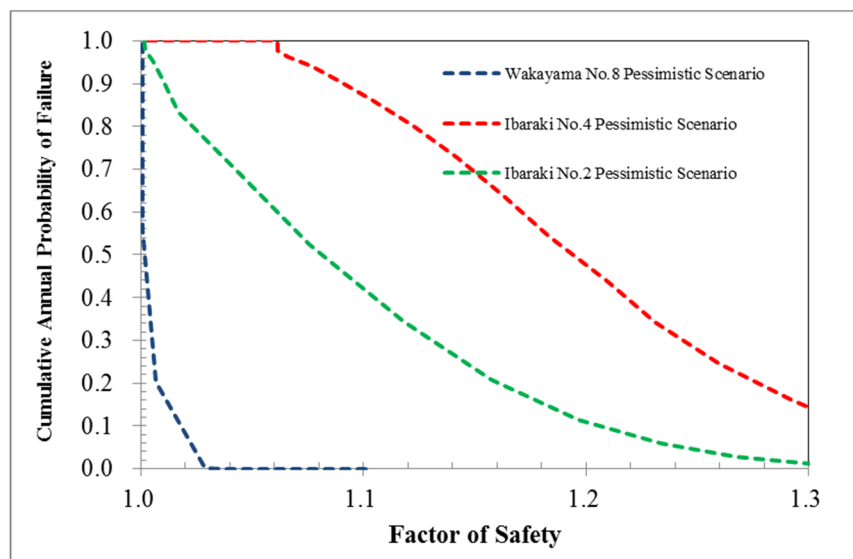
Figure 6.13 Cumulative Annual Probabilities of Failure of risk slopes

The cumulative annual probabilities of failure were plotted and compared for strand and rod types as demonstrated in Fig 6.13 (a) and (b), respectively. For the pessimistic scenario, most of the slopes improved by strand types touched the failure at 2020, roughly, except Ibaraki No.12 while the rod type reached to failure during 2018 to 2020 except Ibaraki No.4, approximately. However, those slopes are quite stable when considering GWT level lower than the failure plane (optimistic scenario). In brief, the rod type seems to be less durable than the strand types that the maintenance should be priority conducted.

In addition, the relationship between $F.S.$ and cumulative probability of failure considering pessimistic scenario is presented in Fig 6.14 (a) and (b) for strand and rod types, respectively. The vertical axis shows the cumulative probability of failure while the horizontal axis is $F.S.$. The results indicate that cumulative probability of failure proportionally decrease to the $F.S.$. However, the reduced rates of each slope are different depending on the slope configuration as well as number of ground anchor on individual slope.



(a) Strand type



(b) Rod type

Figure 6.14 The relationship between $F.S.$ and cumulative probability of failure

CHAPTER 7

ESTIMATE OF THE LIFE CYCLE COST AND DECISION-MAKING ON MAINTENANCE

7.1 Introduction

The Life Cycle Cost, *LCC* is an economic measurement technique to determine the total cost of maintenance over its lifetime, which employed to analysis the lifespan of ground anchors in this paper. Since ground anchors were started to install after 1970 in Japan, consequently, some of them were in severe decayed conditions caused excessive deteriorated or overstressed of pre-stressed forces hence maintenance strategy is required. The deterioration of ground anchors indicated as a reduction of quality or strength affected to the stability of the slope. From such a viewpoint, several statistical model are served to describe a deterioration rate of ground anchor.

The stability of slopes of difference maintenance strategies were illustrated in Fig 7.1. In addition, the stability of slope improved by ground anchors went up after replacing/repairs were conducted. The high-frequency maintenance scenario showed higher *F.S.* with reduced venture to failure; however, the cost of maintenance also increasing. On the other hand, low frequency maintenance plan illustrated lower expense, but high risk of slope collapse with more recovery and miscellaneous expense. Therefore, the *LCC* is adopted as the indicators to evaluate the suitable scenario plan for repair/renew as well as its life span.

In this chapter, the calculation of the Life cycle cost was divided into three categories which are:

4. *LCC* of the Visual inspection test results: considering the failure probability based on the Weibull hazard model and the Markov model with neglect the loss due to slope failure caused the Visual inspection test cannot calculate slope stability. It can be considered as the macroscopic viewpoint.
5. *LCC* of both Visual inspection test and Lift off test results: considering the failure probability based on the Weibull hazard model, excluding the losses because of slope

failure. This result was considered in decision-making on the testing method for establishing the maintenance strategies.

6. *LCC* of the Lift off test results: considering the failure probability based on the Weibull hazard model, including the losses due to slope failure. It can be considered as the microscopic viewpoint.

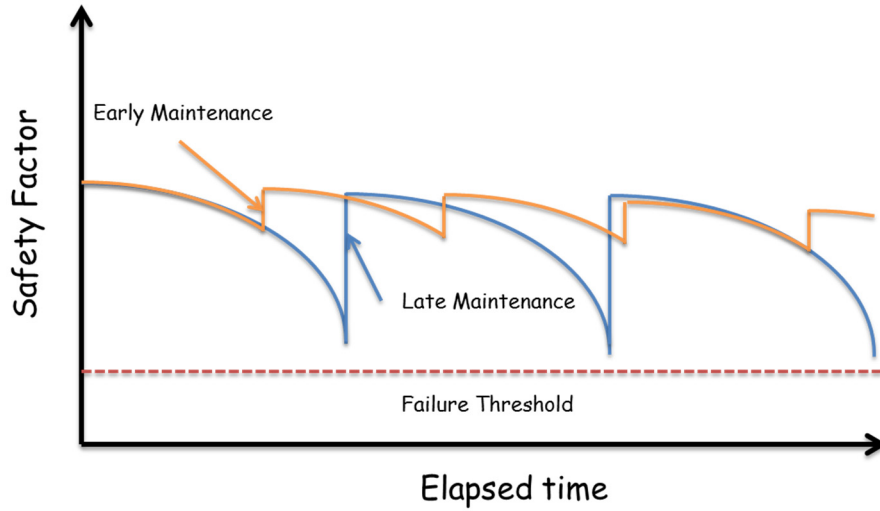


Figure 7.1 Stability of slope improved by ground anchors considering different maintenance strategies

7.2 The Concept of Life Cycle Cost, *LCC*

The *LCC* composed of three components, which are inspection cost, repair cost and recovery cost as mentioned in the previous chapter. The *LCC* can be calculated as follows;

$$\begin{aligned}
 LCC = & \sum_{k=1}^x \sum_{j=1}^{k \cdot t_m} IC_{ins} \left(\frac{1}{1+\rho} \right)^{k \cdot t_m} \\
 & + \sum_{k=1}^x \sum_{j=1}^{k \cdot t_m} \left[\prod_{j=1}^{i-1} (1 - \Delta p_f(t_j)) \Delta p_f(t_i) \right] C_{rep} \left(\frac{1}{1+\rho} \right)^{k \cdot t_m} \\
 & + \sum_{i=1}^t \left[\prod_{j=1}^{i-1} (1 - \Delta p_f(t_j)) \Delta p_f(t_i) \right] C_h \left(\frac{1}{1+\rho} \right)^i
 \end{aligned} \tag{7.1}$$

Where

C_{ins} is the inspection cost

C_{rep} is the repair cost

C_h is the expected losses

ρ is the social discount rate that assumes to be 4%

j represented time after maintenance

i is time after slope failure occurrence

t_m is maintenance time

Δp_f is the failure probability

k is inspection interval.

Note that, there are two types for evaluating the *LCC*, whether considering risk (expected losses) to investigate slope stability in addition to the maintenance work or neglect. In case of the Visual inspection test results, the last term of the *LCC* was abandoned, because the remaining force cannot be measured so that the stability analysis cannot be performed. Therefore, the *LCC* without expected losses can be calculated as:

$$LCC = \sum_{k=1}^x \sum_{j=1}^{k \cdot t_m} IC_{ins} \left(\frac{1}{1 + \rho} \right)^{k \cdot t_m} + \sum_{k=1}^x \sum_{j=1}^{k \cdot t_m} \left[\prod_{j=1}^{i-1} (1 - \Delta p_f(t_j)) \Delta p_f(t_i) \right] C_{rep} \left(\frac{1}{1 + \rho} \right)^{k \cdot t_m} \quad (7.2)$$

The inspection cost is consisting of the Visual inspection test and the Lift-off test. The Visual inspection test was experimented on every ground anchor (approximately 2,000 yen/anchor) while the Lift off test was assumed to perform on the selected spot because it was quite expensive (around 500,000 yen/anchor). In addition, the repair cost depends on the number of anchors's renew cost which was assumed to be a million JPY approximately. Finally, the cost of recovery was calculated following equation proposed by Ohtsu, 2011.

$$C_h = (C_{v0}V + C_{A0}A)x(1 + a) + C_{M0}n \quad (7.3)$$

Where

C_h = recovery cost

C_{v0} = cost of removal per cubic meter

V = volume of debris

C_{A0} = cost of restore per square meter

A = area of restoration

a = miscellaneous expense ratio

C_{M0} = labor and management cost per day

n = working days.

7.3 LCC Considering the Macroscopic Viewpoint

The macroscopic viewpoint considered the failure probability based on the Weibull hazard model and the Markov model with neglect the loss due slope failure caused the Visual inspection test cannot calculate slope stability. Note that, only one ground anchor was considered in each case. Therefore, the inspection expense of each slope was two thousand JPY and the repair cost was a million JPY, respectively.

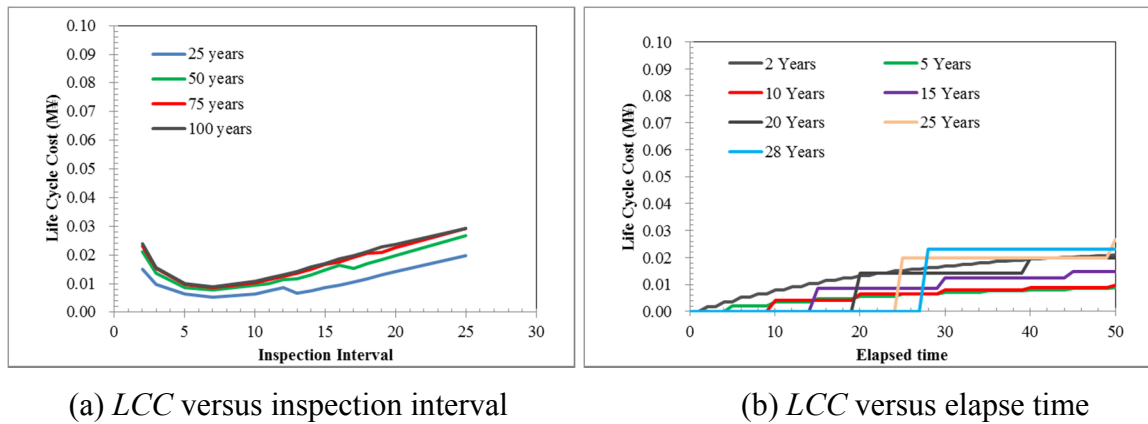
The *LCC* cost was considered by two statistic models as mentioned above. Because of the limitation of the allowable data, two categories were analyzed, which are rod and strand types. There are including two scenarios following the failure criteria of the Visual inspection test. For example, the *LCC* result of the Markov model based on the scenario I (the rank I and II corresponding to failure ranks) denoted as MC-I while the result of Weibull hazard model considering the scenario II (the rank I, II and III corresponding to failure ranks) meant WB-II. Hence, eight scenarios of *LCC* results were compared.

7.3.1 LCC of the Visual inspection test

Figure 7.2 (a) and (b) illustrate comparison of the *LCC* results based on the Visual inspection test results varying inspection intervals versus elapsed time of the rod type (MC-I). The inspection intervals were calculated varies from 2 to 28 years. The high frequency of the inspection interval, the *LCC* increased due to plenty of expense from the inspection while low frequency, the *LCC* increased as well caused high expense of the anchor repair. Therefore, the optimum inspection interval scenario was judged by considering the least *LCC*. In addition, the salvage values of ground anchors were abandoned due to completely deteriorate. Moreover, the *LCC* was focused on difference elapsed time. For example, 25, 50, 75 and 100 years found that they slightly increased. Therefore, the results illustrated on

25 years supposed to be appropriated time due to lowest expense It can be seen that the optimum inspection interval is seven years.

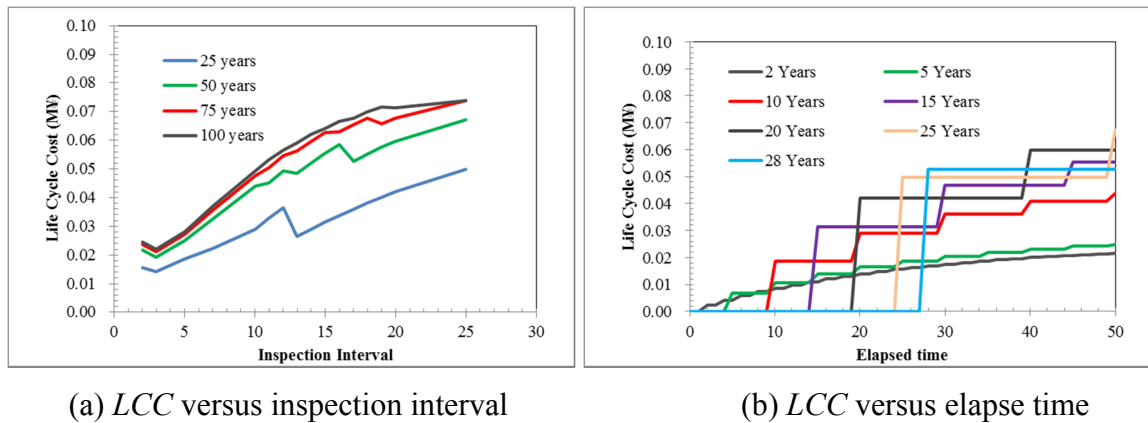
Moreover, the other scenarios; for instance, rod type (MC-II), rod type (WB-I), rod type (WB-II), strand type (MC-I), strand type (MC-II), strand type (WB-I) and strand type (WB-II), were presented in Fig 7.3 to 7.9, respectively.



(a) *LCC* versus inspection interval

(b) *LCC* versus elapse time

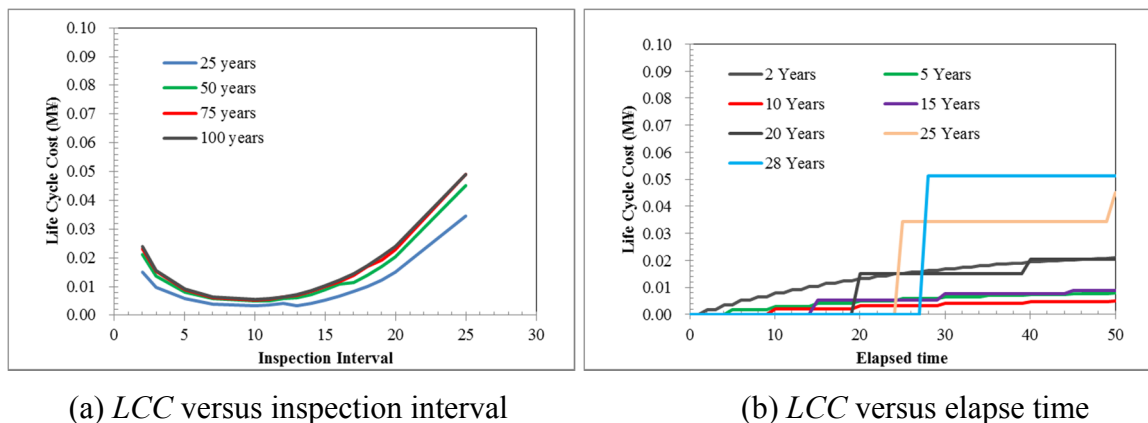
Figure 7.2 Comparison of *LCC* results of the Rod type (MC-I)



(a) *LCC* versus inspection interval

(b) *LCC* versus elapse time

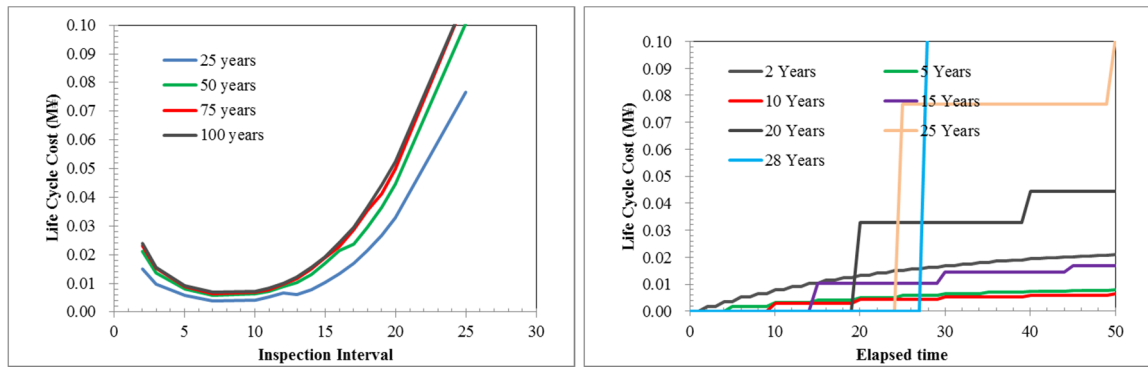
Figure 7.3 Comparison of *LCC* results of the Rod type (MC-II)



(a) *LCC* versus inspection interval

(b) *LCC* versus elapse time

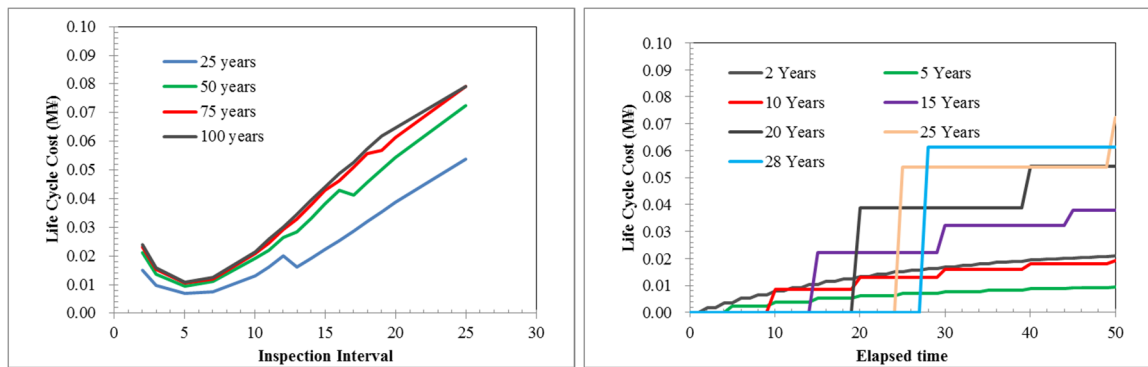
Figure 7.4 Comparison of *LCC* results of the Rod type (WB-I)



(a) *LCC* versus inspection interval

(b) *LCC* versus elapsed time

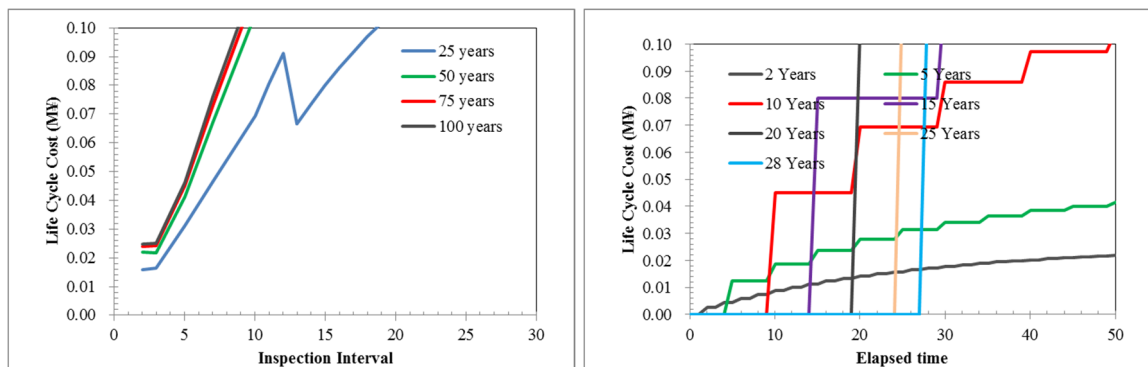
Figure 7.5 Comparison of *LCC* results of the Rod type (WB-II)



(a) *LCC* versus inspection interval

(b) *LCC* versus elapsed time

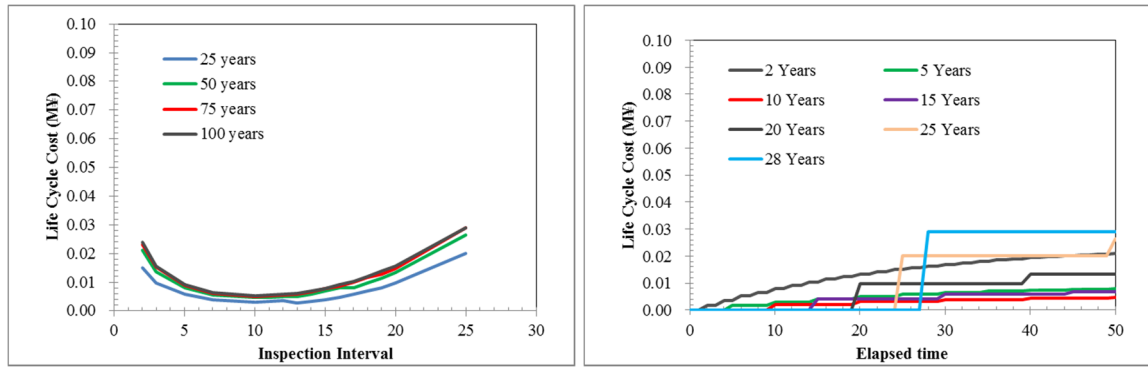
Figure 7.6 Comparison of *LCC* results of the Strand type (MC-I)



(a) *LCC* versus inspection interval

(b) *LCC* versus elapsed time

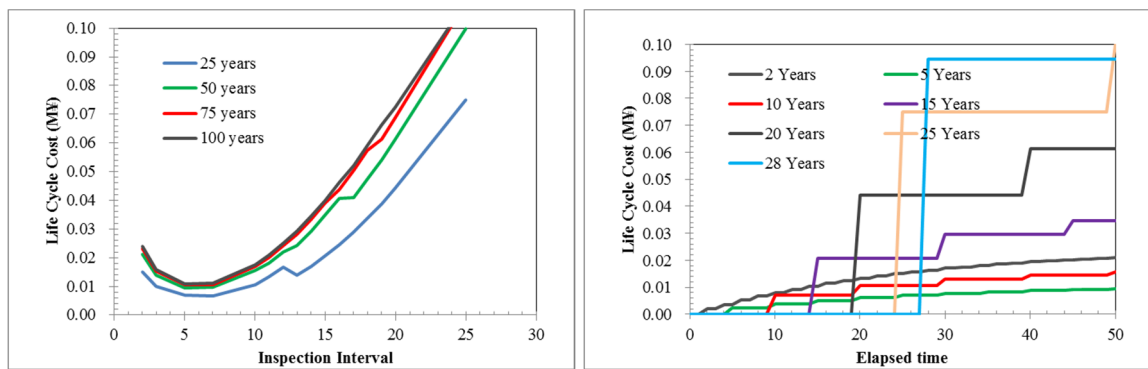
Figure 7.7 Comparison of *LCC* results of the Strand type (MC-II)



(a) *LCC* versus inspection interval

(b) *LCC* versus elapse time

Figure 7.8 Comparison of *LCC* results of the Strand type (WB-I)



(a) *LCC* versus inspection interval

(b) *LCC* versus elapse time

Figure 7.9 Comparison of *LCC* results of the Strand type (WB-II)

Table 7.1 Summary of the *LCC* results of the Visual inspection test

Case	Optimum <i>LCC</i> at 25 years (kJPY)	Optimum Inspection interval (Year)
Rod type (MC-I)	5.31	7
Rod type (MC-II)	14.11	3
Rod type (WB-I)	3.24	10
Rod type (WB-II)	3.97	7
Strand type (MC-I)	7.05	5
Strand type (MC-II)	15.79	2
Strand type (WB-I)	2.85	13
Strand type (WB-II)	6.71	7

Table 7.1 lists the summary results of the *LCC* of each scenario that optimum inspection interval varies from 2 to 13 years. The results, based on the Weibull hazard model revealed the longer optimum inspection interval than the results of the Markov model considering the same scenario as well as the *LCC* expense of the Weibull hazard model were cheaper than the Markov model. The scenario I showed a lower expense with longer optimum inspection interval than the scenario II.

7.3.2 *LCC* of the Lift off test

Figure 7.10 and 7.11 show the *LCC* results various inspection intervals versus elapsed time of the rod and strand types based on the Lift off test results, respectively.

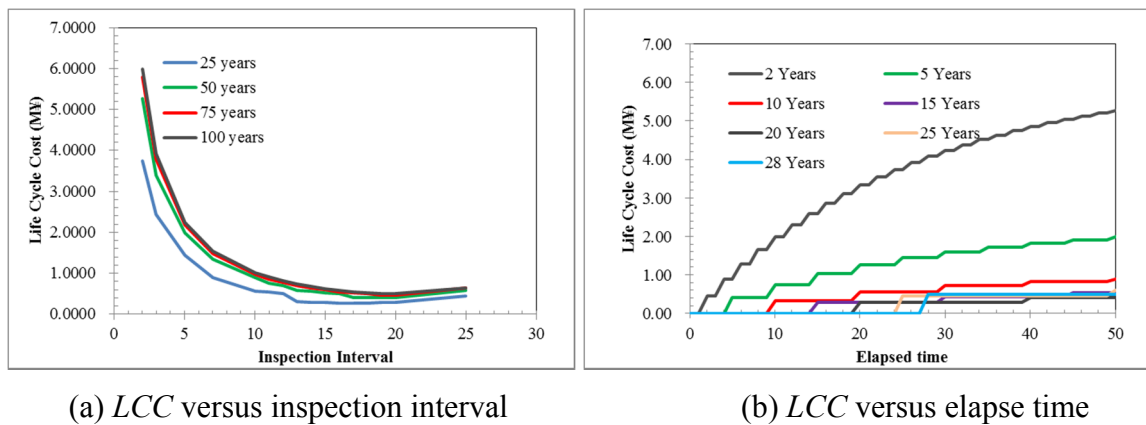


Figure 7.10 Comparison of *LCC* results of the Rod type

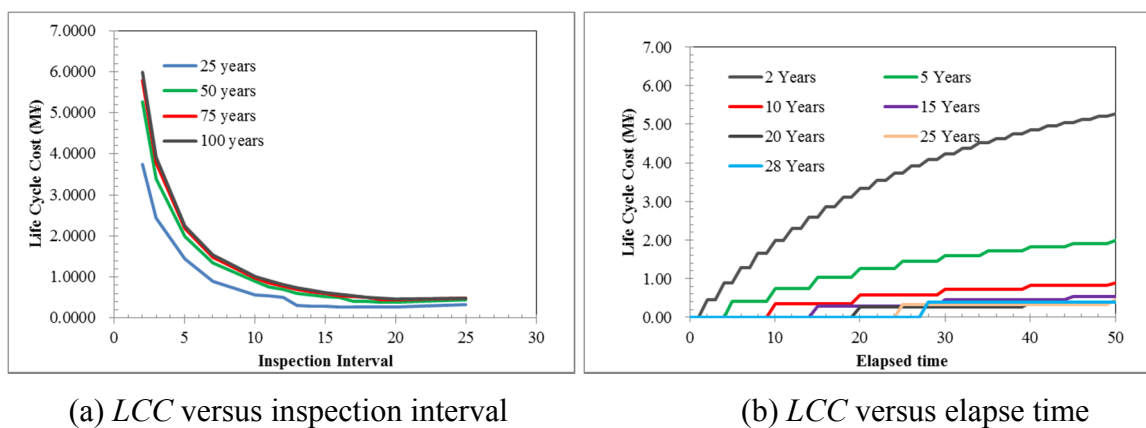


Figure 7.11 Comparison of *LCC* results of the Strand type

It considered the elapsed time of 25 years same with the previous section. The optimum inspection interval of rod and strand types are 17 and 19 years, respectively; however, the

LCC results were slightly different that the rod type demonstrated more expense than the strand type as tabulated in Table 7.2.

Table 7.2 Summary of the LCC results of the Lift off test

Case	Optimum LCC at 25 years (kJPY)	Optimum Inspection interval (Year)
Rod type	275.31	17
Strand type	271.93	19

7.3.3 Comparison of LCC Results between the Visual Inspection and Lift off tests

The comparison of the LCC results between ground anchor types were illustrated in Fig.7.12. The hollow dots represented the scenario II (rank I, II and III corresponding to failure ranks) while the filled dots were scenario I (rank I and II corresponding to failure ranks). The Markov model and the Weibull hazard model denoted as the black and red color, respectively. Both results displayed the similar trend that Weibull hazard model demonstrated lower expense with longer inspection interval than the result based on the Markov model. Moreover, the scenario II showed higher the LCC because the number of failure greater than the scenario I.

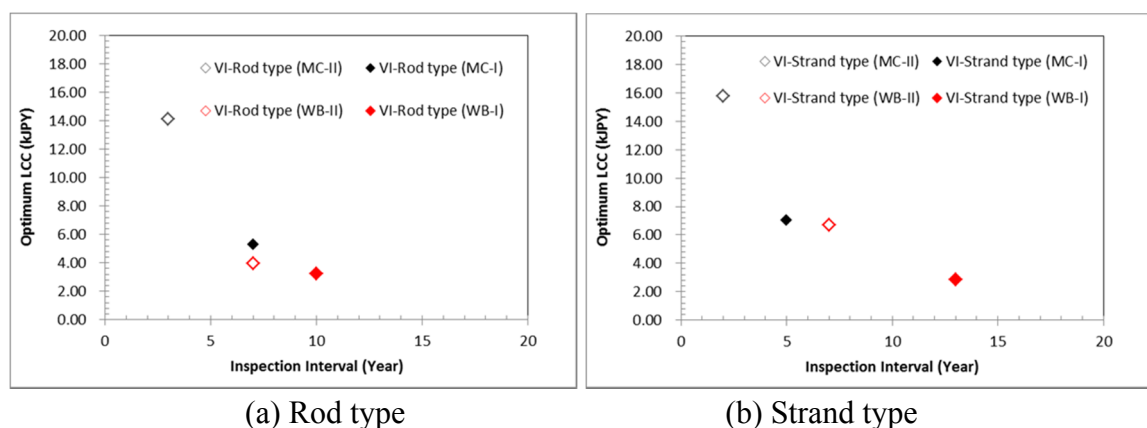


Figure 7.12 Comparison of LCC results between ground anchors type of the Visual inspection test

Figure 7.13 (a) to (b) present the comparison of the *LCC* results between the Markov model and the Weibull hazard model, respectively. The red color represented strand type while the black color indicated the rod type. The filled and the hollow dots were scenario I and II, respectively. The Weibull hazard model revealed the lower *LCC* on every scenario; therefore, it should be the appropriate model for decision making to maintenance. In addition, this model indicated the longer inspection time; hence, it is the profit and advantage of the road administration. The Markov model demonstrated too pessimistic results compared with the Weibull hazard model; therefore, the Weibull hazard model was engaged to be the representative the statistical model to identify the inspection time.

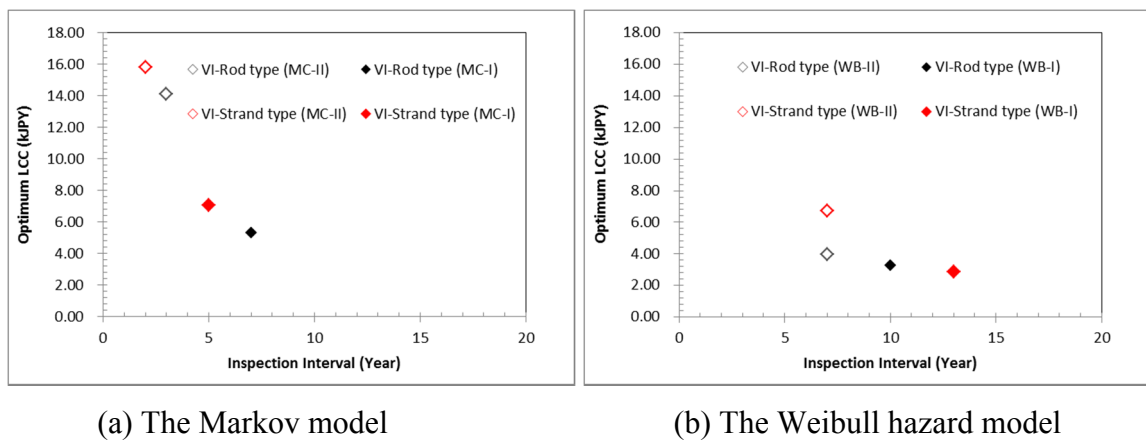


Figure 7.13 Comparison of LCC results between statistical models of the Visual inspection test

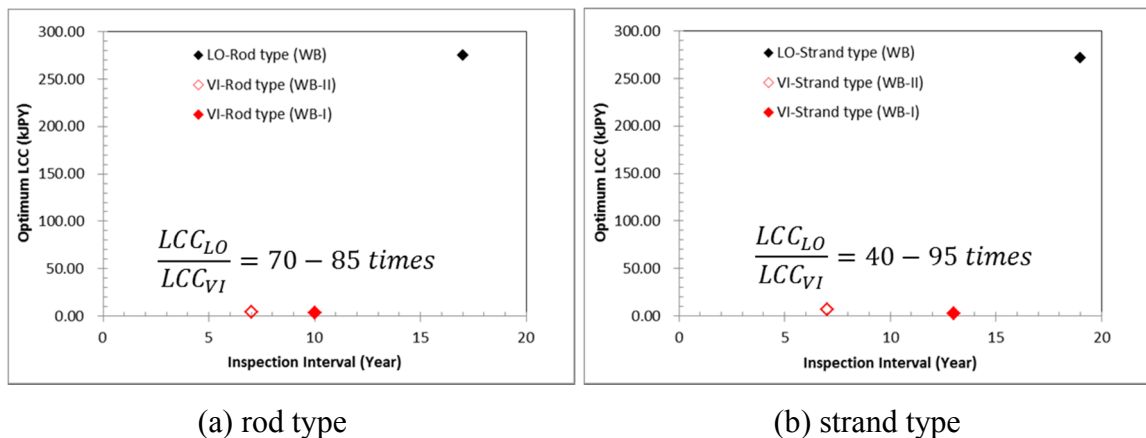


Figure 7.14 Comparison of LCC results between the Visual Inspection test and the Lift off test results

Figure 7.14 (a) to (b) present the comparison of the *LCC* results between the Visual inspection test and the Lift off test results for rod and strand types, respectively. The red color represented the Visual inspection test results denoted as the VI while the black dot indicated the Lift off test result denoted as LO. The *LCC* calculated based on the Lift off test demonstrated higher cost than the Visual inspection test about 70-95 times, since the inspection cost is more expensive as well as the failure probabilities were different that the Visual inspection test showed lower than the Lift off test. Moreover, the suitable inspection time based on the Lift off test were longer than the Visual inspection test.

7.4 *LCC* Considering the Microscopic Viewpoint

Table 7.3 summarizes the input parameters for calculating the *LCC* of the individual risk slopes. Most of them revealed that the repair cost was dominated factor except Fukuchiyama No.8 the recovery cost is the most expense. In fact, the loss due to compensation for damages to vehicles, passenger and private properties, shall be added to recovery cost as the indirect expense, however, it is complicated to evaluate indeed, hence it was abandoned in this study. Seven risk slopes, including Ibaraki No.4, Ibaraki No.2, Wakayama No.8, Kobe No.2, Kyotan No.4, Fukuchiyama No.8 and Ibaraki No.12 were calculated for giving priority to replace/repair strategies. The inspection intervals were considered at 2, 5, 10, 15, 17 and 20 years.

Table 7.3 Summary of input parameters for analysis the *LCC*

Slope Name	Number of anchors	Volume of failure (m ³)	Area of restoration (m ²)	Inspection cost (MJPY)	Repair cost (MJPY)	Recovery cost (MJPY)
Wakayama No.8	395	5,205	9,280	40.29	395.00	125.52
Ibaraki No.4	234	9,441	2,960	23.87	234.00	73.67
Ibaraki No.2	180	7,343	2,300	18.36	180.00	57.27
Fukuchiyama No.8	116	41,430	10,600	11.83	116.00	296.74
Kyotan No.4	172	5,540	1,100	17.54	172.00	36.16
Kobe No.2	85	8,701	2,310	8.67	85.00	63.26
Ibaraki No.12	209	4,782	1,290	21.32	209.00	34.99

Figure 7.15 (a) and (b) illustrate comparison of various *LCC* scenarios versus elapsed time and inspection interval of Ibaraki No.4, respectively. In this context, *LCC* results on each slope related to the individual probabilistic models, including cumulative probability of failure, annual probability of failure attributes. This probabilistic model obtained directly from the Weibull hazard model based on Lift off test results.

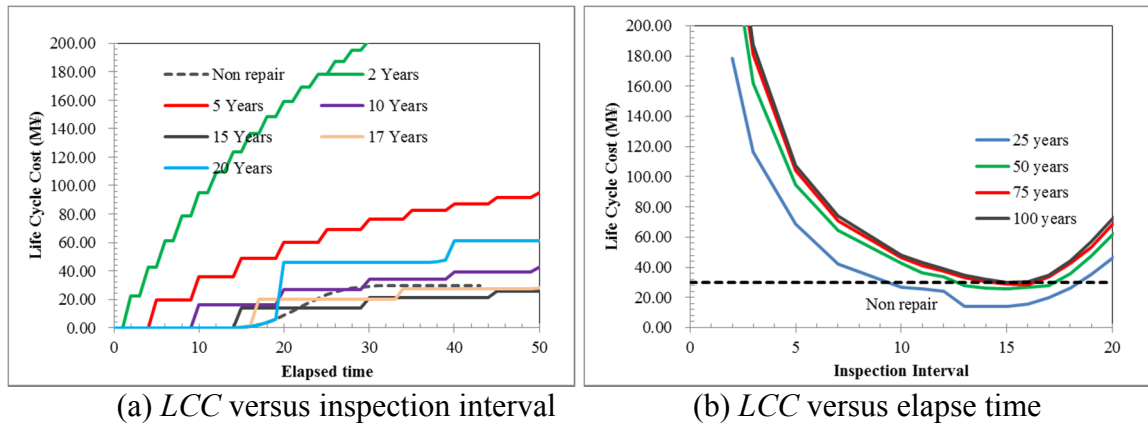


Figure 7.15 Comparison of LCC with difference repair scenarios of Ibaraki No.4

Furthermore, the comparisons of various *LCC* scenarios of other slopes were presented in Fig 7.16 to 7.21 corresponding to Ibaraki No.2, Wakayama No.8, Kobe No.2, Kyotan No.4, Fukuchiyama No.8 and Ibaraki No.12, respectively.

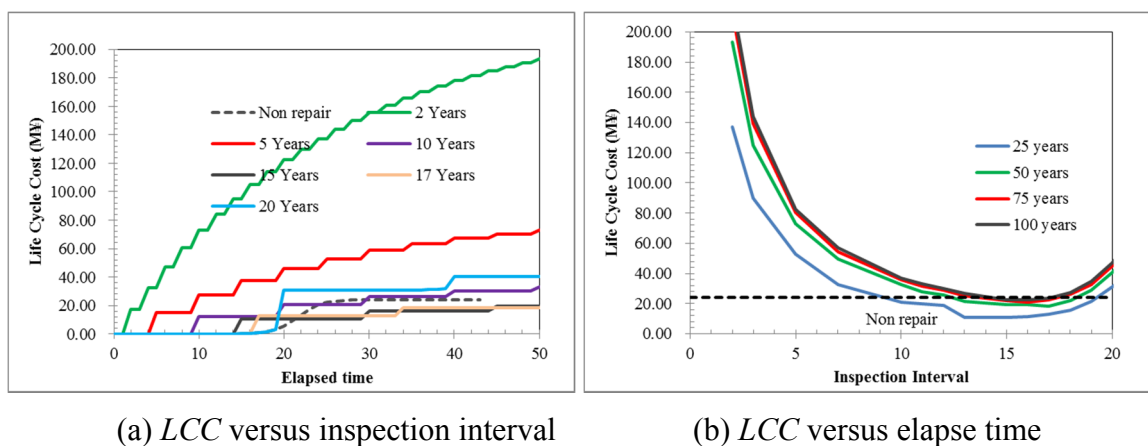
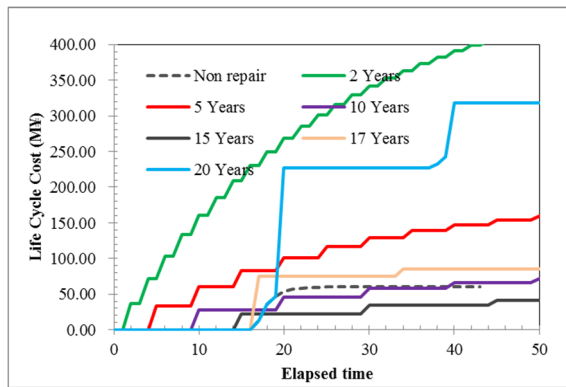
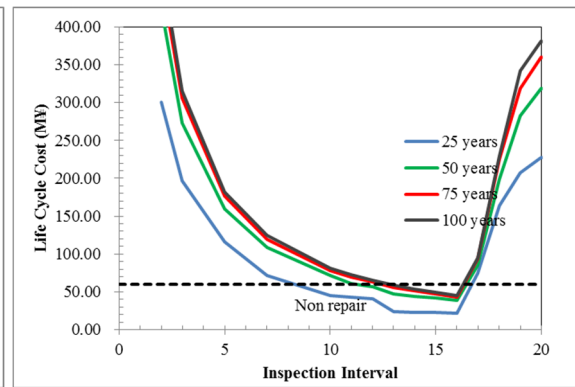


Figure 7.16 Comparison of LCC with difference repair scenarios of Ibaraki No.2

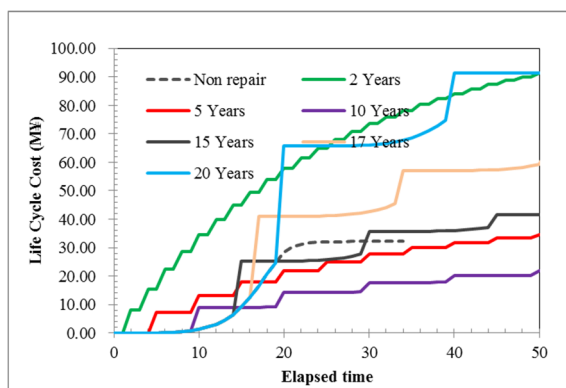


(a) *LCC* versus inspection interval

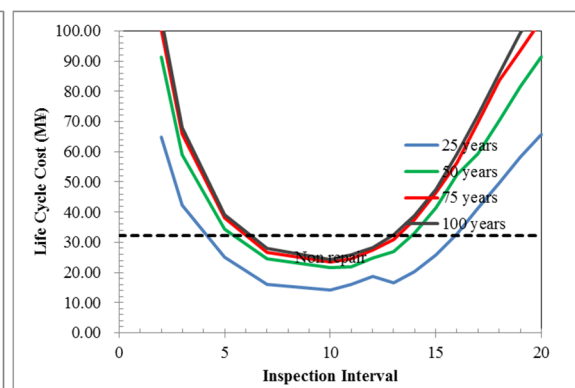


(b) *LCC* versus elapse time

Figure 7.17 Comparison of *LCC* with difference repair scenarios of Wakayama No.8

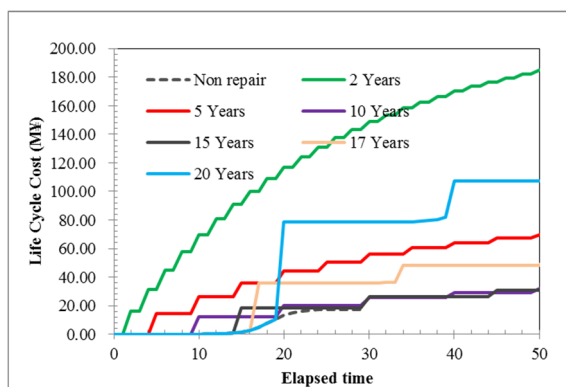


(a) *LCC* versus inspection interval

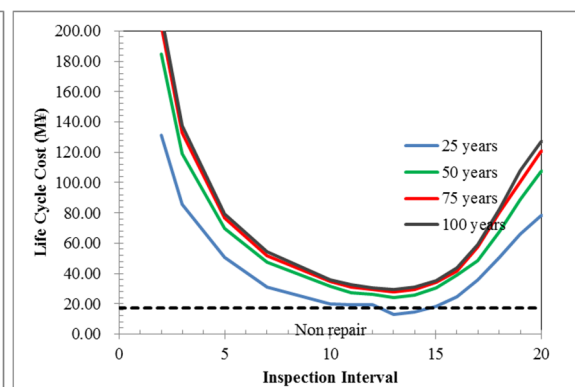


(b) *LCC* versus elapse time

Figure 7.18 Comparison of *LCC* with difference repair scenarios of Kobe No.2

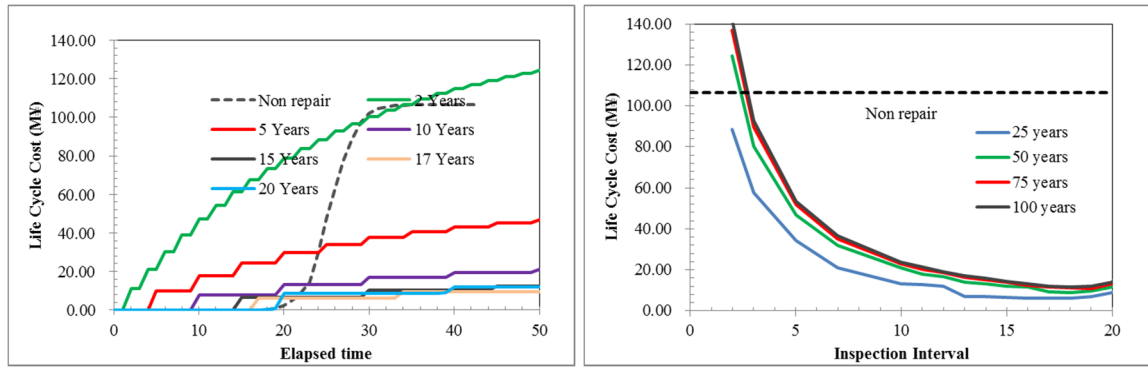


(a) *LCC* versus inspection interval



(b) *LCC* versus elapse time

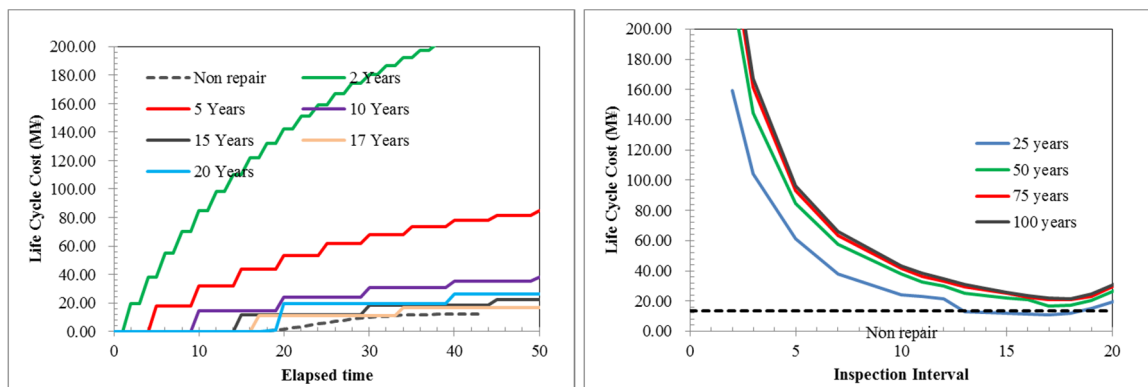
Figure 7.19 Comparison of *LCC* with difference repair scenarios of Kyotan No.4



(a) LCC versus inspection interval

(b) LCC versus elapse time

Figure 7.20 Comparison of LCC with difference repair scenarios of Fukuchiyama No.8



(a) LCC versus inspection interval

(b) LCC versus elapse time

Figure 7.21 Comparison of LCC with difference repair scenarios of Ibaraki No.12

Table 7.4 Summary of Life Cycle Cost analysis results

Slopes	Number of Anchors	Volume of failure (m ³)	Non-repair LCC (MJPY)	Optimum LCC (MJPY)	Optimum Inspection interval (Year)
Wakayama No.8	395	5,205	60.21	39.19	16
Ibaraki No.4	234	9,441	29.86	25.49	14
Ibaraki No.2	180	7,343	23.94	18.37	15
Fukuchiyama No.8	116	41,430	106.60	9.14	17
Kyotan No.4	172	5,540	17.20	23.93	13
Kobe No.2	85	8,701	32.15	21.72	10
Ibaraki No.12	209	4,782	12.58	8.55	17

The results of *LCC* indicated the optimum inspection interval of each slope were various depended on its slope attribute. Fukuchiyama No.8 and Ibaraki No.12 illustrated suitable inspection interval 17 years while Wakayama No.8 was 16 years, Ibaraki No.2 was 15 years, Ibaraki No.4 presented 14 years, Kyotan No.4 was 13 years and Kobe No.2 was 10 years. The other results such as Non-repair *LCC* and Optimum *LCC* were summarized as tabulated in Table 7.4.

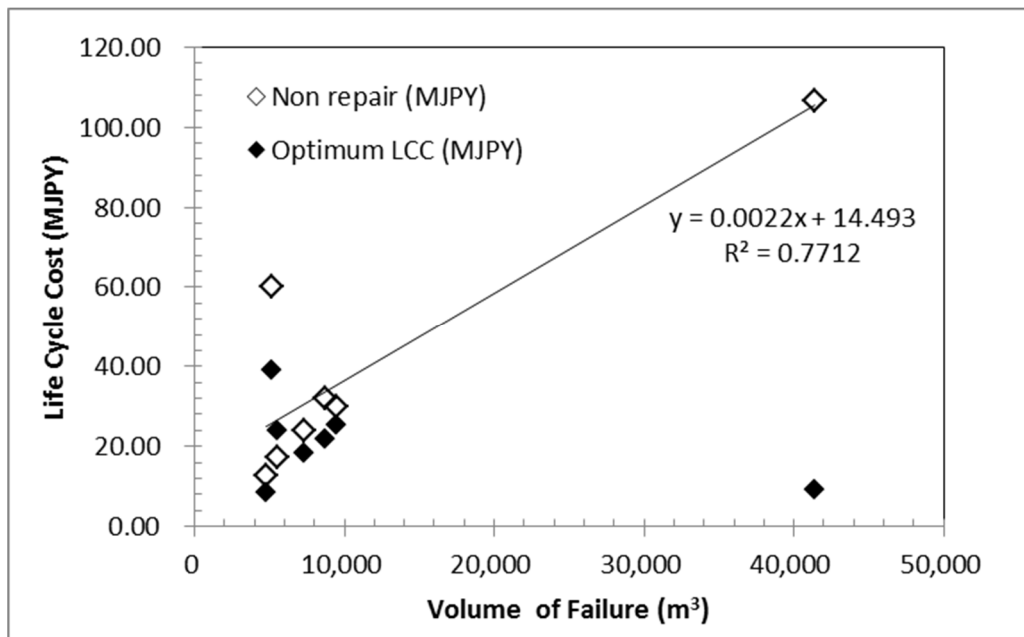


Figure 7.22 *LCC* versus volume of failure of risk slopes

In sharp contrast to this, volume of failure is predominating factor to the *LCC* of Non-repair scenario (see Fig 7.22). These results implied that larger volumes of failure, the recovery proportionally increased. On the other hand, the optimum *LCC* is independent of the volume of failure that the largest failure mass (for instance, Fukuchiyama No.8) does not the most expense on optimum *LCC*. In addition, the optimum *LCC* demonstrated lower expense than the non-repair scenario that is an advantage of the slope failure prevention.

The optimum *LCC* related on the number of ground anchors (see Fig 7.23). The optimum *LCC* grew up explicitly with the number of anchors installed. This result implied that inspection as well as replace/repair costs were the major expense on the optimum *LCC* scenario.

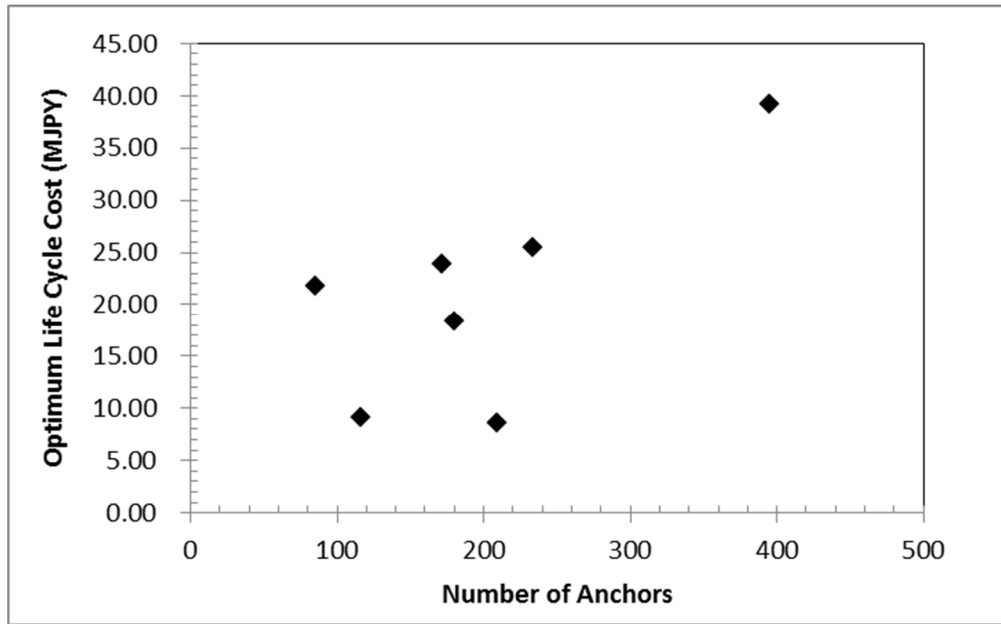


Figure 7.23 Optimum *LCC* versus number of anchors installed

The optimum inspection interval varies from 10 to 17 years depended on the number of ground anchor installed. It might be able to describe that the number of ground anchors is presided parameters to the optimum inspection interval that grew significantly with the number of ground anchor increased as shown in Fig 7.24.

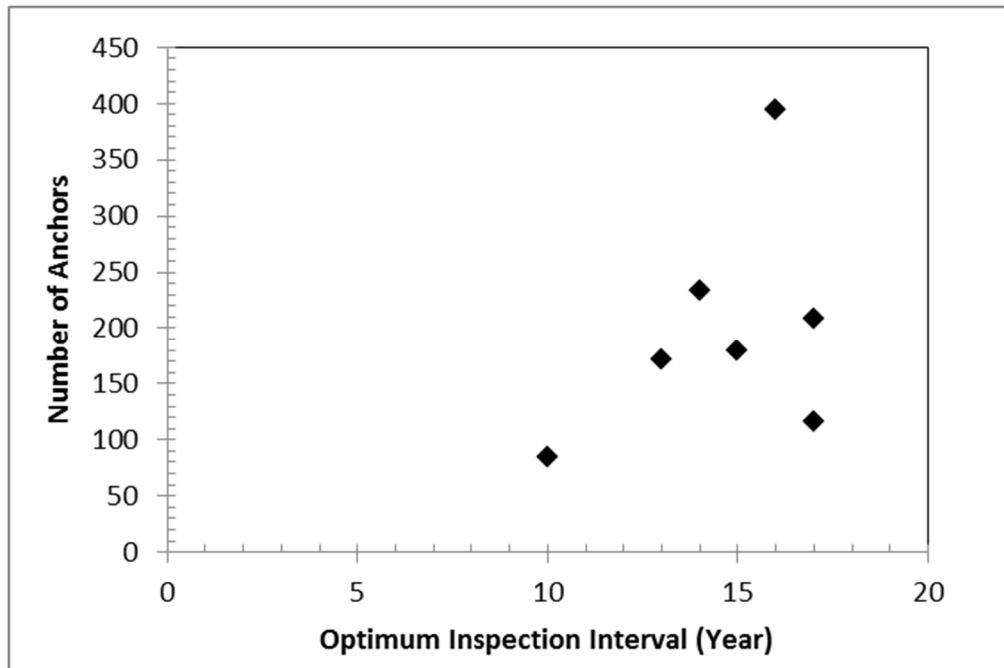


Figure 7.24 Number of ground anchor versus optimum inspection interval

CHAPTER 8

CONCLUDING REMARKS AND FURTHER RECOMMENDATIONS

8.1 Concluding Remarks

This research aims to apply and develop the concepts of infrastructure asset management to enhance the knowledge of maintenance strategies focusing on the slopes improved by ground anchors. Three testing methods were conducted to identify the present condition of ground anchors, including the Visual Inspection test, the Lift off test and the Ultrasonic test.

In Chapter 4, the acquisition of the inspection results and identifies the current condition of those three methods were presented. The first method was the Visual inspection method which is based on the concepts of the quick and non-destructive testing utilizing the light equipment. As a result, the following conclusion can be made:

- The scenario II (the rank I, II and III are corresponding to fail) might be suitable to analyze the decayed rate of slope improved by ground anchors since the scenario I (rank I and II are failure ranks) seemed to be too conservative and inadequate number of failures to calculate.

In order to verify the capability of the anchors instead of the results based on non-laboratory testing, the Lift off test was introduced to measure the existing force directly. However, the difficulty of testing and the expenses is quite expensive; the results were obtained with a limited number of testing. The kriging technique was adopted to interpolate the unknown force nearby testing spots. Therefore, the finding of this method can be presented:

- Four semi-variogram models illustrated similar results of kriging as well as does not distinguish on total force; however, the power model is the most proper to be a representative model for the interpolation because the sill value calculated from semi-variogram does not clearly appeared.

The additional method, namely the Ultrasonic test, was proposed to evaluate the existing force of the anchors as indirect method. The basic concept is that the amplitude wave from the Ultrasonic test proportional increases with the remaining forces obtained by the Lift off test; however, calibration is required. In fact, this method was conducted only a slope;

therefore, it can be used for supplement for the Lift off test only. The indicator kriging was applied to detect the risky zone and to make-decision for additional the Lift off test spots. It could be summarized below:

- The results of reflections on an acoustic wave can be divided into several patterns, including the first, second, third and fourth reflections are corresponding to single, double, triple and quadruple reflected from the second layer; moreover, it is too difficult to explain the behaviors after second reflecting on top of third layers because it cannot identify whether an echo from which layers. Therefore, the echo of the top of third layers was assumed as the results of Ultrasonic test to be calibrated with actual existing force obtained by Lift off test results.
- Because the testing results included the bias therefore the confidence interval was adopted to eliminate both human and equipment errors. The 95% and 99% of confidence interval presented the consisting results with the Lift off test. The degree of the confidence interval plays an important role in the indicator kriging results. Generally, the confidence interval at least of 95% was adequate to analyze because too low confidence interval is inappropriate results while too high value is dispensable due to the same consequence.

The modeling of deterioration process and prediction of future condition was presented in Chapter 5. The results of of both the Visual inspection test and the Lift off test were analyzed and summarized separating between the different types of ground anchors as well as geological conditions. The finding could be summarized as follows:

- The Weibull hazard model is an appropriate model to analyze the deterioration rate of ground anchors because it is the best-fitting compared to the observed data. Moreover, this model provided the rate of failure and the life span, which necessary to evaluate the present conditions and future prediction of the ground anchors stage while another model do not mention.
- Based the results of the Visual inspection test, the strand type anchors are longer life span than the rod type because the higher installed forces, the deteriorated process should take longer. In addition, the old type ground anchors presented shorter life span than the new type because the old type does not coat with a rusting protection. However, considering the different geological conditions, it has quite complicates to

explain the life span between types of ground anchors since it completely conflicted with the previous outcomes because insufficient failure data to analyze. Therefore, the Visual inspection test is inappropriate to use as a primary technique for analyzing the anchor's life span since it judged by the human eye without validation of heavy equipment but might be suitable for the preliminary reconnaissance for quick maintenance on each spot.

- Considering the results of the Lift off test, the strand type anchors seemed to be longer life span than the rod type, which the compatible results with the Visual inspection test. Furthermore, the anchors installed in sedimentary rock demonstrated more durable than anchors in igneous rock. However, the number of ground anchors in the igneous rock is quite small; they were abandoned to analyze the failure probabilities. The statistical approach indicated that seven risk slopes, including Ibaraki No.4, Ibaraki No.2, Wakayama No.8, Kobe No.2, Kyotan No.4 and Fukuchiyama No.8 shall be given priority to replace/repair before 2020 while Ibaraki No.12 was still high performance which shall be considered the maintenance strategies later.
- Finally, they were non-correlation between the Visual inspection and Lift off tests on either microscopic (individual anchor) or macroscopic (slopes) viewpoints; however the Visual inspection test can be used for preliminary test to judge whether ground anchors failure or survives on each spot. Subsequently, those ground anchors were decided to measure the existing force by the Lift off test.

Investigation on stability and failure probability on each slope based on the Lift off test results were presented and compared in Chapter 6. In this chapter, the Visual inspection test results were abandoned because the tension force of each anchor cannot be measured. The important finding of the results is:

- The safety factor and the survival probability results might not be suitable to compare the correlation. Alternatively, the percentage of reduction in performance function is compared instead, it is meaningfully grown with the survival probability; however, it is quite underestimated relationship.
- The cumulative annual probability of failure indicated that most of the slopes improved by strand types touched the failure after 2020, roughly, except Ibaraki No.12

while all of rod type reached to failure during 2018 to 2020, approximately. As a result, the rod type shall be given a priority for maintenance.

Chapter 7 presented the estimate of life cycle cost, *LCC* and decision making on maintenance. This method was utilized to provide the maintenance strategies for the replace/repair on ground anchors. Both macroscopic and microscopic viewpoints were considering. It can be summarized as follows:

- Based on the macroscopic viewpoint, the Weibull hazard model revealed the longer optimum inspection interval as well as lower expense than the results of the Markov model. Therefore, the Weibull hazard model provided more profit and advantages to the road administrators while the Markov model demonstrated too pessimistic results. In addition, even if the Lift off test results presented higher *LCC* but it is more suitable since the Visual inspection test results cannot measure the remaining forces in ground anchors.
- Based on the microscopic viewpoint, the volume of failure is predominating factor to without repair scenario while optimum *LCC* rise proportionally to the number of anchors. In addition, the optimum inspection interval went up with number of anchors installed as interestingly attribute of slope improved by ground anchors.

8.2 Further Recommendations

According to the data obtained, it seemed to be insufficient the number of failure data to evaluate the deterioration rate on the igneous rock of both the Visual inspection and the Lift off test. Moreover, the inspection year is quite short, varying just about 12 to 28 years and without early stage. Consequently, the deterioration rate drastically falls after the first inspection conducted. The additional testing was necessary to validate the accuracy of the predicted results.

In terms of slope stability analysis, the strength parameters like cohesion, c and the internal friction angle, ϕ were assumed to be constant, which might not be suitable to estimate the factor of safety with time. Even though, the reduction of strength parameters slightly decreased, it is the most significant resisting force against slopes collapse while the anchor's force is an additional force. Moreover, the groundwater level shall be measured,

particularly during the monsoon season. The groundwater level plays an important role in the stability of slope analysis since the water is the enemy to soil strengths as well as the acting force was increasingly generated during groundwater rise.

Finally, the indirect losses, including damage to the vehicles, passengers and private properties, was neglected in this studied because it is too difficult to estimate. The indirect losses were calculated considering the expense of the road user during slope failures, which greater than the direct losses. Therefore, it is better be taken into an account when calculated the Life cycle cost.

REFERENCE

- Bohling. G., (2005), *“Introduction to Geostatistics and Variogram Analysis”*, Kansas Geological Survey.
- Casella, George; Berger, Roger L. (2001). *“Statistical inference (2nd ed)”*. Duxbury. ISBN 0-534-24312-6.
- Douglas T.H and Arthur L.J. (1983). *“A Guide to the Use of Rock Reinforcement in Underground Excavation”*. CIRIA, London.
- Dorner, W. (1997). *“Using Excel for Data Analysis,”* Quality Digest, October 1997.
- Everitt,B.S. (2002). *“The Cambridge Dictionary of Statistics”*. CUP. ISBN 0-521-81099-x.
- Fredlund. M., Feng. T. and Thode. R. (2012) *“Tutorial Manual for SVSLOPE”* SoilVision Systems Ltd. Saskatoon, Saskatchewan, Canada
- Hull, John C., Options, (2000) *“Futures & Other Derivatives”*. Fourth edition. Prentice-Hall.
- Hutchinson, D.J., & Diederichs, M.S. (1996) *“Cablebolting in Underground Mines”*. Bitech Publishers Ltd., Vancouver. 416p.
- Kaito, K. (2009), *“Bridge management (2)”*, KU and UTC joint summer training course of road infrastructure asset management.
- Kimoto. S, Ohtsu. H, Miki., T and Kamide., S. (2011) *“A Study on Strategic Maintenance Planning of Ground Anchor Installed at Road Slopes Focusing on Geological Condition”* Proc. of the 10th EIT-JSCE 2011.
- Kimoto. S, (2013) *“Studies on the maintenance and repair plan that takes into account the stability of the slope and the aging of the ground anchor Engineering”* Master Thesis, Kyoto University.
- Krahn. J., (2003), *“The 2001 R.M. Hardy Lecture: The limits of limit equilibrium analyses”*, Canadian Geotechnical Journal, Volume 40, pp.643-600
- Lancaster, T.,(1990).*“The Econometric Analysis of Transition Data”*, Cambridge University Press, 1990..

- Mendes. R.M. and Lorandi. F. (2006) "*Indicator Kriging geostatic methodology applied to geotechnical project planning*" Proc. of the 10th IAEG International Congress.
- Miyatake, H., Oshita. T., Kubo. H. and Takeyama., M (2007), "*A New Manual for Ground Anchor Inspection, Integrity Investigation and Remedial Measures*", International Conference on Ground Anchorage and Anchored Structures in Service
- Morcous, M. (2006). "*Performance prediction of bridge deck systems using Markov Chains*", J. Perform. Constr.Facil., 20(2), 146-155.
- Mendes, R.M.& Lorandi, R.,(2006), "*Indicator kriging geostatistical methodology applied to geotechnics project planning*", Proceedings, 10th Congress of the International Association for Engineering Geology and Environment, CDRom. London, , p.1-12.
- MörTERS, P., and Peres. Y.,(2008). Brownian Motion. Retrieved 25 May 2008.
- Ohtsu, H., Matsuyama, Y. and Supawiwat, N. (2006): "*Evaluation of Road Slope LCC Considering Variation of Performance Deterioration of Slope Countermeasures*" Journal of JSCE F, Vol.62, No.2, pp.405-418 (in Japanese).
- Ohtsu, H. and T. Suwanishwong, T. (2009): "*A Proposal on Road infrastructure asset management associated with rock structures*", Proc. of the Second Thailand Symposium on Rock Mechanics, pp. 71-86.
- Ohtsu, H., Suwanishwong, T., Miki, T. and Kamide, S. (2010): "*Strategic Maintenance Planning of Ground Anchor Based on Inspection Results*". Journal of JSCE F, Vol.66, No.1, pp.158-169 (in Japanese).
- Ohtsu, H. (2011): "*Geotechnical Infrastructure Asset Management*", The Third Edition" Kyoto University Global COE program.
- Otani, y., Iseki, y., Takahashi, Y., Matsuyama, H. and Ohtsu, H.,(2004), "*Study on Life-Cycle Cost Evaluation of Shotcrete Slopes Considering Geo-risk*" Proc. of the Hanoi Geoen지니어ing 2004
- Suksawat. T., Ohtsu. H., Kimoto. S and Kamide., S. (2012) "*Deterioration Forecasting of Ground Anchor Based on Results of the Visual Inspection and the Lift-off Test*" Proc. of the 11th EIT-JSCE 2012
- Suksawat. T., Ohtsu. H., Kimoto. S and Kamide., S. (2013) "*Safety Factor Analysis of Deteriorated Slopes Improved by Ground anchors: Case Study in Japan*" Proc. of the 12th EIT-JSCE 2013

- Suksawat. T., Ohtsu. H., Kimoto. S and Kamide., S. (2013) “A *Statistic Approach to Determinate Failure Probability of Deteriorated Slopes Improved by Ground anchors: Case Study in Kansai, Japan*” Proc. of the Hanoi Geoengineering 2013
- Thanh, L.N. (2009), “*Stochastic optimization methods for infrastructure management with incomplete monitoring data*”, Doctoral thesis, Kyoto University.
- Tobin, J., (1958), “*Estimation of relationships for limited dependent variables*”, *Econometrica*, 26, pp.24-36.
- Tsuda, Y., Kaito, K., Aoki, K., and Kobayashi, K., (2006), “*Estimating markovian transition probability for bridge deterioration forecasting*”, *Journal of Structural Engineering and Earthquake Engineering*, 23(2):241-256

APPENDIX A

VISUAL INSPECTION TEST & LIFT-OFF TEST DATA

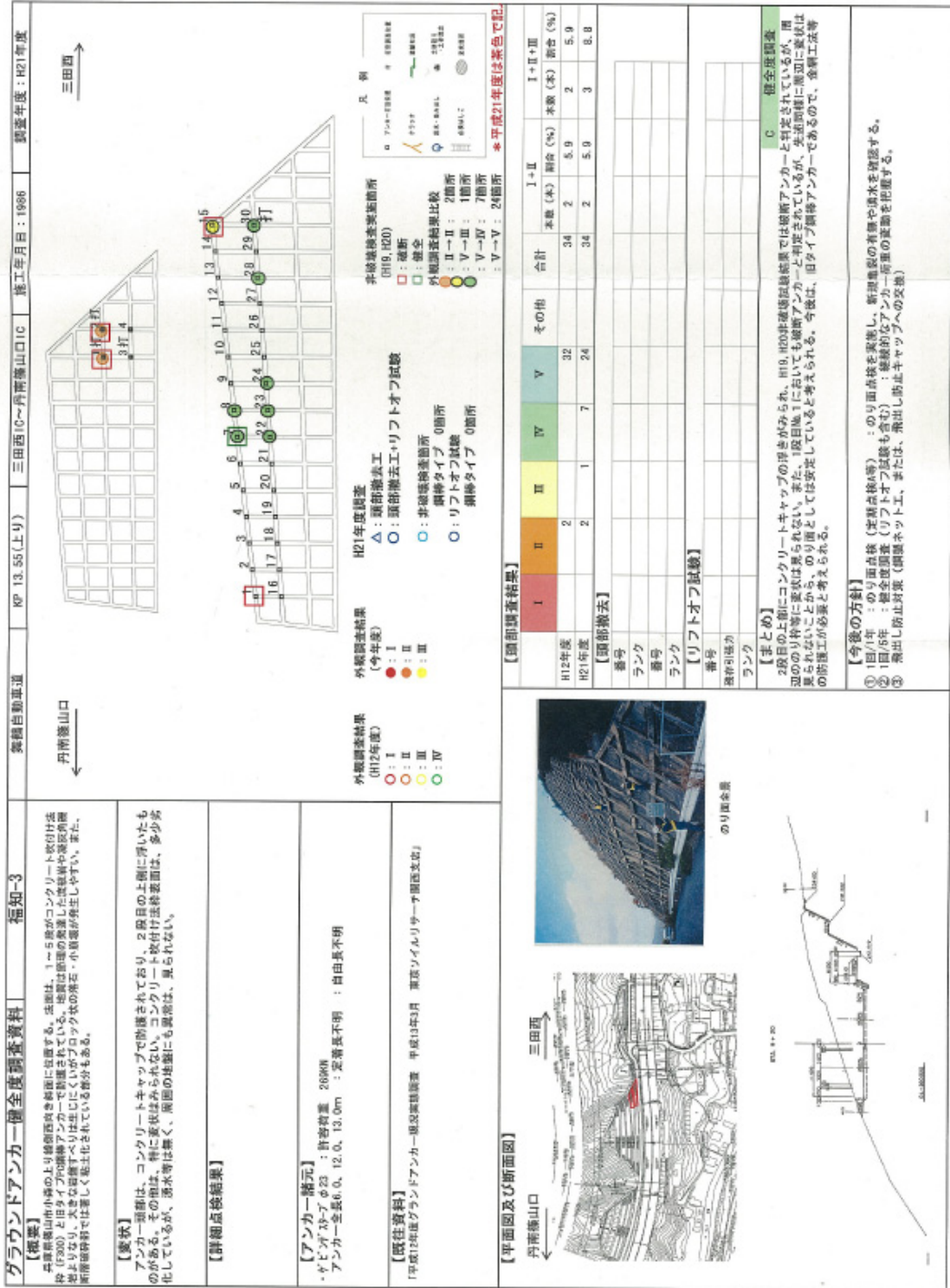


Figure A.4 Fukushi No.3

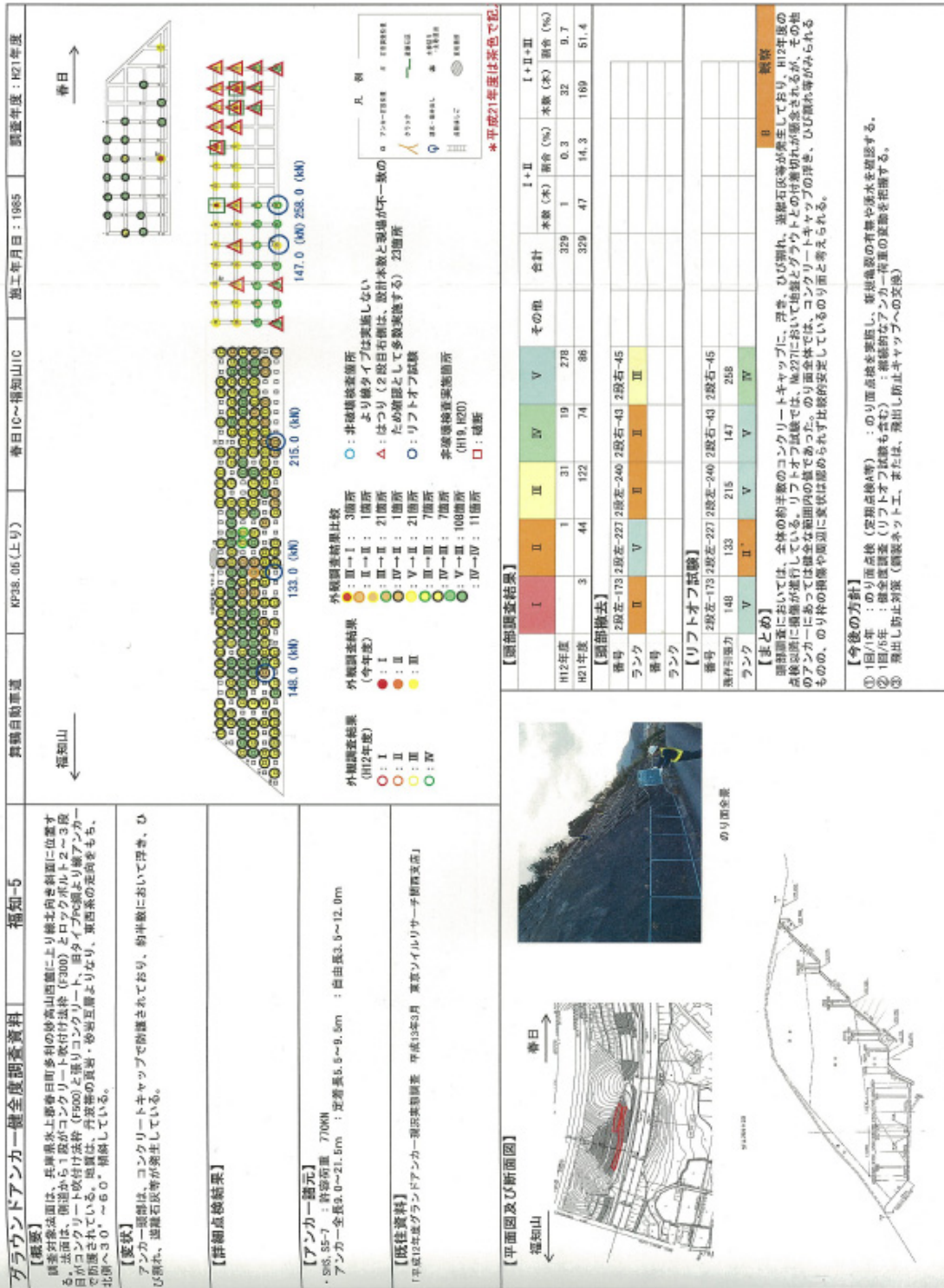


Figure A.6 Fukushi No.5

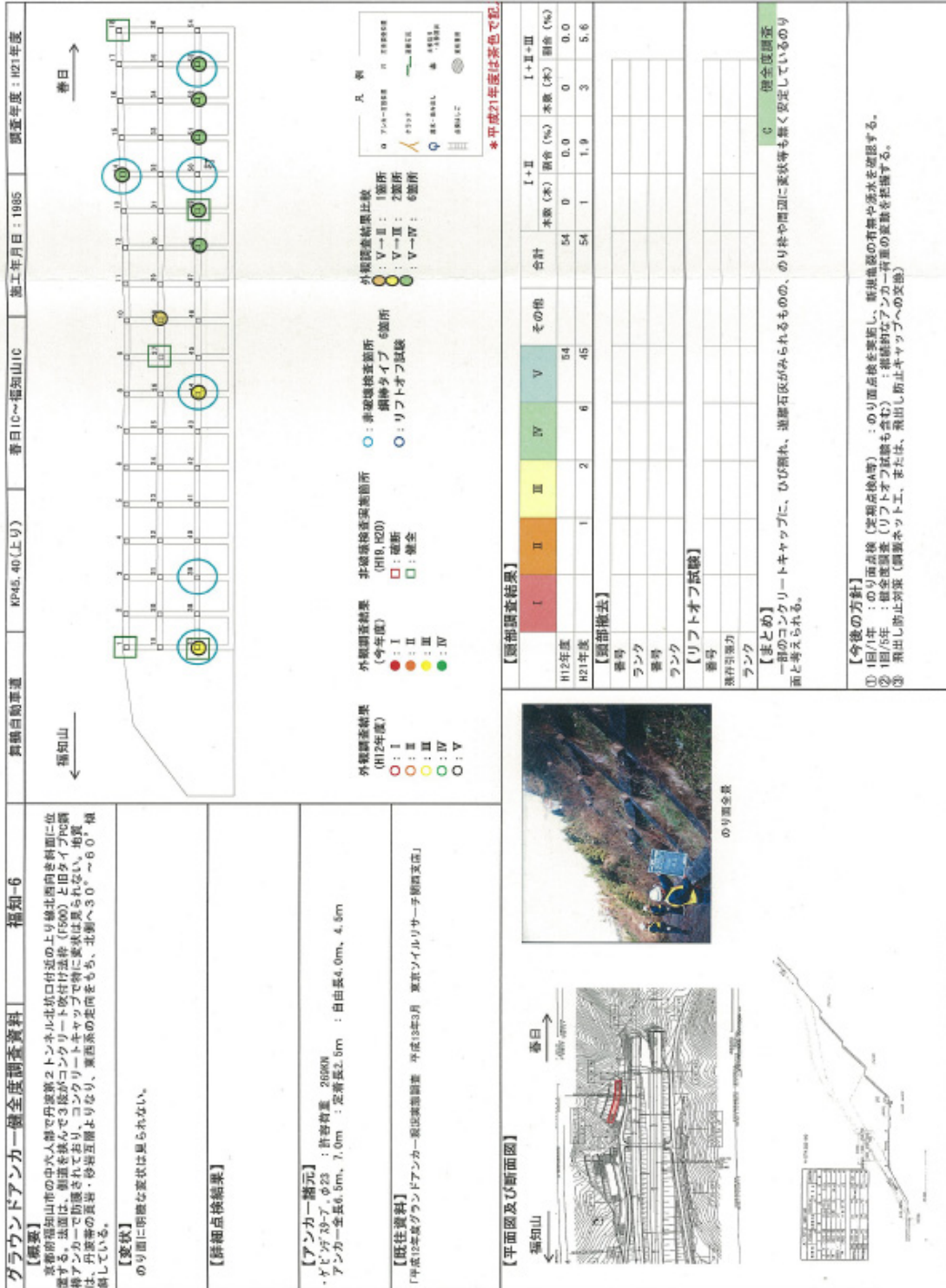


Figure A.7 Fukushi No.6

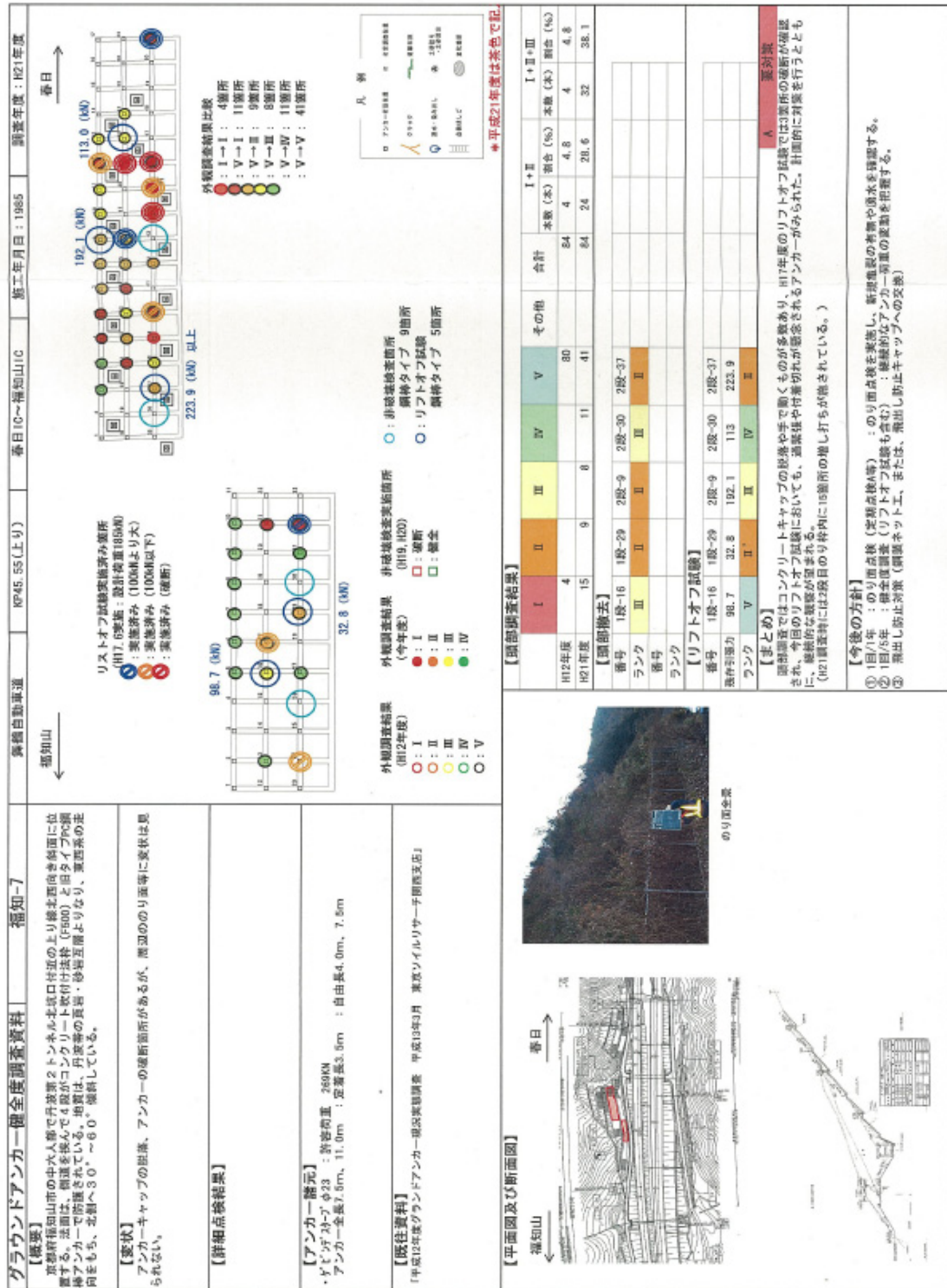


Figure A.8 Fukushi No.7

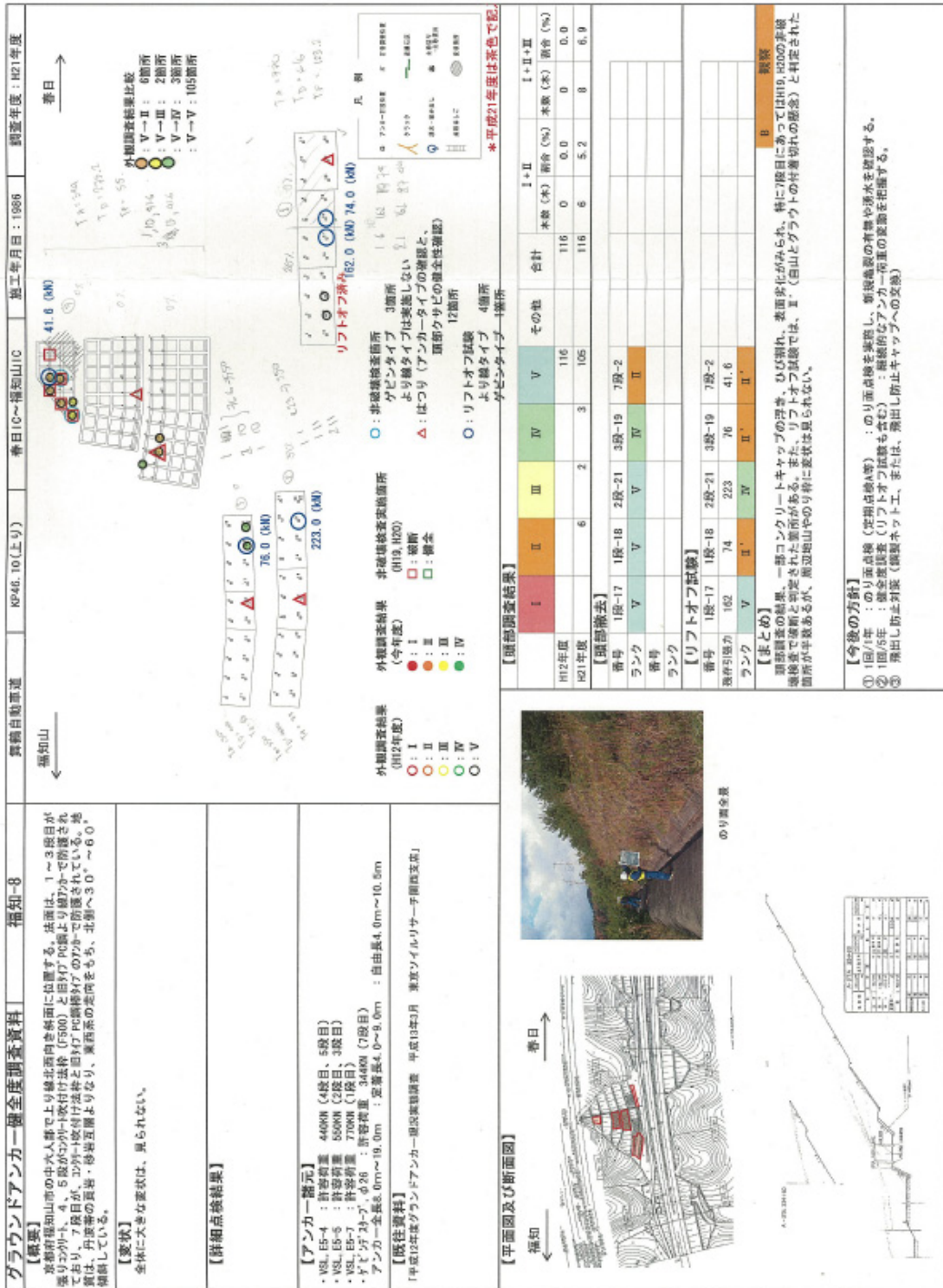


Figure A.9 Fukushi No.8

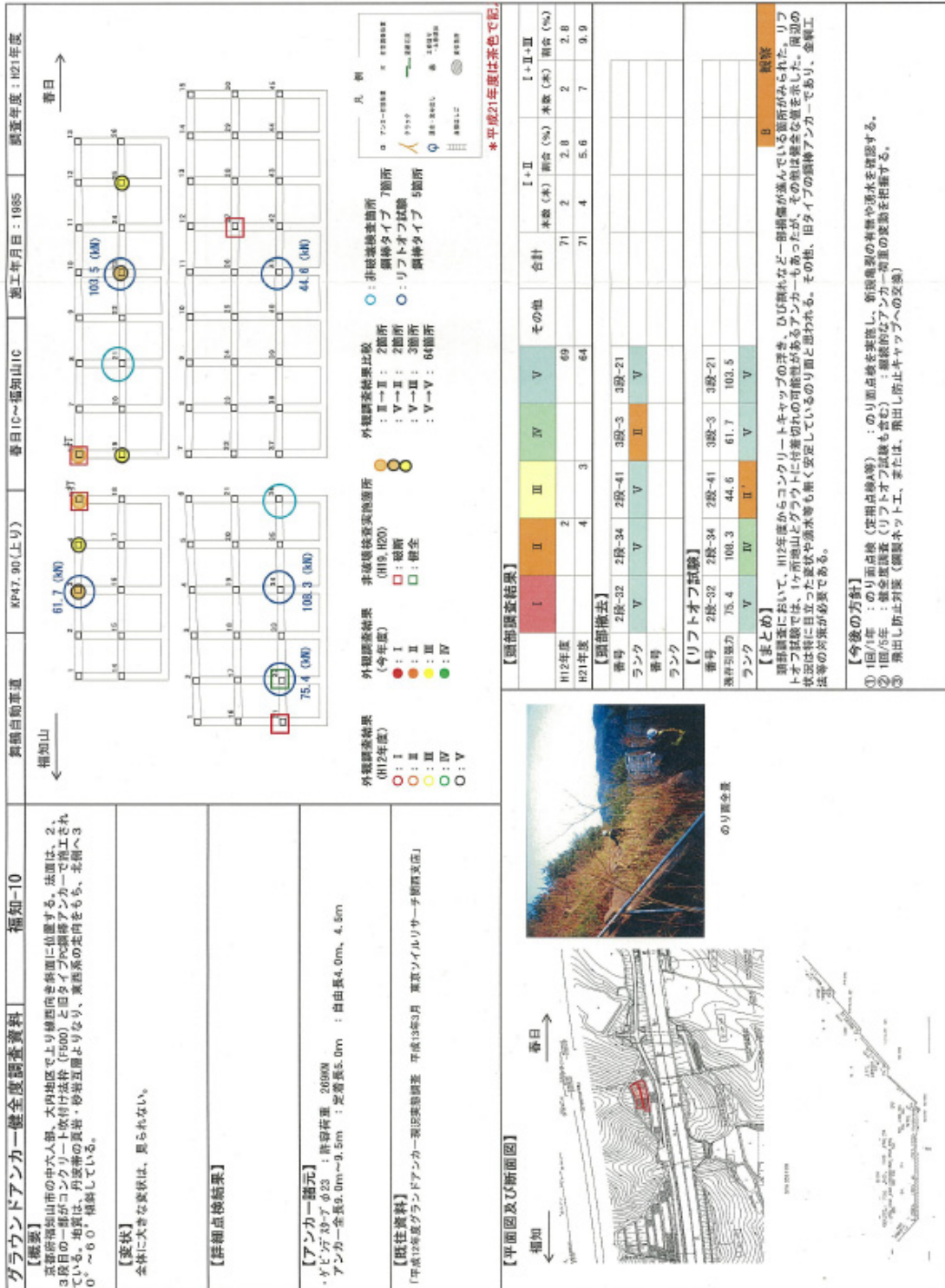


Figure A.11 Fukushi No.10

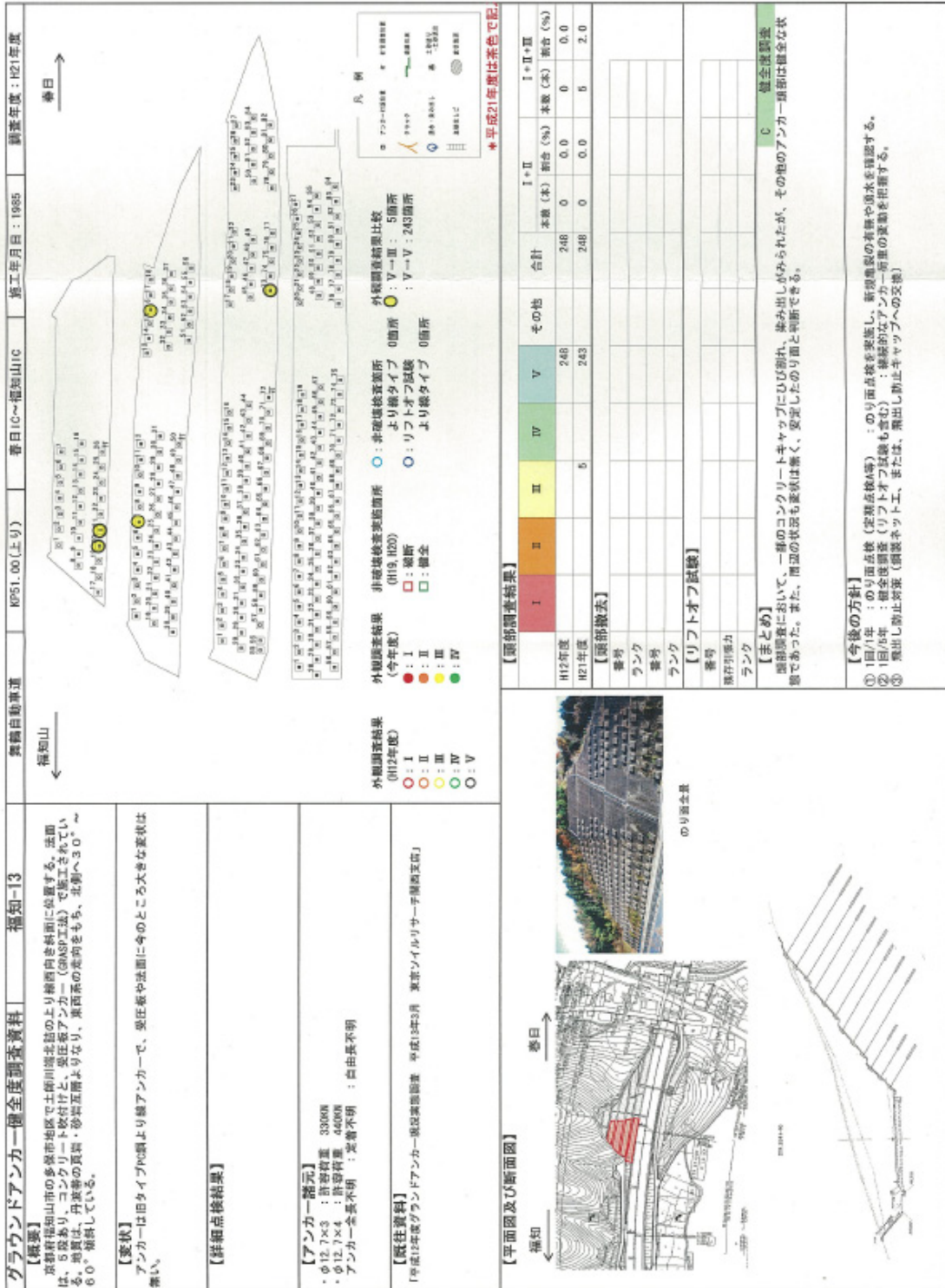


Figure A.13 Fukushi No.13

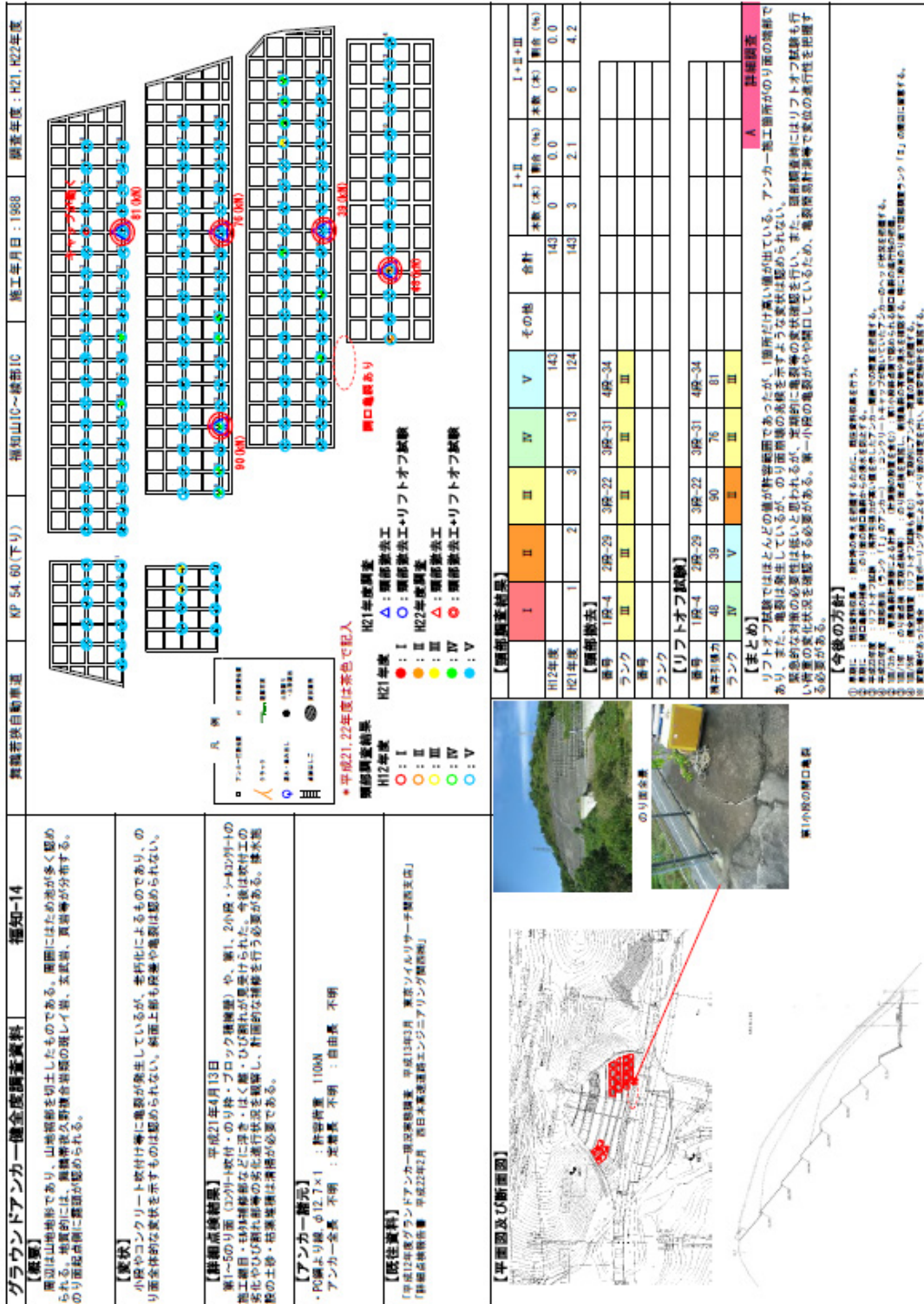
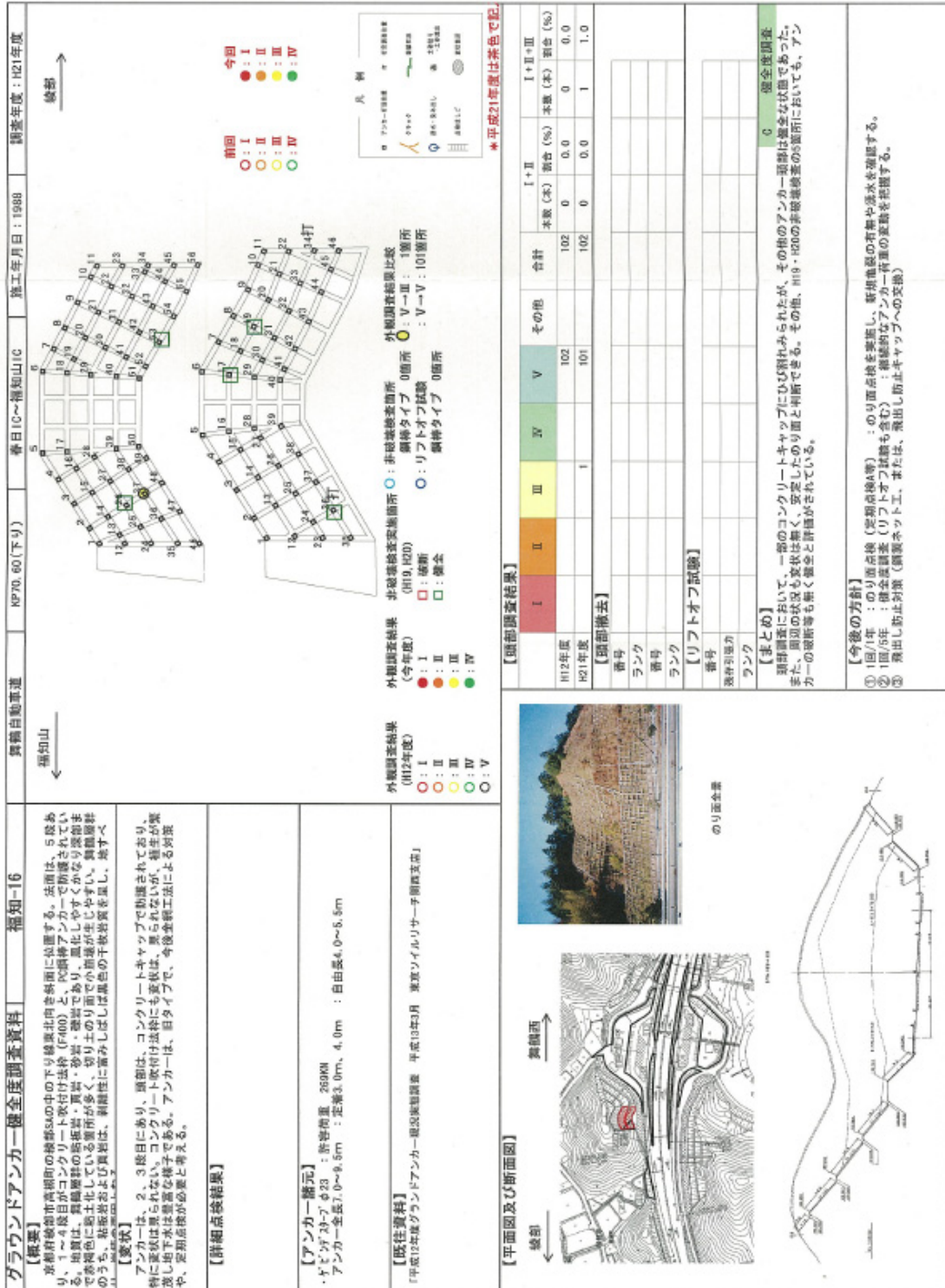


Figure A.14 Fukushi No.14



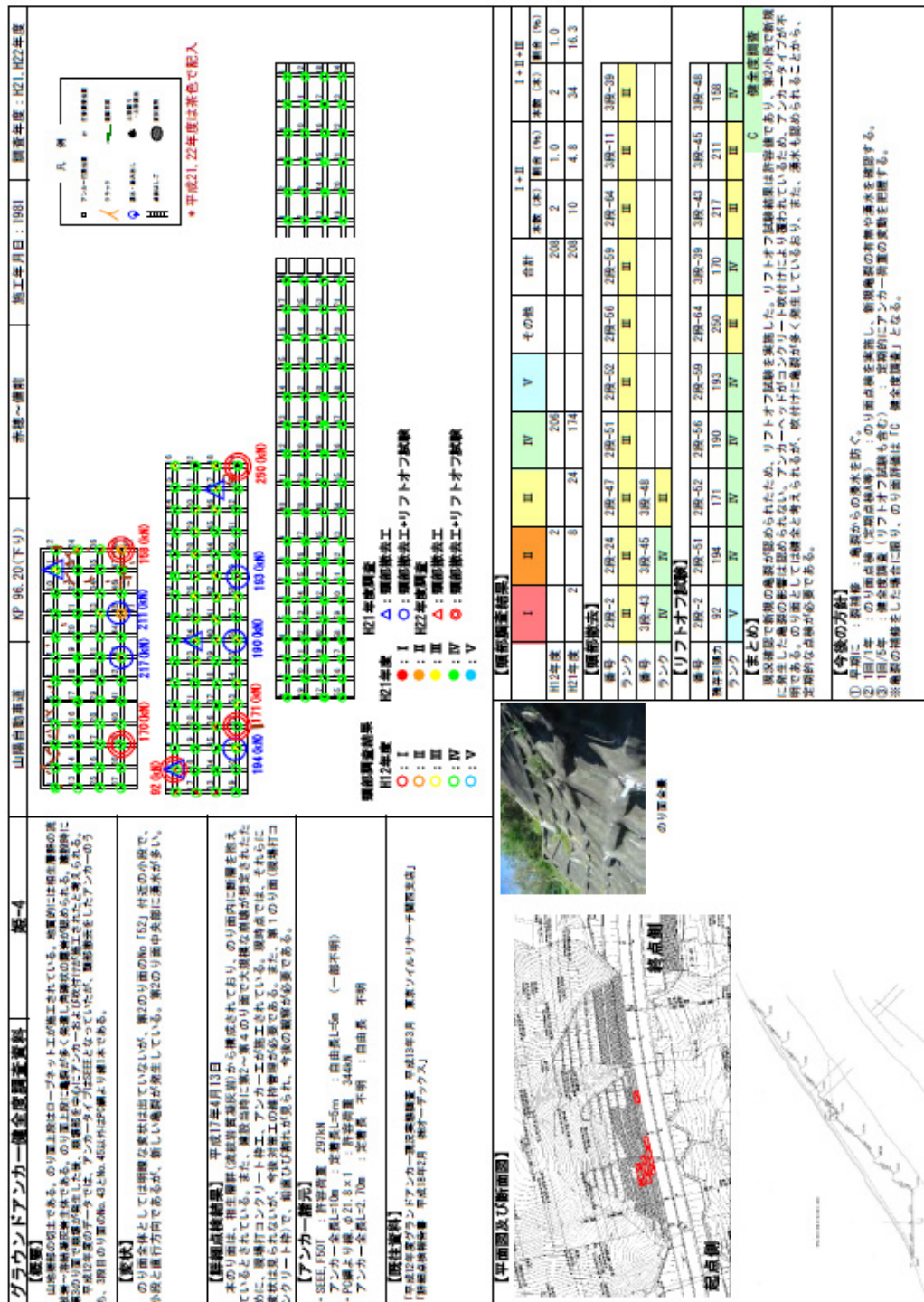


Figure A.22 Himeji No.4

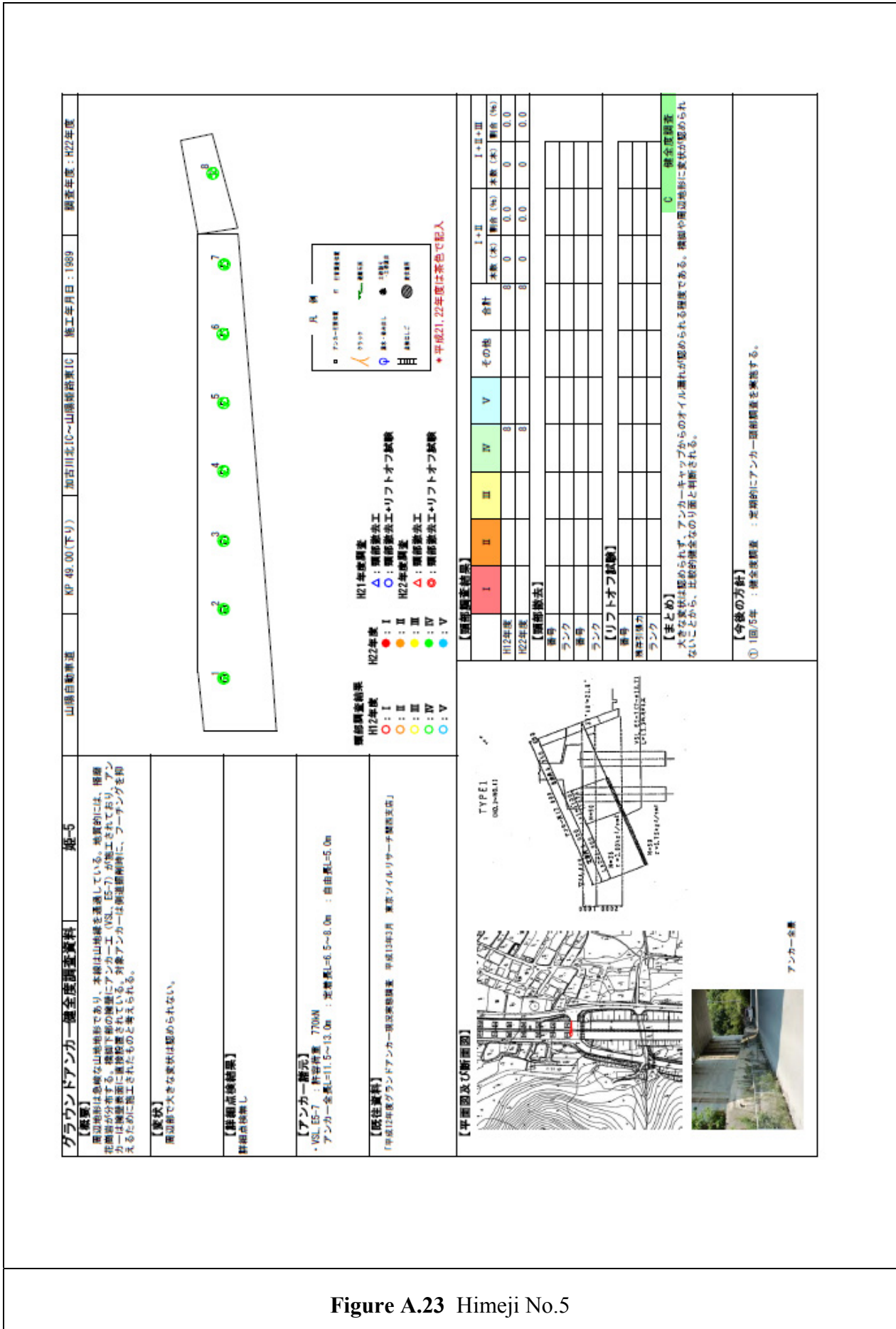


Figure A.23 Himeji No.5

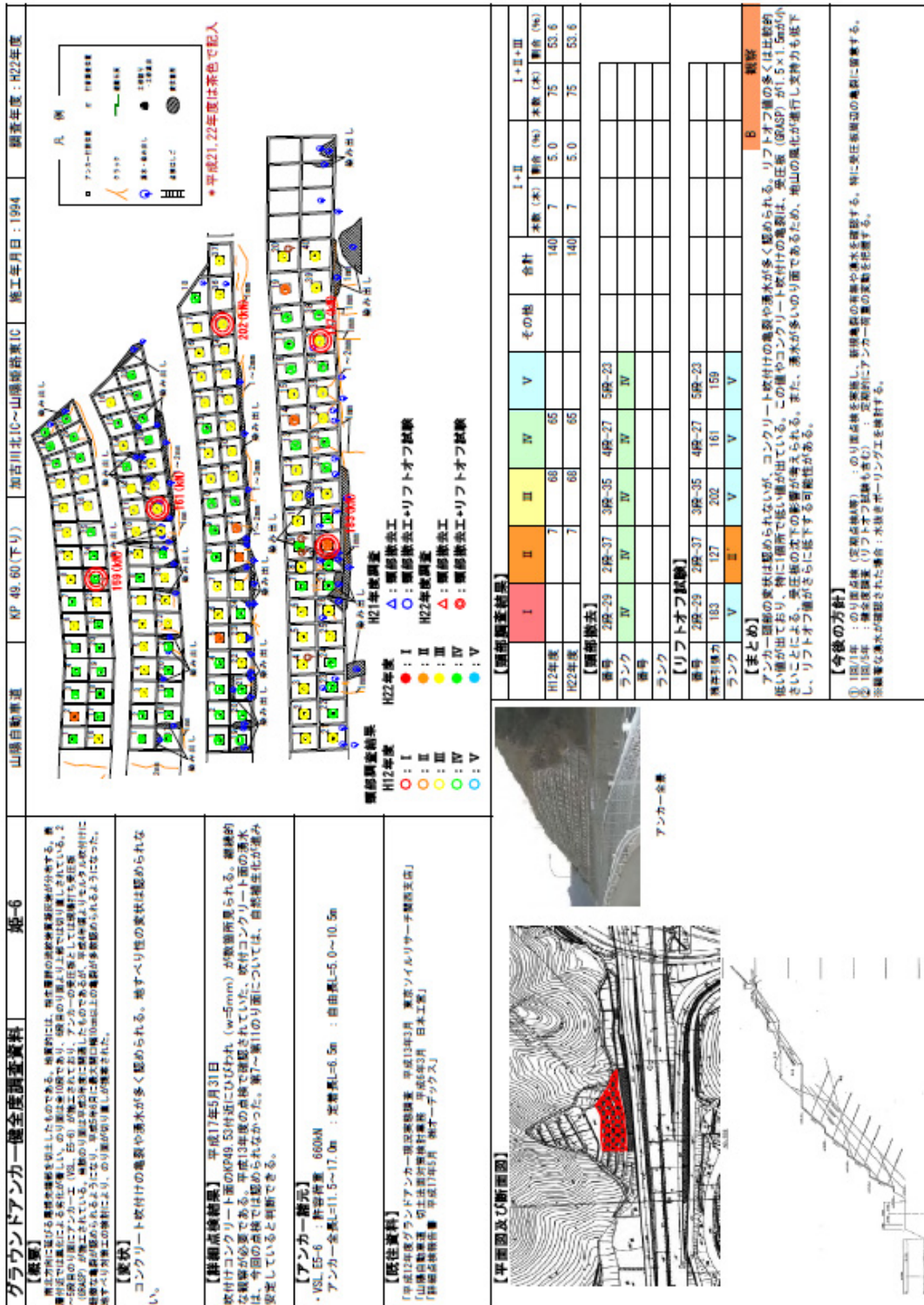


Figure A.24 Himeji No.6

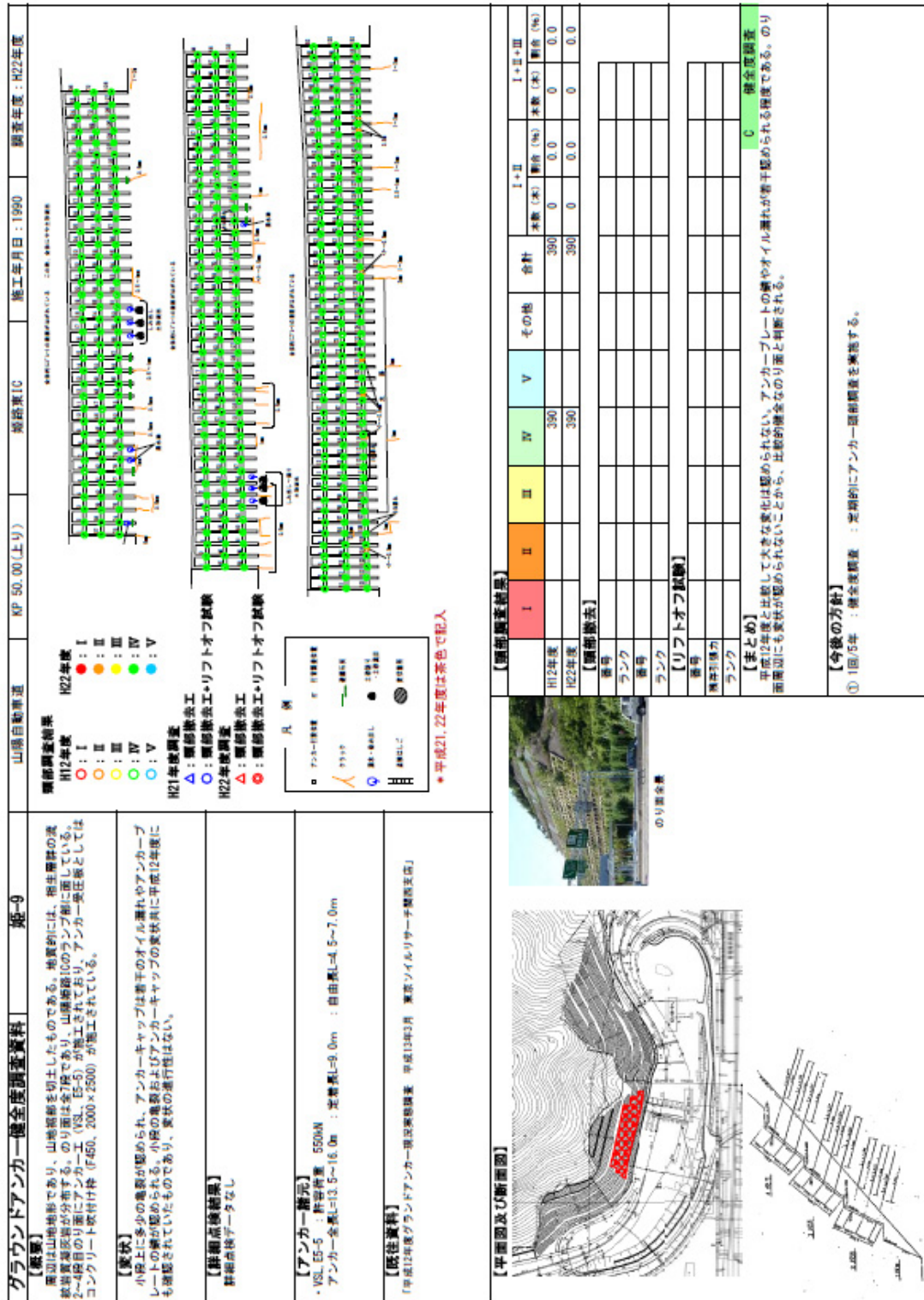


Figure A.27 Himeji No.9

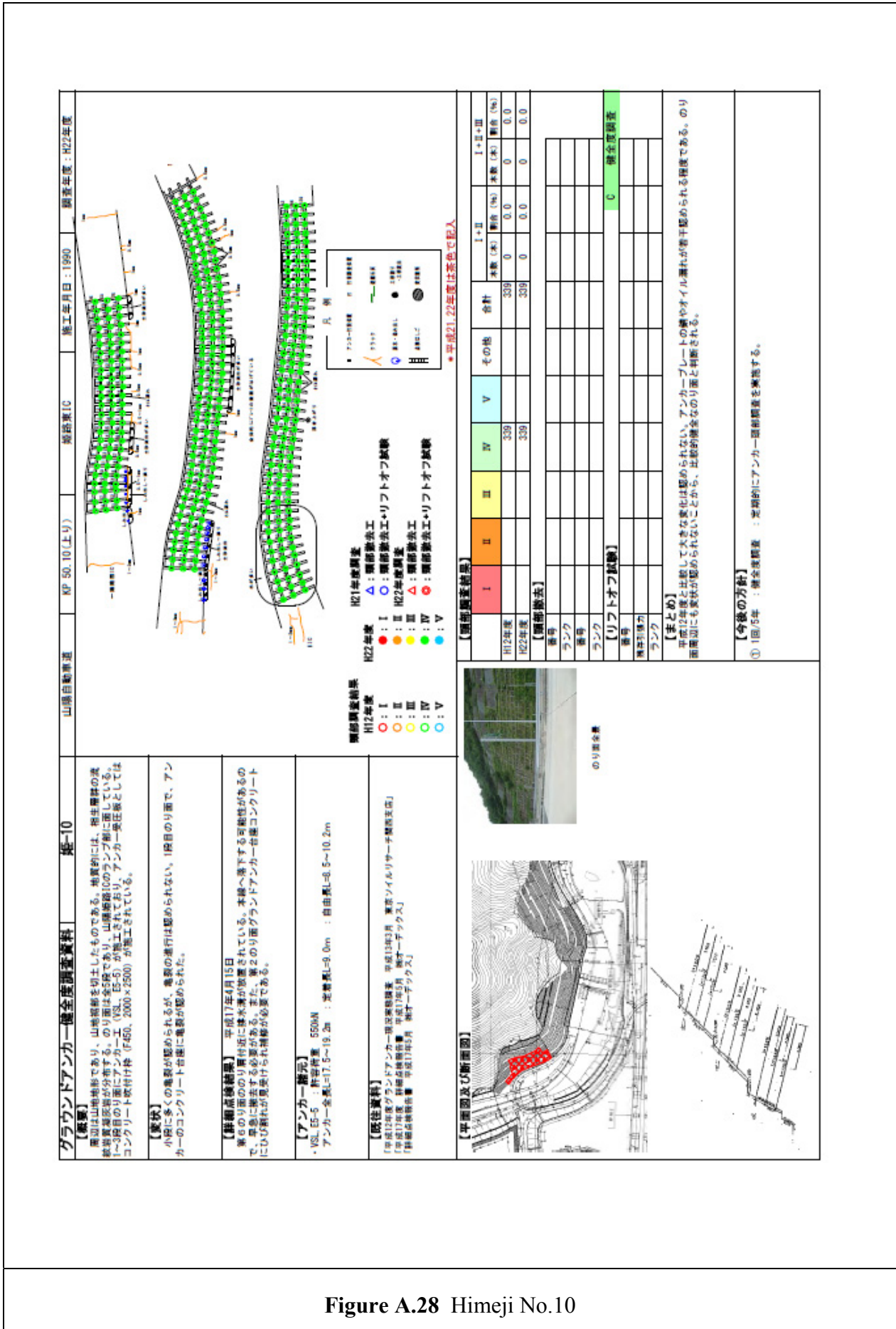


Figure A.28 Himeji No.10

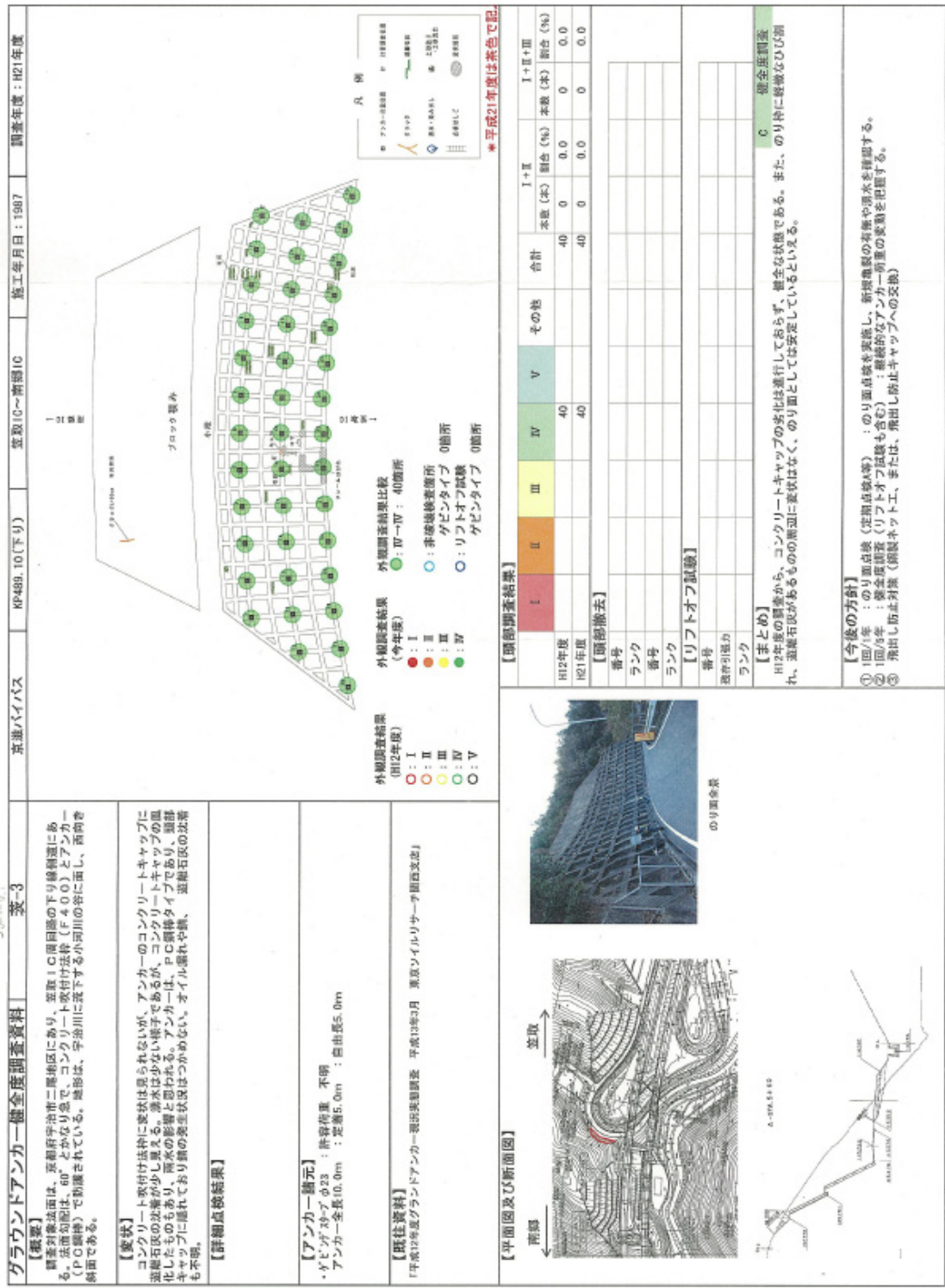


Figure A.31 Ibaraki No.3

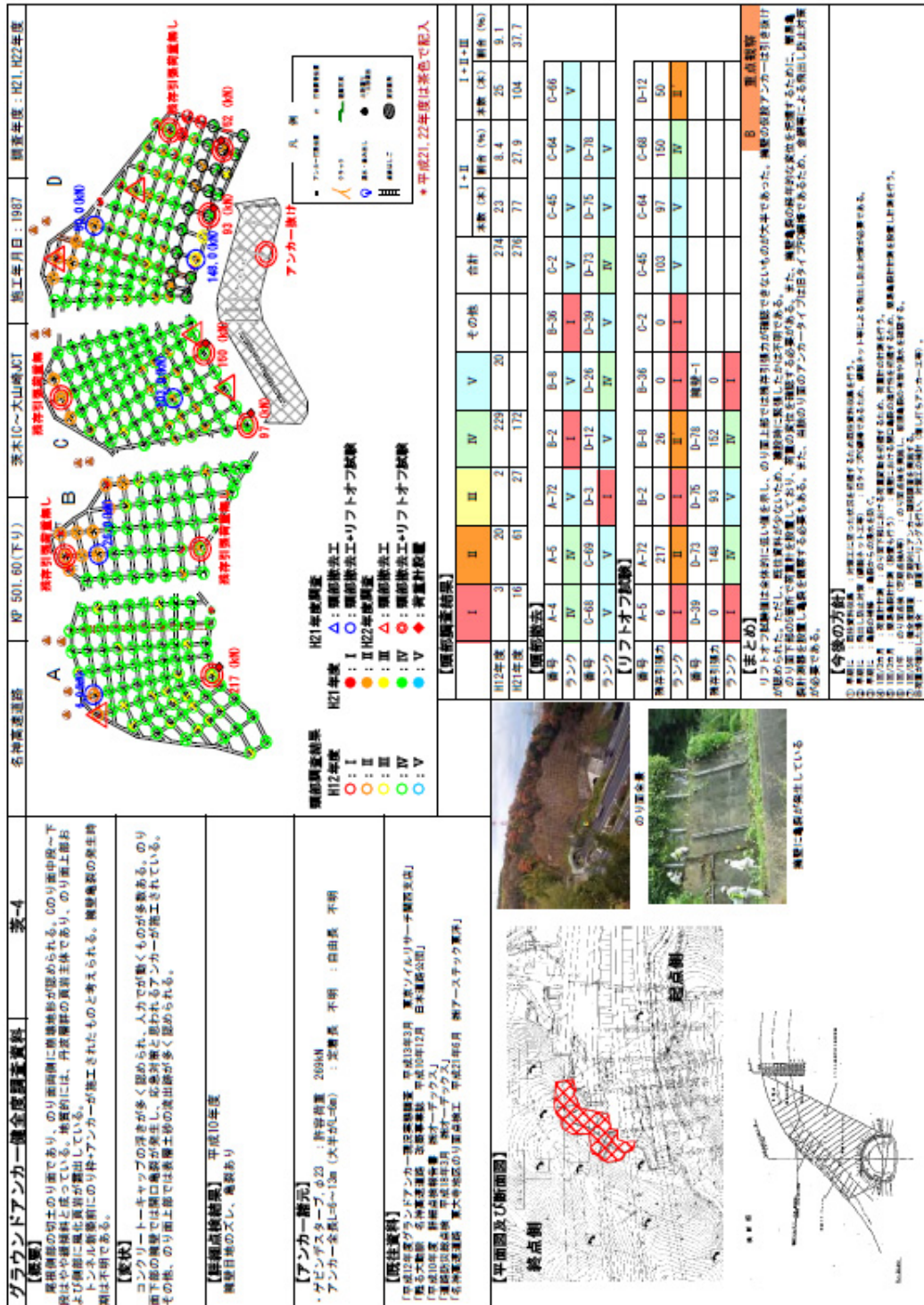


Figure A.32 Ibaraki No.4

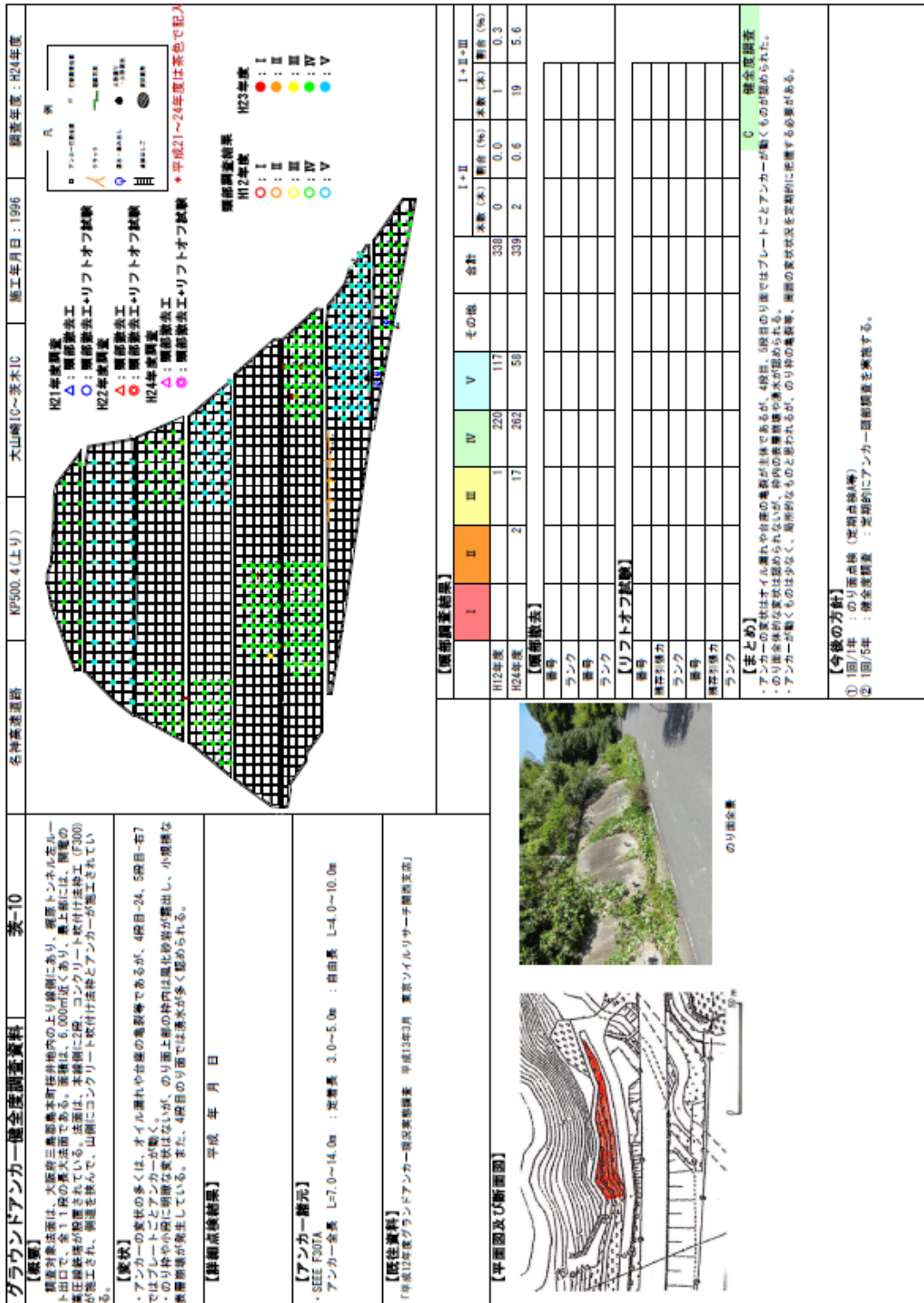


Figure A.38 Ibaraki No.10

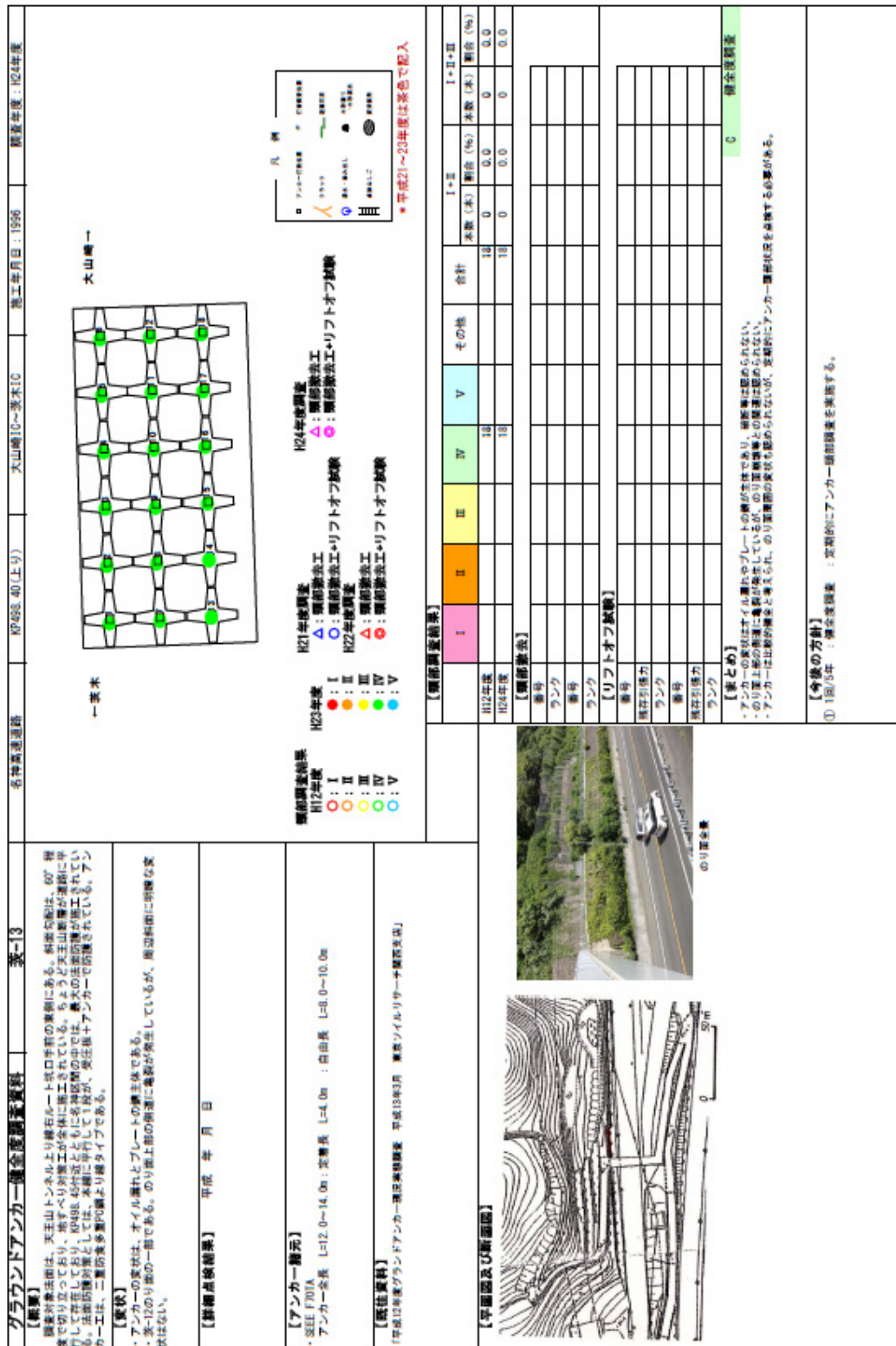


Figure A.41 Ibaraki No.13

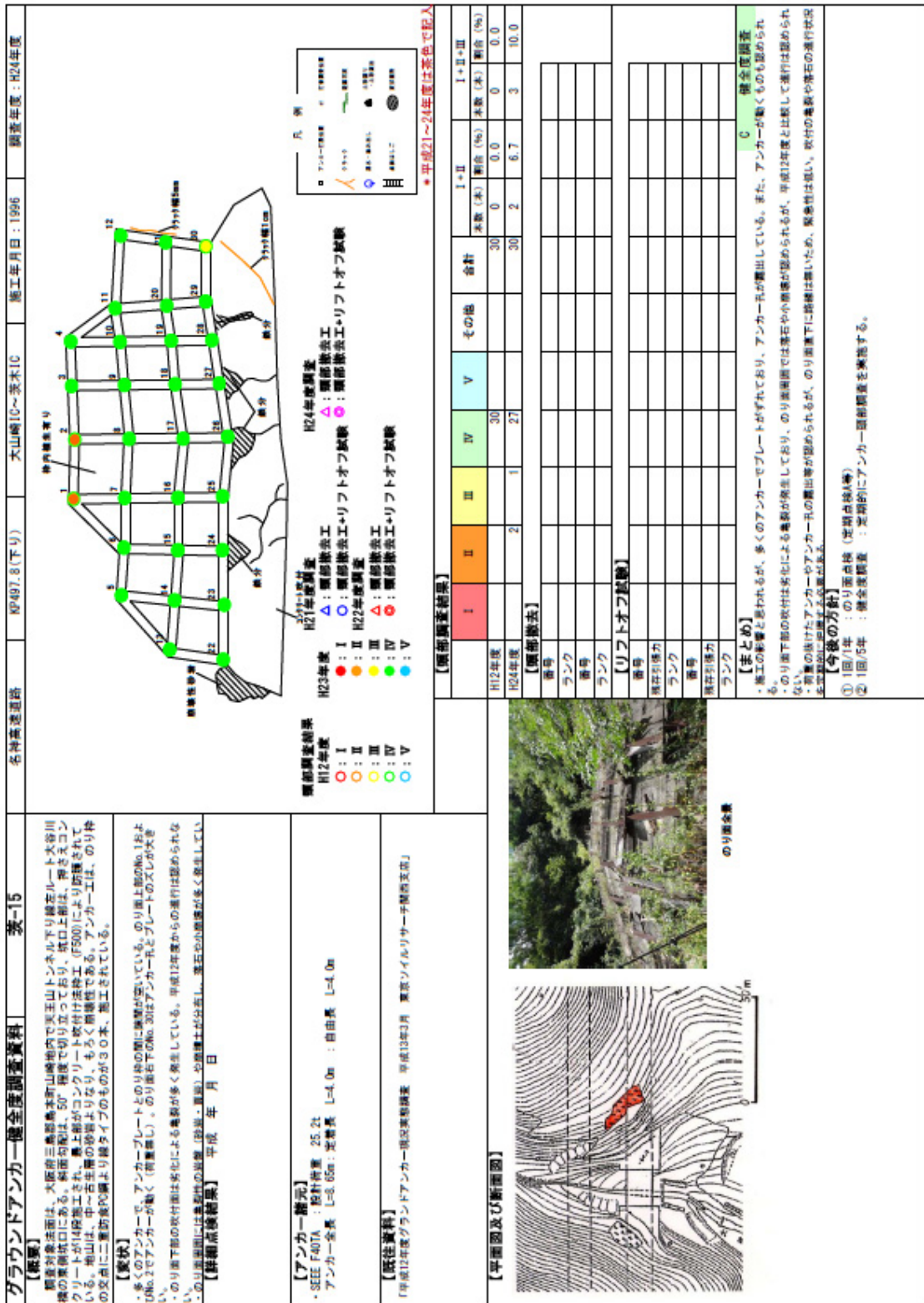


Figure A.43 Ibaraki No.15

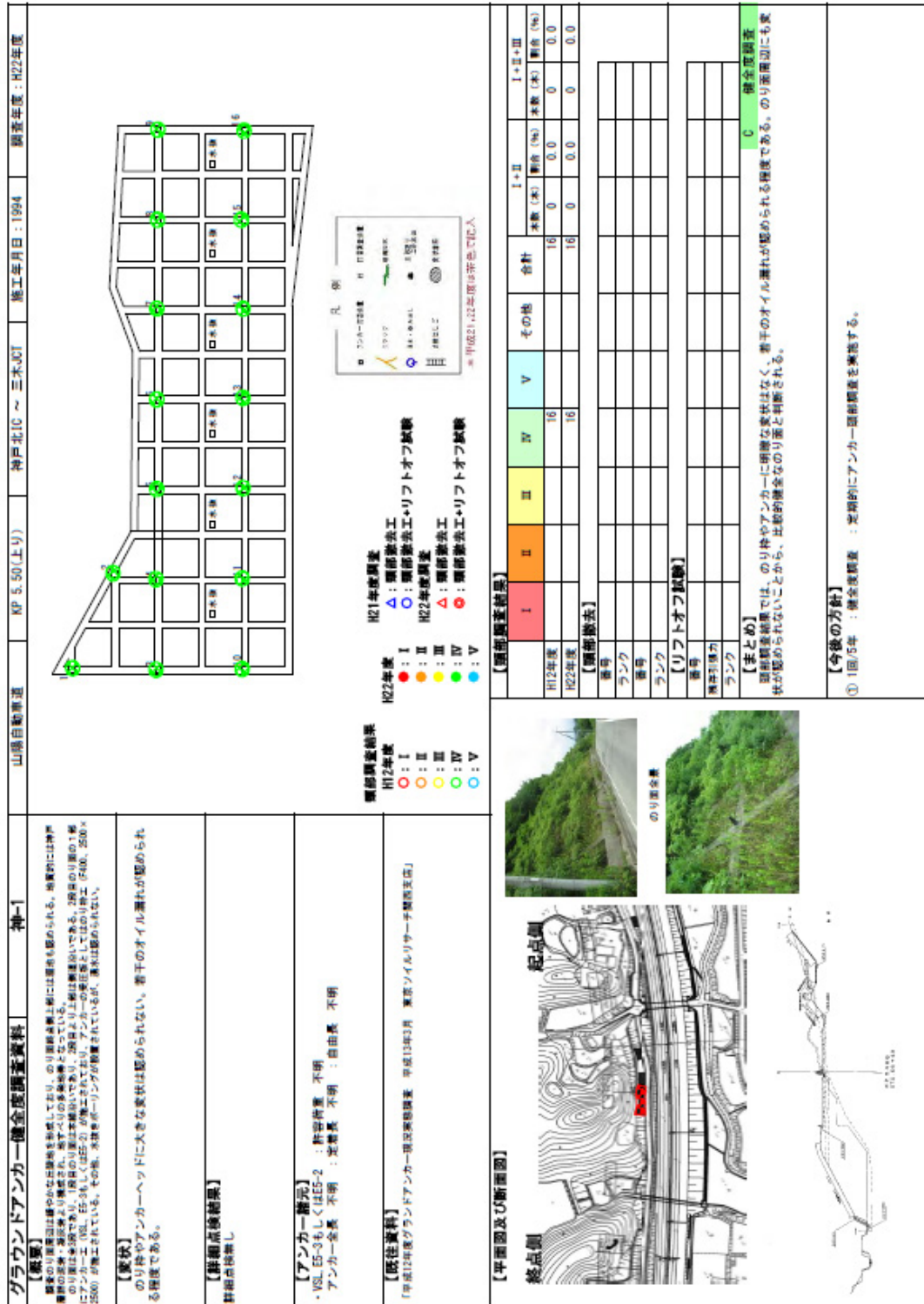


Figure A.45 Kobe No.1

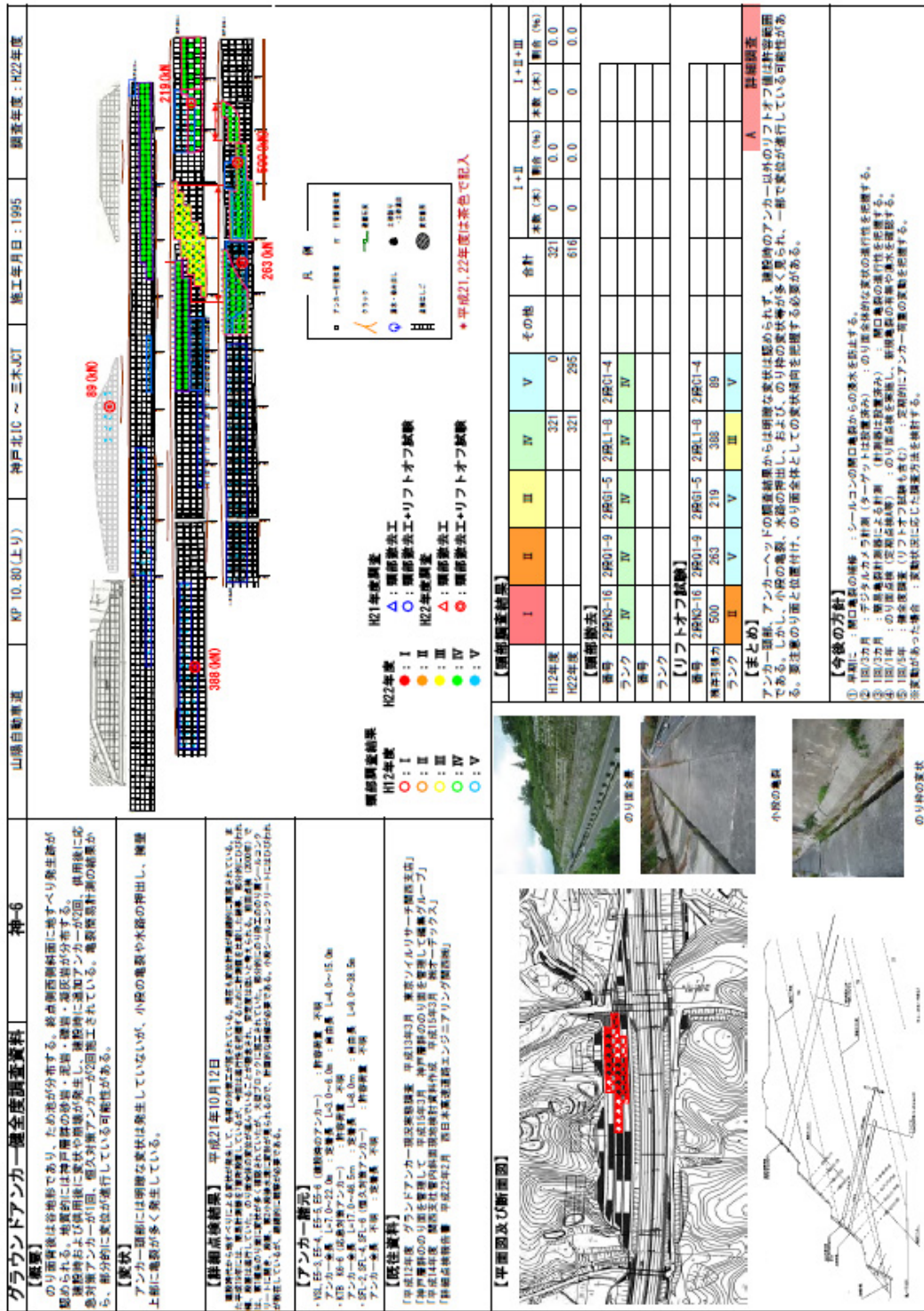


Figure A.50 Kobe No.6

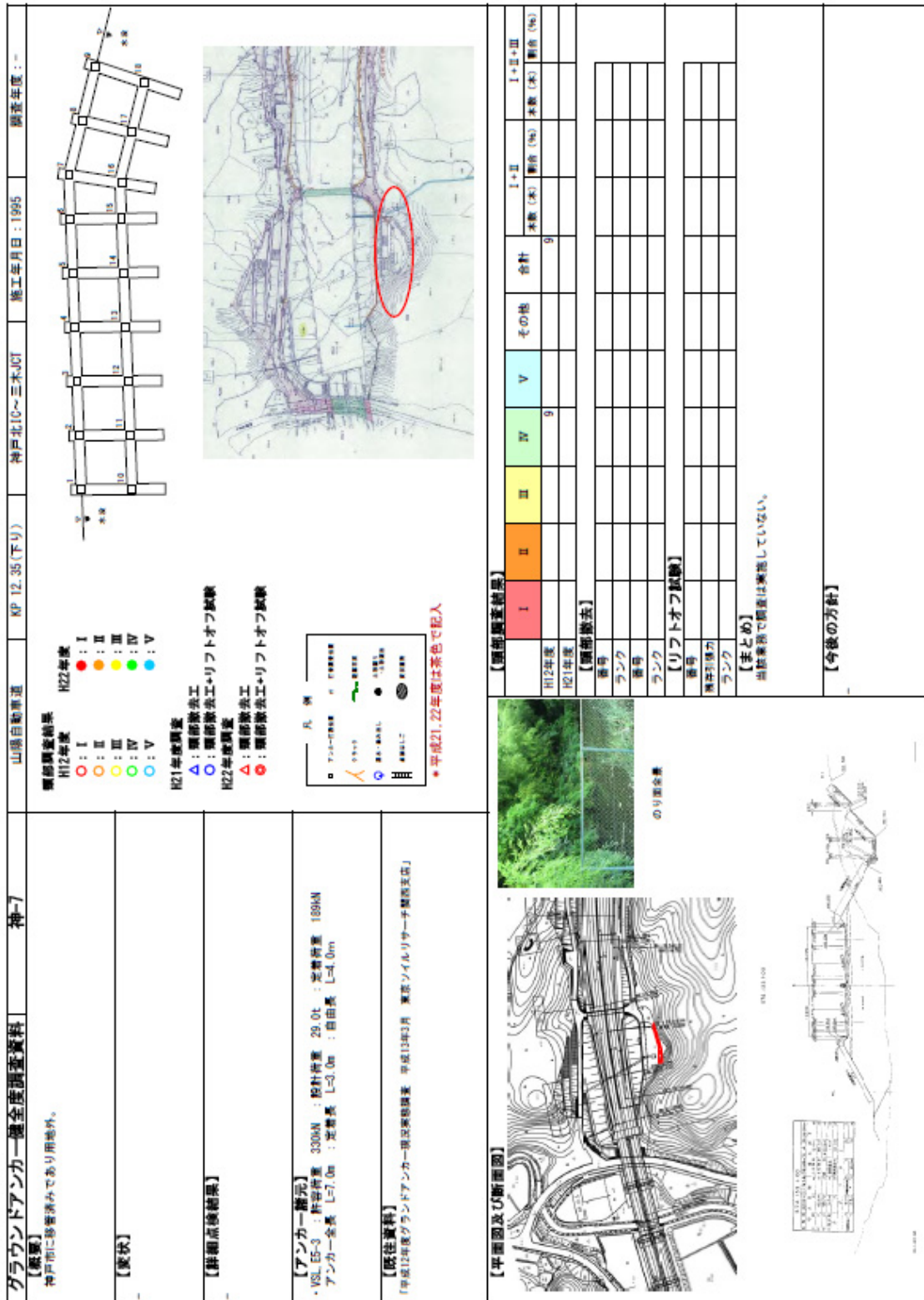


Figure A.51 Kobe No.7

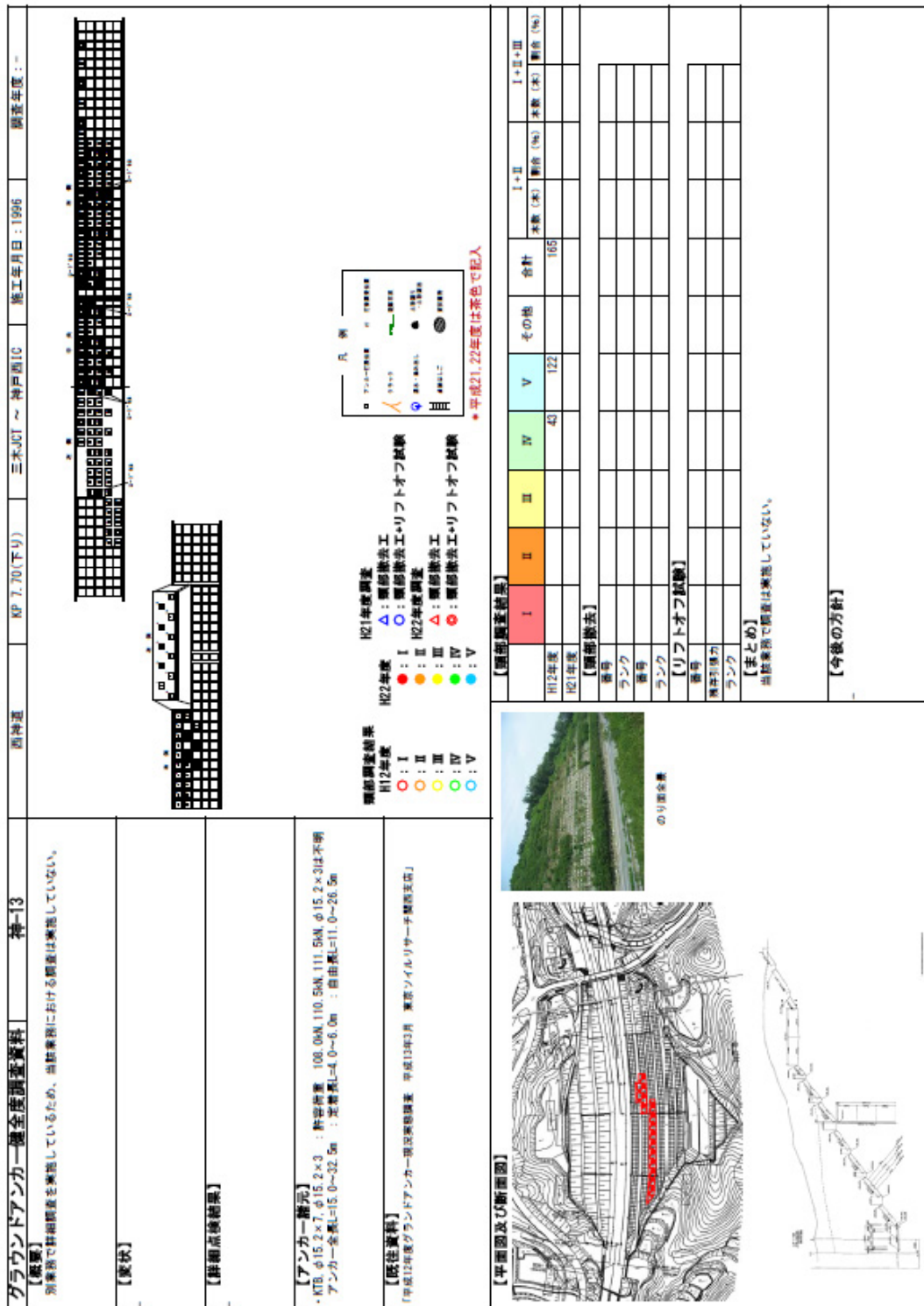


Figure A.56 Kobe No.13

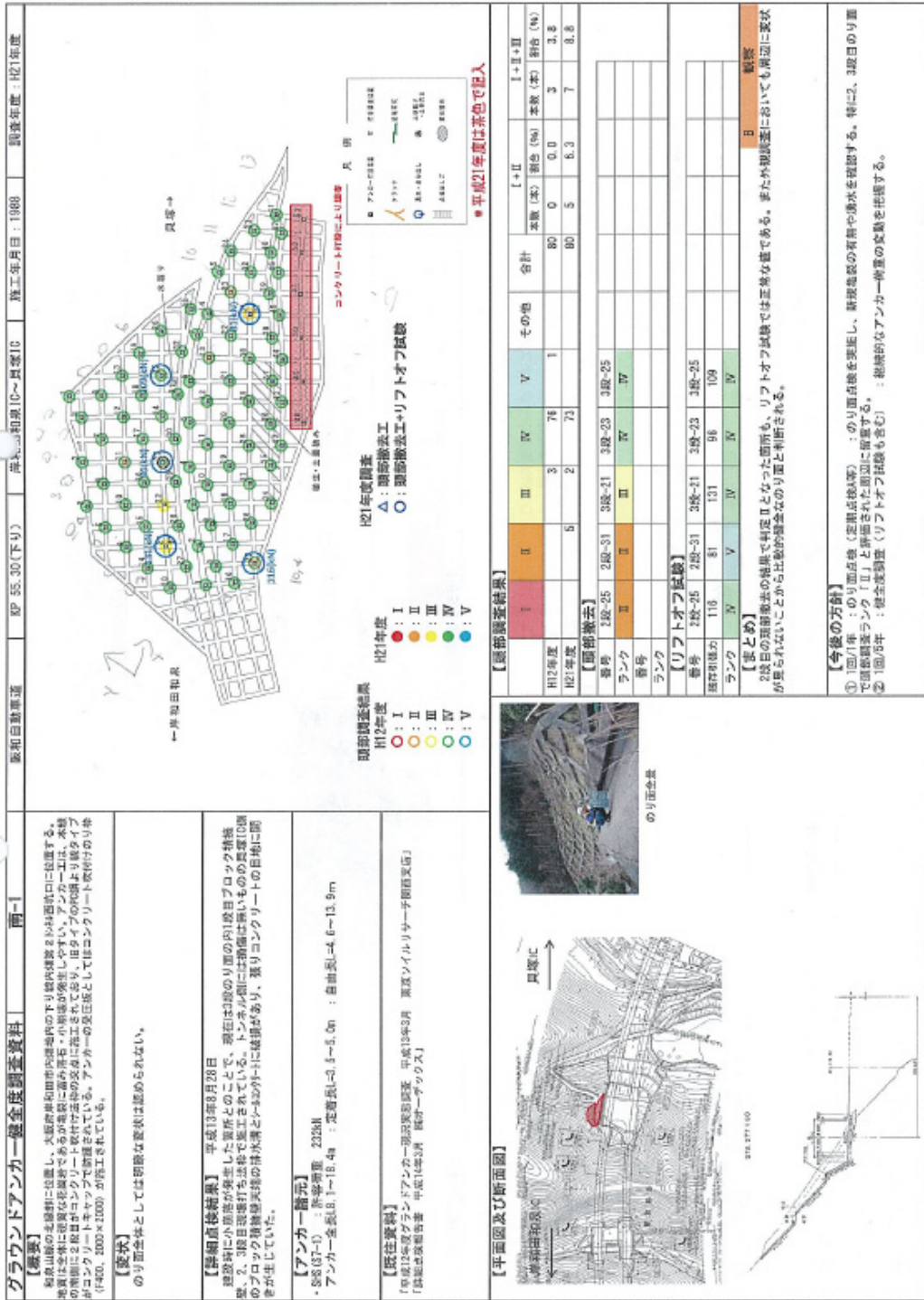


Figure A.63 Minami No.1

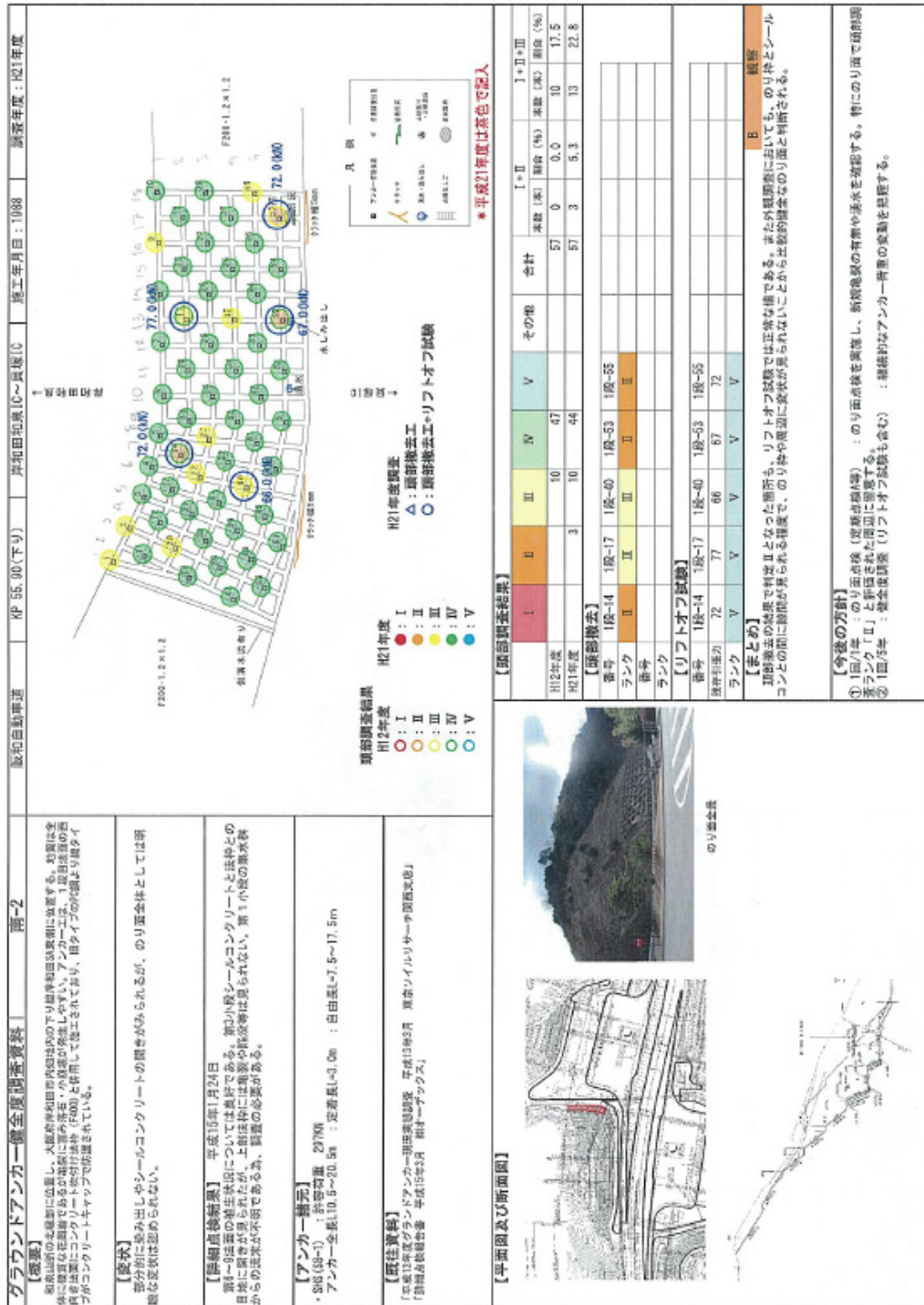
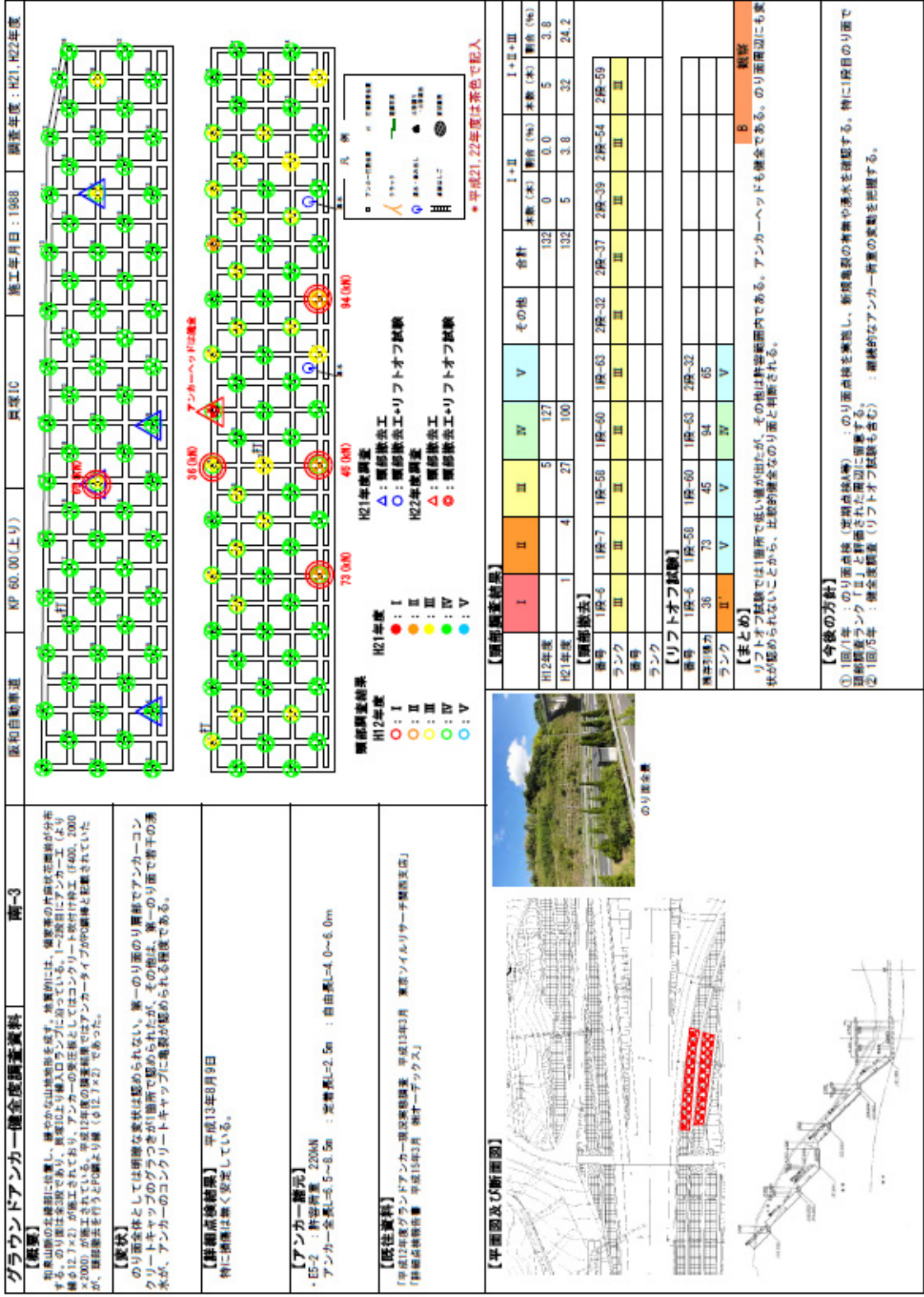


Figure A.64 Minami No.2



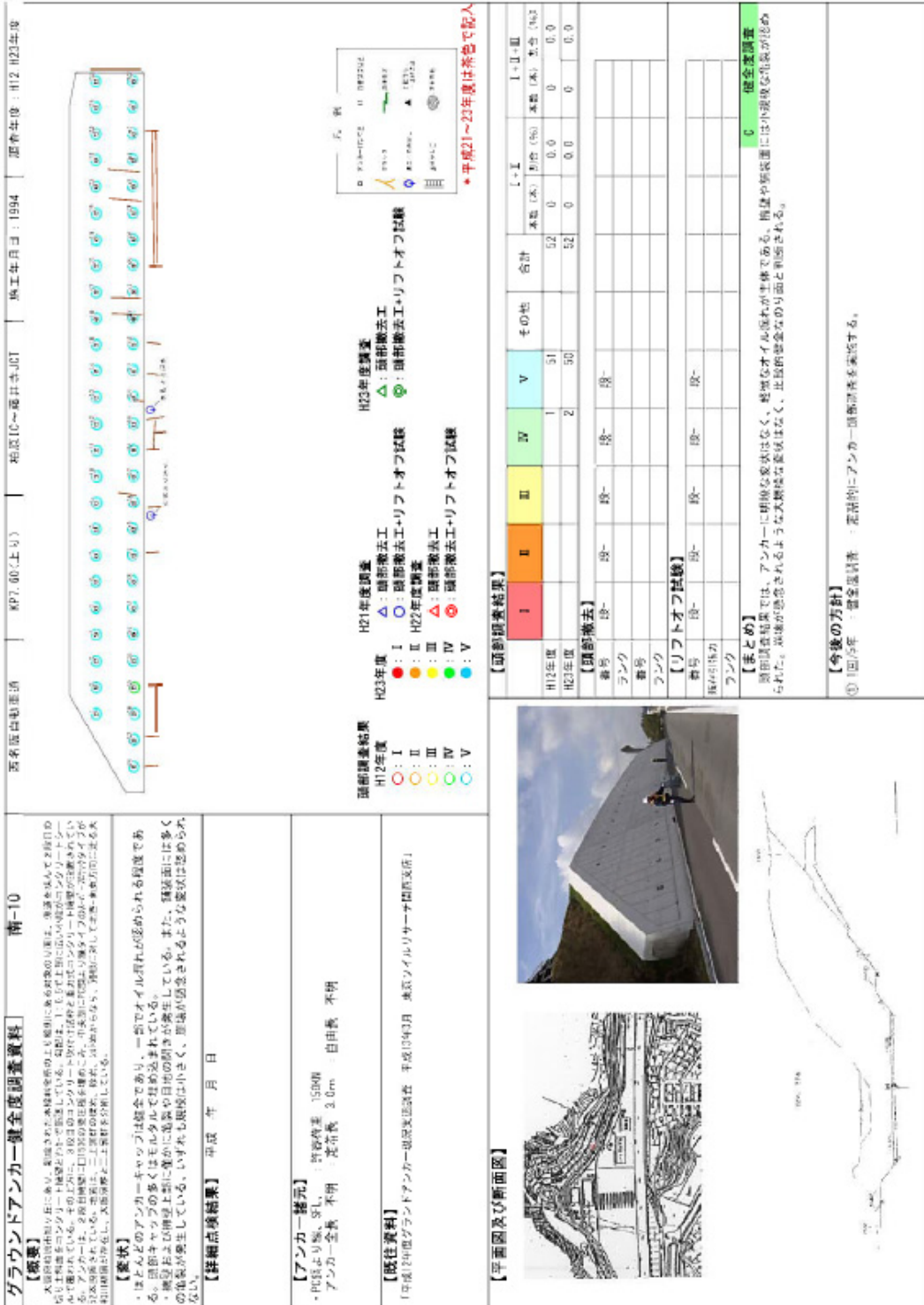


Figure A.72 Minami No.10

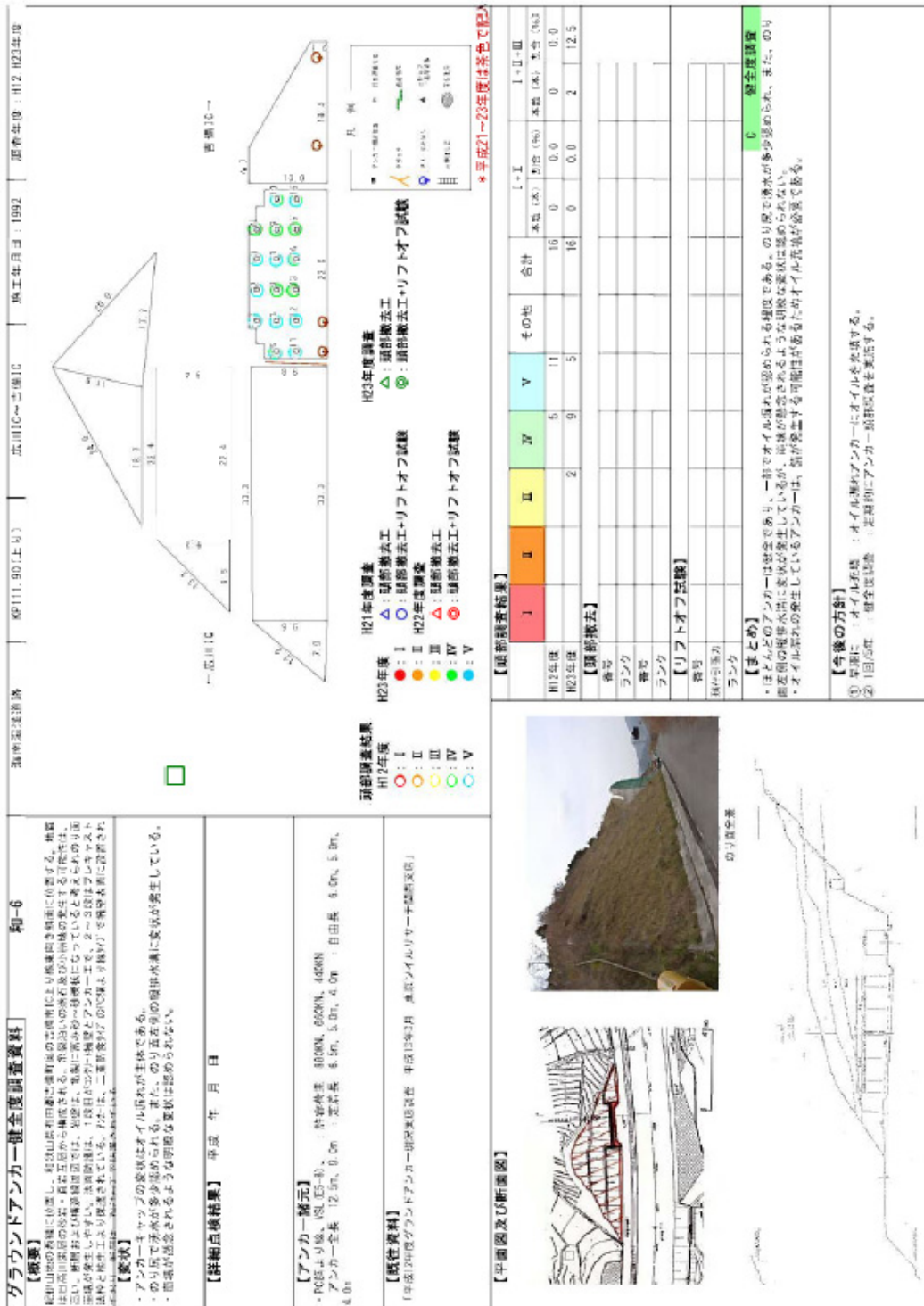


Figure A.79 Wagayama No.6

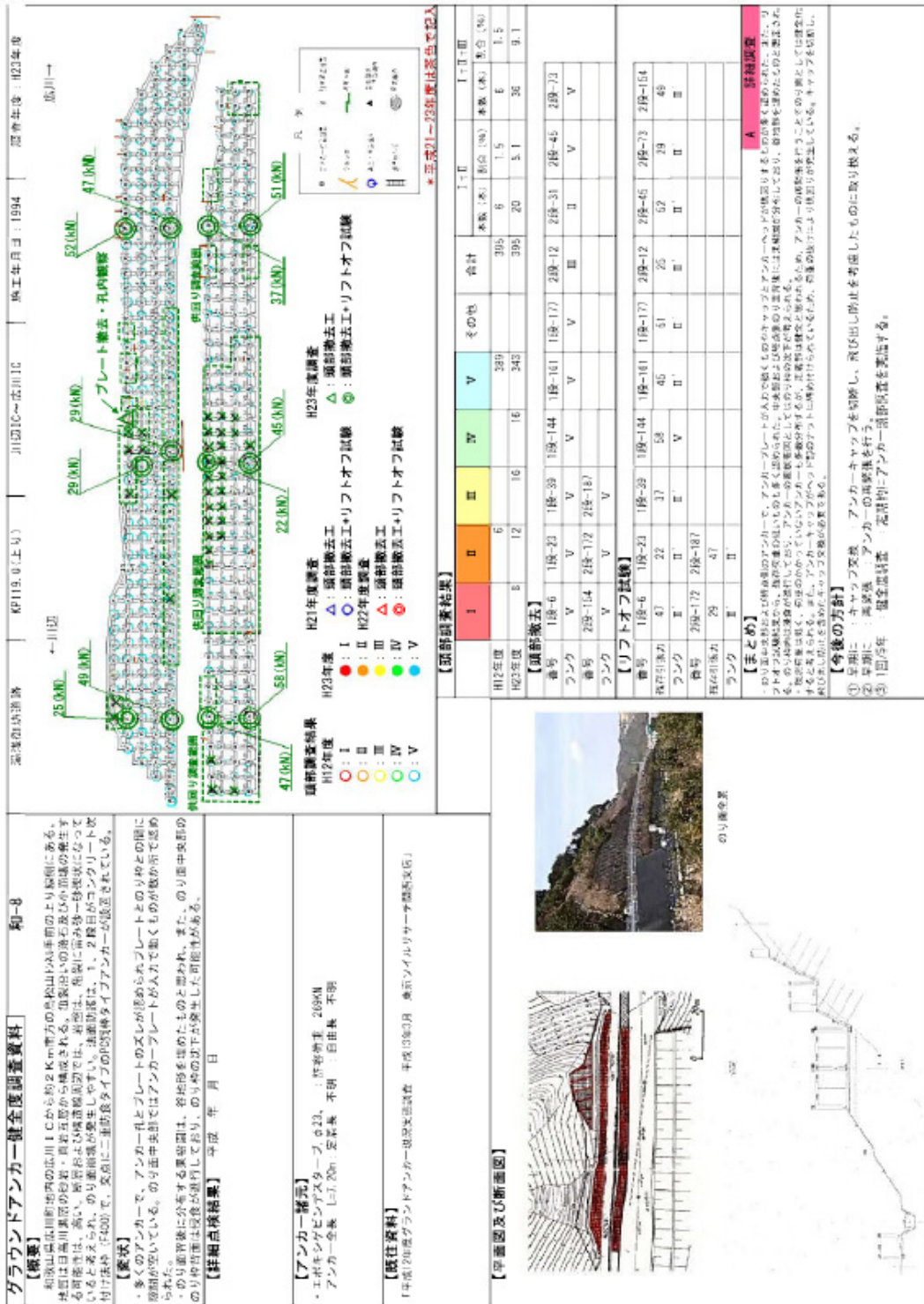


Figure A.81 Wagayama No.8

